REGULATION OF PRODUCTION, MATURATION AND LYTIC RELEASE OF THE RHODOBACTER CAPSULATUS GENE TRANSFER AGENT

by

Alexander Bauer Westbye

B.Sc., University of Oslo, 2008

A THESIS SUBMITTED IN PARTIAL FULFILLMENT OF

THE REQUIREMENTS FOR THE DEGREE OF

DOCTOR OF PHILOSOPHY

in

THE FACULTY OF GRADUATE AND POSTDOCTORAL STUDIES

(Microbiology & Immunology)

THE UNIVERSITY OF BRITISH COLUMBIA

(Vancouver)

April 2016

Abstract

The *Rhodobacter capsulatus* gene transfer agent (RcGTA) is a phage-like particle that mediates horizontal gene transfer between *R. capsulatus* strains, and its production is regulated by several bacterial systems, including quorum sensing and the CckA-ChpT-CtrA phosphorelay. This thesis presents evidence that RcGTA is released from cells by cell lysis, that lysis is modulated by the concentration of inorganic phosphate in the growth medium and that lysis requires an endolysin and holin gene. The expression of the lysis genes is regulated by the histidine kinase CckA, the phosphotransferase ChpT and the response regulator CtrA, and requires phosphorylation of CtrA. The endolysin and holin were characterized by expression in *E. coli*. High resolution electron microscopy images of affinity-purified RcGTA confirmed that RcGTA contains tail fibers and head spikes, and newly revealed the presence of a baseplate-like structure. RcGTA was found to undergo a maturation process similar to that of phages, and this maturation was regulated by the CckA-ChpT-CtrA phosphorelay. Cells lacking CckA produced tail-less particles containing DNA and polytube structures. During particle assembly spikes are attached to the head of RcGTA, and spike formation required *ghsA* and *ghsB*, which appear to be co-transcribed and regulated by CckA-ChpT-CtrA and quorum sensing. Spikes were required for efficient binding of RcGTA to the *R. capsulatus* capsular polysaccharide. Two new regulators of RcGTA, ClpX and DivL, were identified. ClpX was required for transduction, and capsid formation in cells lacking ClpX appeared to halt RcGTA production prior to DNA packaging. DivL appeared to be involved in regulating the CckA kinase activity; however a loss of DivL resulted in opposite phenotypes for an RcGTA overproducer and a wild type strain. Additionally, RcGTA production was found to be stimulated by temporary depletion of amino acids, but did

not require the (p)ppGpp-mediated stringent response or a homologue of the general stress response sigma factor EcfG.

Preface

During my tenure as a graduate student in Dr. Beatty's lab, I had the privilege of working with many excellent peers in a quality research environment. The large majority of the research presented in this thesis was designed, executed and analyzed by myself, with the invaluable input of my supervisor, Dr. J. Thomas Beatty. I did also receive advice from my co-workers, particularly Dr. Paul Fogg, Dr. Cedric Brimacombe, Dr. Hao Ding, Jeanette Beatty and Daniel Jun. During my tenure as a PhD Candidate I supervised and worked with several students, including Yulia Loktionova, Tegan Schellenberg, and Lukas Kater, who provided me with assistance to execute parts of the experiments.

Specific instances where experiments were not fully carried out by me include construction of the *ΔclpX* mutants (performed by Jeanette Beatty), construction of the complementation plasmid pCclpXP and the experiments that resulted in Figure 18A to D (performed by Lukas Kater). The transmission electron microscopy images were obtained by Dr. Calvin Yip (Figure 29, Figure 30D to F, Figure 31), and Keving Kuchinski (Figure 30A to C) with the aid of the UBC BioImaging Facility. Plasmid pRCckA(HA) was constructed jointly by Christina Wiesmann and me. Dr. H. Ding generated strain SBpG*Δ280*, which was used to evaluate the effect of a *ΔdivL* mutation on lysis in this SB1003-derived overproducer strain.

The RNA microarray data for the *cckA* and *ctrA* mutant and the DE442 overproducer were obtained and analyzed by Dr. Ryan Mercer and Dr. Andrew Lang in collaboration with the Beatty lab.

Data analysis was performed by me, and reviewed by Dr. Beatty and other co-authors on publications encompassing the data presented in this thesis.

Much of the research presented in this thesis has been published or is in the process of publication. I am indebted to the editors of Journal of Bacteriology, PLoS One, Journal of Molecular Biology and to the anonymous peer reviewers who gave me very useful and productive feedback during the review process. The relative contributions of each author, and the placement of data within each chapter will be presented in terms of each individual paper in the chronological order in which they were published. In some instances, datasets included in a figure have been slightly changed from the published figure to include relevant information or avoid duplicate representations.

Any material used from publications in this thesis has been done so with explicit permission.

Text and/or modified text from sections 3.1.1.3 and the following figures were published in Fogg PC, Westbye AB, Beatty JT (2012) *One for all or all for one: heterogeneous expression and host cell lysis are key to gene transfer agent activity in Rhodobacter capsulatus.* PLoS One 7(8):e43772: Figure 11A and B. The data I generated for the manuscript, which is presented in this thesis, includes Figure 5 showing that cell lysis is increased in the RcGTA overproducer DE442 and dependent on the growth medium. All other experiments (except Figure 6B, performed by me but not included in this thesis), were performed by Dr. Paul Fogg and are not presented in this thesis. Dr. Paul Fogg wrote the introduction and the majority of the methods, results and discussion sections. I wrote the methods, results and discussion sections relevant to my experiments; editing and critical evaluation were done by all co-authors. Experimental design was the work of Dr. J. T. Beatty, Dr. Paul Fogg, and me.

Text and/or modified text from sections 3.1.1, 3.1.2, 3.1.3.1, 3.3.1, 4.1.1, 4.1.2, 4.1.3,4.2, 4.3 and the following figures were published in Westbye AB, Leung MM, Florizone SM,

Taylor TA, Johnson JA, Fogg PC, Beatty JT (2013) *Phosphate concentration and the putative sensor kinase protein CckA modulate cell lysis and release of the Rhodobacter capsulatus gene transfer agent.* J Bacteriol 195(22):5025-40: Figure 8, Figure 9, Figure 10 (except panel C), Figure 11C to F, Figure 12, Figure 13, Figure 14B to E, Figure 15, Figure 22 and parts of Figure 16A and B. The data I generated for the manuscript, which is presented in this thesis, includes Figure 1, Figure 2C and D, Figure 3, Figure 4, Figure 5, Figure 6, Figure 7, Figure 8 and Figure 9. Experiments not performed by me (Figure 2A and B) were performed by Dr. Molly Leung, Terumi Taylor and Sarah Florizone, and are not presented in this thesis. The introduction, methods, results and discussion section was written by me. Editing and critical evaluation was done by all co-authors. Experimental design was the work of Dr. J. T. Beatty, Dr. Molly Leung, Terumi Taylor, Sarah Florizone, Dr. Paul Fogg, Jeanette Beatty, and me.

Text and/or modified text from sections 3.4.1, 3.4.2, 3.4.3, 3.4.4, 3.4.5, 3.4.6, 3.5.1, 4.3.3, 4.3.4, 4.3.5, 4.7 and the following figures have been accepted for publication in Westbye AB, Kuchinski K, Yip CK, Beatty JT. *The gene transfer agent RcGTA contains head spikes needed for binding to the Rhodobacter capsulatus polysaccharide cell capsule.* J Mol Biol (in press): Figure 24A and B, Figure 25, Figure 26, Figure 27A, B, C and E, Figure 28A and Figure 29. The data I generated for the manuscript, which is presented in this thesis, include Figure 1, Figure 2, Figure 3, Figure 4 and the production of biological material for Figure 5. Transmission electron microscopy (TEM) imaging of samples for Figure 5 was performed by Dr. C. K. Yip. The introduction, methods (except TEM), results and discussion section were written by me. Editing and critical evaluation were done by all co-authors. Experimental design was the work of Dr. J. T. Beatty, Dr. C. K. Yip, Kevin Kuchinski, and me.

Table of Contents

List of Figures

List of Symbols

α	alpha
β	beta
Δ	delta
°	degrees

List of Abbreviations

AI-2	autoinducer-2
ATP	adenosine triphosphate
BLASTP	basic local alignment search tool, protein
bp	base pair
BSA	bovine serum albumin
CA	catalytic and ATPase-binding
cfu	colony forming unit
CPS	capsular polysaccharide
c-di-GMP	cyclic diguanylate
DHp	dimerization and histidine phosphotransfer
DNA	deoxyribose nucleic acid
DMSO	di-methyl sulfoxide
dsDNA	double stranded DNA
EDTA	ethylenediaminetetraacetic acid
ghs	gta head spike
GTA	gene transfer agent
HATPase_C	histidine kinase-type ATPase catalytic
HGT	horizontal gene transfer
HK	histidine kinase
HSL	homoserine lactone
ICE	integrative and conjugative elements
IPTG	isopropyl β-D-1-thiogalactopyranoside

kb	kilo-basepairs
nt	nucleotide
ONPG	ortho-nitrophenyl-β-galactoside
PAGE	polyacrylamide gel electrophoresis
PAS	Per/ARNT/Sim
PCR	polymerase chain reaction
ppGpp	guanosine tetraphosphate
pppGpp	guanosine pentaphosphate
phage	bacteriophage
RcGTA	*R. capsulatus* gene transfer agent
REC	receiver domain
Rif	rifampicin
RNA	ribose nucleic acid
rcf	relative centrifugal force
rpm	rotations per minute
RR	response regulator
SAR	signal anchor release
SDS	sodium dodecyl-sulfate
ssDNA	single stranded DNA
TEM	transmission electron microscopy
TMP	tape measure protein
tmRNA	transfer-messenger RNA
WT	wild type

Acknowledgements

I thank the people and institutes who have made my time as an international graduate student at the University of Bristish Columbia both possible and very pleasurable.

First and foremost, I wish to thank Dr. Tom Beatty for being an excellent PhD supervisor. His encouragement and enthusiasm has allowed me to become a better and independent researcher. I also thank my committee members Drs. Bill Mohn, Curtis Suttle and Erin Gaynor for invaluable input on my project. Additional thanks to Dr. Calvin Yip and Kevin Kuchinski for their assistance with the visualization of RcGTA particles. I also thank Dr. Andrew Lang for providing access to several plasmids and strains which were used for construction and complementation of mutants.

I also thank several present and former members of the Beatty lab, especially Dr. Paul Fogg who taught me several molecular cloning techniques and helped troubleshoot experiments. Thanks to Jeannette Beatty and Lukas Kater, who constructed and performed several important experiments with the *clpX* mutants. I've had several valuable scientific discussions with Dr. Cedric Brimacombe, Daniel Jun, Dr. Rafael Saer, Dr. Hao Ding, Rachel Moens and Christina Wiesman. Big thanks to Yulia Loktionova and Tegan Schellenberg for letting me supervise them. Thanks to Dr. Julian Davies and Iván Villanueva for several discussions on science.

I thank researchers at the Norwegian Defence Research Establishment, Kjeller, and GE Healthcare, Storo, who were instrumental for my interest in scientific research. I also owe many thanks to the late professor Bill Davies (University of Oslo) who sparked my interest in microbiology and encouraged me to apply to UBC.

My time as a graduate student has been extra pleasurable thanks to my stay at St. John's College and the many friendships that were forged there. I'm also grateful for the many

adventures with good friends in the mountains and in Squamish. I especially thank Andrew H, Nicole O, Douglas S, Kjell Erik R, Gaby, Simon N, Niusha, Phil P, Fred V, Kevin K, Daniel J, Camilo R, Natalia M, Liz K, Bill, Dave P, Gareth G, Jan M, Piotr C and Neil M.

I thank my parents for their continued support, and last but not least, special thanks to my partner Bieke Gils and our son Amund.

To my son Amund,

May you discover life’s many wonders.

Chapter 1: Introduction

1.1 *Rhodobacter capsulatus* and the purple nonsulfur bacteria

Rhodobacter capsulatus (previously *Rhodopseudomonas capsulata*) is a purple nonsulfur bacterium and a member of the Alphaproteobacteria. Purple nonsulfur bacteria, as well as the purple sulfur bacteria, are capable of growth using autotrophic photosynthesis and H_2S as a source of reductant. The purple nonsulfur bacteria are typically found in stagnant or eutrophic aquatic environments, and the optimal growth conditions are photoheterotrophic conditions on organic carbon and ammonia (or nitrate), and most members can fix N_2 (Madigan and Jung, 2009).

R. capsulatus is a metabolically very versatile organism and can be cultured phototrophically with either CO_2 or organic carbon, or in darkness by respiratory, fermentative or chemolitotrophic growth using H_2 as the reductant (Madigan and Jung, 2009, Weaver *et al.*, 1975). Together with the nonsulfur bacteria *Rhodobacter sphaeroides* and *Rhodopseudomonas palustris*, *R. capsulatus* has been extensively studied as a model organism for a wide variety of physiological activities.

1.2 Horizontal gene transfer in bacteria

Horizontal gene transfer (HGT; also called lateral gene transfer) is the transfer of a gene to an organism by means other than classical (vertical) inheritance to progeny from a parent. HGT is a common occurrence among prokaryotes and several examples of HGT have been reported for multicellular organisms (Boto, 2014, Soucy *et al.*, 2015). HGT is recognized as providing advantageous traits such as antibiotic resistance, virulence factors, or new metabolic mechanisms (Soucy *et al.*, 2015).

Several mechanisms of HGT among the prokaryotes have been discovered, however most fall within three broad categories: conjugation, natural transformation, or transduction (Frost *et al.*, 2005, Thomas and Nielsen, 2005).

1.2.1 Conjugation

Conjugation is the transfer of genetic material, typically a plasmid, by direct cell-cell contact by a diverse set of mechanisms. The most common mechanism of transfer is through a mating bridge that requires pilus formation by a type IV secretion system encoded on the plasmid (Norman *et al.*, 2009, Thomas and Nielsen, 2005). Conjugation readily occurs between bacteria of different species (Musovic *et al.*, 2006) and is responsible spread of antibiotic resistance in many environments (Carattoli, 2013). Conjugation may transfer DNA between different kingdoms of life: the Alphaproteobacterium *Agrobacterium tumefaciens* transfers the Ti plasmid to plant cells via conjugation during invasion and colonization (Gelvin, 2003).

1.2.2 Natural transformation

Natural transformation is the uptake and recombination of naked DNA from the environment (Johnston *et al.*, 2014, Thomas and Nielsen, 2005). A conserved set of proteins, collectively called Com proteins (e.g., ComEC), are involved in transporting double stranded DNA from the environment to the cytoplasm of the transformed cell. Incoming DNA can either become integrated into the genome by homologous recombination (resulting in transformation) or alternatively be degraded for nutrients. One strand of the incoming dsDNA is degraded in the process of transport, and during transformation the single stranded DNA is bound by DNA processing protein A (DprA) that recruits the recombination protein RecA to allow for homologous recombination. Bacteria capable of taking up DNA are termed competent, and several species exhibit this as a transient feature during laboratory growth (Johnston *et al.*, 2014).

Competence is often regulated by alternative sigma factors or transcription factors. In *Streptococcus pneumoniae* and *Bacillus subtilis*, competence is regulated by pheromones (similar or analogous to quorum sensing, see below) and requires the alternative sigma factor σ^X or transcription factor ComK, respectively (Claverys *et al.*, 2006).

1.2.3 Transduction

Transduction is HGT mediated by bacteriophages (phages) or phage-like particles. Several phages mediate transduction as a by-product of their life cycle either by specifically incorporating a part of the host genome during excision from the prophage state (specialized transduction) or by erroneous packaging of host DNA (generalized transduction). When the phage particle infects a new cell, the bacterial-derived genes may recombine into the new host genome (Frost *et al.*, 2005). Generalized transduction is most commonly observed among phages that utilize a headful packaging mechanism, in which DNA packaging does not require a specific sequence after initiation (Casjens and Gilcrease, 2009).

1.2.4 Other forms of HGT

The transposon is a mobile genetic element that in the simplest form can catalyze intragenic genetic movement, but not transfer to a new host. Transposons move by site-specific excision and integration, and can integrate into conjugative plasmids which allow them to transfer to a new host (Frost *et al.*, 2005). Additionally, some transposons harbor elements to catalyze their own conjugation and are considered members of the integrative and conjugative elements (ICEs) together with other conjugative elements that integrate into the chromosome (Burrus *et al.*, 2002).

Lastly, outer membrane vesicles budding off from bacteria have been proposed to mediate HGT, however there is currently little molecular evidence available to support vesicles having a direct role in HGT (Fulsundar *et al.*, 2014, Schwechheimer and Kuehn, 2015).

1.3 Transduction mediated by phage-like gene transfer agents

In addition to phage-mediated transduction, several bacteria encode small phage-like particles termed gene transfer agents (GTAs) that appear to have evolved to mediate genetic exchange (Lang *et al.*, 2012).

1.3.1 RcGTA, the gene transfer agent of *R. capsulatus*

R. capsulatus produces a GTA termed RcGTA and has become the model system for studying GTAs. GTAs were first reported in 1974 as an unusual mechanism of genetic recombination that shared similarities with transducing phages, but did not cause plaques (Marrs, 1974). Isolation of an RcGTA overproducer mutant Y262 after chemical mutagenesis, which produced approximately 1,000-fold increased levels of RcGTA, allowed for the initial characterization of RcGTA as small bacteriophage-like (phage-like) particles with approximately 30 nm head-diameter. Analysis of the RcGTA nucleic acid indicated that the particle packaged linear dsDNA. Restriction analysis, and later DNA microarray hybridization analysis, indicated that the DNA contained in RcGTA was essentially random, in contrast to phages that preferentially packages their own genome (Hynes *et al.*, 2012, Yen *et al.*, 1979). Later experiments revealed that an ~15 kb gene cluster (Figure 1), containing genes homologues to phage genes, was required for RcGTA production (Lang and Beatty, 2000). Single cell experiments using this promoter revealed that RcGTA is produced by a small (~0.1% to 3%) proportion of the cell population in stationary phase for wild type (WT) cells, whereas this proportion was greatly increased for an RcGTA overproducer strain (Fogg *et al.*, 2012b, Hynes

et al., 2012). H. Ding has recently identified a mutation that appears to be responsible for the RcGTA overproduction phenotype, however it is unclear how this mutation results in the increased production level (H. Ding, unpublished data). Although it has not been demonstrated that RcGTA offers a fitness advantage to the bacterium, it was suggested that RcGTA benefits the bacterial population by increasing diversity in response to a change in environmental conditions (Lang *et al.*, 2012).

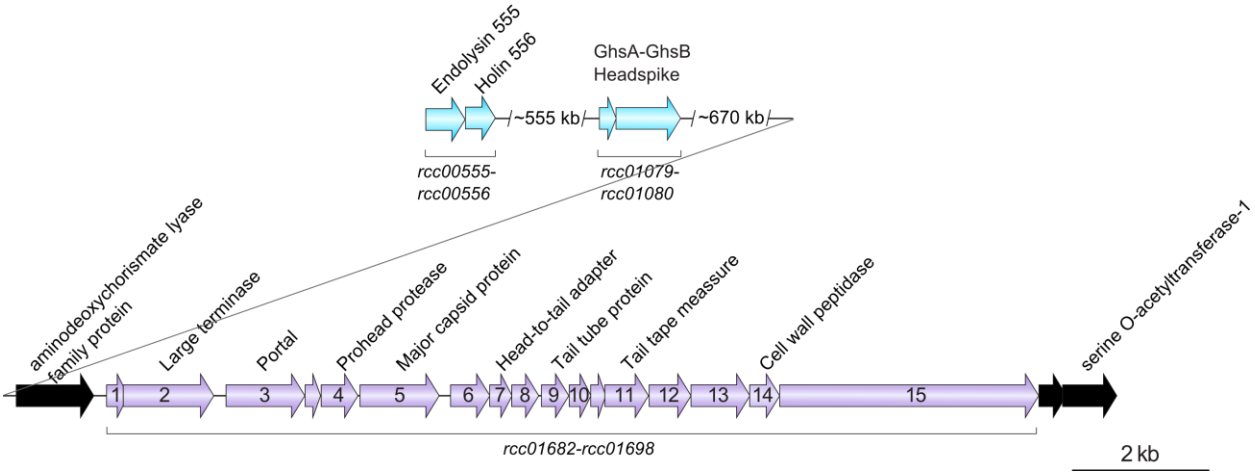

Figure 1 The RcGTA gene clusters

The known ("structural") genes required for formation of RcGTA: the ~15 kb RcGTA primary, lysis and head spike gene clusters. Modified from Lang *et al*. 2013.

1.3.2 GTAs produced by other Alphaproteobacteria, unrelated GTAs and the possible importance of GTAs

An RcGTA-like primary gene cluster is conserved in many members of the Alphaproteobacteria and appears to have been vertically inherited (Lang and Beatty, 2007, Lang *et al.*, 2002, Lang *et al.*, 2012). Recently, functional RcGTA-like activity has been demonstrated, and particles visualized by transmission electron microscopy (TEM) for other organisms such as

Ruegeria pomeroyi and *Roseovarius nubinhibens* (Biers *et al.*, 2008, McDaniel *et al.*, 2010, McDaniel *et al.*, 2012). *Rhodovulum sulfidophilum* was demonstrated to produce a RcGTA-like particle in TEM, and contained a 4.5 kb fragment of DNA (Nagao *et al.*, 2015).

Phylogentically diverse bacteria produce particles that have been recognized as GTAs, because of their transduction potential and the presence of DNase I-protected, non-discrete segments of DNA. However, none of these systems are genetically related to RcGTA (Lang *et al.*, 2012). The spirochaete *Brachyspira hyodyseneriae* produces a particle termed VSH-1, the sulfur-reducing bacterium *Desulfovibrio desulfuricans* produces Dd1, some members of *Bartonella* have been shown to produce BLPs, and *Methanococcus voltae* produces VTA (Anderson *et al.*, 1994, Barbian and Minnick, 2000, Bertani, 1999, Eiserling *et al.*, 1999, Matson *et al.*, 2005). For many of the species, particles were visualized by TEM.

Because GTAs appear to be widespread in prokaryotes and because RcGTA-like genes are widely conserved and maintained in genomes that and appears to encode functional proteins, it has been argued that GTAs may serve a beneficial role to the bacteria (Lang and Beatty, 2007, Lang *et al.*, 2012, Stanton, 2007). It is possible that GTAs increase the rate of HGT in a population when cells are undergoing stress and that this benefits the cells, however no thorough experiments have been performed to investigate this. It can be speculated that RcGTA facilitates the transfer of a beneficial mutation from one subset of a population to cells harbouring another beneficial mutation, thereby producing an additive or synergistic effect. Similarly, a mutation that yields a non-beneficial allele in one genome could yield a beneficial effect on a recipient cell that has one or more alleles that differ from the genotype of the RcGTA producing cell. RcGTA-mediated transduction appears to be strain dependent (Wall *et al.*, 1975), indicating that RcGTA particles may preferentially transduce to related rather than less-related bacteria. DNA contained

in the capsid is protected from nucelases present in the environment, which together with the strain specificity could indicate that RcGTA-mediated transduction is a targeted and efficient mechanism of horizontal gene transfer compared to other horizontal gene transfer mechanisms such as transformation. An alternative beneficial mechanism of GTAs was proposed by Stanton, who suggested that GTAs may provide cells with a temporary diploid state of the genes encoded an incoming DNA fragment, and that this may increase production of beneficial proteins for some of the recipient cells (Stanton, 2007).

1.4 RcGTAs and connections to phages

RcGTA has a phage-like morphology (Yen *et al.*, 1979) and the organization of the primary RcGTA gene cluster is similar to the majority of the late genes of lambdoid phages, with DNA packaging genes followed by head and tail formation genes (Casjens and Hendrix, 2015, Lang *et al.*, 2012). Because of such similarities to phages and the vertical inheritance in the Alphaproteobacteria, it was proposed that RcGTA evolved from an ancestral prophage early in the evolution of the Alphaproteobacteria (Lang and Beatty, 2007).

Virulent phages, such as enterobacterial phage T4, are phages that infect, replicate and release phage progeny from a bacterium (the lytic state) without taking up prolonged residence in the bacterium. In contrast, temperate phages such as lambda can either undergo a lytic process or take up residence as a prophage once inside a bacterium (the lysogenic state). The prophage can reside in the lysogenized bacterium for numerous cell divisions before initiating a lytic cycle to produce numerous copies of the phage and escape the host. Many temperate phages, including enterobacterial phages lambda and Mu, form prophages by integrating their genome into the bacterial chromosome using site-specific recombination or transposition. Other prophages, such as enterobacterial phage P1, replicate as a plasmid inside the host (Campbell, 2005). Most

studied prophages remain latent due to repression of gene expression by a repressor protein, such as the lambda cI repressor. For lambda, a DNA damage-induced SOS response results in cleavage of the cI repressor and induction of the lytic pathway (Little, 2005). During the lytic cycle, the phage expresses the previously latent genes that encode the structural proteins of the particle as well as the DNA packaging machinery.

Phages are classified based on their morphology. The majority of phages have tails, and those containing linear, dsDNA are grouped in the order *Caudovirales* and further divided into three morphological groups based on their tail structure (Ackermann, 2003).

The *Siphoviridae* family contains phages with long, non-contractile and typically flexible tails (Figure 2A); well-studied models include lambda, T1, T5 and HK97, all infecting enterobacteria such as *E. coli,* SPP1 that infects *Bacillus subtilis*, and the lactococcal phages Tuc2009, p2 and TP901-1 (Davidson *et al.*, 2012). Phages with contractile tails are grouped in the *Myoviridae* family and includes the enterobacterial phages T4 and Mu (Leiman and Shneider, 2012). The *Podoviridae* includes phages with short tails such as the enterobacterial phages P22 and T7 (Casjens and Molineux, 2012). RcGTA is morphologically and genetically similar to the *Siphoviridae* family, with several similarities (see below) to phage HK97 (Lang *et al.*, 2012, Yen *et al.*, 1979).

1.5 Phage assembly and maturation

The assembly of long-tailed dsDNA phages (*Siphoviridia* and the contractile *Myoviridae*) follows two separate pathways: a head formation pathway that involves DNA packaging into a preformed head, and a tail formation pathway (Aksyuk and Rossmann, 2011). The two pathways proceed independently; mutations that block the tail formation pathway allow for production of

heads and *vice versa*. After head and tail completion, the two pathways merge to create the infectious particle, or virion.

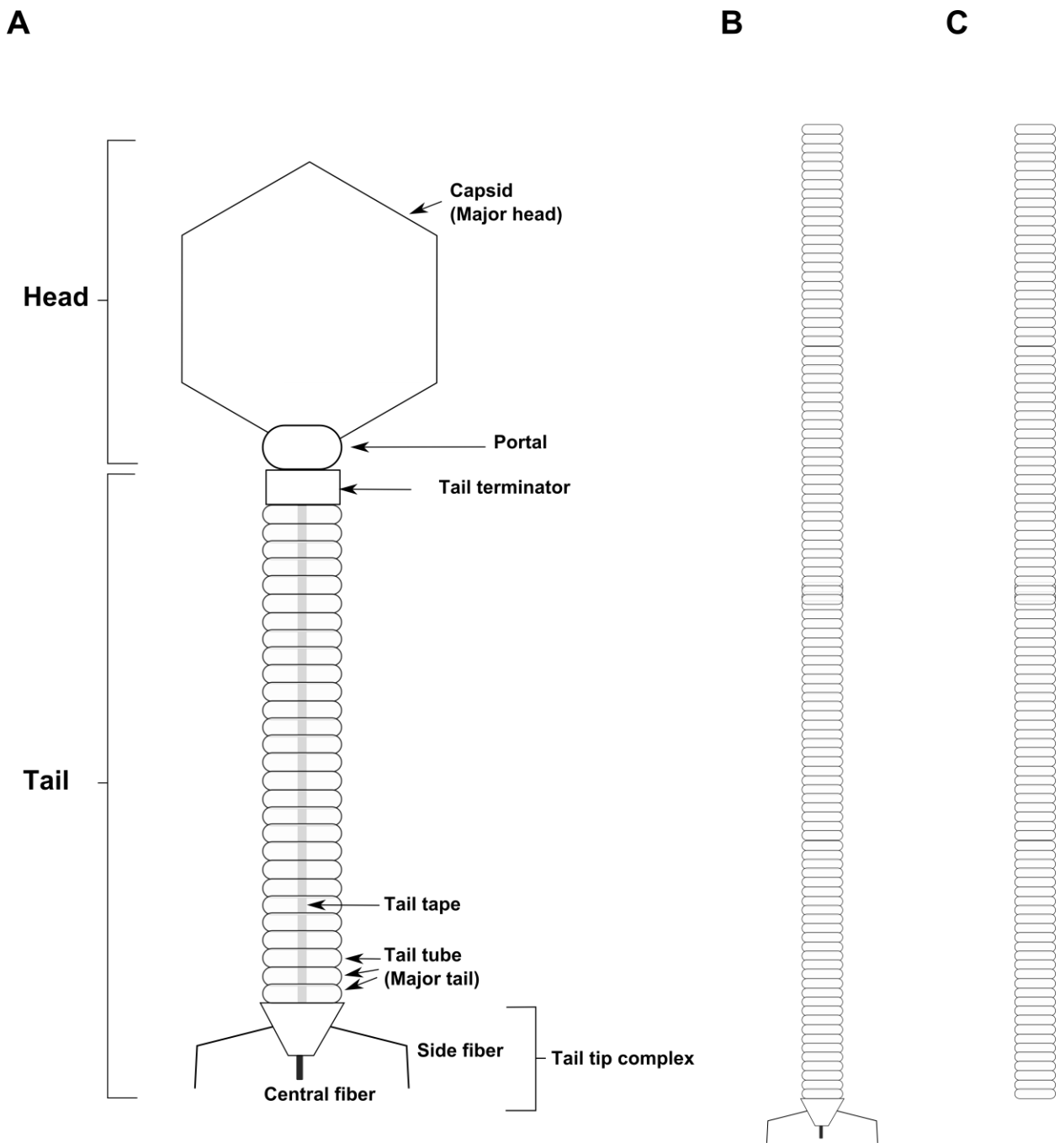

Figure 2 Siphoviridae

A, Siphoviridae are dsDNA viruses with long, non-contractile tails. The head and tail component of the virions assemble by two separate pathways. Several conserved proteins present in matured particles and discussed in text are indicated. **B,** Some tail gene mutants produce excessively long tail-like features termed polytails (**B**) or polytubes (**C**). See text for details. Adapted from Davidson *et al.* 2012.

1.5.1 Head assembly and DNA packaging

The main structure of the DNA-containing head in the *Caudovirales* is called the capsid (Figure 2A) and is typically made up from a minimum of 60 copies of one protein, termed the capsid (or coat) protein (Aksyuk and Rossmann, 2011, Fokine and Rossmann, 2014). RcGTA shows similarity to phage HK97, the most well studied *Siphoviridiae* with respect to head assembly. For HK97, capsid protein assemble into hexameric and pentameric capsomers (Duda *et al.*, 1995b). In contrast, the Myoviridae T4 encodes two separate capsid proteins which form hexameric or pentameric capsomers (Aksyuk and Rossmann, 2011). HK97 capsomers assemble onto the portal protein to form the icosahedric head structure termed Prohead I, with the portal occupying one of the vertexes; however an icosahedric structure is also formed in the absence of the portal protein (Duda *et al.*, 1995b, Hendrix and Johnson, 2012). Similarly, the RcGTA capsid protein is capable of assembly into capsomers and an icosahedric structure when expressed in *E. coli* (Spano *et al.*, 2007). In most phages, including lambda and P22, capsid assembly requires a separate scaffolding protein, however for some phages such as HK97 and T5, the scaffolding role is served by the N-terminal Δ-domain of the capsid protein (Fokine and Rossmann, 2014). For HK97, this domain is cleaved from the mature capsid protein by a protease encoded by a phage gene located directly 5' of the capsid gene, and this intermediate structure has been termed Prohead II (Duda *et al.*, 1995a, Duda *et al.*, 1995b). DNA is subsequently packaged into the head by the terminase complex. The process of DNA packaging appears to trigger the expansion of the capsid, approximately doubling the volume of the capsid. For lambda, head expansion occurs after packaging one third of the genome, whereas T4 DNA packaging and head expansion are uncoupled (Fuller *et al.*, 2007, Rao and Black, 1985). For HK97, head expansion involves autocatalytic covalent crosslinking of the capsid proteins, essentially forming a series of

"chainmail structures" termed Expansion Intermediates, and eventually forming the final Head II structure (Hendrix and Johnson, 2012). Several phages have additional proteins assembled onto the capsid, which are referred to as decorating or accessory proteins depending on the phage system, and are added after expansion but prior to tail assembly. The two most studied proteins are soc from T4, which strengthens the capsid structure, and the essential gpD of lambda, which is required for complete genome packaging (Qin *et al.*, 2010, Sternberg and Weisberg, 1977). Recently, the non-essential T4-decorating protein hoc was reported to be involved for phage binding to intestinal mucosa (Barr *et al.*, 2013). Additionally, many phage capsids contain internal proteins, some of which are injected into the host during infection (Black and Thomas, 2012).

Insertion of DNA into the preformed procapsids is performed by the terminase complex, composed of the large and small terminase proteins, which docks on the portal vertex of the procapsid and packages DNA into the capsid (Casjens, 2011, Feiss and Rao, 2012). Portal proteins form a dodecameric ring at one of the vertexes of the capsid, and DNA enters the capsid through the center of the ring (Casjens, 2011). The movement of DNA into the capsid in an ATP-dependent process is carried out by the N-terminal ATPase domain of the large terminase, which packages DNA into the capsid to a very high concentration (~500 mg/mL) (Black and Thomas, 2012, Sun *et al.*, 2008).

The small terminase protein modulates the activity of the large terminase protein, and is required for recognizing packaging and cut sites. DNA recognition and cutting differ between phages, with lambda having a sequence-specific cut site (*cos*), and P22 having a sequence-specific recognition site (*pac*) but a sequence-independent cut in a region spanning approximately 120 bp centered on the *pac* site (Feiss *et al.*, 1983, Wu *et al.*, 2002).

For many of the phages that use sequence-independent cut sites, DNA packaging proceeds by a headful mechanism, and this has also been suggested to be the DNA packaging strategy for RcGTA, using the terminase proteins (Casjens *et al.*, 2005, Lang and Beatty, 2001). In this process, DNA is packaged into the capsid until the head is sensed to be full, possibly by the portal, and the DNA is cleaved by the C-terminal endonuclease domain of the large terminase protein, resulting in DNA termini lacking a conserved sequence (Casjens, 2011). After packaging and DNA cleavage, the terminase disassociates from the recently packaged capsid and initiates packaging of a new empty capsid with the remainding DNA terminus.

To prevent leakage of DNA from the recently filled head and to form an interface to bind the tail, head completion proteins bind to and "plug" the portal (Tavares *et al.*, 2012). In lambda, protein gpW, encoded 3' of the large terminase is the plug required for DNA retention.

1.5.2 Tail assembly

The best studied *Siphoviridae* tail (Figure 2A) structure is the tail of phage lambda, which is a 135 nm-long flexible tube-like structure, with a 15 nm-long conical tip at the head-distal end, and which is encoded by 11 contiguous genes (Casjens and Hendrix, 2015, Davidson *et al.*, 2012, Katsura, 1983). The conical tip, which is more generically termed the tail tip complex, contains a central fiber that is the receptor binding protein of lambda and a determinant of host range. Other *Siphovirida,* such as the lactococcal phages TP901-1 and p2, as well as the *Myoviridae* T4, have a different tail tip complex termed a baseplate (Leiman *et al.*, 2010, Spinelli *et al.*, 2014).

The recently revised model for lambda tail assembly proposes two converging pathways for initiation, followed by polymerization of the tail tube protein (major tail protein) (Xu *et al.*, 2014). The central fiber protein gpJ assembles to a trimer, to which several proteins (gpI, gpL,

gpK) are added to form the initiater complex (which later becomes the tail tip complex). In parallel, the tape measure protein (TMP) gpH is coated by a helical arrangement of the chaperone gpG, with an occasional inclusion of the chaperone gpGT, the latter produced by a conserved -1 translational frameshift in gpG. The coated tape measure complex binds to the initiator complex, and the tail tube protein polymerizes around the TMP to form 32 hexameric rings (Xu *et al.*, 2014). The length of the tail is dependent on the TMP, which acts as a molecular ruler (Katsura and Hendrix, 1984). After the tail has polymerized to the length determined by the TMP, the tail terminator protein gpU forms a hexameric ring that caps the tail and prevents further polymerization (Pell *et al.*, 2009).

Some tail gene mutations result in the formation of long, tail like structures (Katsura, 1990, Mount *et al.*, 1968). Depending on the presence of the tail tip complex, these structures are categorized as polytails (Figure 2B) or polytubes (Figure 2C). The lambda tail terminator gpU is required for the formation of regular length tails by preventing polymerization of the tail tube protein past the length of the tail tape protein (Katsura, 1990, Mount *et al.*, 1968). In the absence of gpU, long polytails are produced that contain the conical initiator complex and tail fibers. In contrast, double mutants that lack both gpU and either a member of the initiator complex (gpJ, gpI or gpK), the TMP (gpH) or the tail chaperone (gpH) form long tail-like structures termed polytubes that lack the conical tip and side fibers (Katsura, 1990). Similarly, absence of the tail terminator resulted in polytail formation for the phage TP901-1 (Stockdale *et al.*, 2015). The assembly of the lambda tail requires the chaperones gpG and gpGT, the latter a result of a translational frameshift to fuse the *gpG* and *gpT* orfs. Xu *et al.* (2013; 2014) showed that a correct ratio of gpG and gpGT is required for correct tail assembly, and overexpression of gpGT in the presence of the tail tube protein gpV results in polytube formation. Recently, renatured tail

tube protein of the *Bacillus subtilis* phage SPP1 was reported to polymerize and form polytube structures in the absence of any other phage proteins (Langlois *et al.*, 2015).

1.6 The release of phages and RcGTA from cells

1.6.1 Lytic release of dsDNA tailed phages

Most dsDNA tailed phages utilize an endolysin and holin system (described in Figure 3) as well as a spanin complex for the release from the bacterial host, and their combined actions ensure that the host lyses (bursts) to release the phage particles and cytoplasmic content to the environment (Catalao *et al.*, 2013, Young, 2013, Young, 2014). The endolysin is a muralytic enzyme that cleaves peptidoglycan, and the holin a membrane protein that forms holes in the cytoplasmic membrane to allow for passage of the endolysin from the cytoplasm to the periplasm (to access the peptidoglycan). The recently characterized spanin complex appears to promote fusion of the inner and outer membranes of Gram-negative hosts, and is believed to be required for the release of lambda from *E. coli* under natural conditions (Young, 2013).

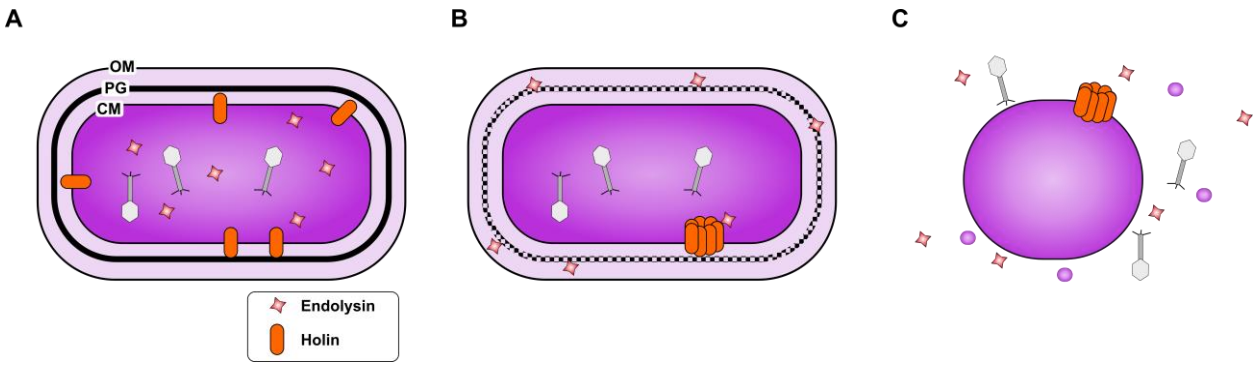

Figure 3 Lysis by canonical endolysin-holin systems

Schematic of the lytic release of phages by a canonical endolysin-holin system. **A,** During late gene expression, catalytically active endolysin and phage particles accumulates in cytoplasm. Holin proteins accumulates in the

cytoplasmic membrane (CM). **B,** Upon triggering of the holins and formation of "holes" in the CM, endolysin proteins are released to the periplasm were they degrade the peptidoglycan (PG) layer. **C,** Loss of the structural support of peptidoglycan results in cell "rounding" and spanin-mediated (not shown) lysis of the cell. The result is release of cytoplasmic material, including phages, to the environment. OM is the outer membrane.

There are currently two separate types of the endolysin/holin system: the initially characterized system of an endolysin and holin (termed canonical), best studied in phage lambda; and the signal anchor release endolysin and pinholin. For lambda, the lysis genes *S*, *R* and *Rz*/*Rz1* encode the holin, endolysin and spanin complex, respectively. These genes are expressed from a late promoter that also initiates transcription of capsid and tail encoding genes (Young, 1992). In addition to encoding the S105 holin the *S* gene also encodes the antiholin S107, which differs from the holin by two amino acids due to the use of an alternative start codon (Bläsi and Young, 1996). S105 and S107 accumulate in the cytoplasmic membrane as dimers. Triggering (activation) of the holin results in the formation of large holes in the cytoplasmic membrane releasing the fully folded endolysin to the periplasm. Holes formed by holins have historically been considered large, and were shown to allow the passage of 480 kDa chimeric endolysin proteins (Wang *et al.*, 2003). Cryo-EM of holin-producing cells recently showed one lesion for most cells, with an average size of 340 nm, however the maximal lesion size exceeded 1 μm (Dewey *et al.*, 2010). The timing of lysis is controlled by the triggering (activation) of the holin, and triggering is dependent on the holin allele. Upon reaching a critical concentration the S105-S107 holin-antiholin forms rafts and subsequent holes in the inner membrane, and this allows the endolysin to access the periplasm. The inhibitory activity of the lambda antiholin S107 is attributed to the N-terminal transmembrane domain of the protein. Prior to triggering, the positive charge resulting from the presence of a lysine and a deformylated methionine prevent

the domain from entering the membrane in the presence of a proton motive force (White *et al.*, 2010). Dissipation of the proton motive leads to insertion of the charged N-terminal domain and formation of active holin (Young, 2013). The timing of lysis is therefore thought to not be regulated in real time but genetically encoded in the holin allele (Wang *et al.*, 2000, Young, 1992). An exception to this occurs for the complex myoviridae T4 and related phages: the release of mature T4 virions from cells is inhibited by secondary infections by T4 phages, a process termed lysis inhibition (Young, 1992). This lysis inhibition was recently found to involve the separately encoded antiholin protein RI. The mechanism of sensing of this superinfection is unknown, but lysis inhibition requires interaction between the soluble domains of phage T4 holin T and antiholin RI, domains which are missing from S-like holins and antiholins from phage lambda and related phages (Moussa *et al.*, 2012, Ramanculov and Young, 2001).

The lambda endolysin R accumulates in a folded and enzymatically activate state in the cytoplasm until released to the periplasm by holin-mediated lesions. The transglycosylase activity of R then cleaves the peptidoglycan that supports the cell shape, resulting in the rounding of cells (Catalao *et al.*, 2013, Young, 2013). The majority of characterized endolysins from phages infecting Gram-negative bacteria consist of a single domain. In contrast, endolysins from phages infecting Gram-positive hosts typically consist of at least two domains: a catalytic and a cell wall binding domain (Loessner, 2005). However, some Gram-negative infecting phages also produce modular endolysins, including the *N*-acetylmuramidase gp61 produced by coliphage N4 (Stojkovic and Rothman-Denes, 2007).

In contrast to the canonical endolysin and holin system, some endolysins are transported across the cytoplasmic membrane independently of the holin by the incorporation of secretion signals (Catalao *et al.*, 2013, Young, 2013). Signal anchor release (SAR) endolysins such as Lyz

from Enterobacteria phage P1 are transported by the *sec* pathway and anchored to inner membrane in an inactive form (Xu *et al.*, 2004). Activation and release of the SAR endolysin from the membrane is mediated by depolarization of the membrane by pinholins. In contrast to the single large membrane lesions formed by canonical holins, the pinholins form multiple small holes of ~ 2 nm diameter (Pang *et al.*, 2009).

The spanin complex appears to be required for fusion of the inner and outer membrane of Gram-negative bacteria, and induction of lambda mutants lacking the spanin complex results in spherical cells lacking the cell wall but supported by the outer membrane (Berry *et al.*, 2012, Young, 2014). However, the requirement of spanins for cell lysis is dependent on the cultivation conditions. In the presence of presence of 10 mM or more divalent cations, cells do not undergo lysis in the absence of spanins Rz or Rz1, whereas lysis occurs in media with lower concentrations of divalent cations. The lambda *Rz1* ORF is completely embedded in the +1 reading frame of *Rz*, and it appears that the majority of the dsDNA phages infecting Gram-negative hosts encode equivalents of the lambda Rz/Rz1 spanins (Summer *et al.*, 2007).

1.6.2 Release of RcGTA

The mechanism and regulation of release of RcGTA from cells had been unclear since the initial report on RcGTA by Marrs (1974). In contrast to phages, RcGTA was found not to produce plaques on a bacterial lawn, and no observable liquid culture lysis was observed for the WT isolates of *R. capsulatus* that produced RcGTA (Marrs, 1974). RcGTA has historically been studied using complex media such as YPS because they yield high transduction frequencies. In contrast, the defined minimal medium RCV was shown to inhibit RcGTA-mediated transduction (Solioz, 1975, Solioz *et al.*, 1975, Yen *et al.*, 1979). Cultivation of the RcGTA overproducer Y262 in the transduction-promoting complex medium PYE, but not the transduction-inhibitory

minimal medium RCV, was reported to result in lysis of 10 – 20% of cells in the culture (Yen *et al.*, 1979), indicating that RcGTA production was accompanied by cell lysis. However, the possibility that lysis could be due to a prophage residing in *R. capsulatus* genome, as opposed to an RcGTA-specific gene, could not be ruled out.

Western blots probed with antibodies raised against the RcGTA capsid protein indicated that strains cultured in RCV medium produced RcGTA, but that the cells did not release RcGTA (Taylor, 2004). Furthermore, preliminary studies indicated that release of RcGTA occurred in RCV medium containing low levels of potassium phosphate, whereas reduced levels of carbon increased intracellular, but not extracellular, levels of RcGTA capsid (Taylor, 2004). In other experiments, it was observed that a mutation in the putative hybrid sensor kinase *cckA* which is required for transduction (see below), resulted in the intracellular accumulation of the RcGTA capsid protein. Furthermore, cells containing this intracellular capsid protein did not release transduction-competent RcGTA upon lysis by exogenous means, indicating that this capsid protein is derived from non-functional RcGTA (Leung, 2010).

1.7 Bacterial regulatory systems controlling RcGTA production

The production of RcGTA has been found to be regulated by several bacterial systems (see below). The primary RcGTA gene cluster is thought to be transcribed from a single promoter, generating a large transcript analogous to the ~26.5 kb late-genes transcript of phage lambda generated from promoter $p_{R'}$ (Friedman and Court, 2005). The promoter of the RcGTA cluster is located ~ 600 bp 5' of the deduced start codon of the first gene, and it is plausible that allows for binding of regulatory elements (Florizone, 2006, Leung, 2010, Westbye *et al.*, 2013). However, no regulator has been demonstrated to interact directly with the promoter or the

untranslated DNA region of the primary RcGTA cluster or any of the accessory gene clusters (lysis and head spike, see Results and Discussion).

1.7.1 Regulation of RcGTA by the GtaI/GtaR quorum-sensing system

RcGTA production is increased upon entry to stationary phase. This is at least partially due to the regulation by the GtaI/GtaR quorum-sensing system that is homologous to the LuxI/LuxR system of *Vibrio fischeri* (Leung et al., 2012, Schaefer et al., 2002). Quorum sensing is a bacterial cell-to-cell communication mechanism, which allows for a uniform response, typically at high cell densities (a quorum). The most well-studied quorum-sensing system is the LuxI/LuxR system, where the *V. fisheri* LuxI acyl homoserine lactone (HSL) synthase produces a diffusible chemical signal, termed an autoinducer (Lazdunski *et al.*, 2004). The autoinducer is sensed by the cognate HSL receptor protein (transcription factor) LuxR. When the concentration of the autoinducer reaches a specific threshold, LuxR is activated and initiates gene expression. In many organisms, the system is autoregulatory, with LuxI expression being activated by LuxR/HSL in a feed-forward loop.

In *R. capsulatus*, the LuxI-homologue GtaI synthesizes a C16 acyl HSL that regulates the activity of the LuxR-homologue GtaR (Leung *et al.*, 2012, Schaefer *et al.*, 2002). GtaR binds DNA and regulates both GtaI and GtaR expression by binding to its own promoter. The transduction levels of a mutant lacking GtaI is reduced to ~20% of WT levels, and this can be restored by addition of exogenous C16 HSL. In contrast, no effect on transduction was observed in the absence of GtaR, and a *ΔgtaIΔgtaR* double mutant showed a WT transduction phenotype. It therefore appears that GtaR is a negative regulator of RcGTA production (Leung *et al.*, 2012). In addition to regulating RcGTA production, GtaI is required for synthesis of the bacterial capsule (see below) (Brimacombe *et al.*, 2013).

1.7.2 The stringent response and general stress response –novel candidates for RcGTA regulation

RcGTA production is stimulated upon entry to stationary phase (Solioz *et al.*, 1975) and appears to be influenced by the carbon level in the growth medium (Florizone, 2006, Leung, 2010). The stringent response is a global stress response activated by many bacteria upon nutrient depletion in stationary phase (Figure 4A). This response is signaled using the alarmones ppGpp and pppGpp (collectively referred to as (p)ppGpp), which result in a drastically altered transcription profile (Hauryliuk *et al.*, 2015). (p)ppGpp production is typically induced by amino acid depletion, however depletion of other nutrients can also stimulate this response. Most studies of (p)ppGpp have focused on *E. coli*, and like most members of the Gammaproteobacteria and the Betaproteobacteria, this bacterium harbours two enzymes involved in (p)ppGpp metabolism: SpoT and RelA. SpoT senses a limitation of several nutrient stresses and is capable of both synthesis and hydrolysis of (p)ppGpp. In contrast, the ribosome-associated RelA enzyme senses amino acid depletion and heat shock and is only capable of (p)ppGpp synthesis. However, most bacteria including *R. capsulatus* harbor a single RelA/SpoT homologue that is capable of both synthesis and hydrolysis of (p)ppGpp (Masuda and Bauer, 2004).

The general stress response system provides cross protection between different stresses. In the Alphaproteobacteria this response is conferred by the sigma factor EcfG (also called SigT), which is itself regulated by the anti-sigma factor NepR and the anti-sigma factor antagonist PhyR, which regulate each other via a partner-switching mechanism (Francez-Charlot *et al.*, 2015a). In *C. crescentus*, the EcfG homologue SigT is involved in a response to carbon depletion and modulates degradation of the response regulator CtrA (Britos *et al.*, 2011). The *R.*

capsulatus genome encodes homologues of these three genes (see section 3.6.4). It therefore appeared plausible that *spoT* or *ecfG* was required for production of RcGTA.

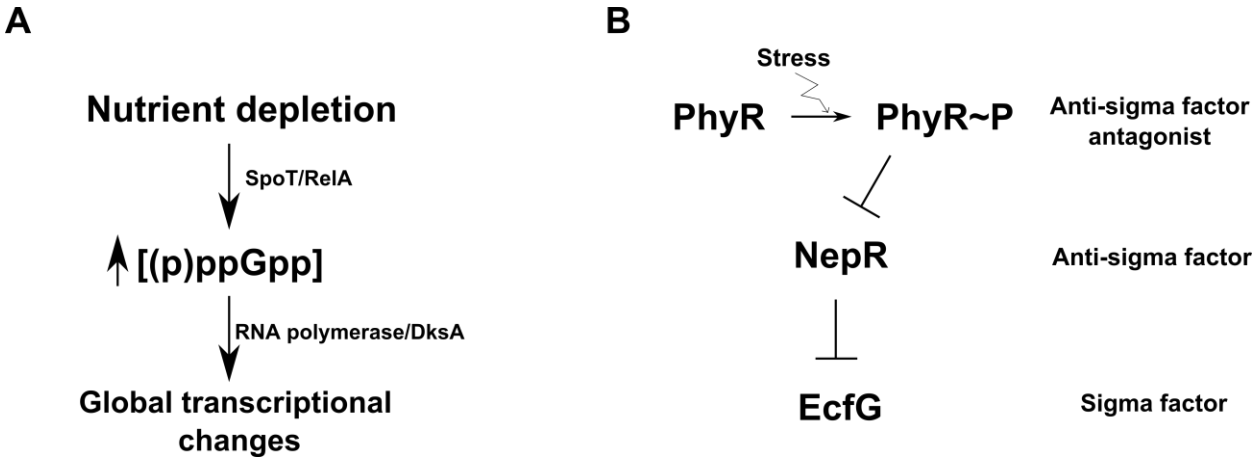

Figure 4 The stringent and general stress responses

A, The stringent response is mediated by ppGpp and pppGpp. Various forms of nutrient depletion induces synthesis of (p)ppGpp. *E. coli* has two enzymes, RelA and SpoT that can synthesize (p)ppGpp, whereas most bacteria have a single enzyme. **B,** The alphaproteobacterial general stress response is mediated by the sigma factor EcfG (SigT). This sigma factor is sequestered by NepR when the response is not activated. Activation of the response results in phosphorylation of PhyR. PhyR~P sequesters NepR by a partner-switch mechanism, freeing EcfG from NepR.

1.7.3 Two component systems and phosphorelays

The first identified regulators of RcGTA production were homologues of the *Caulobacter crescentus* hybrid histidine kinase (HK) CckA and the DNA-binding response regulator (RR) CtrA (Lang and Beatty, 2000), which along with with the histidine phosphotransferase ChpT (Mercer *et al.*, 2012) form a phosphorelay that regulates cell cycling in *C. crescentus* (Curtis and Brun, 2010).

The simplest "phosphorelays" are the two component systems, which are composed of a sensory HK and RR, and considered the major signal transducing system in bacteria, but are also present in eukaryotes (Jung *et al.*, 2012, West and Stock, 2001). Phosphorelays include one or more phosphotransfer proteins between the HK and the RR, and some are branched instead of a single, linear pathway (Jung *et al.*, 2012).

1.7.3.1 Histidine kinases

Most HKs are active as a homodimer and autophosphorylate on a histidine residue in response to a signal. The phosphoryl group is then transferred to an aspartate of the cognate RR, which typically acts as a transcription factor to alter gene expression. For systems where the phosphotransfer involves an intermediate protein termed a phosphotransferase, the term phosphorelay is used.

Two component systems and phosphorelays transfer a phosphoryl from a conserved histidine in the transmitter domain to a conserved aspartate in the receiver (REC) domain for signal transduction (Bhate *et al.*, 2015, Casino *et al.*, 2010, Jung *et al.*, 2012). The prototypical HKs have an extracellular sensor domain that is connected to the transmitter domain by a transmembrane helix. For Class I HKs, the histidine residue is part of a dimerization and histidine phosphotransfer (DHp) domain, that together with a catalytic and ATPase-binding (CA; often referred to as a HK-type ATPase catalytic (HATPase_C) domain), form the transmitter domain. The DHp domain is formed by two antiparallel helices from each peptide in the homodimer to make a four-helical bundle, and the catalytic histidine is part of a conserved sequence of seven amino acids near the membrane-proximal side of the helix: H-D/E-L/I-K/R-T/N-P-L (Figure 5A). For non-hybrid HKs, the membrane-distal part of the DHp domain form

the interface with the RR. The CA domain is situated next to the four-helix bundle and is a highly conserved alpha/beta sandwich (Bhate *et al.*, 2015, Casino *et al.*, 2010).

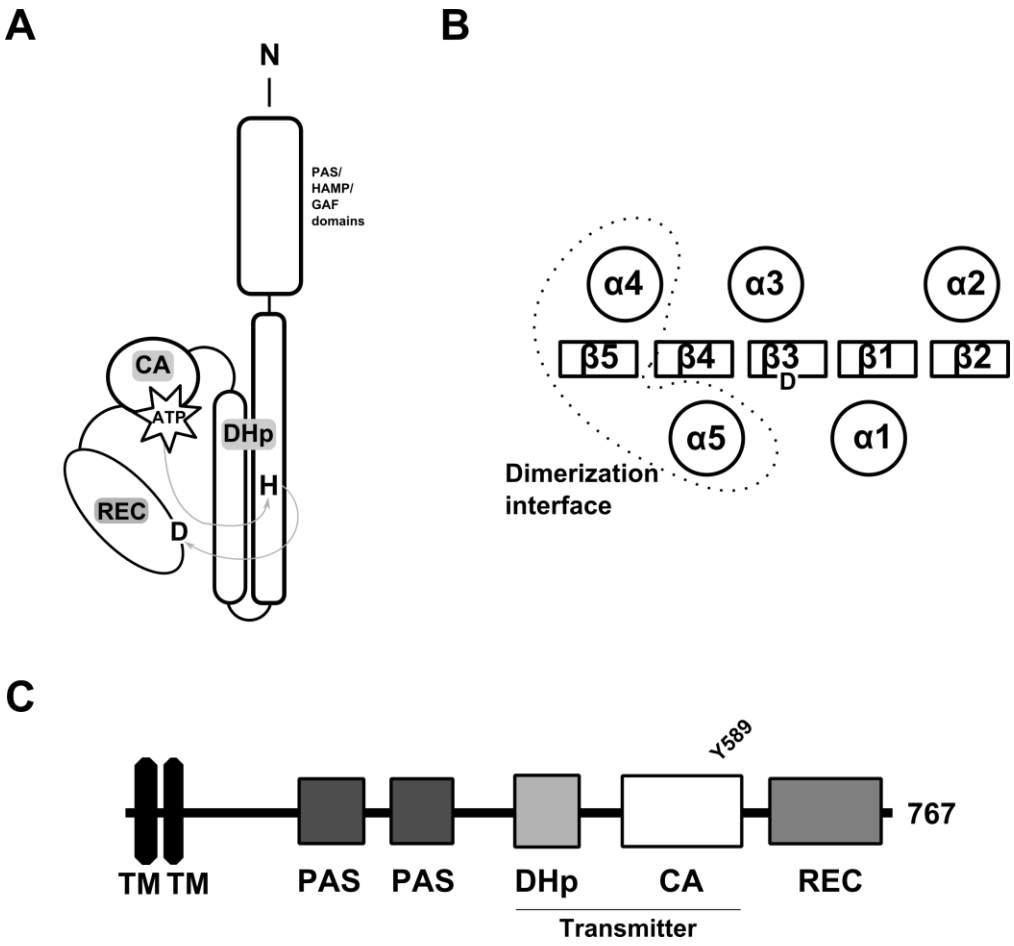

Figure 5 Histidine kinases and response regulators

(**A**) Schematic drawing of the cytosolic part of a hybrid HK; (**B**) the domain organization of a typical response regulator REC domain; (**C**) the predicted domains of *R. capsulatus* CckA, with Tyr 589 indicated. In **A**, grey arrows indicate phosphotransfer from ATP to histidine (H) to aspartate (D). In **B**, α and β indicate alpha-helices and beta-strands, respectively, and D the phosphorylated aspartate residue. See text for details.

A and **B** are based on descriptions in (Casino *et al.*, 2010) and (Bourret, 2010), respectively.

The less common Class II HKs employ a different architecture in which the histidine is part of a histidine phosphotransfer (HPt) domain, which is not located adjacent to the catalytic domain (Jung *et al.*, 2012).

In some phosphorelays, the kinase is a hybrid HK that contains both a transmitter and a receiver domain, and performs an intramolecular phosphotransfer. The phosphoryl signal is then passed on to a histidine in an HPt domain that may be on the same or a separate polypeptide, before the signal is transferred to an aspartate in the receiver domain of the RR.

One ATP molecule binds per CA domain and is held in place by a loop termed the "ATP lid", and binding affinity studies indicate that at least at least one of the CAs contains ATP/ADP at any given time (Bhate *et al.*, 2015). Depending on the HK, during autophosphorylation either the histidine of the DHp domain of the same polypeptide (*cis*-autophosphorylation) or the dimer partner (*trans*-autophosphorylation) attacks the gamma-phosphoryl of the ATP to form His~P and ADP. The aspartate of the receiver domain subsequently attacks His~P resulting in the formation of Asp~P, a reaction that is considerably faster (20-100 min^{-1}) than the autophosphorylation (0.1-5 min^{-1}) (Bhate *et al.*, 2015, Casino *et al.*, 2010).

In addition to phosphorylation of the cognate RR, many HKs can also dephosphorylate an RR, a reaction that is catalyzed by the DHp domain but does not require the histidine residue (Casino *et al.*, 2010). In at least one case, it appears that the primary biological role of a hybrid HK is to act as a phosphatase, with a separate kinase phosphorylating the same RR (Francez-Charlot *et al.*, 2015a).

The sensor domain (also called input domain) of HKs serve as a sensor/interaction module that controls the activity of the transmitter domain by inducing rearrangements of the dimer (Cheung and Hendrickson, 2010, Szurmant *et al.*, 2007). Signal-sensing can affect either

autophosphorylation, phosphatase activity, or both, depending on the HK. The change in activity has been proposed to result from conformational changes in DHp that alters the interaction between the DHp and CA domains, which in turn alters the accessibility of the catalytic histidine (in the DHp domain) to the ATP (bound in the CA domain). Although the conformational change of DHp would also be expected to alter the interaction with the RR, no modulation of the phosphotransfer reaction has been demonstrated (Stewart, 2010).

The most well-studied HKs, such as the *E. coli* NarX and PhoQ, contain extracellular (periplasmic) input domains, and the signal is transmitted to the cytoplasmic transmitter domain by rearrangement of the transmembrane helix (Casino *et al.*, 2010). Other HK proteins have transmembrane or cytoplasmic sensor domains. Several HKs, including CckA (Figure 5), have cytoplasmic sensor domains that adopt a Per/ARNT/Sim (PAS) fold, a five-stranded anti-parallel beta-sheet surrounded by alpha-helices that is found in several modular proteins in addition to HKs involved in signal transduction, such as transcription factors and guanylate cyclases (Moglich *et al.*, 2009). Other common sensor domains are GAF (c-GMP-specific

and c-GMP-stimulated phosphodiesterases, *Anabaena* adenylate cyclases and *Escherichia coli* FhlA) and HAMP (histidine kinases, adenylyl cyclases, methylaccepting proteins, and other prokaryotic signaling proteins) domains (Cheung and Hendrickson, 2010, Szurmant *et al.*, 2007); however such domains are not present in CckA.

The activity of HKs are in several cases regulated by accessory proteins. In enteric bacteria the Rcs phosphorelay controls numerous activities, including motility and biofilm formation, and this phosphorelay is stimulated by the outer membrane protein RcsF (Jung *et al.*, 2012). Response of *Vibrio harveyi* to the "universal" signaling molecule autoinducer-2 (AI-2) requires a phosphorelay composed of the hybrid HK LuxQ, the LuxU phosphotransferase, and

the transcription factor LuxO (Pappas *et al.*, 2004). However, AI-2 is sensed by a periplasmic protein termed LuxP, which is associated with the periplasmic domain of LuxQ. At low concentrations, LuxQ act as a kinase, but binding of AI-2 to LuxP changes the conformation of LuxP, and LuxPQ forms an asymmetric dimer. This in turn is believed to alter the HK to exhibit phosphatase activity (Neiditch *et al.*, 2006).

The two component system PhoR-PhoB regulates the phosphate starvation response in several bacteria, however correct sensing and response to the concentration of phosphate requires the phosphate transporter PstSCAB and the chaperone-like PhoU (Hsieh and Wanner, 2010). Phosphate concentration is sensed by the Pst transporter complex and the signal is conveyed by physical interaction between PstB, PhoU and the PAS domain of PhoR (Gardner *et al.*, 2014). The default expression of the Pho regulon appears to be ON, and is turned OFF at high concentrations of phosphate, because the absence of PhoU results in PhoR having constitutive kinase activity.

1.7.3.2 Response regulators

Phosphorylation of the receiver (REC) domain of a RR by its cognate kinase or phosphotransferase typically changes its activity. Most RRs are modular and contain an output (or effector) domain, although 15% of the RRs in bacterial genomes lack an output domain (Bourret, 2010). The most common output domains are DNA-binding domains of the helix-turn-helix or winged helix families, and the proteins serve as transcriptional regulators. However, RRs with enzymatic, protein-binding or transporter functions have been described (Galperin, 2010).

RRs are typically active as dimers, with dimerization promoted by phosphorylation. REC domains have a conserved topology consisting of a central five-stranded beta-sheet surrounded by a total of five alpha-helices. The highly conserved catalytic aspartate, which becomes

phosphorylated, is found at the C-terminal end of the central beta-sheet (Figure 5B). Phosphorylation rearranges part of the domain to stimulate the formation of a homodimerization interface (Bourret, 2010, Gao and Stock, 2010).

Like many conformational changes in macromolecules, REC domains are believed to exist in an equilibrium between two states, and phosphorylation stabilizes the active, dimer form that in turn changes the activity of the output domain of the RR. This strategy appears essential to the function of many DNA-binding RRs that typically recognize inverted repeats – however dimerization is also common for RRs with other types of output domains such as diguanylate cyclase (GGDEF) domains (Gao and Stock, 2010). It is furthermore recognized that dimerization can also be promoted by the effector domain, such as in DNA binding. In the case of NtrC4 ATPase proteins, phosphorylation causes rearrangements of inactive, preexisting dimers allowing for oligomerization and active ATPase activity (Batchelor *et al.*, 2008).

In addition to being phosphorylated and dephosphorylated by a cognate HK (or histidine phosphotransferase), the REC domain of RRs have inherent autophosphorylation and autodephosphorylation activity *in vitro* (and presumably *in vivo*). In some systems, dephosphorylation is stimulated by auxiliary phosphatases that appear to stimulate the autodephosphorylation activity of the REC domain (Bourret, 2010).

1.7.4 The CckA-ChpT-CtrA phosphorelay

The phosphorelay formed by the hybrid HK CckA, the histidine phosphotransferase ChpT, and the RR CtrA (Figure 6) is widely conserved in the Alphaproteobacteria (Brilli *et al.*, 2010). This phosphorelay has been best characterized in *C. crescentus* where it regulates the cell cycling between sessile stalked cells and motile swarmer cells (Curtis and Brun, 2010, Tsokos and Laub, 2012). The essential RR CtrA is a global regulator that controls over 100 genes

involved in cell division and motility (Laub *et al.*, 2002, Quon *et al.*, 1996). In addition to being a transcription factor, phosphorylated CtrA (CtrA~P) binds to the chromosomal origin of replication and inhibits DNA replication, ensuring that replication only occurs in the sessile stalked cells and not the mobile swarmer cells (Quon *et al.*, 1998). The phosphorylation level of CtrA is controlled by the bifunctional CckA (Figure 6). CckA autophosphorylates on a conserved histidine, and transfers the phosphoryl group to an aspartate in the C-terminal receiver domain of CckA, from where it is transferred to a histidine on ChpT. ChpT then phosphorylates CtrA on a conserved aspartate residue, resulting in dimerization of CtrA~P to form "active CtrA". Additionally, CckA may act as a phosphatase to reverse the phosphoryl transfer pathway, including the dephosphorylation of CtrA~P by ChpT.

In *C. crescentus*, the activity of the CckA membrane protein is controlled by at least two components: 1) The membrane protein DivL stimulates the kinase activity of CckA -- in cells lacking DivL, and overexpressing CckA or expressing a soluble form of CckA, the activity of CckA is primarily as a phosphatase (Chen *et al.*, 2009b, Tsokos *et al.*, 2011); 2) CckA is regulated by levels of the cyclic messenger c-di-GMP, which binds to CckA and inhibits kinase activity while stimulating phosphatase activity, thereby switching the activity of CckA (Lori *et al.*, 2015). In *C. crescentus*, the ability of DivL to stimulate CckA kinase activity is inhibited by phosphorylated DivK, and PleC and DivJ controls the phosphorylation state of DivK (Childers *et al.*, 2014, Tsokos and Laub, 2012). However, homologues of DivK, PleC and DivJ appear to be absent from the Rhodobacterales (Brilli *et al.*, 2010).

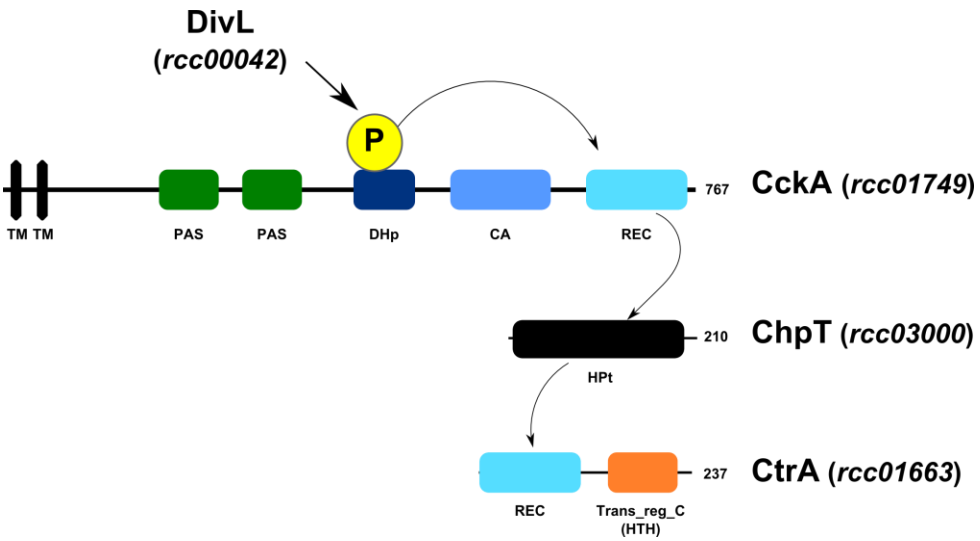

Figure 6 The CckA-ChpT-CtrA phosphorelay

The membrane bound hybrid histidine kinase CckA autophosphorylates, and the phosphoryl group is transferred to the phosphotransferase ChpT, which phosphosphorylates the response regulator CtrA. DivL stimulates the kinase activity of CckA. See text for details.

Recent studies on *Sphingomonas melonis* have revealed an interesting variation on the CckA to ChpT to CtrA theme. In this organism, the proteins CckA and CcsA regulate CtrA phosphorylation levels through ChpT. CckA appears to primarily act as a phosphatase because a loss of CckA results in constitutively active CtrA, and the loss of CckA is offset by a loss of the CcsA (Francez-Charlot *et al.*, 2015b). Despite being a hybrid HK, CcsA differs from CckA by being a soluble protein and having a putative light, oxygen or voltage (LOV) domain.

The requirement of CtrA for viability differs between Alphaproteobacterial lineages. CtrA, as well as DivK, DivL, CckA and ChpT have all been found to be essential for viability of *C. crescentus*. CtrA has also been found to be essential in *Sinorhizobium meliloti*, *Agrobacterium tumefaciens* and *Brucella abortus* (Barnett *et al.*, 2001, Bellefontaine *et al.*, 2002, Curtis and Brun, 2010, Kim *et al.*, 2013). In contrast, CtrA, CckA and ChpT were found to not be essential

in *R. capsulatus* and *R. sphaeroides* (Mercer et al., 2012, Vega-Baray et al., 2015), and CtrA is not essential in *Ruegeria pomeroyi*, *Dinoroseobacter shibae*, *Magnetospirillum magneticum* and *Rhodospirillum centenum* (Bird and MacKrell, 2011, Greene et al., 2012, Wang et al., 2014, Zan et al., 2013). Therfore, the simplest classification of CtrA-containing Alphaproteobacteria is the division into two groups; the CtrA-essential and the CtrA-non-essential group. A more complex classification into four clusters has been proposed by Brilli *et al.* (2010).

Several mutations in CckA have been identified that affect the kinase or phosphatase activity (Chen *et al.*, 2009b, Kim *et al.*, 2013). The CckA(Y674D) gain-of-function mutation reported for *Agrobacterium tumefaciens* appears to make the CckA kinase activity independent of upstream regulators (Kim *et al.*, 2013), and the analogous CckA(Y514D) in *C. crescentus* was recently reported to make CckA non-responsive to c-di-GMP, and thereby unable to act as a phosphatase, resulting in constitutive kinase ON activity (Lori *et al.*, 2015). In contrast, mutation of the autophosphorylated histidine residue in *C. crescentus* CckA to alanine (H322A) abolished kinase activity, but the protein retained phosphatase activity (Chen *et al.*, 2009b).

1.7.5 Proteolytic degradation of *C. crescentus* CtrA by ClpXP

The regulation of the *C. crescentus* CtrA is in part accomplished by the essential protease ClpXP (Figure 7A), which targets CtrA, and mutants lacking ClpXP have defects in chromosome replication and cell division (Domian *et al.*, 1997, Jenal and Fuchs, 1998). The ClpXP protease is composed of a hexamer of the AAA+ATPase ClpX that recognizes and unfolds the substrate, and a 14-mer of the ClpP peptidase, arranged as two stacks of heptamers. Proteins are recognized for degradation by the presence of short unstructured degradation tags, typically at the C-terminus (Baker and Sauer, 2012). However, for some proteins such as the

lambda replication protein O, the degradation tag is present in the N-terminus (Gonciarz-Swiatek *et al.*, 1999).

The best characterized ClpXP degradation tag is the ssrA tag YALAA, which is added to the C-terminus by the transfer-messenger RNA (tmRNA) system (Moore and Sauer, 2007). During ribosome pausing or stalling, a tmRNA charged with alanine can enter an unoccupied A site in the ribosome (where the aminoacyl tRNA would typically enter), and the ribosome may continue translation using the short ORF encoded by the tmRNA, resulting in the release of the incomplete protein containing the ssrA tag. Degradation of these tagged proteins is aided by the adaptor protein SspB (Moore and Sauer, 2007). In *E. coli*, ClpXP is involved in degradation of several stress proteins, including the SOS response repressor LexA and the stationary phase sigma factor RpoS (Neher *et al.*, 2006).

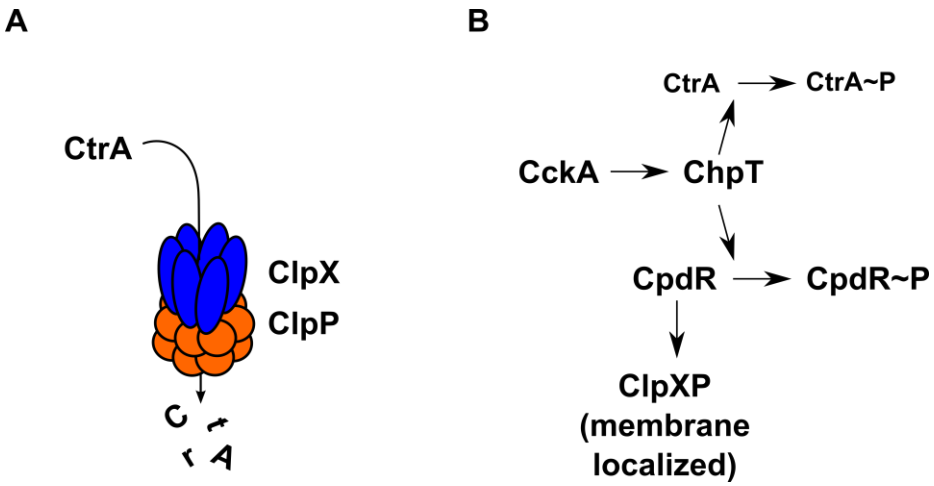

Figure 7 The ClpXP protease

The proteolytic regulation of CtrA by ClpXP (**A**) and regulation of membrane localization of ClpXP (active for CtrA-degradation) by CpdR (**B**) in *C. crescentus*. See text for details.

ClpXP-mediated degradation of CtrA is controlled by the phosphorylation state of CpdR (Figure 7B)(Iniesta *et al.*, 2006). The phosphorylation state of CpdR is controlled by CckA and ChpT, which also control CtrA phosphorylation (see above). In *C. crescentus*, ClpXP and CpdR are essential proteins for laboratory growth. Similarly, in *S. meliloti*, where CtrA is also essential for laboratory growth (see above), the CpdR homologues CpdR1 and CpdR2 are required for localization of the ClpX as well as proper cell differentiation (Barnett *et al.*, 2001, Kobayashi *et al.*, 2009).

A role for ClpXP in regulating *R. capsulatus* CtrA has not been described, but appeared possible based on the conserved nature of the CckA-ChpT-CtrA system in the Alphaproteobacteria (Brilli *et al.*, 2010). Because members of the *Rhodobacter* genus were reported to lack homologues of CpdR (Brilli *et al.*, 2010), it appeared unlikely that CckA (through CpdR-mediated regulation of ClpXP activity) would control proteolysis of CtrA in *R. capsulatus*.

1.8 RcGTA recipient capability

Most studies of RcGTA have focused on the production of RcGTA; however, for transduction to occur, the DNA packaged into RcGTA needs to recombine into a recipient cell's genome. Early studies indicated that RcGTA-borne DNA is integrated by RecA-mediated homologous recombination, and the requirement for RecA was later confirmed (Brimacombe *et al.*, 2014, Genthner and Wall, 1984). More surprising, it was recently discovered that the ability to receive RcGTA, termed recipient capability, is regulated by the same bacterial systems that regulate RcGTA production, and requires natural transformation-like proteins (Brimacombe *et al.*, 2014, Brimacombe *et al.*, 2015).

1.8.1 The capsular accessory receptor

R. capsulatus cells are covered by a polysaccharide capsule, and this capsular polysaccharide (CPS) appears to function as an initial binding receptor for RcGTA, but is not essential for the transduction process (Brimacombe *et al.*, 2013, Omar *et al.*, 1983). Production of CPS requires the putative polysaccharide biosynthesis cluster *rcc01081-rcc01086* as well as the putative glycosyl transferase *rcc01932,* and is regulated by the quorum sensing system GtaI-GtaR, that also regulates RcGTA production (Leung *et al.*, 2012, Schaefer *et al.*, 2002).

1.8.2 A natural transformation-like system is required for recipient capability

The CckA-ChpT-CtrA phosphorelay is involved in regulating the ability of cells to receive RcGTA, although the details have not been fully established. Cells lacking the RR CtrA show no detectable levels of recipient capability, whereas mutations of *cckA* and *chpT* have less dramatic effects. CtrA was found to regulate several homologues of natural transformation genes, including DprA and Com genes, which were found to be essential for recipient capability (Brimacombe *et al.*, 2014).

By comparison to natural transformation systems, it was proposed that RcGTA injects the DNA into the periplasmic space of *R. capsulatus,* from where the DNA is transported into the cytoplasm by a Com system, and recombined into the genome with the aid of DprA and RecA (Brimacombe *et al.*, 2014, Brimacombe *et al.*, 2015).

1.9 The importance of research into RcGTA and knowledge gaps addressed

The conservation of functional RcGTA-like genes and particles in many alphaproteobacteria indicates that GTAs provide an evolutionary benefit to the bacteria. Little is known about the biology of GTAs compared to genuine phages, and to HGT by transformation or phage-mediated generalized transduction. Knowledge gained from experiments on the model

RcGTA of *R. capsulatus* are likely to be applicable to other RcGTA-like particles, and possibly to the unrelated GTAs of other species. Additionally, because the RcGTA morphology and the encoding genes are similar to genuine bacteriophages, studies of RcGTA will provide novel knowledge about regulatory systems in the Alphaproteobacteria and the protein structures of tailed bacteriophages.

This thesis research was performed to address the following knowledge gaps about RcGTA: How is RcGTA released from cells, and is the absence of RcGTA release from cells cultured in high phosphate and the absence of release from a *ΔcckA* mutant related? Does the CckA-ChpT-CtrA putative phosphorelay control release and assembly of RcGTA? Do proteins that in *C. crescentus* are connected to CckA-ChpT-CtrA-pathway regulate RcGTA? How does RcGTA recognize the bacterial cell? How do media containing reduced concentrations of carbon stimulate capsid production?

Chapter 2: Materials and Methods

2.1 Bacterial strains and growth conditions

The rifampin resistant RcGTA WT strain SB1003 and the RcGTA-overproducer strain DE442 were used to study RcGTA production. Strain SB1003 (Solioz and Marrs, 1977) is a rifampin-resistant derivative of strain B100 (Hillmer and Gest, 1977, Rapp *et al.*, 1986, Solioz *et al.*, 1975), a spontaneous phage-free mutant of the environmental isolate B10 (Marrs, 1974, Weaver *et al.*, 1975). DE442 is of uncertain providence, but likely a rifampin-resistant *crtG* mutant derived from the RcGTA overproducer strain Y262 (Yen *et al.*, 1979), which was derived from strain BB103 [BB103 is reported to be a spontaneous streptomycin-resistant derivative of strain B10 (Lang and Beatty, 2000)]. The genome of strains DE442 and SB1003 have been sequenced (Ding *et al.*, 2014, Strnad *et al.*, 2010). Promoter activity of mutants was carried out in either DE442 or the WT B10 background, as described. For RcGTA transduction assays, rifampin sensitive B10 was used as the recipient. In binding assays, B10 or the B10-derived CPS mutants *Δ1081* or *Δ1932* (Brimacombe et al., 2013) were used. For transduction using B10 and derivatives as donors, spontaneous rifampin resistant strains were used. Cells were cultured in the minimal medium RCV (Beatty and Gest, 1981) for general growth or promoter activity studies, unless otherwise mentioned.

R. capsulatus were cultured in YPS or RCV (Wall *et al.*, 1975) media. The composition of YPS is 0.3% (wt/vol) yeast extract, 0.3% (wt/vol) Bacto peptone, 2 mM $MgSO_4$ and 2 mM $CaCl_2$. The composition of RCV is 0.1% (wt/vol) $(NH_4)_2SO_4$, 0.4% (wt/vol) DL-malic acid, 9.6 mM KPO_4, 15 ng/mL biotin, 1 μg/mL niacin and 5% (vol/vol) “Super salts”. Super salts contains 0.04% (wt/vol) EDTA, 0.4% (wt/vol) $MgSO_4 \cdot 7H_2O$, 0.15% (wt/vol) $CaCl_2 \cdot 2H_2O$, 0.024% (wt/vol) $FeSO_4 \cdot 7H_2O$, 0.002% (wt/vol) Thiamine-HCl and 2% (vol/vol) “Trace elements”. Trace

elements contains 1.59 mg/mL $MnSO_4 \cdot H_2O$, 2.8 mg/mL H_3BO_3, 0.04 mg/mL $(CuNO_3)_2 \cdot 3H_2O$, 0.24 mg/mL $ZnSO_4 \cdot 7H_2O$ and 0.75 mg/mL $Na_2MoO_4 \cdot 2H_2O$.

For studies of the effect of phosphate on RcGTA production, cells were cultured in the modified YPSm medium contained a reduced concentration of $MgSO_4$ and $CaCl_2$ (0.5 mM each), pH 6.8; the RCVm medium lacked KPO_4 (the only phosphate source in RCV), contained 14.7 mM K^+ (by neutralizing the malic acid carbon source with KOH), and was buffered with 20 mM 3-morpholinopropane-1-sulfonic acid (MOPS), adjusted to pH 6.8 with HCl. Cultures were supplemented with salts adjusted to pH 6.8 with HCl or NaOH to an initial concentration, as described below. For resuspension experiments measuring lysis, strains were cultured in RCVm containing 10 mM KPO_4, and cells were harvested by centrifugation and resuspended in RCVm defined medium or 20 mM Tris-HCl buffer (pH 6.8) to an OD_{660} of 5.0 or 0.5.

For RcGTA-binding experiment involving the *ΔghsB* head spike mutant, recipient cells were cultured in YPS.

Cultures were generally inoculated to an optical density at 660 nm of 0.15 (approximately 7.2 * 107 CFU/ml) and incubated photoheterotrophically for 24 h (promoter activity experiments) or 40 h (transduction, binding, lysis or gel migration experiments) at 30 °C in 16.5 mL capped glass tubes and RcGTA recipient cells which were cultured chemoheterotropically in the dark at 30 °C, unless otherwise noted. For RcGTA affinity purification, cells were cultured photoheterotrophically in 200 mL capped glass bottles with YPS medium (Wall *et al.*, 1975). Cultures were supplemented with tetracycline HCl (0.5 ug/ml), kanamycin sulfate (10 ug/ml), or gentamicin sulfate (3 ug/ml) or spectinomycin (10 ug/ml), as appropriate.

Escherichia coli strain DH5α (Sambrook *et al.*, 1989) lambda pir was used for general cloning work. For conjugation of plasmids to *R. capsulatus*, *E. coli* S17-1 (Simon *et al.*, 1983)

lambda pir or TEC5 (Taylor *et al.*, 1983) were used. For overexpression of *rcc00555*, *E. coli* BL21(DE3) was used, and cells were induced at an OD600 of 0.5 by addition of 1 mM isopropyl-D-1-thiogalactopyranoside (IPTG). *E. coli* were cultured in LB medium (Sambrook *et al.*, 1989) supplemented with either ampicillin (100 ug/ml), tetracycline HCl (10 ug/ml), kanamycin sulfate (50 ug/ml), gentamicin sulfate (10 ug/ml) or spectinomycin (50 ug/mL), as appropriate.

2.2 Construction of targeted mutants and complementation plasmids

Genetic constructs are listed in Table S1. For the construction of the translationally in-frame *ΔphoB* strain mutant, the N-terminal and C-terminal regions of *phoB* (*rcc03498*) and flanking regions were amplified using the primer pairs `accctgttcg`**`gagctc`**`gacccgatcg` and `tgttgcgcaggatcc`atcgatcagct, and `aatggcggcgcggatcc`cgtg and `atctaga`tgcaggaaatggcgggggcg. The amplicons were cloned into the suicide plasmid pZJD29A that encodes gentamicin resistance and the *sacB* counter-selection marker (Z. Jiang and C. E. Bauer, personal communication) by digestion and ligation of the SacI (**bold**), BamHI (underlined) and XbaI (*italic*) sites. To conjugate the plasmid into *R. capsulatus*, 100 uL culture of *E. coli* S17-1 lambda pir containing plasmid was pelleted (3,500 rcf, 2 min), the pellet washed in RCV and mixing with the cell pellet of 400 uL of *R. capsulatus* cells and spotted onto RCV. After 16h incubation, mating spots were spread on RCV media containing gentamicin for selection for single-crossover recombinants. After growth in RCV broth for ~20 generations, second-crossover recombinants containing the desired mutation were obtained by plating on RCV agar medium containing 5% (wt/v) sucrose. The correct mutation was confirmed by the absence of the WT PCR-band and by DNA sequencing.

The *R. capsulatus* strain DE442-derived *ΔcckA* mutant was created by amplifying the genomic segment of SB1003 *ΔcckA* (Mercer *et al.*, 2012) containing the truncated *cckA* (interrupted by a kanamycin resistance cassette), using primers `taagtagtcgacgatctggtgctggt` and acaatggtcgacacgctttcgcacag. The resultant 1.8-kb amplicon was cloned into the plasmid pUC19 (Sambrook *et al.*, 1989) SmaI site. Replacement of the native DE442 *cckA* gene was performed by transduction, as described by Aklujkar et al. (Aklujkar *et al.*, 2000). The *trans*-complementing *cckA*-containing plasmid was constructed by amplifying DE442 genomic DNA with primers `atattctagaggtgctggtcgatgcgccct` and `atataagcttctgcagcccgagaccgaggc`. The resultant 2.8-kb fragment was cloned into the lowcopy-number, broad-host-range plasmid pRK415 (Keen *et al.*, 1988) by ligation to the introduced XbaI and HindIII sites to create pRCckA.

The strains DE442 *ΔchpT* and DE442 *ΔctrA* were created by transduction of the kanamycin resistance interrupted alleles from SB1003 *ΔchpT* (pD51E) and SB1003 *ΔctrA* (pD51E).

Strain DE555 (DE442 *Δrcc00555*) was created by RcGTA-mediated transduction of a KIXX-disrupted (kanamycin resistance) knockout fragment as described by Hynes *et al.* (2012). The *rcc00556* complementation/expression plasmids were constructed by amplifying DE442 genomic DNA with primers `atatccatggggctgatcgggacgat` and `atatggatcctgcctttgcggtgcccgaaaa`. The resultant 0.67-kb fragment was cloned into pIND4 (Ind *et al.*, 2009) or pIND4Gm (see below) to create pI556 or pI556Gm, respectively, using the introduced NcoI and BamHI sites. Plasmid pIND4Gm was created by amplifying the *aacC1* gene from plasmid pZJD29A using primers `atatcccgggttgacataagcctgttcggt`

and atatcccgggcttgaacgaattgttaggtg. The resultant 0.78-kb fragment was ligated into the XmaI site of plasmid pIND4 to create plasmid pIND4Gm.

To construct *ΔghsB* mutants, a *ghsB* (*rcc01080*) containing fragment was amplified using primers atatgaattcaatcggcaaactcgaaggagagac and atatagcgctccggcaaaacaaggcagcat and cloned into pUC19 using EcoRI and and BamHI. An *aacC1* cassette (conferring gentamycin resistance) (see above) was ligated into the resultant plasmid cut with AgeI and NgoMIV, deleting 54% of the *ghsB* orf, to create pU1080Gm. For the mutation of *rcc01691* (tail tube protein), the amplicon obtained using primers atattctagaggatttgccacggcgaagg and atatgagctcatctcgaccgtgcgcagatc was cloned into pCM62 (Marx and Lidstrom, 2001) using XbaI and SacI, a fragment deleted and replaced by KIXX from pUC4KIXX (Barany, 1985) (conferring kanamycin resistance) by FastCloning (Li *et al.*, 2011) using primer pairs ggagttcttcgcccaccccaggtgcccgagtttcaggtc and cggcagcgtgaagcttcccttccagcgaggtcacatcga, and tcgatgtgacctcgctggaagggaagcttcacgctgccg and gacctgaaactcgggcacctggggtgggcgaagaactcc to create pC1691KIXX. The mutations were transduced into DE442 or SB1003 and derived strains using DE442 to create the *ΔghsB* and *Δ1691* mutations. To construct the markerless, translationally in-frame *ΔghsA* mutant, a *ghsA* (*rcc01079*)-containing fragment was amplified using primers atatgagctcacgcggggtgcctgtgtgac and atattctagatggcccgggttttgccccag and cloned into pUC19 using SacI and XbaI. FastCloning was used to delete 59% of the *ghsA* ORF using primers gacatatggacgtcgtgacctataccg and

cggtataggtcacgacgtccatatgtc. The fragment was transferred to pZJD29A using SacI and XbaI. First and secondary crossovers were obtained as described above.

The GhsA complementation plasmid pCghsA, containing containing *rcc01079* and the promoter region, was constructed by amplifying the region using atattctagaagatcatcctgggcctgcc (forward) and atatgagctcgcgacaccattcacggcata (GhsA-reverse) The amplicon was cloned into pCM62 using the SacI and XbaI sites to create pCghsA. The GhsB complementation plasmid pCghsA-ghsB, containing *rcc01079-rcc01080* and the upstream native promoter, was constructed by amplifying the region using the above forward primer and atatgagctctcgctctgccagaaccgcaa (GhsB-reverse). The amplicon was cloned into pCM62 using the SacI and XbaI sites to create pCghsA-ghsB. A C-terminal 6 His tag (underlined) was introduced to GhsB by using the above forward primer and atatgagctcaatgatgatgatgatggagcgccccggccgg to create pCghsA-ghsB_His.

The *ΔclpX* mutants were constructed by amplifying the entire *clpX* (*rcc02608*) orf including ~500 bp upstream cctcgcgatctagaacaccatgc and ccaccgagctccagtgttttgc. The 1.8 kb amplicon was cloned into pCM62 using XbaI and SacI to create pCclpX. The *aacC1* cassette was amplified from pZJD29A using taagcaaccggtttgacataagcctgttcggt and tgcttaccatggcttgaacgaattgttaggtg and cloned into the AgeI and NcoI site pCclpX deleting 20% of *clpX*. The *ΔclpX* mutants were created by transduction from DE442. To create plasmid pCclpXP, containing ~500 bp upstream of *clpP* and the *clpP-clpX* orfs, the 2.7 kb

amplicon obtained using atattctagacggtgacgaaagcctcggtg and atatgagctccacctccgcatctttggccc was cloned into the SacI and XbaI site of pCM62.

The *ΔdivL* mutant was constructed by amplifying *divL* (*rcc00042*) using atatgagctcctggcgcgaggacgagaccg and atattctagagcactctagcggccctgccc and cloned into pUC19 using SacI and XbaI. SmaI-cut *aacC1* amplicon was ligated into the NaeI-cut vector in reverse orientation. The construct was conjugated into DE442 using TEC5 and mutants created by transduction. The complementation plasmid pCdivL was constructed by amplifying ~500 bbp upstream of divL using atatgagctcctatcgctaccccgagctgg and atattctagatcttgcatggccgcactcta. The 2.2 kb amplicon was ligated into pRK415 using XbaI and SacI

The histidine auxotrophic strain *ΔhisB* was created by amplifying *hisB* (*rcc01183*) using atatctgcagcacctcaggccgcaaggcca and atatgagctcgaaggcggcctcggcgatgt and cloned into pUC19 using PstI and SacI. A SmaI excised KIXX fragment was introduced into the XhoI site in forward orientation, disrupting the 5' half of *hisB*. The *ΔhisB* mutant was created by transduction to SB1003 using TEC5 and DE442. The markerless serine auxotrophic strain *ΔserB* was created by amplifying *serB* (*rcc03445*) upstream and downstream fragments using primer pairs atat**gagctc**cgctcggaacccgcacacca and atattctagaggtgaccgtgaccgcctcca, and atattctagagcggcgcaatgcgagatcc and atat*gtcgac*gcttcggtgacgcccgagca. The amplicons were joined using XbaI (underlined) and cloned into the SacI (**bold**) and SalI (*italized*) sites of pZJD29A. The *ΔserB* mutant was created by conjugating the suicide plasmid to SB1003 and selecting for primary and secondary crossovers as described above.

The *ΔspoT* single mutant was created by transduction to SB1003 of the tetracycline marked *spoT* mutation from the *hvrA spoT* double mutant strain SM05 (Masuda and Bauer, 2004). A *ΔhvrA* single mutant was similarly produced using transduction, selecting for kanamycin resistance. The *spoT* complementation plasmid pIspoT was created by amplifying the coding region of *spoT* (*rcc03317*) using primers `atatccatggtcgatgtcgaagacct` and `atatggatcctcagggtttgcgcgacaggt`. The amplicon was cloned into pIND4 using NcoI and BamHI to create pIspoT.

The *ΔecfG* mutant, lacking a putative general stress sigma factor, was constructed by amplifying ecfG (*rcc02291*) using `atattctagagcaagcccctcctccggcac` and `atatgagctccccgttcgtcgccgtcagca`, and the resultant amplicon ligated into pUC19 using XbaI and SacI. Inverse PCR using `ccggggatggggccgcag` and `ggtgacattgcgggtcagcgaa` was used to delete 78% of the coding region of *ecfG*. The fragment was moved to the suicide plasmid pZJD29A using XbaI and SacI, and this plasmid was conjugated into SB1003 to create the *ΔecfG* mutant using primary and secondary crossover as described above.

2.3 Construction of promoter reporter plasmids

The translationally fused promoter-*lacZ* reporter plasmid pXCA-555, used to measure *rcc00555* expression was constructed using primers `atatctgcaggcgtgctgcccgacctcttt` and `atatggatccatccgatccccttggctgag` to amplify strain SB1003 DNA and incorporate the PstI and BamHI sites. The resultant PCR fragments were digested and ligated into plasmid pXCA601 (Adams *et al.*, 1989) to create an in-frame fusion to *lacZ* (the **G** of the *rcc00555* AT**G** start codon becomes the first G of the GGATCC BamHI cut site).

Plasmid pXCA-ghsA was constructed by amplifying a fragment containing the *ghsA* (*rcc01079*) annotated start codon and 354 bp 5' using `atatctgcagacgcggggtgcctgtgtgac` and `atatggatccatatgtctctccttcgagtttgcc`. The resultant amplicon was cloned into plasmid pXCA601 using the PstI and BamHI sites to create a fusion of the start codon to *lacZ*.

2.4 Construction of pET28a(+)-derived plasmids and recombinant protein production

The *rcc00555* overexpression plasmid pET-555C was created by amplifying SB1003 genomic DNA using primers `atatccatgggatctgtctacgagattgc` and `atatctcgaggccccatgccgccacccg`. The 0.63-kb amplicon was ligated between into the pET28a(+) NcoI/XhoI sites to create plasmid pET-555C. Plasmid pET-555C contained a mutation resulting in an amino acid substitution from phenylalanine to leucine at the C-terminal end (the catalytic site is predicted to be in the N terminus).

To create the *ghsB* (*rcc01080*) overexpression plasmid pETghsB_C, SB1003 genomic DNA was amplified using primers `atat`**`gagctc`***`CCATGG`*`tcgcgcttggtcttggcc` and `atat`*`tctaga`*`CTCGAGgagcgccccggccgg` and the amplicon cloned into pUC19 using introduced SacI (**bold**) and XbaI (*italized*) sites. A sequence verified fragment was excised and cloned into pET28a(+) using the NcoI (*ITALIZED*) and XhoI (UNDERLINED) sites to create pETghsB_C.

Cells were cultured to OD_{600} of 0.6 and protein production induced by addition of IPTG (1 mM) and cells incubated at 30°C for 4h. For Rcc00555 protein, (555C), cells were resuspended in 20 mM NaCl, 20 mM Tris, pH 8.0, 20 mM imidazole lysis buffer. For GhsB protein, cells were resuspended in 50 mM $NaPO_4$, pH 8.0, 300 mM NaCl, 10 mM imidazole lysis buffer. Cells were passed through a French press, and lysate was cleared (16,000 rcf, 30 min).

Protein was purified using a nickel-nitrilotriacetic acid (Ni-NTA) gravity column. Fractions were eluted by increasing imidazole concentrations were collected. Rcc00555 was eluted using 450 mM imidazole and GhsB eluted starting at 150 mM imidazole. GhsB protein-containing fractions were pooled and twice dialysed against 100 volumes of 50 mM $NaPO_4$ (pH 8.0), 10 mM NaCl, then passed through a 0.2 µm pore size filter. Final protein concentration was ~0.7 mg/mL.

2.5 Construction of the new RcGTA 6 His tagged capsid plasmid pRhoG5CTH

pRhoG5CTH was created by excising the 6 His-tagged RcGTA major capsid orf from pOrf5CTH (Chen *et al.*, 2009b) and cloned into pRhokHi-6 (Katzke *et al.*, 2010) using NdeI and HindIII.

2.6 Affinity purification of RcGTA

R. capsulatus cells expressing 6 His-tagged capsid protein (pRhoG5CTH) or 6 His-tagged GhsB protein (pCghsA-ghsB_His) were pelleted at 6800 rcf for 10 min. Culture supernatant was collected and Tris-HCl pH 7.8 was added to 10 mM. Supernatant was further cleared by centrifugation at 17,000 rcf for 15 min, and passed through a glass microfiber filter (Whatman EPM2000) followed by a 0.2 um sterile filter. The filtrate was loaded on a gravity column containing ~ 3 mL Ni-NTA beads (Qiagen) equilibrated with BSA-free G-buffer (G*-buffer; 10 mM Tris-HCl pH 7.8, 1 mM $MgCl_2$, 1 mM $CaCl_2$, 1 mM NaCl). Beads were washed with ~ 200 mL G*-buffer containing 40 mM imidazole, and chimeric RcGTA eluted using 400 mM (pRhoG5CTH containing cells) or 150 mM (pCghsA-ghsB_His) imidazole in G*-buffer. Eluate was dialysed using G*-buffer and concentrated using a 100 kDa cutoff-ultrafiltration device (Amicon Ultra-0.5).

2.7 Transposon mutagenesis and screening

Transposon mutagenesis was performed using plasmid pRL27, which contains a Tn5 encoding a hyperactive transposase, an R6K origin of replication and kanamycin resistance (Larsen et al 2002 Arch Microbiol). After conjugation, Tn5-mutants were selected on RCV agar medium containing kanamycin. For *rcc01079* promoter activity screen, pRL27 was conjugated into DE442(pXCA-1079) and mutants were plated on RCV agar containing kanamycin, tetracycline and X-gal.

2.8 RcGTA transduction assay

RcGTA activity was determined as previously described (Westbye et al 2013). 100 µL of 0.2 µm pore-size filtered culture supernatant, or supernatant diluted in G-buffer (10 mM Tris-HCl pH 7.8, 1 mM $MgCl_2$, 1 mM $CaCl_2$, 1 mM NaCl, 500 µg/mL BSA Fraction V) was mixed with 400 µL G-buffer and 100 µL rifampin-sensitive B10 cells cultured to stationary phase in RCV medium, pelleted at 3500 rcf for 10 min, and resuspended in 0.4 volumes G-buffer in 5 mL polystyrene tubes. The mixture was incubated for 1 h at 30 ºC with agitation, then 900 uL of RCV were added and tubes reincubated for 3 h. The mixture was transferred to 1.7 mL microfuge tubes, centrifuged 5 min at 3,500 rcf and the resultant pellet suspended in a small volume and spread on RCV or YPS agar plates containing 80 ug/mL rifampin. Rifampin-resistant colonies were enumerated after 2 (YPS) or 3 (RCV) days.

2.9 RcGTA binding assay

RcGTA binding was determined using an adsorption assay (Brimacombe *et al.*, 2013). In short, recipient cells were cultured to the stationary phase, mixed with filtered culture supernatant

for 1 h, and the mixture was centrifuged to pellet the cells. After filtration, this supernatant was used in a transduction assay to determine the residual transduction frequency after cell adsorption. This ratio was calculated by dividing the transduction frequency of adsorbed supernatant to a no-cell adsorption control.

2.9.1 Enzymatic lysis for RcGTA transduction

A 10 mL culture was centrifuged at 3,500 rcf for 10 min and the resultant pellet was suspended in 1 ml of 20 mM Tris-HCl pH 7.8, 50 mM EDTA, 250 mM sucrose and 0.5 mg/ml lysozyme. Samples were subjected to four freeze-thaw cycles between dry-ice and ~40 °C temperatures, then 9 ml of 20 mM Tris-HCl pH 7.8, 0.5 mM $MgCl_2$ and 0.1 mg/ml DNase I were added, and samples incubated at room temperature for 10 min to reduce viscosity. Samples were centrifuged and the supernatant was filtered through a 0.2 µm pore diameter filter before being used in RcGTA transduction assays. The concentration of protein (lysozyme and DNase I) in the lysis buffer was subtracted from sample values before normalization to total protein.

2.9.2 Mechanical lysis by French press

Cultures or suspended cell pellets were lysed by passage through a French press mini pressure cell (Aminco) at 900 psi. The resultant lysate was centrifuged at 16,000 rcf for 5 min to produce a cleared lysate unless otherwise stated.

2.9.3 Lysis for native agarose gel electrophoresis

Culture was lysed by the addition of 0.2% Triton X-100, 10 mM Tris pH 8.0 and 50 µg/mL lysozyme (Sigma), followed by incubation at 30 ºC for 1 h. Samples were centrifuged at 16,000 rcf for 5 min to produce a cleared lysate.

2.10 Western blot

Liquid culture samples of ~1.5 mL (normalized to OD at 660 nm) were pelleted at 16,000 rcf for 5 min. For SB1003-derived samples, the culture supernatant was concentrated ~10-fold using a vacuum centrifuge concentrator. SDS-PAGE separation was performed using a 10% separation and 4% stacking gel, and proteins were transferred to a BioTrace NT nitrocellulose blotting membrane (Pall Life Sciences) using a Mini Trans-Blot apparatus (Bio-Rad) in electroblot buffer (27.5 mM Tris-base,192 mM glycine and 20% methanol) at 30 V overnight. Membranes were initially blocked with 5% milk in TBS-T (1.2% w/vol Tris-base, 1% NaCl, 0.1% Tween-20, adjusted to pH 7.5 with HCl), then probed with rabbit anti-capsid serum, washed 3 times with TBS-T, then probed with horse radish peroxidase-conjugated donkey anti-rabbit antibody. Membranes were developed using using luminol and *p*-coumaric acid (Haan and Behrmann, 2007).

2.11 Agarose gel electrophoresis

DNA fragments were analysed using agarose gel electrophoresis, typically using 0.8% slab agarose gels in 0.5x TBE (40 mM Tris-Cl, 45 mM boric acid, 1 mM EDTA, pH 8.3). Gels were staining with ethidium bromide and DNA visualized using UV-light.

For native agarose gel electrophoresis of RcGTA particles, filtered culture supernatant or cell lysates were treated with 100 ug/mL DNase I at 30 ºC for 1 h. Ten uL were loaded on a 0.8 % agarose TBE slab gel, unless otherwise stated.

2.12 Visualization of spheroplast-like structures

Cultures were centrifuged at a low speed (16,000 rcf) for 30 min. The supernatant was aspirated and the resultant cell pellet and the upper semitransparent layer were separated by gently suspending the upper layer using a micropipette. For ultracentrifugation, 10 ml of culture

were initially pelleted by centrifugation at 3,500 rcf for 10 min, and the supernatant was transferred to a fresh tube. For SB1003-derived strains, the low-speed centrifugation step was repeated 3 times due to poor pellet formation. Three ml of the cleared supernatant were centrifuged at 37,000 rcf for 10 min. The resultant pellet was suspended in 10 µL of 2.5 mM NaCl, 100 mM Tris-HCl, pH 7.8. Vesicles were visualized in a light microscope using a 100-X magnification oil-immersion objective.

Lysozyme treatment was performed by adding 0.25 mg/ml lysozyme (Sigma) and 1.3 mM EDTA (pH 8) to resuspended cell pellets, followed by incubation for 30 min at 30 °C.

2.13 Propidium iodide staining

Cultures of *E. coli* were pelleted by centrifugation, washed and suspended in 10 mM $MgSO_4$, pH 6.5. Propidium iodide was added to 0.2 mM, cells incubated for 30 min at RT and cells visualized on agarose-coated microscope slides. Fluorescence microscopy was performed using a mercury lamp (HBO, 50 W) for excitation and the Zeiss filter set 15.

2.14 Biofilm formation

To quantify biofilm material formed on the walls of culture tubes, the culture was discarded and tubes gently rinsed with water. White/opaque material was stained with 1.5 mL of 0.1% wt/vol crystal violet in dH_2O for 1 min and tubes rinsed gently with 5 volumes water. For quantification, bound crystal violet was eluted using 1 mL ethanol and the absorbance of the eluate measured at 600 nm.

2.15 Enzymatic assays

2.15.1 Endolysin activity determination by zymogram

Zymography was performed as previously desctibed (Fogg *et al.*, 2012b). In short, crude peptidoglycan isolated from *R. capsulatus* was incorporated into an SDS-polyacryl amide gel.

After electrophoresis, protein(s) were renatured and the gel stained using coomassie brilliant blue. Activity was visible as a clearing against the uniform blue background at the predicted size of Rcc00555.

2.15.2 Beta-galactosidase

Gene expression (defined in this thesis as the combined activity of transcription and translation initiation) was determined by measuring the β-galactosidase activity of cells containing a promoter-*lacZ* reporter construct. *lacZ* was fused to the annotated start codon of a DNA sequence containing ~500 bp upstream included any predicted promoters, as described in detail in section 2.3 and previously (Leung, 2010, Leung *et al.*, 2012). Five mL of culture were pelleted at 6,800 rcf for 10 min and the pellet washed and suspended in Z-buffer (60 mM Na_2HPO_4, 40 mM NaH_2PO_4, 10 mM KCl, 1 mM $MgSO_4$, 50 mM β-mercaptoethanol, pH 7). Cells were lysed by sonication, and the lysate cleared by centrifugation at 16,000 rcf for 5 min. Cleared cell lysate was added to Z-buffer to a total volume of 500 uL, and the enzymatic reaction initiated by addition of 200 uL of *o*-nitrophenyl-β-galactoside (ONPG; 4 mg/mL in 60 mM Na_2HPO_4, 40 mM NaH_2PO_4, pH 7). Absorbance at 420 nm was monitored over time and β-Galactosidase activity was calculated by

$$U = 1000 \times \frac{\Delta A_{420nm}/\Delta t_{min}}{4.5 \times C_{protein}} \times \frac{V_{reaction}}{V_{lysate}}$$

where $C_{protein}$ is the concentration of total protein (mg/mL) determined by a Lowry assay and V indicates volumes.

2.15.3 Malate dehydrogenase

Malate dehydrogenase activity was performed as previously described (Fogg 2012, Westbye et al 2013). 100 µL of 0.2 µm pore-size filtered culture supernatant or lysate were

mixed with 0.2 mM NADH and 100 mM KPO_4 (pH 7.4) in a total volume of 980 ml. The assay was initiated by the addition of 20 µl of 10 mM oxaloacetic acid, and the decrease in absorbance at OD_{340} over time was measured in a U-3010 spectrophotometer (Hitachi). The ΔA340/min was calculated from the initial linear portion of the curve using the Time Scan function of UV Solutions 2.1 (Hitachi) software. Activity was calculated in units/ml using the equation:

$$\left(\frac{\Delta A_{340nm}/\Delta \mathrm{t}_{min}}{6.22 \times 10^3}\right) \times \left(\frac{\mu mol}{L}\right)$$

2.16 Total protein determination by the Lowry method

Total protein concentration was determined by the the Lowry method using BSA as the standard (Peterson, 1983).

Chapter 3: Results

3.1 Release of RcGTA is mediated by regulated cell lysis

The mechanism of release of RcGTA had not been well studied. Because most tailed dsDNA phages are release by cell lysis, this appeared to be the most likely mechanism of release. Therefore, the release mechanism of RcGTA was investigated with a focus on a possible lytic mechanism.

3.1.1 Inhibition of RcGTA release by phosphate

Preliminary experiments showed that the concentration of phosphate in the growth medium RCV influences the partitioning of the RcGTA capsid protein between the cell pellet and culture supernatant after centrifugation (Leung, 2010, Taylor, 2004), and it was suggested that nutrient-dependent regulation of RcGTA, possibly through the PhoB-dependent phosphate starvation response system, may be a regulator of RcGTA release (Leung, 2010).

3.1.1.1 High concentrations of phosphate inhibit RcGTA transduction

To investigate the role of phosphate in RcGTA transduction and release, modified versions of the complex medium YPS (YPSm) and minimal medium RCV(RCVm) were developed to allow varied phosphate concentrations while minimizing the effects on buffering capacity and potassium concentration, or the formation of insoluble precipitates. Reducing the concentration of $MgSO_4$ and $CaCl_2$ in YPS medium to 0.5 mM (each) allowed for addition of KPO_4 (pH 6.8) to 10 mM without formation of precipitates (not shown). Because KPO_4 serves as both the main buffering agent, and the sole potassium source in RCV, the modified phosphate-free medium was developed to have a level of potassium equal to the classical RCV medium by neutralizing the malic acid component by addition of KOH, and a high buffering capacity by the addition of 4-morpholinepropanesulfonic acid (MOPS, pH 6.8) to 20 mM.

Transduction frequencies from cells cultured in YPSm medium containing KPO_4 or the alternative phosphate source $NaPO_4$ (both at 10 mM) were decreased to 37% and 27%, respectively, indicating that the addition of high levels of phosphate reduces the transduction frequency when cultures are grown in YPSm (Figure 8A). In contrast, the addition of MOPS increased transduction frequencies, indicating that the decreased transduction frequency from the addition of phosphate salts was not due to an increased buffering capacity. The decreased transduction frequency was accompanied by a decrease in the amount of the RcGTA capsid protein present in the culture supernatant and an intracellular accumulation for cultures supplemented with KPO_4 or $NaPO_4$. In contrast, addition of KSO_4, KNO_3 or MOPS had little or no effect (Figure 8B).

To more fully study the effects of phosphate on RcGTA transduction, the transduction frequency from RCVm containing increasing concentrations of KPO4 was investigated. The concentration of inorganic phosphate in YPS was determined to be ~0.5 mM using a malachite green colorimetric assay (not shown; Bioassay Systems Cat. No POMG-25H). A growth curve of *R. capsulatus* cultured photoheterotrophically in RCVm containing different concentrations of phosphate was performed to investigate the phosphate effect during laboratory growth conditions. Cultures containing an initial concentration of 4, 1, 0.5 or 0.3 mM KPO_4 grew at similar rates and reached similar densities, while cultures containing 0.1 or 0 mM KPO_4 showed a marked reduction in growth rate and final densities (not shown). Based on the growth curves and the measurements of inorganic phosphate levels in YPS, RCVm containing 0.5 mM KPO4 was subsequently used as the standard condition for low phosphate.

RcGTA donors grown in RCVm 0.5 mM transduced markers at high levels (Figure 8C), in contrast to the minimal transduction typically observed when using classical RCV medium

that contains 9.6 mM KPO_4 (not shown). Increasing concentrations of phosphate in RCVm were accompanied by decreasing transduction frequencies, with supernatant from 10 mM KPO_4 cultures reduced to 0.4% of frequencies observed using cultures grown in the presence of 0.5 mM KPO_4 (Figure 8C). To confirm that the increased release of RcGTA was not due to a reduced buffering capacity, the final pH of culture media were compared. A very small difference in pH was observed between the cultures (Figure 8D). Furthermore, the omission of MOPS from media containing 10 mM KPO_4 did not result in an increased level of transduction (Figure 8C), despite having a markedly reduced buffering capacity indicated by an increase in the final culture pH (Figure 8D).

Low concentrations of phosphate (0.5 and 2.0 mM) stimulated the release of RcGTA capsid protein to the culture supernatant, while high concentrations (5.0 and 10 mM) resulted in an intracellular accumulation of capsid protein (Figure 8E).

Therefore, it appeared that the presence of inorganic phosphate in high (millimolar) concentrations inhibited the release of RcGTA from cells to the culture supernatant.

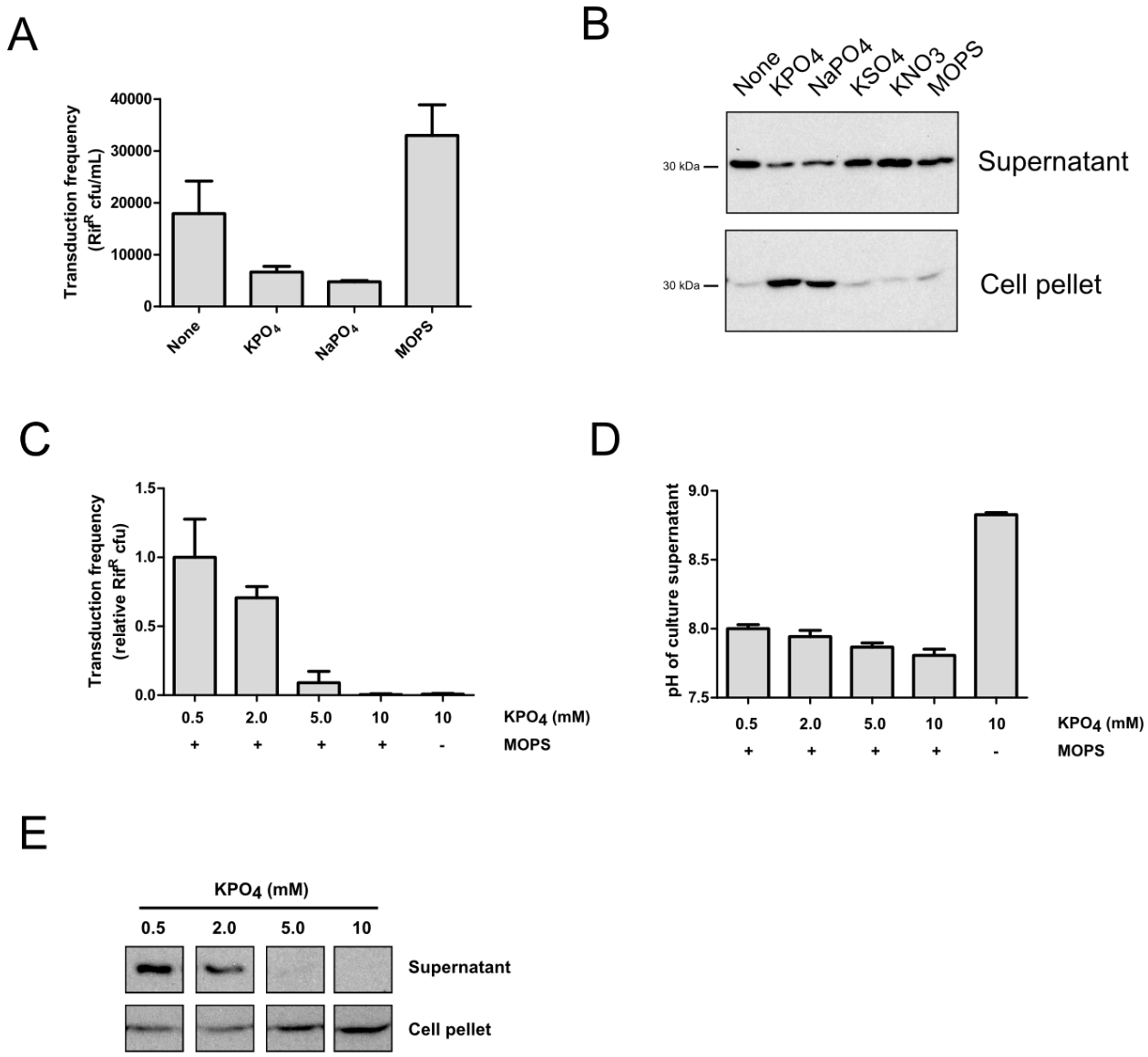

Figure 8 High concentration of phosphate inhibits RcGTA transduction and release

Transduction frequencies from filtered culture supernatant (**A** and **C**), western blots using anti RcGTA capsid serum for the presence of RcGTA in culture supernatant and cell pellet fraction (**B** and **E**) and pH of culture supernatant (**D**). SB1003 was cultured in YPSm medium supplemented with KPO_4, $NaPO_4$, KSO_4, KNO_3 or MOPS as indicated (**A** and **B**), or RCVm supplemented with KPO_4 and MOPS as indicated (**C**, **D** and **E**).

The total amount of capsid produced (intracellular and extracellular) appeared similar for cells cultured in the differing concentrations of phosphate (Figure 8B and E), indicating that phosphate concentration did not influence production of the capsid protein. To confirm that the RcGTA gene cluster was not differentially expressed when cultured in low *vs*. high phosphate concentration, expression of the RcGTA *orf1* was measured using the *lacZ* reporter plasmid p601-g65 (Leung *et al.*, 2012). The β-galactosidase activity increased 2.4-fold for cells cultured in 10 mM KPO_4 compared to 0.5 mM (Figure 9A), apparently contradicting the results shown in Figure 8. Because the reporter assay utilizes the cell fraction of the culture (and not the cell-free culture supernatant), β-galactosidase produced by cells in 0.5 mM KPO_4 activity could presumably be released from cells together with the RcGTA capsid protein. Promoter activity was therefore also measured in the strain SB555 (SB1003 *Δrcc00555*), a recent mutant of a predicted endolysin with reduced release of RcGTA (Hynes *et al.*, 2012) (this mutation blocks cell lysis, see Section 3.1.2). In the *Δ555* background, cells cultured in the presence of 10 mM KPO_4 had an activity 1.2-fold greater than in the presence of 0.5 mM KPO_4 (Figure 9B), indicating that phosphate concentration does not influence the activity of the RcGTA promoter. Furthermore, the high/low phosphate difference observed for SB1003 was likely due to a loss of β-galactosidase activity released from cells rather than a differential activity of the RcGTA promoter.

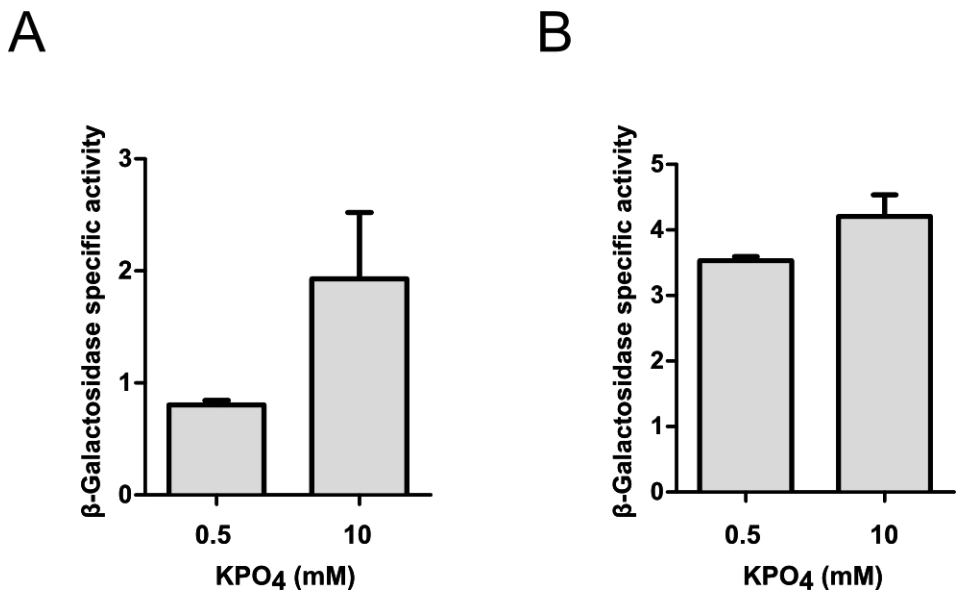

Figure 9 Phosphate concentration does not increase RcGTA promoter activity

RcGTA promoter activity (β-galactosidase activity) of the RcGTA promoter-*lacZ* reporter plasmid p601-g65 for SB1003 cells (**A**) and cells of the RcGTA-release deficient strain SB555 (**B**) cultured in RCVm medium supplemented with 0.5 or 10 mM KPO_4.

3.1.1.2 Phosphate-dependent release of RcGTA from cells does not require the PhoB-dependent phosphate starvation response

Depletion of phosphate induces the PhoB-dependent phosphate starvation response in many bacteria (Lamarche *et al.*, 2008), and I hypothesized that RcGTA was induced by a similar response. In many bacteria, PhoB induces the expression of alkaline phosphatase in conditions of limiting phosphate, and alkaline phosphatase activity is widely used as an indicator of Pho regulon induction (Wanner, 1993).

To investigate whether cultivation in low levels of phosphate resulted in a phosphate starvation response, measurements of residual inorganic phosphate and alkaline phosphatase activity were performed. RCVm containing 0.5 mM KPO_4 was found to be essentially devoid of

inorganic phosphate at the timepoint used to harvest RcGTA, whereas 0.4 and 2.6 mM residual phosphate were detected in media initially containing 2.0 and 4.0 mM KPO_4 (Figure 10A), indicating that the cells were capable of accumulating approximately 1.4 to 1.6 mM KPO_4 from the growth medium. Similarly, the production of alkaline phosphatase was elevated in a medium containing 0.5 mM KPO_4, compared to 2.0 or 4.0 mM (Figure 10B), indicating that cells in 0.5 mM KPO_4 initiated a cellular response to increase phosphate acquisition.

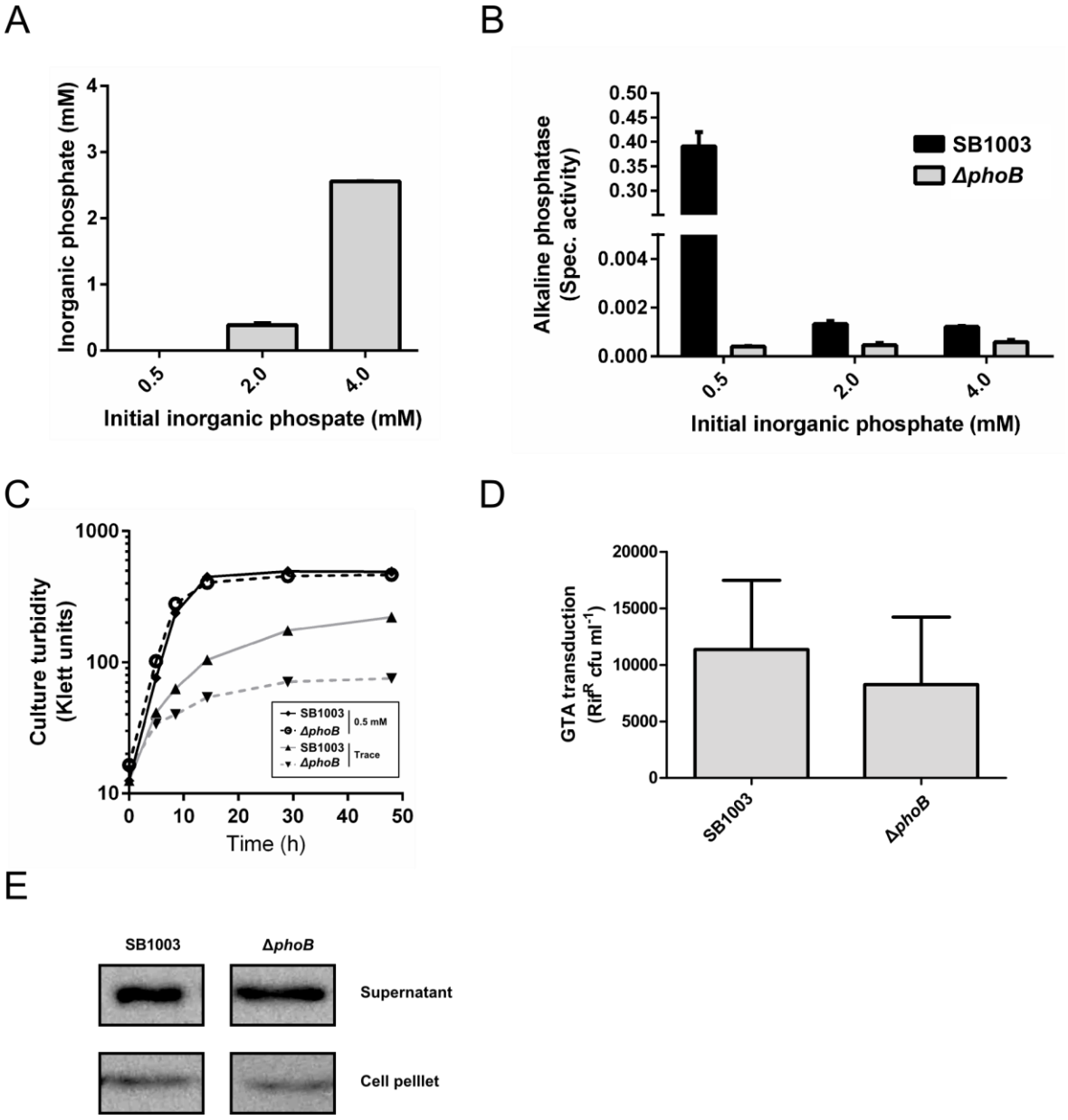

Figure 10 The PhoB-dependent phosphate starvation response is not required for RcGTA production and release.

A. Residual inorganic phosphate in culture supernatant, measured by a malachite green assay. **B.** Alkaline phosphatase activity for SB1003 and the *ΔphoB* mutant. **C.** Culture turbidity monitored over time for SB1003 and SB1003*ΔphoB* inoculated in RCVm containing 0.5 mM or trace amounts of KPO_4. **D.** Transduction frequencies of SB1003 and *ΔphoB.* **E.** Western blot of SB1003 and *ΔphoB* cells probed with RcGTA capsid protein anti-serum. For **D** and **E**, cells were cultured in RCVm 0.5 mM KPO_4. Concentration of KPO_4 (mM) is indicated.

The *R. capsulatus* genome was found to encode one predicted homologue of PhoB, encoded by *rcc03498*, and a markerless deletion of 93% of *rcc03498* was constructed (*ΔphoB*). Transfer of exponentially growing cells from RCV to a RCVm medium containing trace amounts of inorganic phosphate resulted in reduced growth for the *ΔphoB* strain compared to SB1003 (Figure 10C), whereas no major growth defect was observed in media containing 0.5 mM (Figure 10C). In contrast to WT, the resultant *ΔphoB* mutant was found to not produce alkaline phosphatase when cultured in RCVm 0.5 mM (Figure 10B). Therefore, *rcc03498* encodes a functional homologue of PhoB that regulates the *R. capsulatus* phosphate starvation response.

To determine whether a PhoB-dependent response regulates RcGTA release, transduction frequencies and RcGTA capsid release of the *ΔphoB* mutant were compared to the parental strain. No difference in transduction frequency (Figure 10D) or RcGTA release (Figure 10E) were observed for the *ΔphoB* mutant compared to the parental WT strain. Because the release of RcGTA was observed in conditions of excess phosphate (2 mM, Figure 8E and A) and PhoB was not required for transduction or release of RcGTA (Figure 10D and E), this indicates that the influence of phosphate concentration on RcGTA transduction and release is not due to a phosphate depletion/starvation response.

3.1.1.3 The concentration of phosphate modulates cell lysis of the RcGTA-overproducer strain DE442

During my PhD thesis research, RcGTA was proposed to be released from cells through cell lysis (Lang *et al.*, 2012), similar to the release mechanism utilized by tailed bacteriophages

such as lambda (Young, 2013). However, no study of the mechanism of RcGTA release had been undertaken. To facilitate the study of release, the RcGTA overproducer phenotype of strain DE442 was exploited. RcGTA overproducers have previously been used to facilitate the study of RcGTA production (Leung, 2010, Yen *et al.*, 1979).

Pigmented cell-free culture supernatant was observed for DE442 cultured photoheterotrophically and semiaerobically to the stationary phase (40 h) in the complex medium YPS (not shown). Absorption spectroscopy scans of 0.2 um-filtered semiaerobic culture supernatant revealed that DE442 released a large amount of the membrane bound photosynthetic pigment light harvesting complex 2 (LH2) to the culture supernatant (Figure 11A). Much less LH2 was observed in the supernatant of DE442 cultivated in the 9.6 mM KPO_4-containing medium RCV, while no pigments were detected in the supernatant of SB1003 cultured in either YPS or RCV (Figure 11A).

Because lysis entails the release of cytoplasmic components, the activity of the citric acid cycle enzyme malate dehydrogenase, normally confined to the cytoplasm, was measured in the culture supernatant and compared to French-pressed whole culture activities. High levels of malate dehydrogenase activity were detected in DE442 cultures grown semiaerobically in YPS, with 45% of the whole culture activity confined to the (cell-free) supernatant fraction (Figure 11B). In contrast, 11% of the malate dehydrogenase activity was confined to the culture supernatant of cells cultured in RCV medium. Cultures harvested in the exponential phase (16 h), when RcGTA production is low (Florizone, 2006), contained much less malate dehydrogenase activity in the supernatant (3% and 2% of the total for YPS and RCV, respectively). In contrast to the RcGTA overproducer DE442, the WT SB1003 released very low to non-detectable levels of malate dehydrogenase under all conditions (Figure 11B). Therefore, cultivation of the RcGTA

overproducer strain DE442 in growth medium promoting RcGTA release was accompanied by a large amount of cell lysis, which indicated that RcGTA is released through lysis of the host.

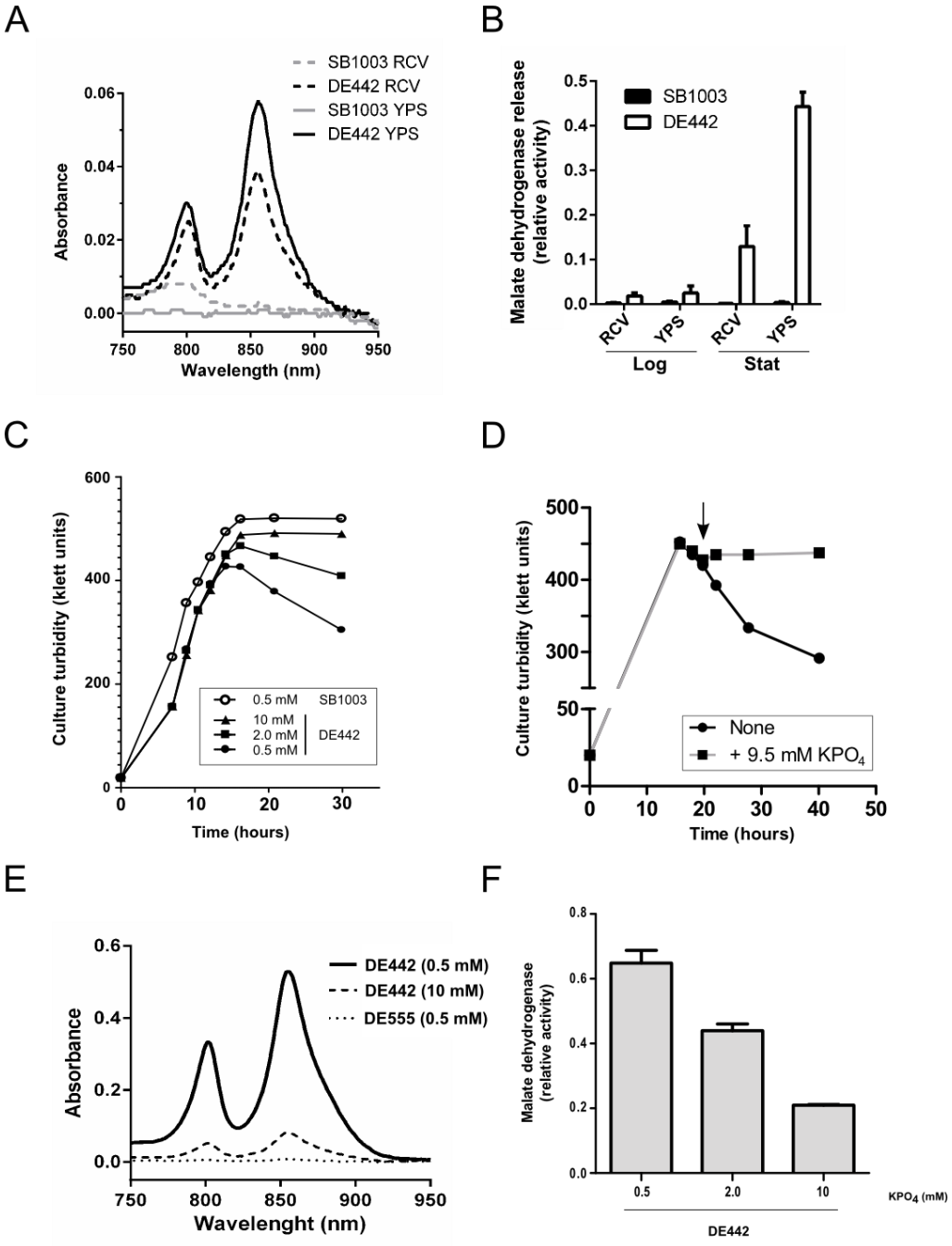

Figure 11 Phosphate-modulated lysis of the RcGTA overproducer DE442

A, Absorbance scan of filtered culture supernatant, showing 800 nm and 850 nm absorption peaks of the photosynthetic pigment LH2. **B,** Malate dehydrogenase activity of culture supernatant relative to French-pressed total culture activity. **C,** Culture turbidity of SB1003 and DE442 cultured photoheterotrophically in RCVm. **D,** Culture turbidity of DE442 cultured RCVm 0.5 mM KPO_4. Arrow indicates addition of trace (none) or 9.5 mM

KPO_4 to culture. **E,** Absorbance scan (LH2 region) of culture supernatant for DE442 and endolysin-knockout DE555 cultured in RCVm with 0.5 or 10 mM KPO_4. **F,** Malate dehydrogenase activity of culture supernatant relative to French-pressed total culture activity.

Cells were cultured semiaerobically in RCV or YPS medium (**A** and **B**) or photoheterotrophically in RCVm with the indicated concentration of KPO_4 (**C** to **F**). Culture density was measured by Klett-Summerson photoelectric colorimeter.

Induction of phage lambda results in cell lysis of the *E. coli* host, observable by a decrease in culture turbidity, due to the expression of specific lysis genes encoded by lambda (Campbell, 1961, Garrett *et al.*, 1981). Because the high levels of transduction observed in RCVm 0.5 mM compared to 10 mM KPO_4 (Figure 8C) was not due to an increased activity of the RcGTA promoter (Figure 9), but rather appeared to influence the release of RcGTA from cells (Figure 8E), I hypothesized that phosphate concentration in the growth medium modulates cell lysis.

Growth kinetics of DE442 were monitored by turbidity during photoheterotrophic growth for 30 h in RCVm containing different levels of KPO_4. During the logarithmic phase of growth, no difference was observed between cultures containing low or high levels of KPO_4. However, at entry into stationary phase at approximately 14 h, the turbidity of the 0.5 mM cultures, and to a lesser extent 2.0 mM, decreased while the 10 mM cultures leveled off (Figure 11C). Furthermore, addition of 9.5 mM KPO_4 after the onset of the decline in turbidity of 0.5 mM cultures rapidly halted the decrease (Figure 11D). In contrast, no decrease in turbidity was observed for the RcGTA WT-level strain SB1003 cultured in 0.5 mM KPO_4 (Figure 11C).

A wavelength scan of cell-free supernatant from DE442 cultured in RCVm 0.5 mM KPO_4 resulted in a large LH2 absorbance peaks (Figure 11E), confirming that DE442 released

the membrane bound photosynthetic pigment in high concentrations. In contrast, the LH2 absorption peaks were much smaller for cells cultured in 10 mM KPO_4. For DE442 cultured in 0.5 mM KPO_4, ~65% of the total malate dehydrogenase activity of the culture was present in the supernatant fraction (Figure 11F), indicating that the majority of the cells had lysed and released their cytoplasmic content. For 10 mM KPO_4 cultures, a smaller portion (~20%) of the malate dehydrogenase was released to the culture supernatant.

R. capsulatus forms rod-like cells (Weaver *et al.*, 1975). In rod shaped cells, degradation of the peptidoglycan layer, which supports the cell shape, by an endolysin result in the formation of rounded cells (Berry *et al.*, 2012). Inspection of DE442 0.5 mM KPO_4 cultures by phase contrast microscopy revealed the presence of numerous spheroplast-like vesicles or rounded cells of various diameters, while few (DE442 10 mM) or none (SB1003 0.5 mM) were observed for the cultures which did not drop in density (not shown).

Centrifugation (16,000 rcf, 30 min) of DE442 cultured in 0.5 mM to separate cells from the medium resulted in a pigmented culture supernatant and a pellet containing two layers: A lower dense cell pellet layer, and an upper translucent layer (Figure 12A). Microscopy of the translucent layer revealed it to consist mainly of vesicles, while the dense lower pellet consisted of mostly rod shaped cells (Figure 12B). To assess whether the vesicles could be the result of cells lacking the structural support of peptidoglycan, resuspended cells were treated with EDTA and lysozyme, which resulted in structures similar to the spheroplast-like vesicles observed for cells cultured in a low concentration of phosphate (Figure 12B).

To address whether a low amount of vesicles was produced by SB1003 cultured in 0.5 mM KPO_4, cells were removed from culture by low speed centrifugation (3,500 rcf, 10 min) and the supernatant ultracentrifuged (37,000 rcf, 10 min) resulting in a small pigmented pellet

(Figure 12C). In contrast, DE442 produced a large pigmented pellet. Microscopy of the suspended SB1003-derived pellet revealed several spheroplast-like vesicles (Figure 12D), indicating that SB1003 cultured in 0.5 mM KPO_4 produces a small amount of spheroplast-like vesicles.

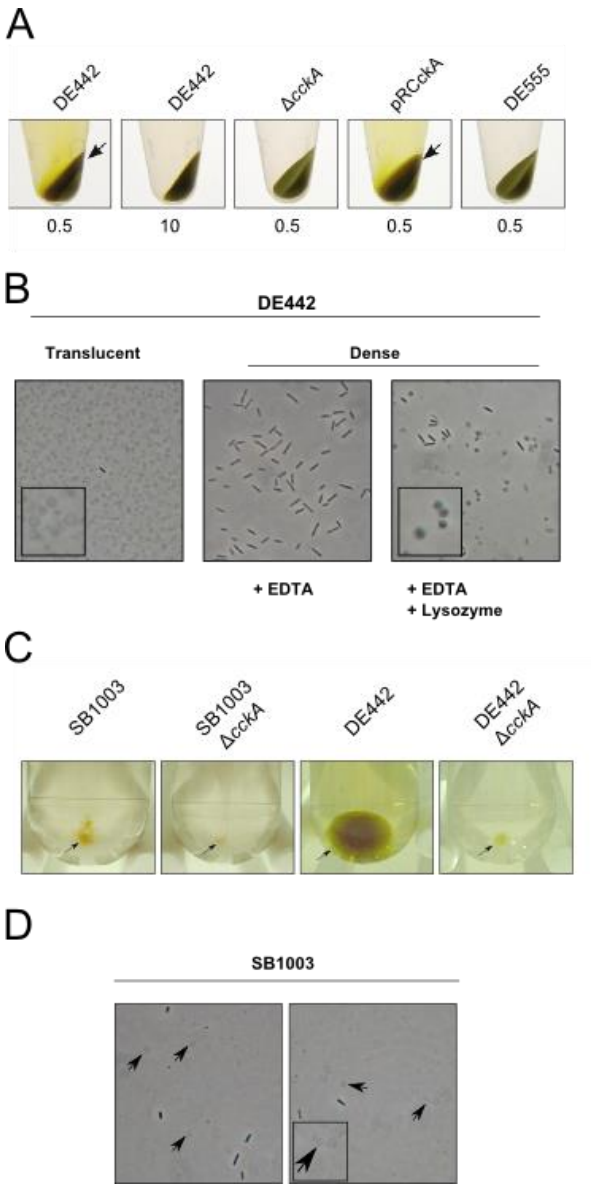

Figure 12 DE442 produces spheroplast-like vesicles

A, Cell pellets of cultures centrifuged at 16,000 rcf for 30 min. The concentration of KPO_4 is indicated, and arrows point at the upper, translucent pellet layer. **B,** Phase-contrast microscopy of the DE442 upper translucent and lower dense pellet layer. The lower dense pellet was treated with or without lysozyme as indicated. **C,** Pellet resulting from ultracentrifugated (37,000 rcf, 10 min) culture supernatant. **D,** Phase-contrast microscopy of resuspended SB1003-derived ultracentrifuged pellet. Insets show enlarged vesicles.

3.1.1.4 Inhibition of cell lysis does not require *de novo* protein synthesis

To investigate whether the effect of the phosphate concentration on cell lysis requires active growth, DE442 cells cultured in 10 mM phosphate were collected and resuspended in RCVm medium or a salt-free Tris-HCl buffer in the presence or absence of 10 mM phosphate. Malate dehydrogenase was readily detected after 30 min incubation in the absence of phosphate, but to a lesser degree in the presence of phosphate, in a concentration-dependent manner (Figure 13A), whereas other salts did not affect the release of malate dehydrogenase. Inhibition of protein synthesis by gentamicin (Sarre and Hahn, 1967) did not reduce the amount of malate dehydrogenase released (Figure 13B) compared to that for untreated cells, although the antibiotic inhibited growth (Figure 13C).

Therefore, actively growing cells and protein synthesis are not required for the inhibitory effect of phosphate on cell lysis.

In summary, release of RcGTA from cells is dependent on the concentration of inorganic phosphate present in the culture medium. The release of RcGTA is accompanied by cell lysis evidenced by the release of the photosynthetic pigment of LH2, the cytoplasmic enzyme malate dehydrogenase and the formation of spheroplast-like structures. The effect on cell lysis and RcGTA release by phosphate concentration is independent of the PhoB-dependent phosphate starvation response, and inhibition of cell lysis was found to be independent of both active growth and protein synthesis.

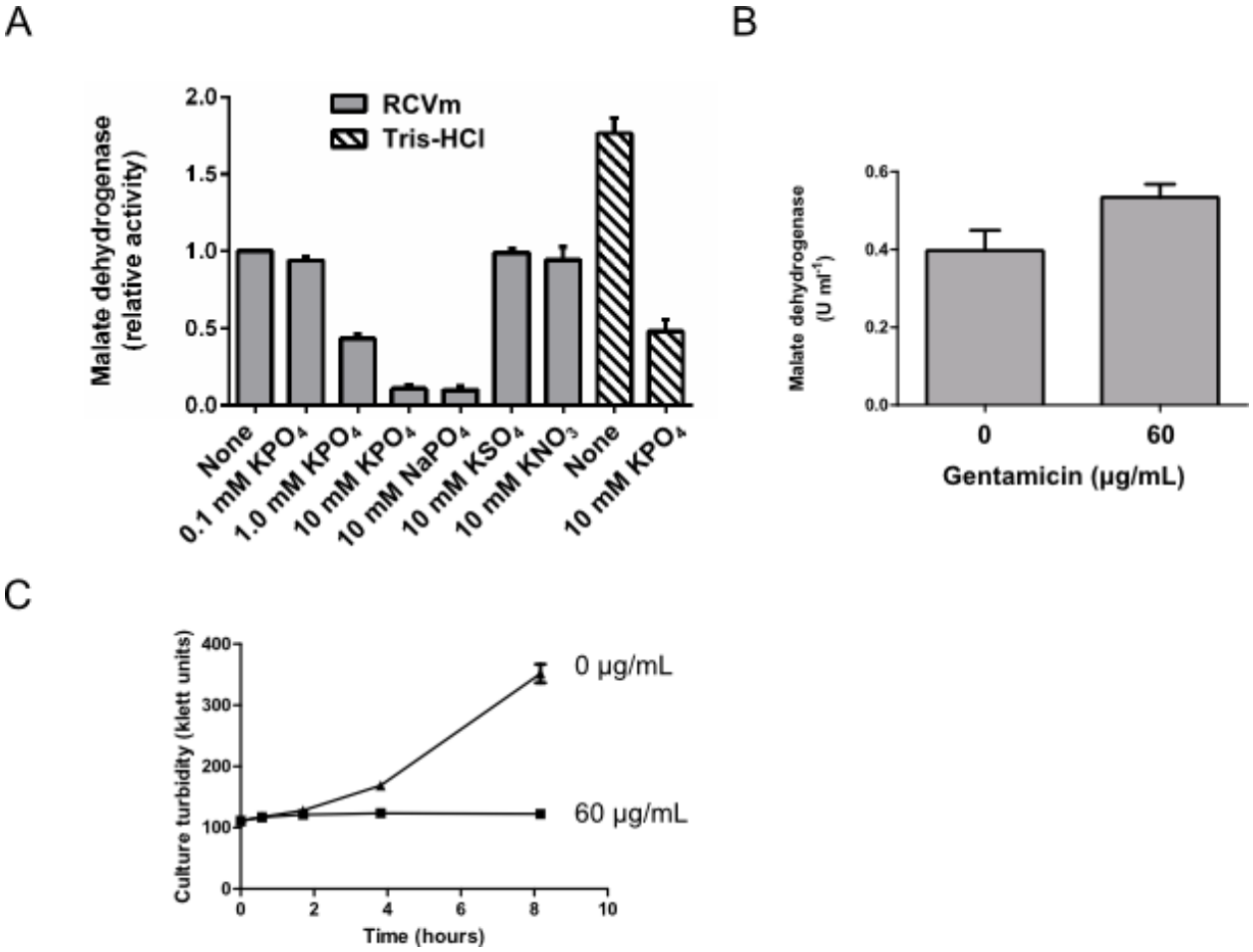

Figure 13 Inhibition of cell lysis by phosphate occurs in the absence of de novo protein synthesis

Malate dehydrogenase activity (**A** and **B**) and culture turbidity (**D**). **A,** DE442 resuspended in RCVm or Tris-HCl pH 6.8 buffer containing indicated salts. **B,** DE442 treated with 0 or 60 µg/ml gentamicin and resuspended in RCVm lacking phosphate. **C,** Turbidity of cultures treated with 0 or 60 µg/mL gentamicin. Cells were grown in RCVm containing 10 mM KPO_4 and resuspended to an OD_{660} of 5.0 (A) or 0.5 (B). For panel **A,** activity is expressed relative to the activity in RCVm lacking phosphate. For panel **B**, activity was multiplied by 10 for direct comparison with experiments using an OD_{660} of 5.0. Error bars represent the standard deviations of three biological replicates.

3.1.2 Cell lysis is mediated by the endolysin Rcc00555 and holin Rcc00556

3.1.2.1 *rcc00555* and *rcc00556* are required for cell lysis and RcGTA release

Most tailed bacteriophages utilize an endolysin/holin system for escape from the host cell (Young *et al.*, 2000, Young, 2013). Recently, it was reported that a putative lysozyme encoded by *rcc000555* is required for release of RcGTA from SB1003 cells (Hynes *et al.*, 2012). Bioinformatic analysis using PFAM indicated that *rcc00555* encodes a modular protein, consisting of an N-terminal glycosyl hydrolase domain (PF05838) and a C-terminal peptidoglycan binding domain (PF09374) (Figure 14A). BLASTP of Rcc00555 against the NCBI refseq_protein database indicated the protein to be conserved in several Alphaproteobacteria, including *R. sphaeroides* and the two reported GTA producers *Roseovarius nubinhibens* and *Ruegeria pomeroyi*. Sequence alignment using NeedleP of Rcc00555 to the characterized PF05838-founding endolysin gp61 from coliphage N4 (Stojkovic and Rothman-Denes, 2007) indicated a 37% sequence identity over the entire protein, and Rcc00555 contained the catalytically active EGGY motif (Figure 14A and Figure S1) but lacked the N-terminal export signal. The sequences of the homologous proteins from *R. sphaeroides*, *R nubinhibens* and *R. pomeroyi* similarly aligned well with the coliphage N4 endolysin gp61 (Figure S1).

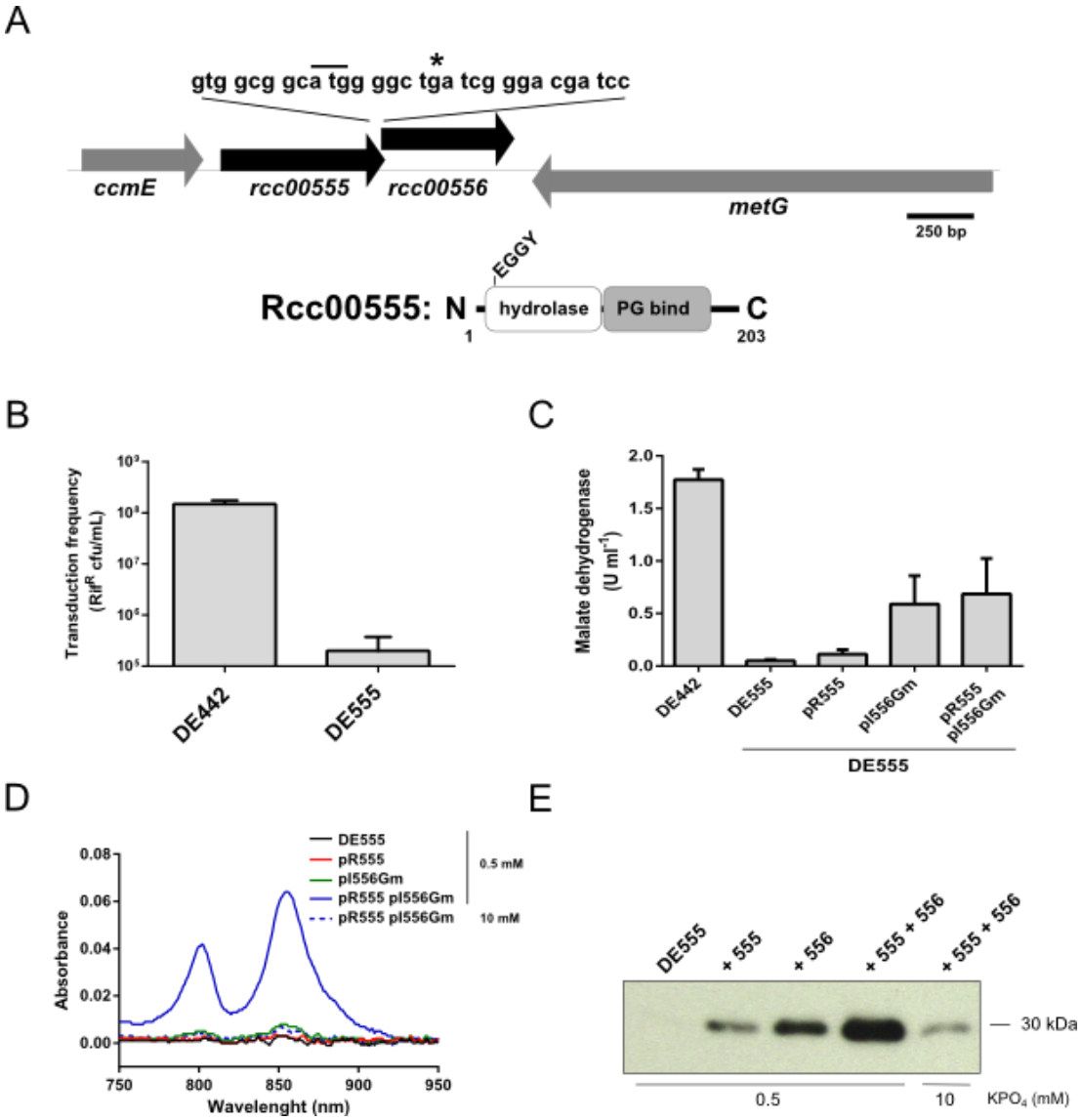

Figure 14 *rcc00555* and *rcc00556* are required for cell lysis

A, Genetic context of the predicted endolysin *rcc00555* and holin *rcc00556*, and predicted domains in Rcc00555. Annotated *rcc00555* stop codon (*) and *rcc00556* start codon (line), predicted glycosyl hydrolase (hydrolase) and peptidoglycan binding (PG bind) domains and active site residues EGGY are indicated. **B,** Transduction frequency of DE442 and the *Δrcc00555* strain DE555 culture supernatant. **C,** Malate dehydrogenase activity present in culture supernatant of indicated strains. **D,** Photosynthetic pigment LH2 present in culture supernatant of DE555 complemented with pR555 and/or pI556Gm. **E,** Restoration of capsid protein production by plasmids pR555 and/or pI556Gm. Concentration of KPO_4 in culture medium is indicated for **D** and **E**.

To test whether Rcc00555 functions as an endolysin, the *rcc00555* orf was disrupted in DE442 using a kanamycin-resistance marker to create strain DE555. Transduction from DE555 was greatly impaired (Figure 14B), extending the observation of Hynes et al (Hynes *et al.*, 2012) from strain SB1003 to DE442. The mutant strain DE555 was impaired for cell lysis when cultured in 0.5 mM KPO_4: Release of malate dehydrogenase to culture medium was 3% of the parental strain DE442 levels (Figure 14C), and production of spheroplast-like vesicles (not shown) and release of pigments were mitigated (Figure 14D). However, *trans*-complementation of the mutant strain DE555 by plasmid pR555, which expresses the *rcc00555* orf (Hynes *et al.*, 2012), did not restore cell lysis. Because the *rcc00555* orf overlaps the putative holin *rcc00556* orf, I hypothesized that the kanamycin resistance cartridge in the disrupted *rcc00555* impairs transcription of the downstream holin (*rcc00556*). Simultaneous complementation of the *rcc00555*-disrupted strain DE555 with *rcc00555*- and *rcc00556*-expressing plasmids pR555 and pI556Gm increased the release of pigments to the supernatant, and this release was dependent on the phosphate concentration (Figure 14D). Furthermore, release of the RcGTA capsid protein to the culture supernatant was greatly increased when DE555 contained both plasmids pR555 and pI556Gm, compared to DE555 containing either plasmid singly (Figure 14E), and this release was dependent on phosphate concentration.

3.1.2.2 Expression of the *rcc00556*-encoded holin in the absence of the *rcc00555*-encoded endolysin results in release of a cytoplasmic enzyme, but not membrane-bound photosynthetic pigments

Partial restoration of the release of malate dehydrogenase was observed for DE555 containing pI556Gm in the absence of pR555 (*rcc00556*-positive and *rcc00555*-negative). The

activity was similar to that of DE555 complemented by both plasmids pR555 and pI556Gm, but 33% of the activity measured for WT DE442 (Figure 14C), indicating that *rcc00556* encodes a holin that produces a hole large enough for soluble proteins to escape the cytoplasm, but do not allow release of membrane bound LH2 pigments. *rcc00556* therefore appears to encode is a classical holin, and not a pinholin as the latter form holes too small to allow proteins to escape the cytoplasm (Young, 2013).

In contrast, the release of vesicular photosynthetic pigments required both the *rcc00555* putative endolysin and *rcc00556* putative holin, and this release was inhibited for cells cultured in 10 mM KPO_4 (Figure 14C). Therefore, malate dehydrogenase appears to be released from cells by a combination of diffusion through *rcc00556* holin-mediated holes and *rcc00555* endolysin-dependent cell lysis, whereas the release of intracytoplasmic membrane vesicles containing photosynthetic pigments requires endolysin-mediated cell lysis.

3.1.2.3 *rcc00555* encodes an endolysin

In preliminary biochemical characterizition of Rcc000555, the *rcc00555* open reading frame was expressed with a C-terminal His-tag from plasmid pET-555C in *E.coli* BL21 DE3, and the protein purified by affinity chromatography.

Resuspension of *E. coli* cells induced to express 555C in 0.1 volume of water after centrifugation resulted in a markedly less turbid sample than non-induced cells, or cells containing the empty vector pET28a(+) (Figure 15A). Furthermore, phase contrast microscopy of cells expressing *rcc00555* revealed the presence of rounded cells or vesicles, and extensive cell lysis (not shown). No inhibition of lysis was observed by the addition of 10 mM KPO_4, indicating that the concentration of phosphate does not inhibit the lytic activity of Rcc00555 (Figure 15A).

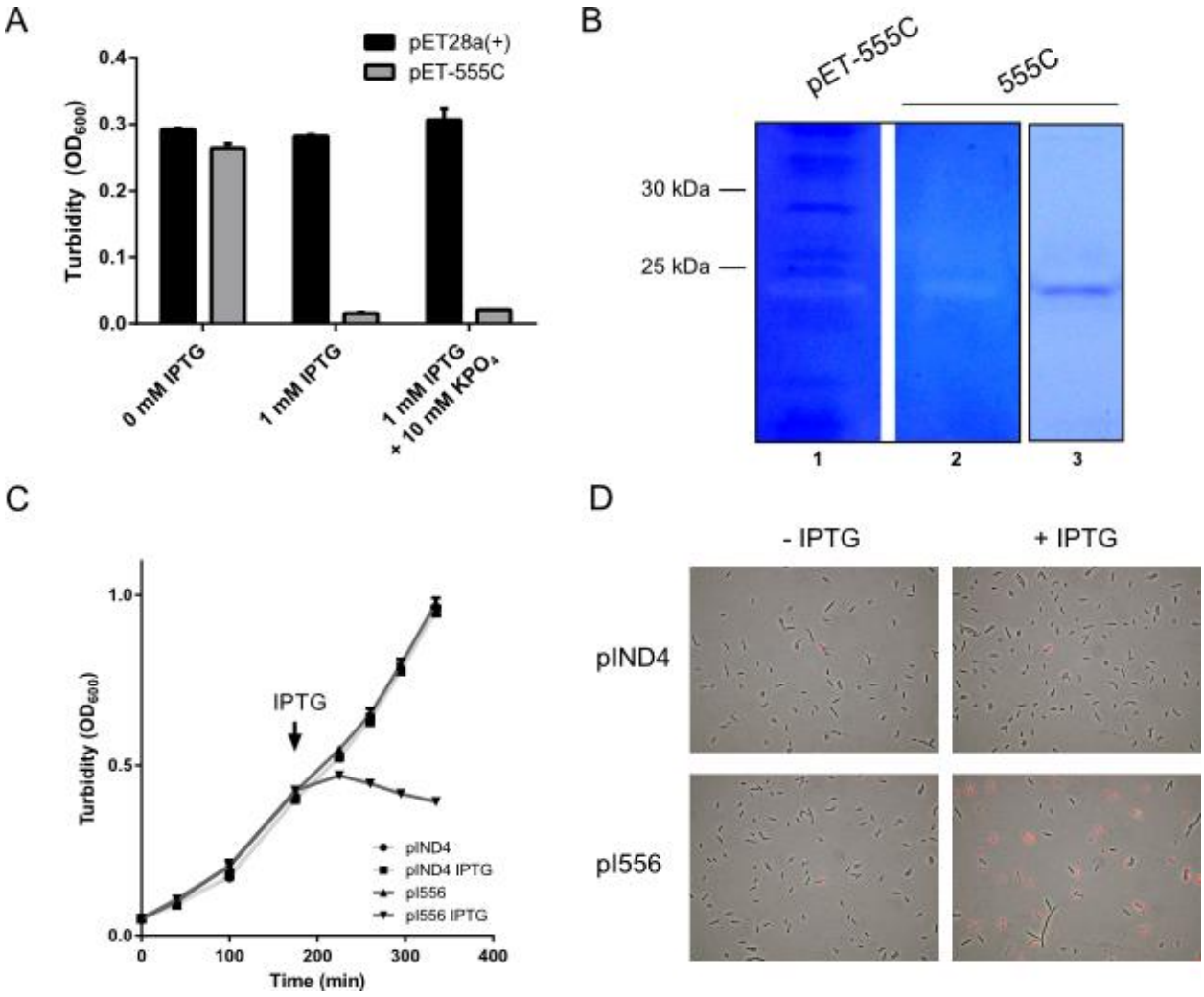

Figure 15 Recombinant expression of the *rcc00555* endolysin and *rcc00556* holin in *E. coli*

The lytic and peptidoglycan-degrading activities of *rcc00555* (**A** and **B**) and holin-like activity of *rcc00556* (**C** and **D**) expressed in *E. coli* are shown. **A,** Turbidity after resuspension in dH_2O of induced *E. coli*. **B,** Lane 1, zymogram of *E. coli* culture lysate; lane 2, affinity-purified 555C protein; lane 3, SDS-PAGE of purified 555C protein. The approximate migration of the markers is indicated. **C,** Growth curves of *E. coli*. Arrow indicates induction time point. **D,** Propidium iodide staining of *E. coli* after induction of *rcc00556* expression. Cells were induced by addition of 1 mM IPTG. Error bars represent the ranges for two (**A**) or the standard deviations for three (**C**) biological replicates.

The His-tagged 555C protein was purified using Ni-NTA chromatography, and the eluate yielded a band of the predicted size of 22.9 kDa (Figure 15B, lane 3). To test whether 555C had peptidoglycan-degrading activity, zymography was performed in an SDS-polyacrylamide gel that contained SB1003-derived peptidoglycan, and the peptidoglycan visualized by staining with Coomassie brilliant blue. A clearing at the position corresponding to the 555C band against a blue background was observed for the cell lysate (Figure 15B, lane 1) and purified 555C (Figure 15B, lane 2). Therefore, Rcc00555 has peptidoglycan–degrading activity, consistent with this protein being an endolysin.

3.1.2.4 *rcc00556* encodes a holin

Holins form holes, or lesions, in the bacterial inner membrane, which depolarize the membrane and effectively kill the cell (Wang *et al.*, 2000). The *rcc00556* orf was transcribed in *E. coli* from the IPTG-inducible promoter on plasmid pI556. Induction of expression rapidly halted growth, whereas no effect on growth was observed with the empty vector control (Figure 15C). To confirm that the membrane potential of the cells was disrupted, cells were stained with propidium iodide, which is not permeant to live cells. About 50% of the cells induced to express *rcc00556* fluoresced when treated with propidium iodide, whereas very few fluorescent cells were observed for uninduced and empty vector control cells (Figure 15D), indicating that the high level expression of *rcc00556* killed *E. coli*. This is in agreement with the results obtained for *R. capsulatus*, where low level expression of *rcc00556* resulted in the release of the cytoplasmic enzyme malate dehydrogenase to the culture supernatant (Figure 14C). Therefore, the *rcc00556* gene product alone appears to be sufficient to depolarize bacterial cytoplasmic membranes by forming a hole, as has been found for bacteriophage holins (Wang *et al.*, 2000), consistent with the hypothesis that Rcc00556 is a holin.

3.1.3 Regulation of cell lysis by the CckA-ChpT-CtrA phosphorelay

3.1.3.1 Cell lysis and expression of 555-556 is regulated by CckA, ChpT and CtrA

All components of the putative phosphorelay CckA-ChpT-CtrA are required for RcGTA-mediated gene transduction. However, cells lacking CckA and ChpT produce the RcGTA capsid protein which is not released from cells (Mercer *et al.*, 2012), a phenotype similar to the effect of high concentrations of phosphate (Figure 8). Because the release of RcGTA was found to be associated with cell lysis and required the endolysin 555 and holin 556, I hypothesized that the CckA-ChpT-CtrA putative phosphorelay regulated expression of the Rcc00555-556 lysis system. This hypothesis was tested by disruption of either *cckA*, *chpT* or *ctrA* in a DE442-background, and it was found that all three knockouts resulted in undetectable release of photosynthetic pigments (Figure 16A), indicating that an intact CckA-ChpT-CtrA phosphorelay is required for cell lysis.

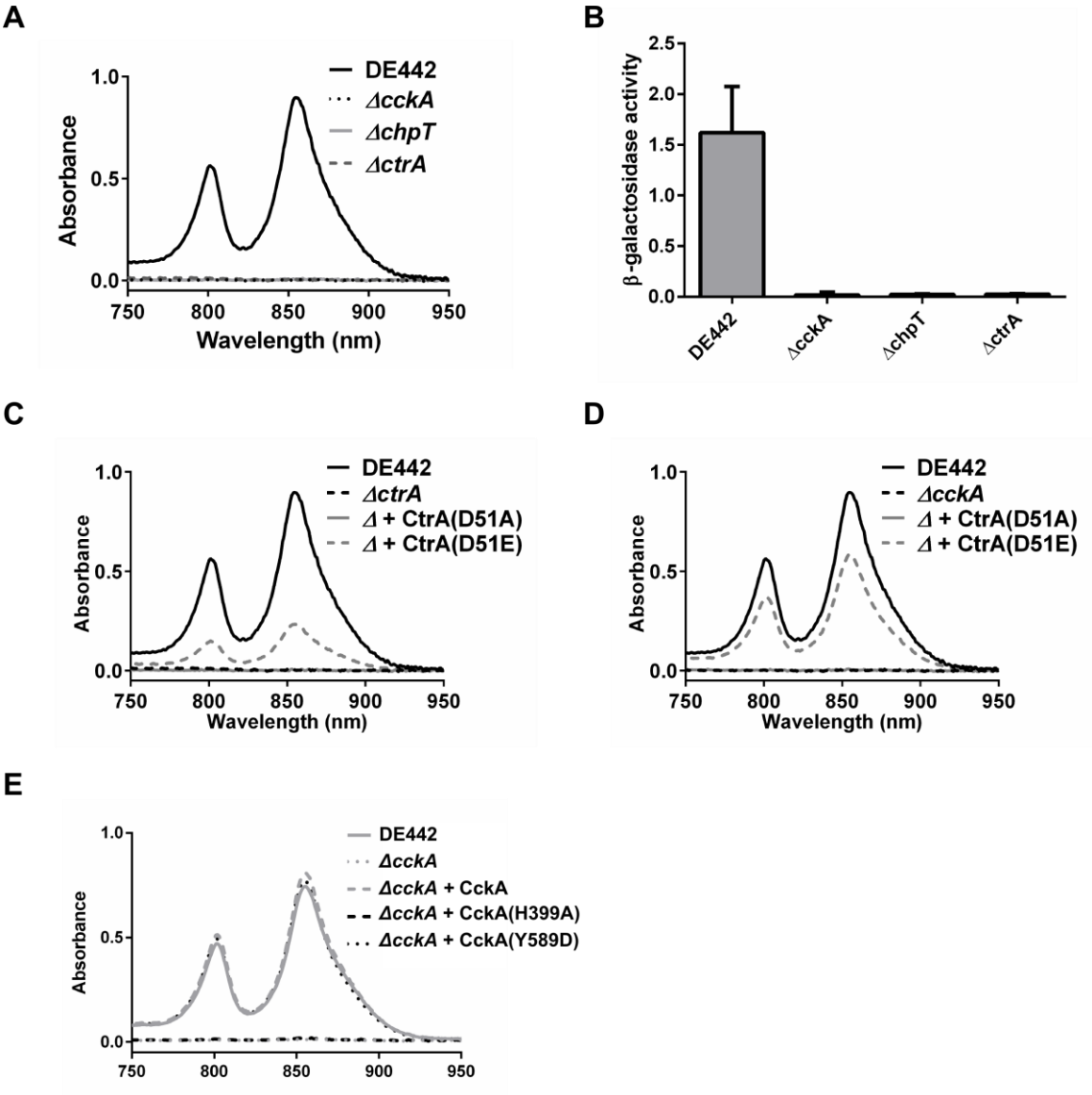

Figure 16 Cell lysis is regulated by the CckA-ChpT-CtrA phosphorelay

Release of membrane bound photosynthetic pigment LH2 (**A**, **C**, **D** and **E**) and endolysin-holin promoter activity (**B**) for DE442 and DE442-derived mutants *ΔcckA*, *ΔchpT* and *ΔctrA*. **A,** LH2 pigment present in culture supernatant for indicated strains. **B,** Promoter activity (β-galactosidase activity) of cells containing the endolysin-holin promoter-*lacZ* reporter plasmid pXCA-555. **C** and **D**, Effect of the non-phosphorylatable CtrA(D51A) and phosphomimetic CtrA(D51E) on cell lysis for *ΔctrA* (**C**) and *ΔcckA* (**D**) mutant. Effect of predicted CckA kinase activity mutants CckA(HxxA) and CckA(Y589D) on cell lysis by (**E**).

To evaluate whether the CckA-ChpT-CtrA phosphorelay regulates expression of the Rcc00555-556 endolysin-holin system, the promoter-reporter plasmid pXCA-555 was constructed to contain 247 bp of 5' sequences and the annotated start codon of *rcc00555* fused in-frame to a *lacZ* reporter coding sequence. Disruption of *cckA*, *chpT* or *ctrA* reduced the β-galactosidase activity to 1.1%, 1.5% or 1.6%, respectively, of the parental strain DE442 levels (Figure 16B). In contrast, cultivation of strain DE555 containing plasmid pXCA-555 in a medium supplemented with 10 mM KPO_4 did not decrease the β-galactosidase activity compared to supplementation with 0.5 mM KPO_4 (Figure S2), consistent with the conclusion that high concentrations of phosphate inhibit cell lysis by a post-translational effect.

Therefore, the expression of the Rcc00555-556 endolysin-holin system is regulated by the CckA-ChpT-CtrA putative phosphorelay, consistent with the lack of lysis (Figure 16A) and the absence of RcGTA capsid release of from *cckA* and *chpT* mutants (Mercer *et al.*, 2012).

3.1.3.2 CtrA~P is required for cell lysis

In *C. crescentus*, the HK CckA is required for phosphorylation of CtrA to produce active CtrA~P (Curtis and Brun, 2010). Mutation of the aspartate (D) in the *C. crescentus* CtrA receiver domain to a glutamate (E) mimicks the role of the aspartate phosphorylation (D~P) (Domian *et al.*, 1997). Because expression of this CtrA(D51E) mutation in an *R. capsulatus cckA* mutant partially restored release of capsid protein (Mercer *et al.*, 2012) and *cckA* was required for lysis (Figure 16A), I hypothesized that phosphorylated CtrA was required for cell lysis. Introduction of the phosphomimetic CtrA(D51E), but not the non-phosphorylatable CtrA(D51A) into DE442 *ΔctrA* increased the release of photosynthetic pigments to the culture supernatant (Figure 16C), indicating that CtrA~P activates cell lysis, while non-phosphorylated CtrA had no effect.

If the absence of lysis in the *cckA* mutant is solely due to a lack of CtrA~P, then expression of the phosphomimetic CtrA(D51E) in the *cckA* mutant should restore cell lysis. Introduction of CtrA(D51E) to the DE442 *ΔcckA* mutant restored cell lysis, whereas no effect was observed when CtrA(D51A) was present in the *ΔcckA* mutant (Figure 16D). To confirm that the kinase activity of CckA is required for lysis, the catalytic histidine H399 was replaced by an alanine using site-directed mutagenesis to create plasmid pRCckA-HA (encoding CckA(H399A). The analogous mutation in *C. crescentus* CckA results in a protein with no kinase activity, but which retains phosphatase activity (Chen *et al.*, 2009b). Introduction of this pRCckA-HA to DE442*ΔcckA* did not restore lysis, in contrast to the WT allele encoded by pRCckA (Figure 16E).

Therefore, the absence of cell lysis in the *cckA* (and presumably in the *chpT*) mutant was due to an absence of CtrA~P, and the kinase activity of CckA is essential for this CtrA phosphorylation.

Based on the results in this thesis and described above, the results of Mercer *et al* (2012), and the conserved nature of the CckA-ChpT-CtrA phosphorelay in the Alphaproteobacteria (Bellefontaine et al., 2002, Kim et al., 2013, Pini et al., 2015, Willett et al., 2015), it appears that *R. capsulatus* CckA, ChpT and CtrA form a phosphorelay.

3.2 The RcGTA regulators ClpX and DivL, and a role for CtrA in cell division of *R. capsulatus*

3.2.1 The ClpX chaperone is required for RcGTA production and proper cell division

Because RcGTA production is regulated by CckA, ChpT and CtrA, and appears to function similarly to the phosphorelay in *C. crescentus* and *S. meliloti*, I hypothesized that the proteolytic regulation of CtrA by ClpXP that exists in other species was also conserved in *R.*

capsulatus. Because CtrA, ChpT and CckA are not essential for growth of *R. capsulatus*, I hypothesized that a loss of a component of the ClpXP protease, encoded by *rcc02608* (ClpX) and *rcc02609* (ClpP), would not be lethal. Furthermore, the resultant mutant was expected to have altered levels of CtrA that would result in dysregulation of RcGTA production. Because ClpP is a member of other proteases, such as ClpAP (Baker and Sauer, 2012), a *clpX* mutant was constructed to investigate the role of ClpXP in RcGTA production.

The predicted *R. capsulatus clpX* (*rcc02608*), which is located downstream of *clpP* (Figure 17A), was readily deleted by transduction of a *ΔclpX::aacC1* allele (conferring gentamicin resistance), yielding several gentamicin-resistant colonies, thereby indicating that ClpX, and presumably ClpXP, are not essential for viability of *R. capsulatus* under laboratory conditions. The resultant *ΔclpX* strain exhibited several growth defects, including a tendency to form extended lag phases (not shown), and increased doubling time (4 h) compared to the parental WT strain SB1003 (2.2 h). *R. capsulatus* cells are rod shaped, often in short chains (Weaver *et al.*, 1975). Inspection of *ΔclpX* cells by phase contrast microscopy revealed extensive cell filamentation compared to SB1003 (Figure 17B and C), indicating that *clpX* is required for proper cell division of *R. capsulatus*, as has been reported for *C. crescentus* (Jenal and Fuchs, 1998).

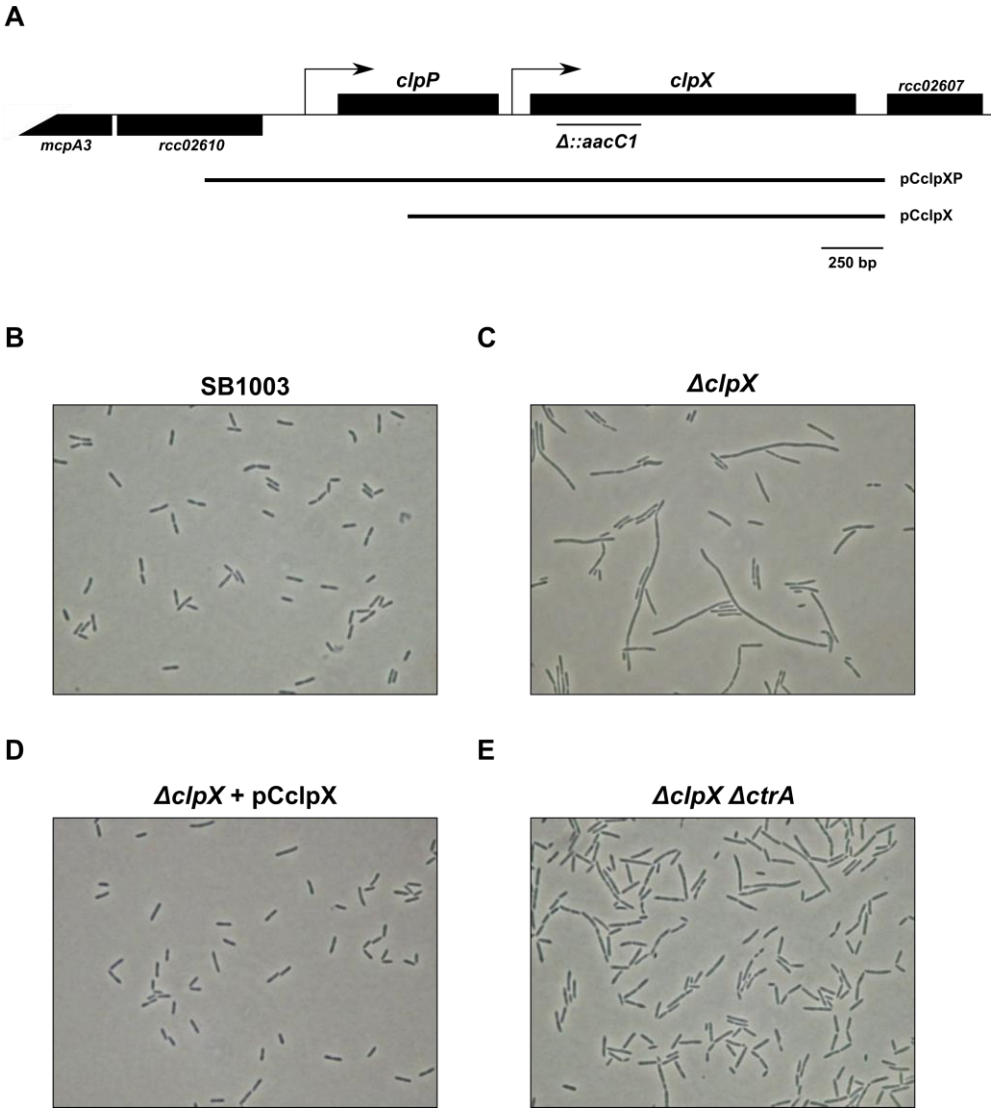

Figure 17 Cell filamentation defects of *ΔclpX* mutant

Genetic context of *clpX* (**A**) and phase contrast microscopy of strains (**B** to **E**). **A,** The *clpP* (*rcc02609*) and *clpX* (*rcc02608*) open reading frames with predicted promoters indicated by bent arrows. Encoded upstream of *clpP* is a hypothetical protein of unknown function and a protein predicted to contain methyl-accepting chemotaxis, HAMP and PAS domains. The orf downstream of *clpX* is annotated as "NADH ubiquinone oxidoreductase subunit, NDUFA12 family" protein. The region deleted and replaced by the *aacC1* casette (*Δ::aacC1*) to create the *ΔclpX* mutant and the inserts contained in complementation plasmids pCclpX and pCclpXP are indicated. **B,** The WT strain SB1003. **C,** SB1003 *ΔclpX.* **D,** SB1003 *ΔclpX* containing plasmid pCclpX expressing *clpX* in *trans*. **E,** SB1003 *ΔclpX ΔctrA* double mutant.

In *E. coli*, *clpX* is part of an operon with *clpP*, where *clpP* is the promoter-proximal gene (Gottesman *et al.*, 1993), however a weak promoter is present between *clpP* and *clpX* (Yoo *et al.*, 1994). Using BPROM, I similarly detected a putative promoter upstream of *clpP* as well as a promoter in the intercistronic region between *clpX* and *clpP* of *R. capsulatus* (Figure 17A). To determine whether *R. capsulatus clpX* expression is dependent on the promoter upstream of *clpP*, I created two complementation plasmids: Plasmid pCclpXP that contains the *clpP*/*clpX* orfs and the predicted promoter upstream of *clpP*, and plasmid pCclpX that contains *clpX* and the putative intercistronic promoter, but lacking the majority of *clpP* (Figure 17A).

Introduction of plasmid pCclpX (Figure 17D) and pCclpXP (not shown) to the *ΔclpX* strain eliminated the majority of the cell filamentation. Introduction of the *pCclpX* plasmid to the WT strain produced a similar minor alteration in cell shape to that of *ΔclpX* complemented with pCclpX, while no effect was observed by an empty plasmid (not shown). This indicates that the *clpX* mutation is not polar and that in contrast to *E. coli*, *R. capsulatus clpX* expression does not require the putative promoter upstream of *clpP*. *clpX* and *clpP* appear therefore to not be predominantly expressed as an operon. Furthermore, changes in the levels of ClpX protein and/or the ClpX:ClpP ratio, appear to have a small influence on cell shape.

To investigate whether *clpX* is required for RcGTA production, RcGTA capsid production was monitored over time (Figure 18 A), and transduction frequencies using the *clpX* mutant as donor were compared to the WT strain SB1003 after growth for an equivalent number of cell divisions (Figure 18B). Typical levels of RcGTA capsid protein were detected for SB1003 both intracellularly and extracellularly starting at 24 h after inoculation of a liquid medium culture. In contrast, elevated levels of capsid protein were detected both intracellularly

and extracellularly for the *ΔclpX* mutant, compared to SB1003 from 40 h onward (Figure 18A). Despite the elevated levels of capsid protein present outside of cells, no transduction was detected using the *ΔclpX* mutant as a donor (Figure 18B), indicating that the capsid protein produced and released by a *clpX* mutant does not represent transduction-capable RcGTA, analogous to the transduction-incompetent capsid protein accumulating inside a *cckA* mutant (Leung, 2010).

The activity of the RcGTA primary gene cluster promoter was elevated in the *ΔclpX* mutant (1.8-fold of SB1003, Figure 18C), consistent with the increased production of capsid protein (Figure 18A). Compared to the lysis-deficient *ΔcckA* mutant (Figure 16), the extracellular presence of the capsid protein in *ΔclpX* mutant cultures indicates cell lysis (Figure 18A). Activity of the endolysin-holin promoter was increased in the *ΔclpX* mutant (2.6-fold of SB1003, Figure 18C), and LH2 pigments were clearly detected in the culture supernatant of a DE442 *ΔclpX* mutant (Figure 18), confirming that the *clpX* mutation does not block cell lysis, unlike the *ΔcckA* mutation.

Therefore, ClpX (presumably as part of a ClpXP) is not required for expression of RcGTA genes, however ClpX is required for production of transduction-capable RcGTA. This was further investigated below (sections 3.3.3 and 3.5.3).

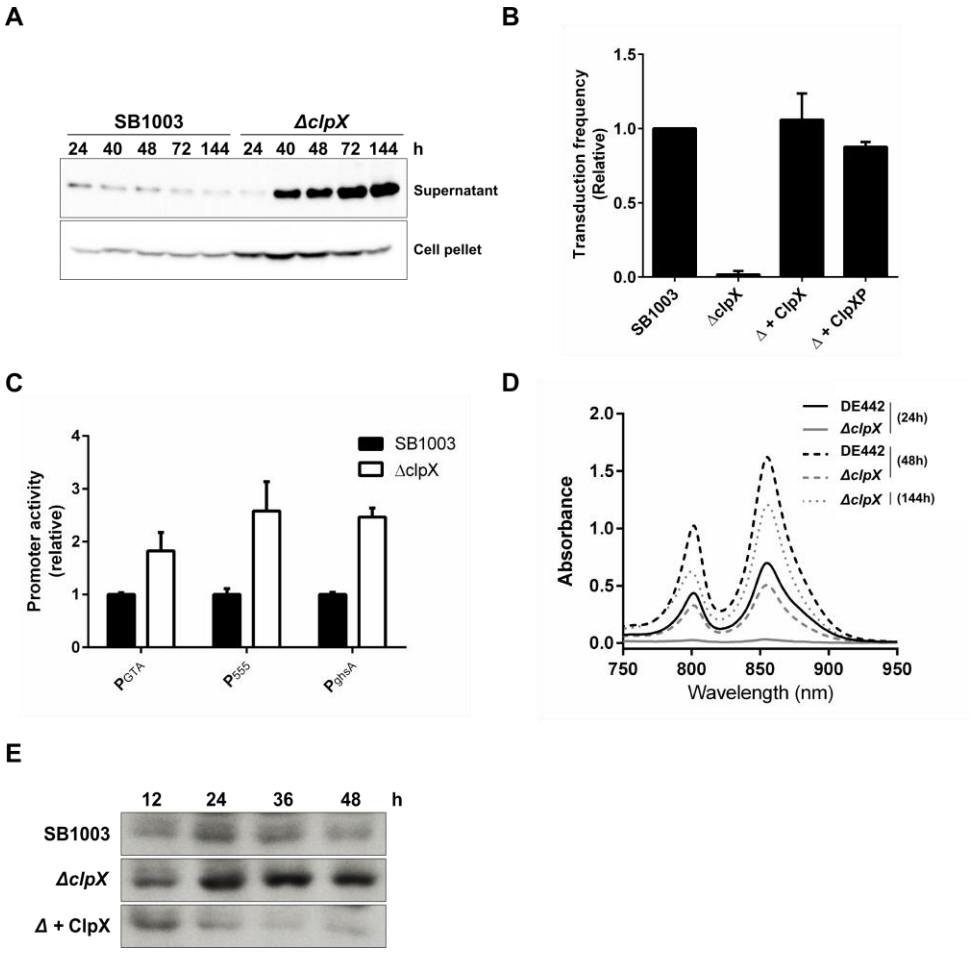

Figure 18. ClpX is required for RcGTA transduction, but not expression of RcGTA genes, and regulates CtrA levels.

A, Western blot of SB1003 and SB1003 *ΔclpX* cultures probed with RcGTA capsid anti-serum. **B,** Transduction frequencies of SB1003, SB1003 *ΔclpX*, and SB1003 *ΔclpX* complemented with plasmid pCclpX or pCclpXP. **C,** Promoter activity (β-galactosidase activity) of SB1003 or SB1003 *ΔclpX* cells containing promoter-*lacZ* reporter plasmids for the RcGTA cluster (using plasmid p601-g65), endolysin-holin (plasmid pXCA-555) or the RcGTA head fiber (pXCA-ghsA) promoter. **D,** Presence of the photosynthetic pigment LH2 in culture supernatant for DE442 and DE442 *ΔclpX*. **E,** Western blot of SB1003, SB1003*ΔclpX,* and SB1003*ΔclpX* complemented in *trans* by plasmid pCclpX, probed with *C. crescentus* CtrA anti-serum.

In **B** and **C**, values are expressed relative to SB1003 levels. Bars show the average and error bars represent standard deviation of two biological replicates.

3.2.2 Dysregulation of CtrA mediates cell filamentation.

Loss of *clpX* resulted in cell filamentation of *R. capsulatus* (Figure 17C). Similarly, the loss of ClpXP or perturbation of CtrA and CtrA~P levels result in filamentation of *C. crescentus* (Domian *et al.*, 1997, Jenal and Fuchs, 1998). I therefore hypothesized that the cell filamentation phenotype observed for the *R. capsulatus ΔclpX* mutant was due to elevated levels of CtrA.

Western blot analysis of *R. capsulatus* cells probed with serum raised against the *C. crescentus* CtrA protein showed a band of increased intensity at the predicted molecular weight of CtrA in the *ΔclpX* mutant, relative to the parental strain SB1003, and not in the strain complemented in *trans* by plasmid pCclpX (Figure 18E). It therefore appears that *R. capsulatus* CtrA is proteolytically degraded by ClpXP.

To test whether the elongated cell phenotype would be offset by removing CtrA, a *ΔclpX ΔctrA* double mutant was constructed. The *ΔclpX ΔctrA* double mutant produced cells with an intermediate phenotype between WT and the single *clpX* mutant (Figure 17E), indicating that a large part of the cell division defect of the *clpX* mutant results from elevated levels of CtrA.

On the basis of the different phenotypes when a *ΔcckA* mutant was complemented with the non-phosphorylatable or phosphomimetic CtrA proteins, the loss of *cckA* appeared to result in a lack of phosphorylation of CtrA (Figure 16D). Because a loss of CtrA phosphorylation (*ΔcckA*) or absence of CtrA (*ΔctrA*) had not been reported to cause cell division defects, I hypothesized that the major cause of the division defects in the *ΔclpX* mutant was due to elevated levels of CtrA~P. In *C. crescentus*, CckA controls the level of CtrA phosphorylation, and altered phosphorylation levels of CtrA result in cell morphology defects (Chen *et al.*, 2009b, Lori *et al.*, 2015, Tsokos *et al.*, 2011). Mutation of a conserved tyrosine to aspartate in CckA had been shown to turn the bifunctional CckA kinase/phosphatase into a constitutive kinase (Kim *et al.*,

2013, Lori *et al.*, 2015), and this residue is conserved in *R. capsulatus* CckA (Figure 19A). I therefore hypothesized that the analogous CckA(Y589D) mutation in *R. capsulatus* (Figure 19B) would increase CtrA phosphorylation, which would help me to evaluate whether an increase in CtrA~P concentration results in division defects.

Consistent with previous reports, the *ΔcckA* and *ΔctrA* mutants had no gross cell morphology defects compared to the WT strain SB1003 (Figure 19C to E left panels). Introduction of plasmid pRCckA (encoding the WT CckA) to SB1003 or *ΔcckA* did not alter cell morphology (Figure 19C and D, middle panels), however introduction of pRCckA-YD (encoding the CckA(Y589D) mutation) to either SB1003 or *ΔcckA* resulted in extensive cell filamentation (Figure 19C and D, right panels), indicating that increased CckA kinase activity results in cell filamentation. Because introduction of pRCckA-YD into the WT strain SB1003 resulted in filamentation, the CckA(Y589D) allele (at least when expressed from a plasmid) is dominant over the WT allele (Figure 19C). This genetic dominance indicates that the rate of ChpT phosphorylation by the combined WT and mutant alleles of CckA is greater than the phosphatase activity of WT CckA. Furthermore, because no filamentation is observed for the WT strain SB1003, this indicates that the levels of CtrA~P in SB1003 are generally low.

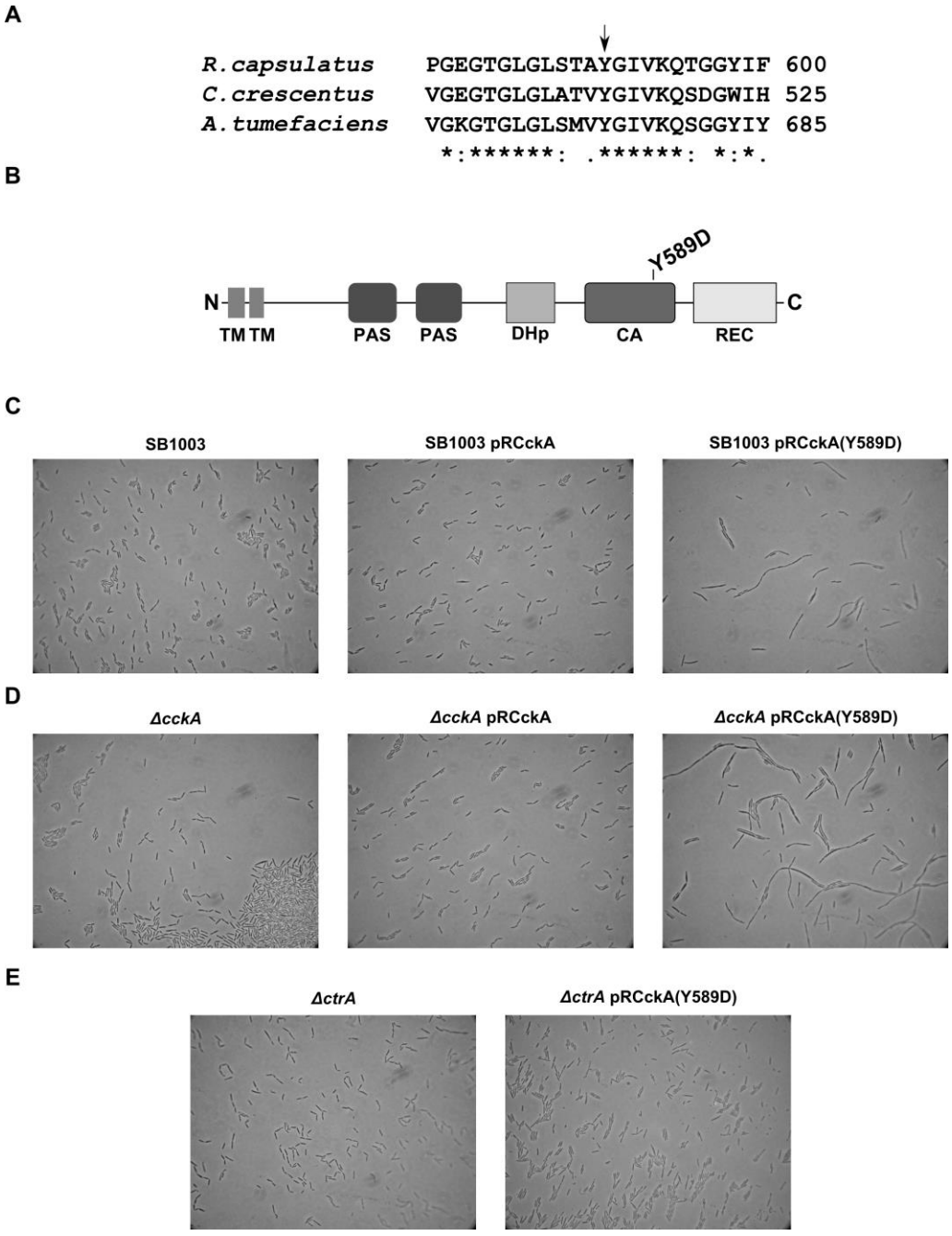

Figure 19. CckA with predicted constitutive kinase activity results in cell filamentation.

A, Sequence alignment of CckA from *R. capsulatus*, *C. crescentus* and *A. tumefaciens* showing the sequence around the conserved tyrosine (arrow). **B,** Schematic representation of the *R. capsulatus* CckA protein, with the Tyr 589 mutated to Asp in plasmid pRCckA-YD indicated. **C** to **E,** Phase contrast microscopy of cells of SB1003,

SB1003*ΔcckA* or SB1003*ΔctrA*, and strains containing plasmid pRCckA (expressing WT CckA) or pRCckA-YD (expressing CckA(Y589D).

Because the CckA(Y589D) mutation was hypothesized to result in an increased CtrA phosphorylation, I investigated whether the cell morphology change in a CckA(Y589D) mutant could be reversed by the elimination of CtrA. Introduction of pRCckA-YD into a *ΔctrA* mutant did not result in filamentation of the cells (Figure 19E, right panel), in contrast to the effects observed for SB1003 and *ΔcckA* (Figure 19C and D, right panels). Therefore, cell filamentation appears to result from the increased phosphorylation of CtrA by CckA(Y589D) and indicates that the CckA-ChpT-CtrA phosphorelay, despite not being required for cell division, is nonetheless involved in regulating cell division in *R. capsulatus*, as in *C. crescentus* and other species (Pini *et al.*, 2015, Quon *et al.*, 1996, Wang *et al.*, 2014, Willett *et al.*, 2015). Furthermore, my results are consistent with CckA and CtrA forming a phosphorelay (involving ChpT), and support the interpretation that the filamentation observed for the *clpX* mutant is largely due to an excess of the CtrA protein (Figure 17).

3.2.3 The enigmatic RcGTA regulator DivL.

3.2.3.1 A truncated homologue of *C. crescentus* DivL regulates RcGTA production

In *C. crescentus*, the kinase activity of CckA is regulated by DivL (Tsokos *et al.*, 2011); however no full length homologue of DivL was found to be encoded in the *R. capsulatus* genome using BLASTP combined with domain analysis. A transposon screen in the overproducer strain DE442 using a promoter-reporter plasmid that requires CckA, ChpT and CtrA for expression (the *ghsA/B* promoter-*lacZ* reporter plasmid pXCA-ghsA, see Chapter 3.4) identified *rcc00042* (Figure 20A) as required for expression of the *ghsA/B* promoter. BLASTP

analysis indicated that *rcc00042* encodes a protein similar to the *C. crescentus* DivL protein (not shown). The amino acid sequence of Rcc00042 is 38% similar to the N-terminal part of *Caulobacter crescentus* DivL, but lacks the C-terminal, non-functional histidine kinase-specific DHp and CA domains of *C. crescentus* DivL (Figure 20B). Interestingly, expression of *rcc00042* is down-regulated in a *ctrA* mutant, and a putative CtrA binding site is present in the *rcc00042* 5' region (Mercer *et al.*, 2010). Therefore *rcc00042* appeared to encode a truncated homologue of the *C. crescentus* DivL protein. Because *C. crescentus* DivL is required for CckA kinase activity, and because the transposon insertion appeared to turn off the *cckA* dependent *ghsA* promoter (see Figure 26A), we hypothesized that the *R. capsulatus* DivL homologue (Rcc00042) is similarly required to activate the kinase activity of CckA, resulting in phosphorylation of CtrA. A targeted disruption of *rcc00042* was therefore constructed (referred to as *ΔdivL*).

Comparison of the effect of the *ΔdivL* mutation in the strains WT SB1003 and the RcGTA-overproducer DE442 revealed, surprisingly, that the mutation had opposite effects on RcGTA production. The DE442 *ΔdivL* mutant decreased RcGTA transduction to 0.3% of the parental DE442 (Figure 21A), similar to the effect observed from a loss of CckA, and transduction was restored by introduction of DivL in *trans*. In contrast, the SB1003 *ΔdivL* mutation increased transduction 145-fold compared to SB1003, and *trans* complementation partially restored the transduction to 8-fold of SB1003 (Figure 21B). Similarly, capsid protein levels were greatly increased for the SB1003 *ΔdivL* mutant compared to SB1003 (Figure 21C).

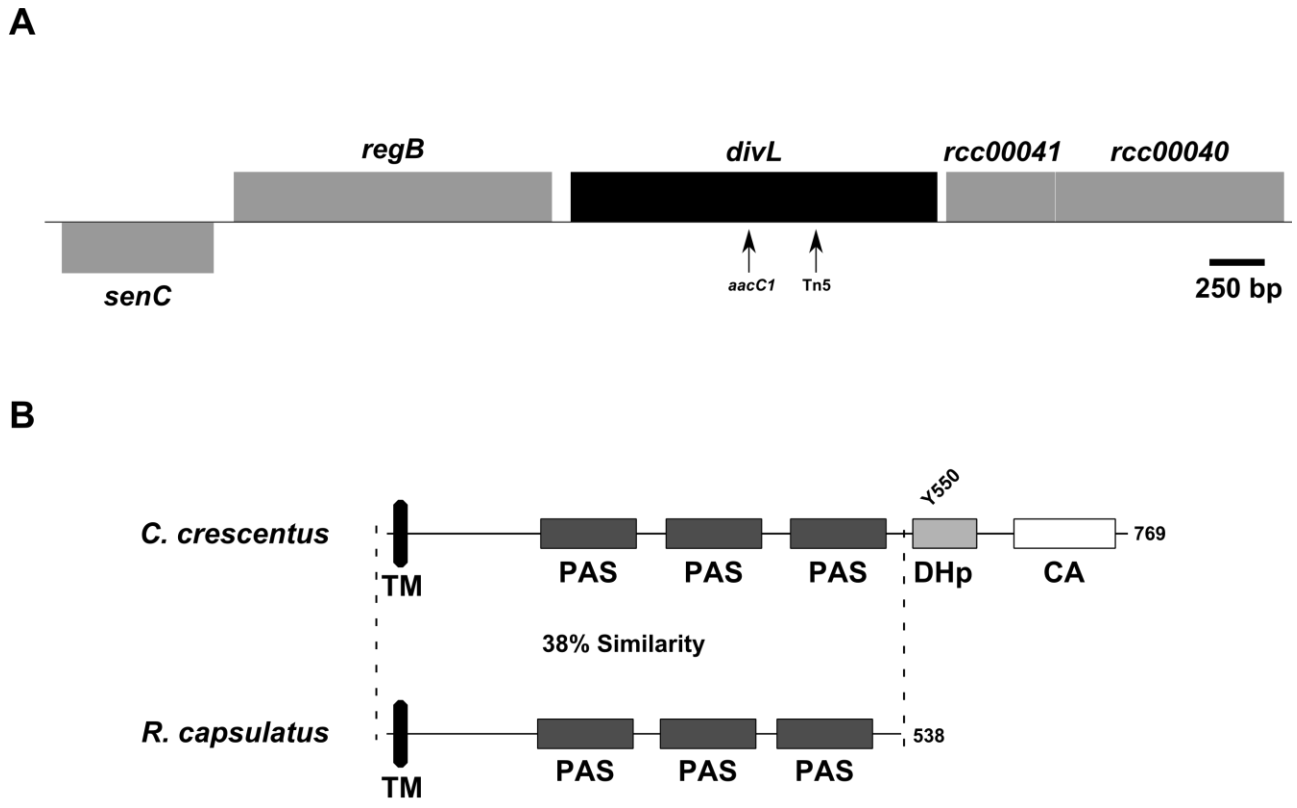

Figure 20 *R. capsulatus* DivL

A, The genetic context of *divL* (*rcc00042*). The redox regulator RegB and SenC (involved in respiration and photosynthesis gene expression) are encoded upstream of *divL*. A predicted member of the TsaE threonyl-carbamoyl adenosine biosynthesis proteins (*rcc00041*) and a predicted phosphotransferase (*rcc00040*) are encoded 5' of *divL*. The insertion site of the transposon and the NaeI site used to introduce *aacC1* to create *ΔdivL* are indicated by an arrow. **B,** Comparison of predicted domains in *C. crescentus* and *R. capsulatus* DivL proteins. The 38% amino acid sequence similarity of the conserved N-terminal region indicated. The tyrosine (Y550) occupying the typical histidine position in DHp is indicated.

To investigate whether the increase in RcGTA production observed for SB1003 *ΔdivL* was accompanied by increased expression of the RcGTA primary gene cluster, I measured the transcriptional activity of this gene cluster promoter using the reporter plasmid p601-g65 (Westbye *et al.*, 2013). The absence of DivL increased promoter activity 3.1-fold compared to the WT strain (Figure 21D), however similar increases were observed in response to the absence of CckA or ChpT, which increased activity 2.6 and 3.1-fold of WT, respectively. In contrast, the absence of CtrA reduced expression of this reporter to 28% of the WT strain, consistent with the absence of production of RcGTA in *ctrA* mutants (Lang and Beatty, 2000, Mercer *et al.*, 2012). The increased expression appeared to be independent of cell lysis, as the lysis-deficient SB555 strain (*Δ555*) had activity comparable to the WT strain (1.3-fold increased).

Therefore, DivL is involved in regulating RcGTA production; however the phenotypic effects of a loss of *divL* appeared to depend on the strain background. The *ΔdivL* mutation is the first example of a regulatory mutation exerting opposite effects on RcGTA production in different strain backgrounds.

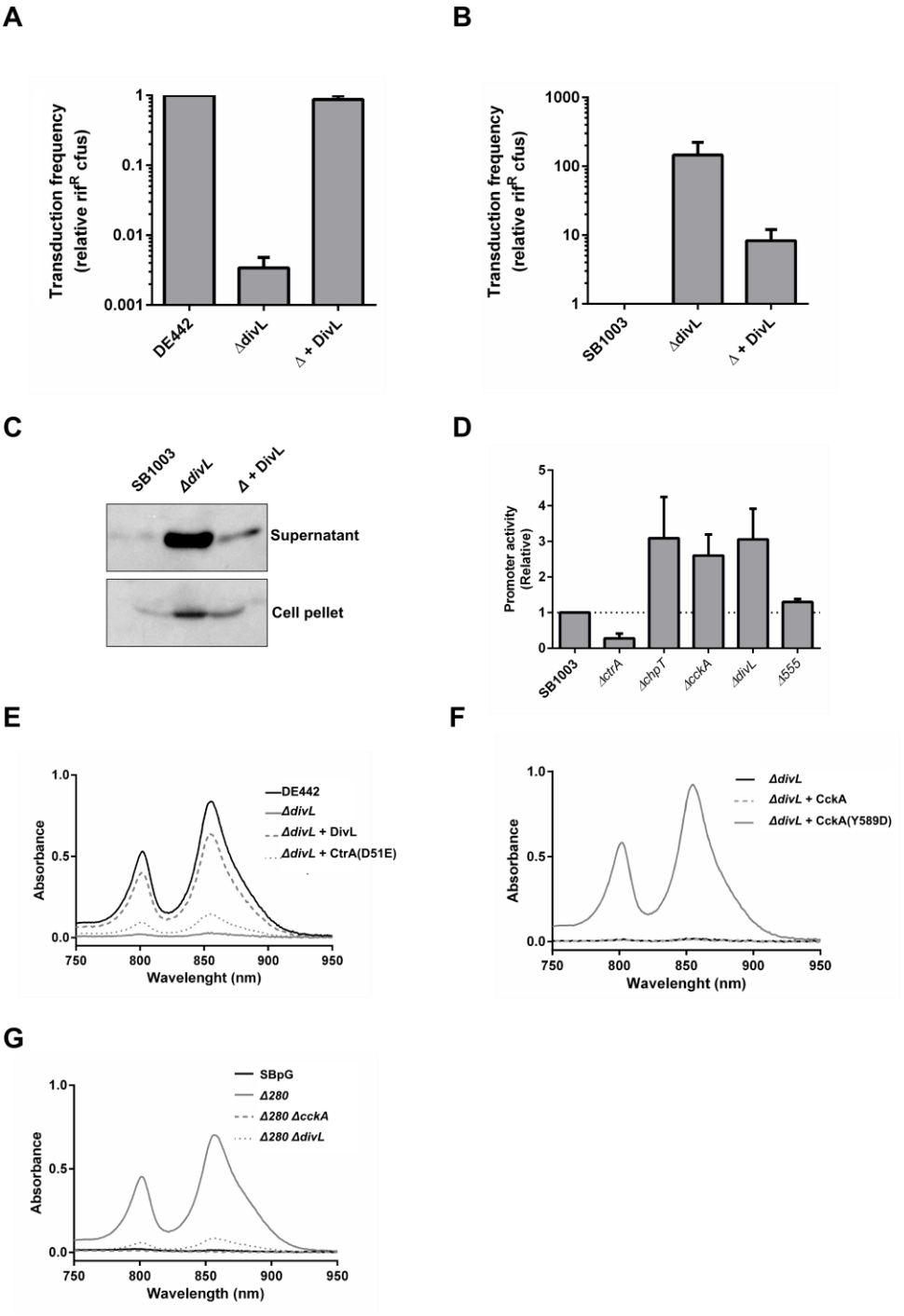

Figure 21 RcGTA is regulated by a DivL homologue

Transduction frequencies (**A** and **B**), western blot (**C**), absorbance spectra of culture supernatant (**D**, **E** and **F**), and promoter activity (**G**). **A,** DE442, DE442 *ΔdivL* and DE442 *ΔdivL* complemented in *trans* by plasmid pCdivL. **B,** SB1003, SB1003 *ΔdivL*, and SB1003 *ΔdivL* complemented in *trans* by pCdivL. **C,** Culture supernatant and cell

pellet fraction probed using RcGTA capsid protein anti-serum. **D,** Promoter activity (β-galactosidase activity) of strains harboring the RcGTA primary gene cluster promoter-*lacZ* reporter plasmid p601-g65. **E,** DE442, DE442 *ΔdivL*, and DE442 *ΔdivL* containing complementation plasmid pCdivL or pD51E encoding the phosphomimetic CtrA(D51E) protein. **F,** DE442 *ΔdivL* and DE442 *ΔdivL* containing plasmid pRCckA or pRCckA-YD (encoding CckA(Y589D). **G,** The WT-derived SBpG, the RcGTA-overproducer mutant SBpG *Δ280* and the double mutants SBpG *Δ280ΔcckA* and SBpG *Δ280ΔdivL*.

Bars represent means and error bars represent standard deviation of a minimum of three biological replicates.

3.2.3.2 DivL modulates CtrA phosphorylation

RcGTA regulatory mutant phenotypes are more distinct in the overproducer DE422 because of an increase in signal to noise when measuring RcGTA phenotypes (such as capsid production), and allows for easy detection of cell lysis by the presence of extracellular LH2 pigments. I exploited this to investigate the role of DivL using cell lysis as a reporter for the presence and phosphorylation state of CtrA. I found that *cckA*, *chpT*, *ctrA* and phosphorylation of CtrA are required for DE442 cell lysis (Figure 16A to E), and CtrA~P was reported to be required for the release of RcGTA from the WT strain SB1003 (Mercer *et al.*, 2012).

No release of the LH2 pigment to culture supernatant was detected for DE442 *ΔdivL* (Figure 21E). Introduction of plasmid pD51E, encoding the phosphomimetic CtrA(D51E) allele, into DE442 *ΔdivL* partially restored cell lysis (Figure 21E), indicating that DE442 *ΔdivL* lacks phosphorylated CtrA~P.

The *R. capsulatus* CckA(Y589D) mutation appeared to increase phosphorylation of CtrA (Figure 19). The analogous mutation in *A. tumefaciens* and *C. crescentus* CckA proteins have been reported to make CckA a constitutive kinase, and independent of the upstream regulator DivL and c-di-GMP levels (Kim *et al.*, 2013, Lori *et al.*, 2015). Introduction of pRCckA-YD into

DE442 *ΔdivL* (and to DE442 *ΔcckA*, see Figure 16E), but not the WT-encoding pRCckA, restored cell lysis (Figure 21F), indicating that in DE442 DivL is a regulator of CckA kinase activity and required for CtrA phosphorylation.

DE442 was created by chemical mutagenesis and contains hundreds of point mutations, and lacks the 133 kb plasmid pRCB133 present in the WT parental strain SB1003 (H. Ding unpublished and (Ding *et al.*, 2014)). Hao Ding recently identified a point mutation in *rcc00280* that explains the majority of the overproducer phenotype of DE442 (in preparation). Similarly, a knockout of *rcc00280* in a WT RcGTA background (strain SBpG, derived from SB1003 by insertion of a fluorescent protein gene between the RcGTA promoter and g1) yielding SBpG*Δ280* results in an RcGTA overproduction phenotype with accompanying cell lysis (Ding unpublished, and Figure 21G). Because the SBpG*Δ280* mutant lacks the multiple point mutations of DE442 relative to SB1003 and therefore is more closely related to SB1003 than DE442, the effect of the *ΔdivL* mutation on cell lysis was investigated in the strain SBpG*Δ280.* Disruption of *divL* reduced, but did not abolish, the release of LH2 pigment to the supernatant fraction compared to the parental strain SBpG*Δ280* (Figure 21G). In contrast, no lysis was observed for a SBpG*Δ280ΔcckA* double mutant (Figure 21G).

Based on the above results, it appears that the DivL protein is required for CckA kinase activity in the RcGTA overproducer strain DE442, consistent with the role of DivL in *C. crescentus* (Tsokos *et al.*, 2011). In the WT and the WT-derived RcGTA overproducer strain SBpG*Δ280*, the role of DivL appears to be more complex: a SB1003 *ΔdivL* mutant had increased transduction frequency (Figure 21B) and expression of the RcGTA primary cluster promoter was increased (Figure 21D) for SB1003. However, loss of CckA and ChpT, despite being required for release and transduction (Mercer *et al.*, 2012), had a similar effect on the promoter reporter

(Figure 21D). The *ΔdivL* mutation reduced, but was not required for observable cell lysis for the WT-derived overproducer strain SBpG*Δ280* (Figure 21F). It therefore appears that DivL is involved in regulating the phosphorylation state of CtrA through CckA in the WT strain SB1003.

3.3 RcGTA maturation I: genetic analysis of CckA, CtrA phosphorylation and ClpX

3.3.1 The *cckA* mutant produces DNA-containing, transduction incompetent RcGTA particles

The putative hybrid HK CckA is required for transduction and production of the lysis machinery, however not for the synthesis of the RcGTA capsid protein (Florizone, 2006, Mercer *et al.*, 2012). Furthermore, the intracellular contents of an overproducer strain Y262 *ΔcckA* mutant, although containing the capsid protein, were found to be incapable of transduction, indicating an RcGTA defect (Leung, 2010). Because DE442 produces increased levels of RcGTA compared to WT strains and Y262 (not shown), I decided to exploit this phenotype to investigate the role of CckA on the production of transduction-competent RcGTA particles.

The DE442 *ΔcckA* mutant accumulated intracellular capsid protein (Figure 22A), similar to SB1003 *ΔcckA* and Y262 *ΔcckA* mutants (Leung, 2010, Mercer *et al.*, 2012). To investigate whether the intracellular capsid protein represented functional RcGTA, transduction frequencies of intracellular and extracellular fractions were measured. Transduction was readily detected from DE442-derived culture supernatant (extracellular fraction), and dependent on phosphate concentration (Figure 22B). As expected, very low levels were detected for the *ΔcckA* mutant. Transduction frequencies observed for DE442 freeze-thaw cell lysates (intracellular fraction) were 7.8-fold higher for cells cultured in 10 mM phosphate compared to of 0.5 mM phosphate (Figure 22C), indicating that for DE442 the intracellular capsid levels (Figure 22A) correlated

with transduction levels (Figure 22C). In contrast, extremely low transduction frequencies were observed for equivalent lysates of *ΔcckA* cells, with transduction levels of 0.0075% or 0.010% (0.5 and 10 mM phosphate, respectively) of the level of the parental strain despite elevated capsid protein levels (Figure 22C), and this was complemented by CckA *in trans*.

Therefore, the majority of the capsid protein present in DE442 *ΔcckA* cells is not associated with functional RcGTA particles.

The assembly of phages is a multistep process (Aksyuk and Rossmann, 2011), and I hypothesized that CckA was required for one or more maturation steps to produce transduction-capable RcGTA. Loss of the predicted capsid prohead protease, encoded by *rcc01686* resulted in RcGTA capsid which migrated on SDS-PAGE at a higher molecular weight than WT (Figure S3). In contrast, the RcGTA capsid protein of *ΔcckA* cells (Figure 22A) migrated at a rate identical to that of the 30-kDa proteolytically cleaved protein of WT strains, indicating formation of a processed head structure analogous to that of prohead II or a later maturation stage of phage HK97 (Hendrix and Johnson, 2012). To determine whether CckA is required for DNA packaging and/or maturation of the RcGTA particle, culture supernatants and cell lysates were analyzed by native agarose gel electrophoresis (Serwer and Griess, 1999).

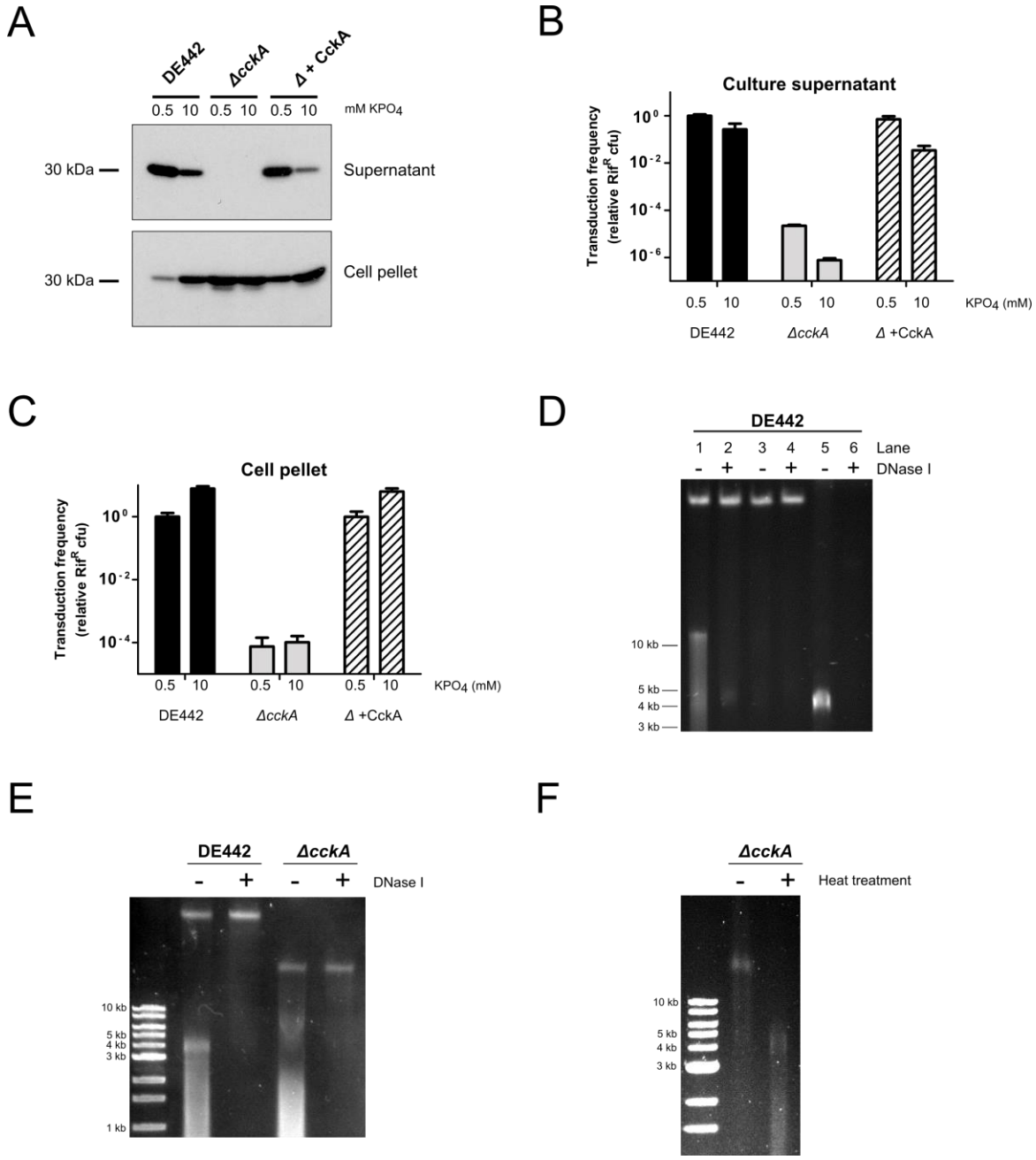

Figure 22 CckA is required for maturation of RcGTA

Western blots (**A**), transduction frequencies (**B** and **C**), and native agarose gels (**D** to **G**) of DE442, DE442 *ΔcckA*, DE442 *ΔcckA* complemented *in trans* by pRCckA, as indicated. **A,** Blots probed using RcGTA capsid protein antiserum. The approximate migration of the 30-kDa marker is indicated. **B,** Culture supernatants (extracellular fraction). **C,** Freeze-thaw-lysed cells (intracellular fraction). **D,** Lanes 1 and 2, filtered DE442 culture supernatant; lanes 3 and 4, resuspended pellet of supernatant after ultracentrifugation; lanes 5 and 6, heat-treated samples. **E,**

Native gel of cell lysates obtained by passage through a French press. **F,** Native gel of *ΔcckA* lysate obtained by passage through a French press subjected to DNase I followed by heat treatment.
Cells were cultured in RCVm medium (**A**, **B**, **C**, **E**), RCV (**F**) or YPS (**D**). Samples were normalized to the total amount of protein in French press lysates of culture (**A** and **B**), or cell pellet (**C**). Error bars represent the standard deviations of three biological replicates.

Filtered (0.2 µm pore size) DE442 culture supernatant contained an apparently large (>10 kb) DNA band revealed by ethidium bromide staining (Figure 22D, lane 1). This band was protected from DNase I digestion (Figure 22D, lane 2), in contrast to other DNA present (Figure 22D, compare lanes 1 to 3), and was pelleted by ultracentrifugation. Heat treatment, used to release DNA from viral particles (Duda *et al.*, 2009), resulted in an essentially complete conversion of the large DNA band to an ~4-kb band that was no longer protected from DNase I digestion (Figure 22D, lanes 5 and 6). Similarly, gel excision of the large DNA band, followed by guanidine thiocyanate protein denaturation and DNA purification by silica column chromatography, resulted in an ~4-kb band (not shown). These results strongly indicate that the large DNA band represents the ~4-kb DNA fragments inside RcGTA particles (Yen *et al.*, 1979), which migrate to the position of a larger DNA fragment because of a slower electrophoretic mobility of RcGTA particles compared to free DNA.

DE442 *ΔcckA* produced a DNase I-protected band that migrated to a position intermediate between the band from DE442 lysates and the 10-kb DNA size standard (Figure 22E). Heat treatment of *ΔcckA* mutant lysates resulted in a conversion of this band to a species migrating to the ~4-kb region of the gel (Figure 22F). Therefore, it appears that the *ΔcckA* mutant produces a capsid containing DNA, and therefore packages DNA; however, the

extremely low transduction frequency and the altered electrophoretic mobility indicate that almost all the particles fail to undergo maturation to produce transduction-capable RcGTAs.

3.3.2 Phosphorylation of CtrA is required for maturation of RcGTA.

Mercer *et al.* (2012) reported that introduction of both non-phosphorylatable CtrA(D51A) and phosphomimetic CtrA(D51E) restored capsid production in a *ΔctrA* mutant, however only CtrA(D51E) restored transduction. Because cell lysis was found to be restored in the *ΔcckA* mutant by introduction of the phosphomimetic CtrA(D51E) (Figure 16), I hypothesized that the maturation defect observed for the *ΔcckA* mutant was due to a lack of CtrA phosphorylation.

Cells lacking CtrA did not produce DNase I-protected DNA (Figure 23A), consistent with the requirement of CtrA for RcGTA capsid production and transduction (Mercer *et al.*, 2012). Introduction of the non-phosphorylatable CtrA(D51A) allele to the *ΔctrA* strain produced a band migrating at the same position as the band from the *ΔcckA* mutant, but no WT-band (Figure 23A). An unknown additional band migrating slower than the band in the *ΔcckA* mutant was also observed. Introduction of the phosphomimetic CtrA(D51E) appeared to produce a series of intermediate bands, however a band at the position of the WT RcGTA was absent. For the *ΔcckA* mutant, introduction of CtrA(D51E), but not CtrA(D51A) the resulted in the presence of a DNase I protected band at the position of the WT-band (Figure 23A), although there was a series of intermediate bands (see also migration of DE442 *ΔghsA* complemented in trans with *ghsA*, Figure 27E). Therefore, phosphorylation of CtrA appears to be essential for maturation of RcGTA to transduction competent particles. Because the nonphosphorylatable CtrA(D51A) restored production of a DNase I protected band in a *ΔctrA* mutant, and this band appeared to be identical to the band observed in the *ΔcckA* mutant, it appears that CtrA, but not phosphorylation of CtrA, is required for formation of the transduction-deficient RcGTA intermediate produced by

the *ΔcckA* mutant (Figure 22). Furthermore, because the phosphomimetic CtrA(D51E) restored formation of the WT-band in the *ΔcckA* mutant, but not in *ΔctrA,* it appears that both non-phosphorylated and phosphorylated CtrA are required for efficient maturation of RcGTA, at least in the overproducer strain DE442.

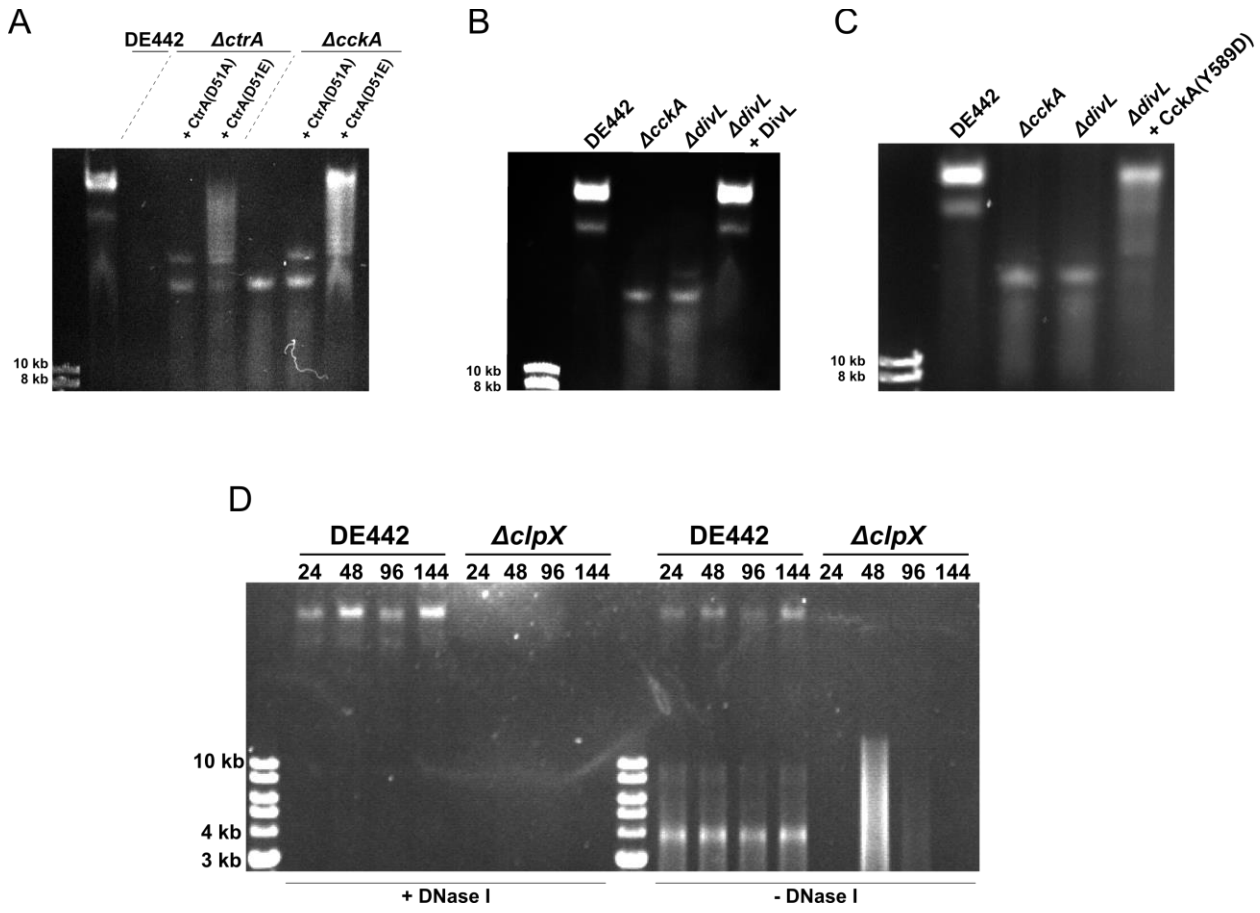

Figure 23 The effects of CtrA phosphorylation, loss of *divL* and loss of *clpX* on RcGTA maturation.

Native gels of cell lysate subjected to DNase I, unless otherwise noted. **A,** DE442, DE442 *ΔctrA* and DE442 *ΔcckA* contain plasmids pD51A and pD51E. **B,** DE442, DE442 *ΔcckA*, DE442 *ΔdivL* and DE442 *ΔdivL* complemented *in trans* by pCdivL. **C,** DE442, DE442 *ΔcckA*, DE442 *ΔdivL* and DE442 *ΔdivL* containing plasmid pRCckA-YD encoding CckA(Y589D). **D,** DE442 and DE442 *ΔclpX* cultured for the times indicated above each lane (in h).

The *R. capsulatus* DivL protein appears to regulate CckA kinase activity and thereby CtrA phosphorylation, at least in DE442 (Figure 21). Consistent with an absence of CtrA phosphorylation, the DE442 *ΔdivL* mutant lacked the DNase I protected WT DNA band but produced a band migrating at the same rate as the *ΔcckA* mutant, and this was complemented by DivL in *trans* (Figure 23B). Furthermore, the presence of the WT DNA band was restored by introduction of the predicted DivL-independent CckA(Y589D) allele into the *ΔdivL* mutant (Figure 23C). Therefore, DivL is required for maturation of RcGTA in DE442, consistent with DivL regulating CckA kinase activity.

3.3.3 Maturation defects of the *ΔclpX* mutant differ from those of the *ΔcckA* mutant

Both *ΔcckA* and *ΔclpX* mutants produce transduction deficient, matured capsid protein, however the phenotypes of these two mutants differed as the *ΔclpX* mutant released RcGTA from cells to the culture supernatant wheras *ΔcckA* did not (Figure 22A, Figure 18A).To investigate whether the capsid protein released from the *clpX* mutant (Figure 18A) was derived from DNA-containing, but transduction deficient particles similar to those produced by a *cckA* mutant, culture supernatant was treated with DNase I and analyzed using native gel electrophoresis. Although the RcGTA DNase I protected band characteristic of WT particles was readily detected in DE442 culture supernatant, no such band was detected for the DE442 *ΔclpX* mutant (Figure 23D) despite the elevated levels of capsid protein (Figure 18A), indicating that the capsid protein produced by the *ΔclpX* mutant is not in the form of a DNA-containing particle. Furthermore, no DNase I sensitive ~4 kb band was enriched in the DE442 *ΔclpX* mutant, in contrast to the parental strain DE442. However, a smear of DNase I sensitive DNA was observed for the *ΔclpX* mutant cultured for 48 h, but not 24 h, which appears to correlate with the release

of capsid protein and cell lysis of DE442 *ΔclpX* (Figure 18A and D), and could indicate leakage of packaged DNA from an immature particle.

3.4 RcGTA maturation II: an RcGTA maturation gene required for efficient adsorption to capsule coated cells

3.4.1 *ghsB* encodes an RcGTA attachment factor

To better understand the maturation defects of *ΔcckA* particles (see section 3.3.1), I inspected RNA microarray data of *ΔcckA* and *ΔctrA* mutants compared to WT obtained by collaboration with A. Lang's lab. The RcGTA gene cluster genes were all expressed in a *ΔcckA* mutant (not shown). However, the two orfs *rcc01079* and *rcc01080* (hereon referred to as *ghsA* and *ghsB*) were found to be downregulated compared to WT in the absence of either CckA or CtrA. Because *ghsA* and *ghsB* are located directly adjacent to a capsular receptor biosynthetic gene cluster (Brimacombe *et al.*, 2013) (Figure 24A), co-purify with RcGTA (Chen *et al.*, 2009a), and are required for maximal frequencies of RcGTA-mediated gene transduction (Lang *et al.*, 2012) I hypothesized that *ghsB* encodes a protein involved in the attachment of RcGTA to the cellular capsule.

Bioinformatic analysis of *ghsA* and *ghsB* detected no conserved domains from the PFAM or SMART databases (http://pfam.xfam.org; http://smart.embl-heidelberg.de). However, homology modelling of the predicted GhsB using Phyre2 (Figure 24B and C, and Table S2) and Swiss-model (http://www.sbg.bio.ic.ac.uk/phyre2; http://swissmodel.expasy.org) indicated a similarity to carbohydrate-binding proteins and members of the immunoglobulin superfamily. The top ranked templates (Table S2) were to carbohydrate binding modules (CBMs), which are non-catalytic domains typically present on modular glycoside hydrolases and promote the

association of the enzyme to insoluble polysaccharides (Boraston *et al.*, 2004). Further bioinformatics analysis of the predicted structure using 3DLigandSite (http://www.sbg.bio.ic.ac.uk/3dligandsite/) indicated that tyrosine 177 (Figure 24C) may be involved in binding carbohydrates.

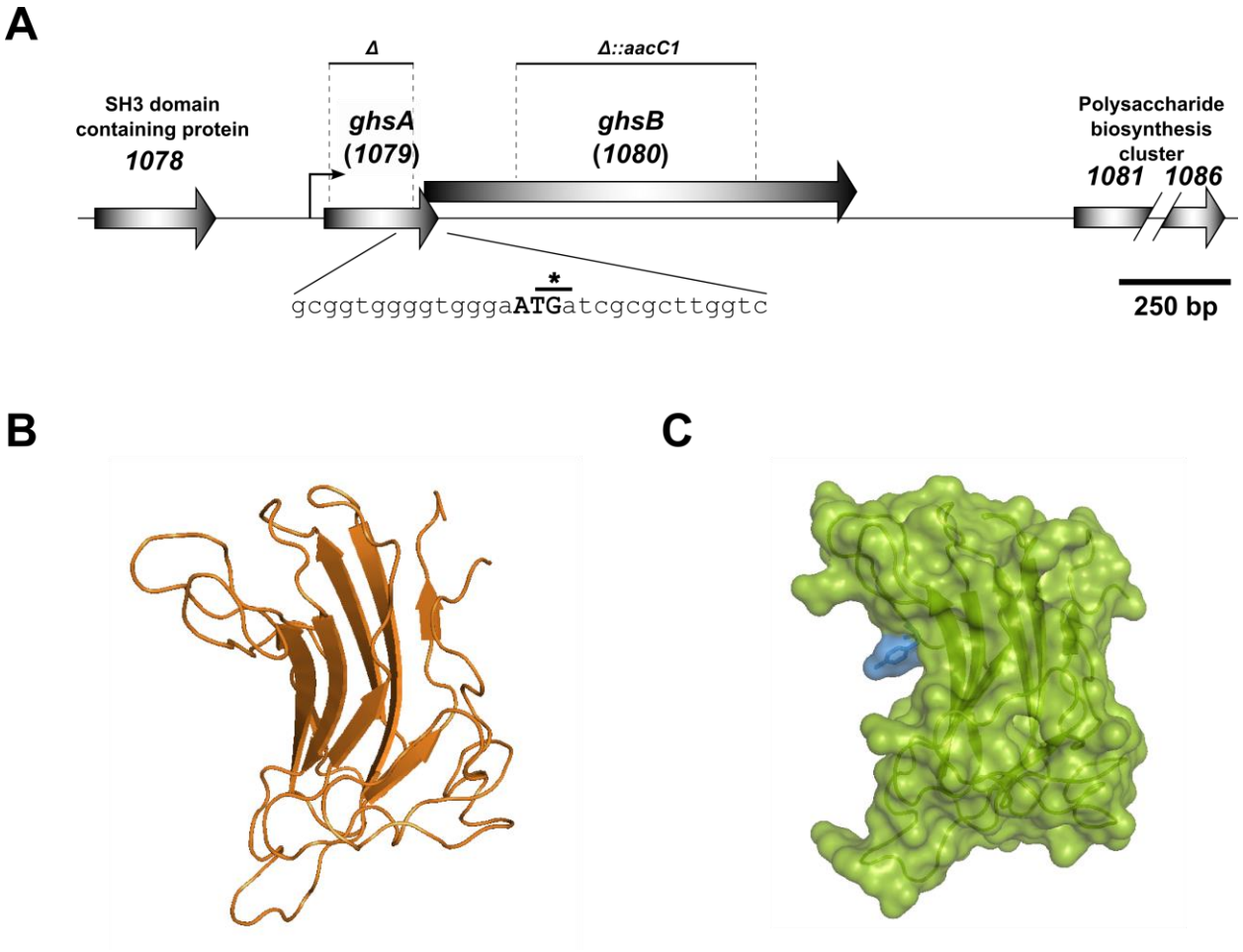

Figure 24 Genomic context of *ghsA-ghsB* and predicted structural model for GhsB

The genomic context of the overlapping ORFs *ghsA* (*rcc01079)* and *ghsB (rcc01080)* (**A**) and Phyre2 predicted structural model (residues 85-256, deemed confidently predicted) of GhsB (**B** and **C**). **A,** The uncharacterized ORF *rcc01078* predicted to produce an SH3-domain containing protein is present upstream, and the polysaccharide biosynthesis cluster *rcc01081-1086* required for capsule production is present downstream. Annotated stop codon for *ghsA* (star), start codon for *ghsB* (UPPERCASE) and putative *ghsA/ghsB* promoter (bent arrow) are indicated.

Fragments deleted to construct *ΔghsA* and *ΔghsB* are indicated above orf. Drawn to approximate scale as indicated by the 250 bp bar. **B**, Ribbon model of GhsB. **C**, Surface model of GhsB, showing predicted tyrosine 177 (blue) predicted to be involved in binding carbohydrate.

The models of GhsB (**B** and **C**) were based on Phyre2 predicted structure, see text for details.

To test whether GhsB was required for RcGTA attachment to the CPS, I created a deletion mutant of *ghsB* (*ΔghsB*) in the RcGTA overproducer strain DE442. A western blot of culture supernatant probed with RcGTA capsid antiserum indicated that the *ΔgshB* mutant releases amounts of RcGTA capsid protein similar to the parental strain (Figure 25A, bottom). However, the transduction frequencies in experiments using the *ΔghsB* mutant as a source of RcGTA were 4% of the parental strain, indicating that RcGTA particles lacking GhsB had a severe impairment in transduction efficiency (Figure 25A, top).

To test whether *ghsB* is required for RcGTA to efficiently bind to cells, I assessed the binding affinity to recipient cells by comparing the transduction frequency of a solution of RcGTA particles before and after binding to cells. Adsorption of DE442-derived RcGTA (WT-RcGTA) to capsule-producing WT strain B10 cells reduced the residual transduction frequency to 2.7% of the value compared to a no-cells control (Figure 25B). In contrast, RcGTA from the DE442 *ΔghsB* mutant (ΔGhsB-RcGTA) had a residual transduction frequency of 44% (Figure 25B). I interpret this ~16-fold difference as indicating that GhsB is required for maximal adsorption of RcGTA to WT cells.

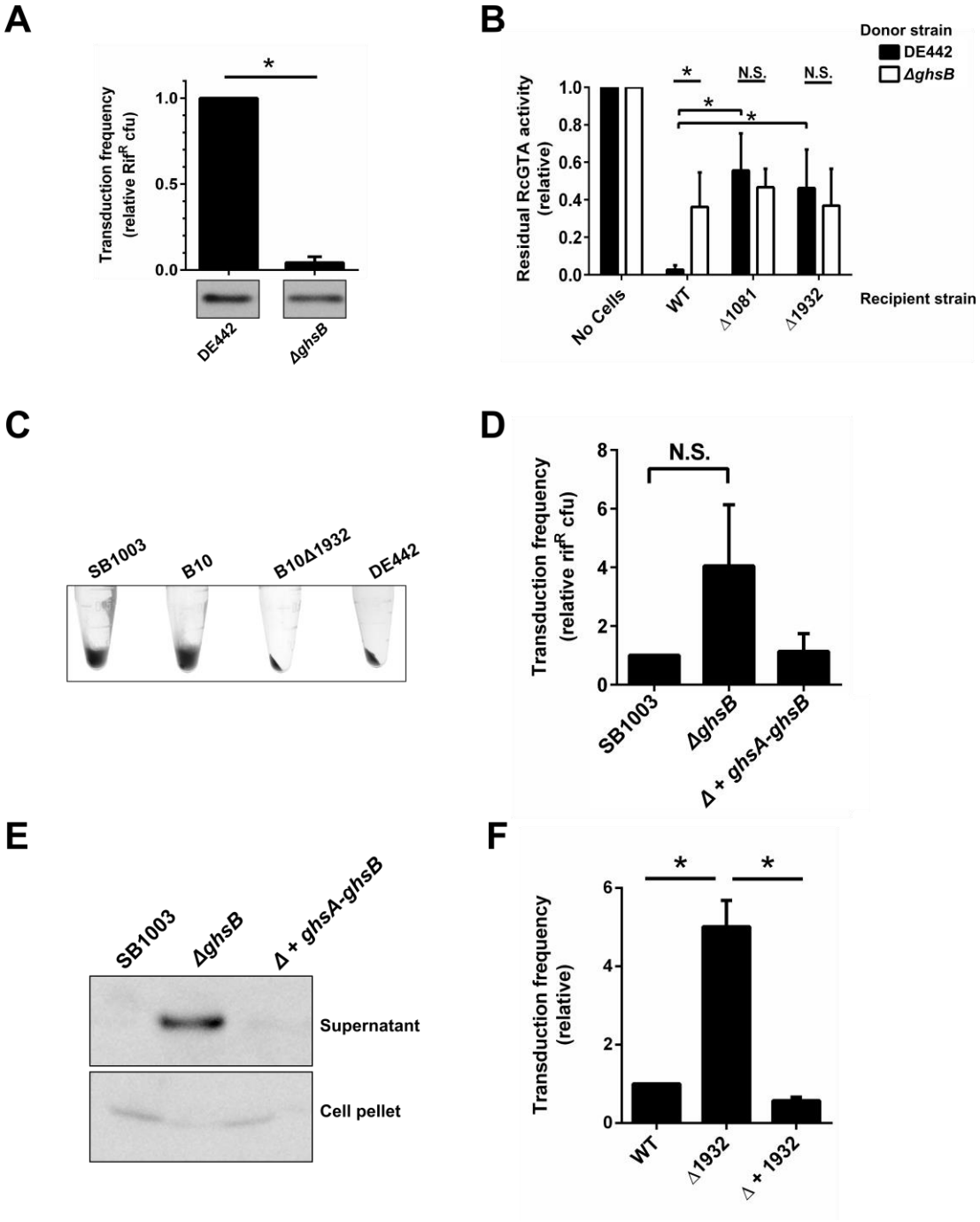

Figure 25 GhsB is required for maximal adsorption of RcGTA to cells.

A, Transduction frequencies of RcGTA from overproducer DE442 and DE442 *ΔghsB* to WT recipient strain B10 (top), and western blot showing RcGTA capsid protein levels in cell-free culture supernatants (bottom; cropped from the same blot). **B,** Cell binding affinity of RcGTA. Residual RcGTA activity in DE442 or DE442 *ΔghsB*

derived supernatant after adsorption to WT B10 cells, capsule-less B10 *Δ1081* and B10 *Δ1932* relative to a no-cells control. **C,** Macroscopic assay for capsule production by WT strains SB1003 and B10, capsule-less B10 *Δ1932* mutant and RcGTA overproducer strain DE442. The presence of capsule is indicated by the absence of a tight cell pellet. **D,** Transduction frequencies using cell-free culture supernatants of the WT strain SB1003, mutant SB1003 *ΔghsB*, and *trans*-complemented SB1003 *ΔghsB*(pCghsA-ghsB). **E,** Western blot showing RcGTA capsid protein levels in the cell-free culture supernatant and cell pellet fractions of the WT strain SB1003, mutant SB1003 *ΔghsB*, and *trans*-complemented SB1003 *ΔghsB*(pCghsA-ghsB). **F,** Transduction frequencies of rifampin resistant B10, capsule-less B10 *Δ1932* and *trans*-complemented B10 *Δ1932*(pI1932). Error bars represent the standard deviation between three (**A**, **C** and **E**) or four (**B**) biological replicates.

To test whether the cell attachment-defects of ΔGhsB-RcGTA are dependent on capsule production, I compared the adsorption of WT-RcGTA and ΔGhsB-RcGTA to the capsule null mutants B10 *Δ1081* and B10 *Δ1932*, which lack a predicted group 1 glycosyl transferase and a WecA homologue, respectively (Brimacombe *et al.*, 2013). No statistically significant difference between WT-RcGTA and ΔGhsB-RcGTA binding affinity to the two CPS-mutants Δ*1081* and Δ*1932* was detected (Figure 25B), indicating that the binding difference between WT-RcGTA (containing GhsB) and ΔGhsB-RcGTA depends on CPS production by the recipient cell. Therefore, the GhsB protein appears to be involved in binding of RcGTA to the CPS.

3.4.2 Transduction frequencies of recipient cells are highly dependent on binding of RcGTA to CPS

In WT *R. capsulatus* cultures RcGTA is produced by ~0.15 to 3 % of the cells (Fogg *et al.*, 2012a, Hynes *et al.*, 2012) and cells are covered by CPS (Brimacombe *et al.*, 2013), whereas the mutant strain DE442 is an RcGTA overproducer in which ~26% of cells produce RcGTA, and which appears to contain a lower level of CPS than the WT strains SB1003 and B10 (Figure

25C). Because RcGTA binding to cellular CPS appears to be dependent on GhsB (see above), it was hypothesized that in a WT strain population GhsB-containing particles would be predominantly bound to cells, resulting in a lower number of RcGTA particles in the culture supernatant compared to otherwise isogenic mutant strains lacking either the RcGTA capsule attachment factor (*ΔghsB*) or cellular capsule production (*Δ1932*).

The mutant strain SB1003 *ΔghsB* was found to have a 4.1-fold greater transduction frequency when compared to the WT strain SB1003 (Figure 25D). However, a western blot probed with RcGTA capsid antiserum indicated that the slightly increased transduction frequency from the SB1003 *ΔghsB* culture supernatant was due to a greatly increased amount of RcGTA capsid protein, compared to the parental WT strain SB1003 (Figure 25E). Similarly, reduced levels of capsid protein were present in the cell pellet fraction of the SB1003 *ΔghsB* mutant (Figure 25E). I attribute this difference between *ΔghsB* mutants of SB1003 (Figure 25D and E) and DE442 (Figure 25A) to be due to a combination the greater amount of capsule present on strain SB1003, relative to strain DE442, and the reduced amount of RcGTA produced by strain SB1003 relative to strain DE442. To confirm that the absence of capsule in the RcGTA-producing strain results in increased transduction frequencies of the culture supernatant, amount of RcGTA (as indicated by transduction frequency) produced by the capsule-less B10 *Δ1932* mutant was compared to the parental WT strain B10. The absence of capsule production resulted in a 5-fold increase in transduction (Figure 25F). Therefore, in WT-derived populations the absence of RcGTA-to-CPS binding, either from loss of GhsB on RcGTA, or loss of CPS on producing cells, results in much more RcGTA present in the culture supernatant.

3.4.3 Expression of *ghsA/ghsB* is regulated by the phosphorelay homologues CckA-ChpT-CtrA, and quorum sensing

The annotated start codon of *ghsB* overlaps the last two codons of *ghsA* (Figure 24A), and so it appeared likely that these two ORFs are co-transcribed. A putative promoter upstream of *ghsA* (Figure 24A) was predicted using Softberry BPROM (http://www.softberry.com/all.htm) (Solovyev and Salamov, 2011), and a segment of DNA containing this putative promoter was found to initiate transcription after fusion to *lacZ*, supporting the promoter prediction. The resultant pXCA-ghsA promoter-reporter plasmid was used to investigate regulation of *ghsA*/*ghsB* expression in several regulatory mutants.

RcGTA-dependent gene transduction is greatly decreased in knockout mutants of the phosphorelay CckA-ChpT-CtrA homologues (Mercer *et al.*, 2012), and *cckA* was found to be required for lytic release of RcGTA (Westbye *et al.*, 2013). The *ghsA/ghsB* promoter activity (*β*-galactosidase activity) of the reporter plasmid pXCA-ghsA was measured in *ΔcckA*, *ΔchpT* and *ΔctrA* knockout strains, and I observed that the absence of CckA or ChpT reduced the activity to 0.3% of the parental strain, whereas the absence of CtrA reduced the activity to less than 0.1% of parental levels (Figure 26A). Therefore, the CckA-ChpT-CtrA phosphorelay is required for expression of *ghsA/ghsB*, consistent with the aforementioned microarray data.

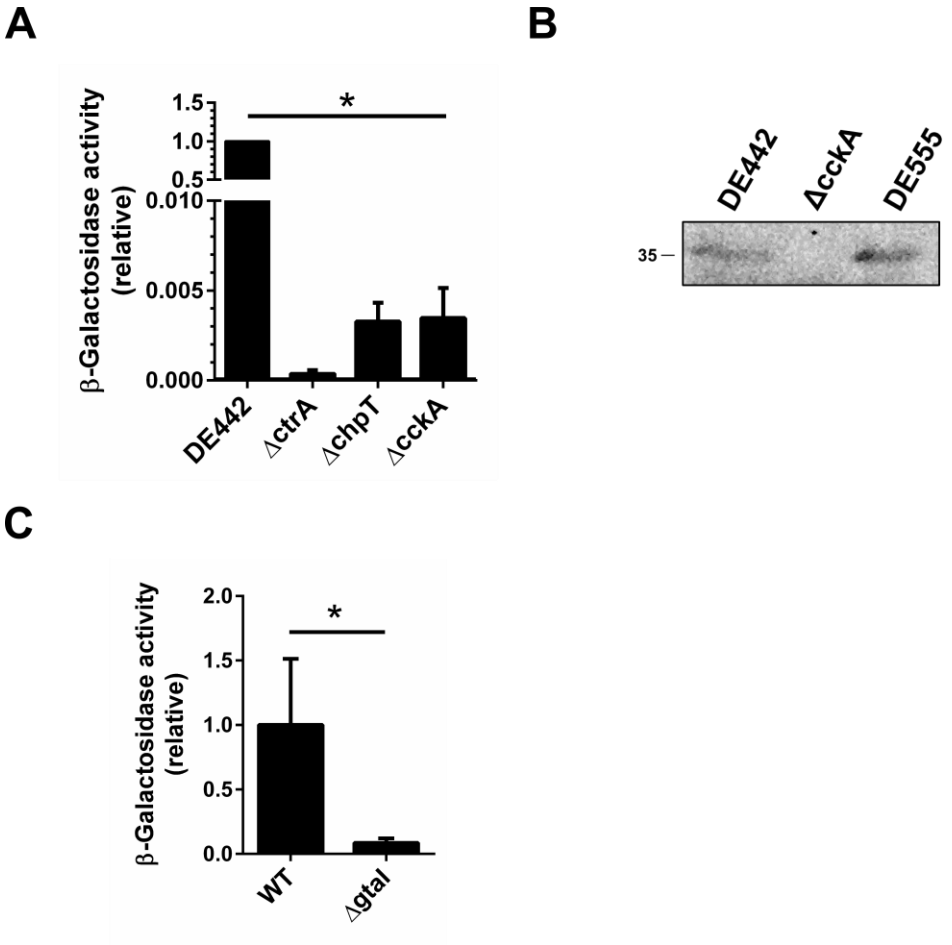

Figure 26 *ghsA/ghsB* expression is regulated by CckA-ChpT-CtrA and GtaI

Promoter activities (*β*-galactosidase activities) of cells containing the *ghsA/ghsB* promoter reporter plasmid pXCA-ghsA (**A** and **C**), and detection of 6xHis-tagged GhsB in the cellular fraction (normalized by OD_{660}) (**B**). **A,** Strain DE442 compared to mutants DE442 *ΔctrA*, DE442 *ΔchpT* and DE442 *ΔcckA*. **B,** Western blot probed with anti-6xHis antibody of strain DE442 compared to mutants DE442 *ΔcckA* and DE555 containing plasmid pCghsA-ghsB_His (expresses 6xHis-tagged GhsB). **C,** WT strain B10 and mutant B10 *ΔgtaI*. Error bars represent the standard deviation between three biological replicates.

To confirm that the reduced transcription of *gshA-ghsB* as indicated by the reporter plasmid results correlated with the amount of GhsB production, I created a C-terminally 6xHis-tagged version of GhsB (predicted mass: 33.7 kDa), and performed a western blot of cells probed

with an anti-6xHis antibody. A band migrating close to the 35 kDa marker was detected in the overproducer strain DE442, and of increased intensity in the endolysin-negative lysis-deficient strain DE555 (Figure 26B) (Westbye *et al.*, 2013). In contrast, no band was visible for the lysis-deficient DE442 *ΔcckA* mutant (endolysin expression requires CckA, see section 3.1.3.1), indicating that production of GhsB requires CckA, consistent with the promoter activity data (Figure 26A).

RcGTA production is differentially regulated in different culture growth phases, accomplished in part through quorum-sensing regulation. An acyl-homoserine lactone (C16-acyl-HSL) synthesized by GtaI is an inducer for RcGTA and regulates CPS production (Brimacombe *et al.*, 2013, Schaefer *et al.*, 2002). To test whether *ghsA/ghsB* expression is similarly regulated by GtaI, I compared the promoter activity of plasmid pXCA-ghsA in the WT strain B10 to that of the mutant B10 *ΔgtaI*. The promoter activity in cells lacking GtaI was reduced to 8.5 % of the parental strain (Figure 26C), indicating that *ghsA/ghsB* expression is dependent on quorum sensing.

3.4.4 GhsB is a CckA-dependent maturation factor, and located on the RcGTA capsid

Loss-of-function mutants of the putative hybrid HK gene *cckA* produce transduction-deficient RcGTA particles that, although containing DNA, have altered native gel electrophoresis migration compared to WT-RcGTA (see section 3.3.1). Based on this, I suggested that CckA is required for the production of one or more maturation factors required for fully functional RcGTA particles. Because *cckA* is required for activity of the promoter upstream of *ghsA* and *ghsB*, I hypothesized that GhsB is a CckA-dependent maturation factor, and tested this hypothesis by evaluation of the native gel electrophoresis migration properties of ΔGhsB-RcGTA particles.

ΔGhsB-RcGTA particles contain DNA, based on the presence of a DNase I-resistant band that stained with ethidium bromide, which after heat treatment migrated at ~4.5 kb, characteristic of RcGTA-DNA (Figure 27A). However, intact ΔGhsB-RcGTA migrated at a distinctly faster rate than WT-RcGTA (Figure 27A), and this phenotype was complemented by *ghsA/ghsB* in *trans* using plasmid pCghsA-ghsB. Therefore, GhsB appears to be a CckA-dependent maturation factor. Furthermore, the migration rate of ΔGhsB-RcGTA was distinct from that of ΔCckA-RcGTA particles (Figure 27B), and introduction of the *ΔghsB* mutation into the *ΔcckA* strain did not alter gel migration compared to *ΔcckA* alone, consistent with the requirement of CckA for GhsB expression (Figure 26A and B). Because the particles produced by the *ΔcckA* and *ΔcckAΔghsB* strains show the same gel migration phenotype, and different from that of *ΔghsB* alone, the *ΔcckA* mutation is dominant over the *ΔghsB* mutation, apparently because maturation factors in addition to GhsB are absent in a *cckA* mutant.

GhsA and GhsB were reported to co-purify with RcGTA (Chen *et al.*, 2009a), indicating that they are components of the mature particle. It was previously suggested these two proteins are tail fibers (Lang *et al.*, 2012), which would be consistent with our experiments described in the preceding text. However, some phages contain structures on the capsid that are involved in attachment to recipient cells (Barr *et al.*, 2013, Guerrero-Ferreira *et al.*, 2011). With this in mind, I deleted the RcGTA predicted major tail (tail tube) gene *rcc01691*, which encodes a Phage_tail_2 PFAM family (PF06199) member and is present 5' of the predicted gpG/gpGT chaperone genes, similar to the lambda major tail protein gene gpV (Casjens and Hendrix, 2015, Lang and Beatty, 2001). Because RcGTA is morphologically similar to long tailed phages, this *Δ1691* mutation was expected to block the tail assembly pathway but allow for the production of DNA-filled heads.

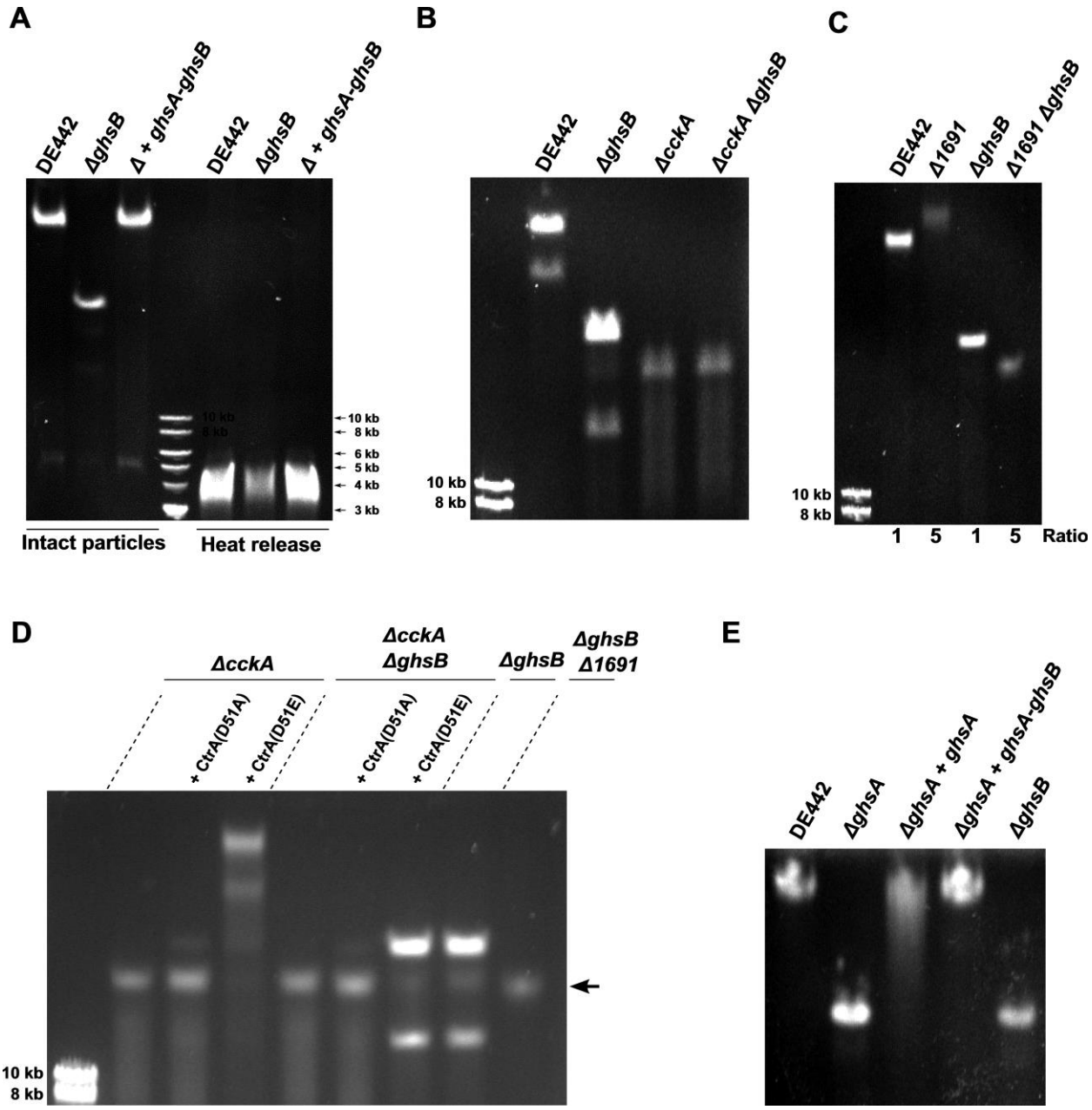

Figure 27 GhsB influences RcGTA gel migration and is located on the RcGTA head.

Native agarose gel migration of intact RcGTA particles (DNase I-resistant bands) stained for DNA obtained from indicated strains. **A,** DE442, mutant strain DE442 *ΔghsB*, and *trans*-complemented DE442 *ΔghsB*(pCghsA-ghsB). Lanes to the right of ladder are heat released, DNase-untreated samples. **B,** DE442, mutant DE442 *ΔghsB*, the regulatory mutant DE442 *ΔcckA*, and double mutant DE442 *ΔcckAΔghsB*. **C,** DE442, the major tail protein mutant

DE442 *Δ1691*, mutant DE442 *ΔghsB*, and the double mutant DE442 *Δ1691ΔghsB*. **D,** DE442*ΔcckA*, DE442 *ΔcckAΔghsB* double mutant, DE442 *ΔghsB* and DE442 *Δ1691ΔghsB* double mutant, containing plasmids pD51A or pD51E as indicated. **E,** DE442, DE442 *ΔghsA*, *trans*-complemented DE442 *ΔghsA*(pCghsA) and DE442 *ΔghsA*(pCghsA-ghsB), DE442 *ΔghsB*.
The ratio of the volume of sample loaded is indicated at the bottom of each lane in **C**.

As expected, the *Δ1691* mutant was unable to perform transduction (not shown), and in native gel electrophoresis produced a DNase I-resistant, ethidium bromide-stained faint band with an altered migration rate compared to the WT-RcGTA (Figure 27C), which I attribute to DNA-replete, head-only RcGTA particles. Because a lack of GhsB strongly influenced the native gel migration of RcGTA (Figure 27A), a deletion of *ghsB* in the *Δ1691* mutant was expected to change the migration rate only if GhsB were associated with the head. In contrast, no migration change would be expected if GhsB were associated with only the tail. The *Δ1691/ΔghsB* double mutant produced a distinct gel band that had an increased gel migration rate compared to WT-RcGTA, Δ1691-RcGTA, and ΔGhsB-RcGTA, consistent with GhsB being located on the RcGTA head as opposed to the tail.

Expression of the phosphomimetic CtrA(D51E), but not the nonphosphorylatable CtrA(D51A) in the *ΔcckA* mutant restored an RcGTA band at the position of the WT gel migration (Figure 23A and Figure 27D), but also produced a smear or ladder-like pattern. To investigate whether this could be due to induction of *ghsB* expression by CtrA(D51E), a gel migration experiment was performed using the *ΔcckAΔghsB* double mutant. Expression of CtrA(D51E), but not CtrA(D51A), in this double mutant resulted in a band similar to the *ΔghsB* mutant with no smear above this band (Figure 27D), consistent with *ghsB* expression requiring CtrA~P.

To test whether GhsA is also required for RcGTA maturation, a markerless and inframe deletion of *ghsA* was created. The resultant DE442 *ΔghsA* strain produced a particle that migrated at the same position as the *ΔghsB* mutant (Figure 27E). Introduction of *ghsA* in *trans* from plasmid pCghsA mostly restored the WT band, although a faster-migrating smear was observed analogous to the bands observed for CtrA(D51E) complemented strains (Figure 23A). Introduction of plasmid pCghsA-ghsB to *ΔghsA* restored the WT band, with no smear.

It therefore appears that GhsA and GhsB are both maturation factors, and the absence of *ghsA* produces an identical gel migration shift from DE442 to an absence of *ghsB*.

3.4.5 GhsA and GhsB homologues are present in two *R. capsulatus* phages.

Because similar Ig-domains are found in proteins that are otherwise unrelated and from different phages, it has been proposed that such Ig-like domains present in phage genomes are transferred extensively by horizontal gene transfer (Fraser *et al.*, 2007). Bioinformatic analysis of GhsA and GhsB using BLASTP (http://blast.ncbi.nlm.nih.gov) and Emboss Needle (http://www.ebi.ac.uk/Tools/psa/emboss_needle) indicated that homologues are encoded in the genomes of two phages reported to infect *R. capsulatus*. GhsA and GhsB have 48.7% and 87.7% amino acid similarity to gp57 and gp58 of the prophage RcapMu, which is resident in the SB1003 genome (Fogg *et al.*, 2011). GhsA and GhsB are also similar to two proteins encoded in the genome of phage RcapNL (unpublished, GenBank NC_020489) having 70.6% and 20.6% similarity, respectively, to gp29 and gp30. In both cases, the two orfs are located next to each other in the same order as *ghsA* and *ghsB*. It therefore appears possible that the *ghsA* and *ghsB* have been acquired from either a common ancestor shared with phages infecting *R. capsulatus*, or transferred by horizontal gene transfer.

In summary, GhsB is required for efficient binding to cells containing the polysaccharide capsule. The *ghsA* and *ghsB* genes appear to be co-transcribed, and require the CckA-ChpT-CtrA phosphorelay and the GtaI/GtaR quorum sensing system for maximal expression.

3.4.6 An attempt to biochemically characterize GhsB

The orf encoding GhsB was cloned into expression vector pET28a(+) to create a C-terminally 6xHis tagged recombinant protein. GhsB-6His was expressed using the IPTG-inducible T7 promoter, and soluble protein purified using Ni-NTA, to a concentration of 0.7 mg/mL (Figure 28A).

Because the genetic and bioinformatics studies indicated that GhsB was a polysaccharide binding protein that is required for RcGTA binding to the polysaccharide capsule of B10 (Figure 25), several assays were attempted to investigate interaction with the capsule. I was unable to detect protein-cell binding (Figure 28B), inhibition of transduction or auto agglutination of cells in the presence of 6xHis GhsB (not shown). A reproducible GhsB-dependent effect was observed on the cell pellet of B10 during RcGTA transduction assays. After collecting cells by centrifugation, samples containing B10 cells and GhsB protein did not form a typical pellet, but rather formed a "smear" along the wall of the tube, which was independent of addition of RcGTA (Figure 28C). B10 samples lacking GhsB did not show this phenotype (Figure 28C). The effect was less pronounced for capsule-less B10*Δ1932* cells, but proved less reproducible (not shown).

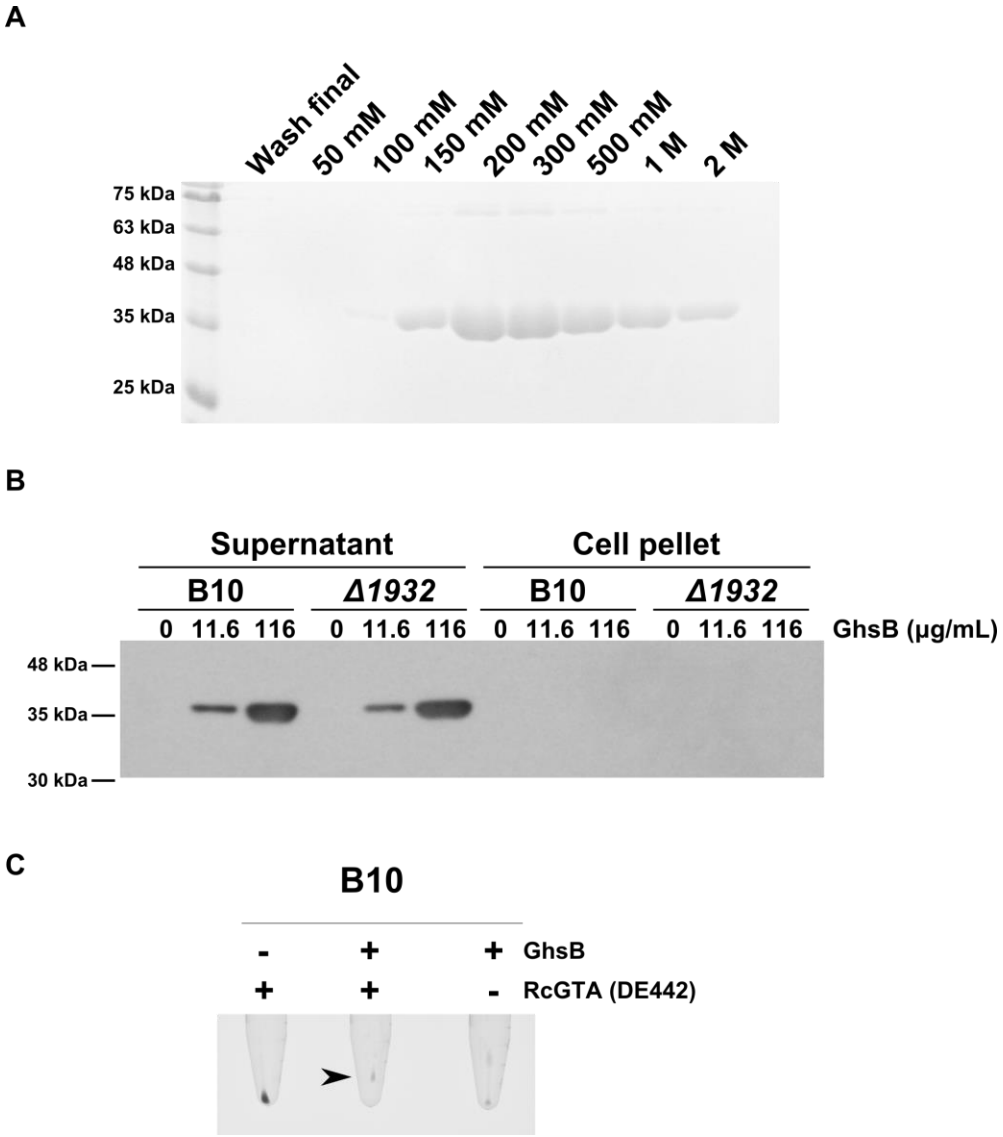

Figure 28 Production of recombinant GhsB-6His

A, SDS-PAGE of eluted fractions of C-terminally 6xHis tagged GhsB protein from Ni-NTA column, stained with Coomassie brilliant blue. The concentration of imidazole in each elution is indicated above the lanes. **B,** Western blot of B10 or capsule-less B10 *Δ1932* cells incubated with purified GhsB protein, probed with anti-6xHis antibody. Cells resuspended to OD_{660} of 0.3 in 50 mM $NaPO_4$ 10 mM NaCl were incubated with purified GhsB-6His protein at indicated concentrations (above lanes) for 1h. Cells were separated from supernatant fraction by centrifugation (16,000 rcf, 5 min), samples separated on SDS-PAGE, and western blotted. **C,** Effect of GhsB-6His addition to B10 cells on cell pellet formation in a transduction assay. Arrowhead indicates smear.

3.5 RcGTA maturation III: electron microscopy of RcGTA

3.5.1 GhsB is required for the formation of head spikes, and RcGTA particles have tail side fibers and an intricate baseplate

The initial description of RcGTA morphology reported the presence of spike-like structures on the RcGTA capsid, and suggested the presence of a tail side fiber (Yen *et al.*, 1979). Because GhsB is involved in cell attachment (Figure 25B) and appears to be located on the head (Figure 27C), we hypothesized that GhsB is involved in forming head spikes. I affinity-purified His-tagged RcGTA particles from the DE442 parental and the *ΔghsB* mutant strains using a modification of the method of Chen *et al.* (2009), and visualized the particles using TEM with negative staining. Images were obtained of RcGTA particles in side view (Figure 29A and B), as well as particles that appeared to be attached head-down, tail-up (Figure 29C and D. Additional images in Figure S4 and Figure S5). The TEM of WT-RcGTA (Figure 29A) showed particles with an ~30 nm diameter capsid and short, striated tails (45 to 50 nm long, ~8 nm wide), consistent with previous reports of RcGTA (Chen *et al.*, 2009a, Yen *et al.*, 1979).

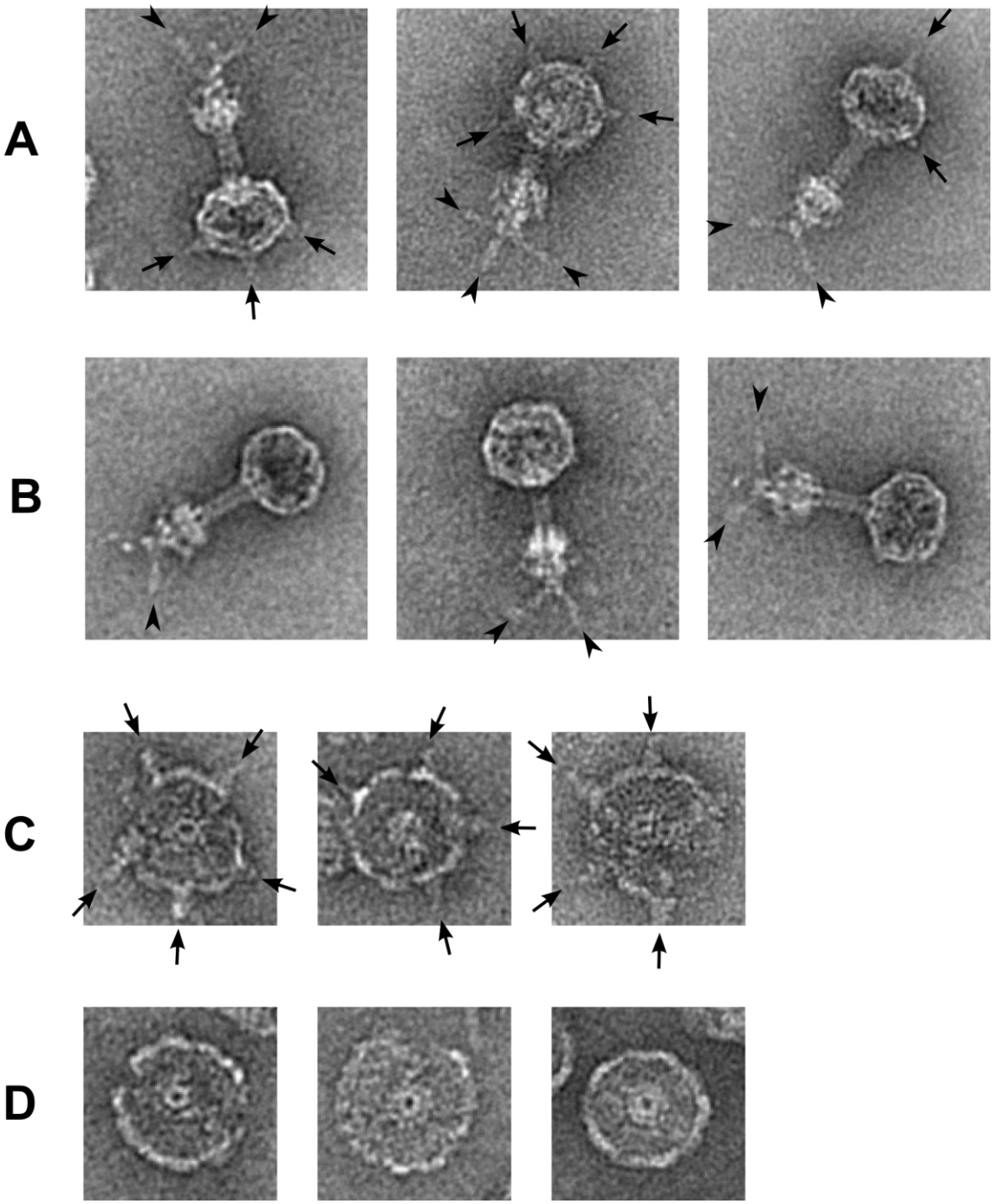

Figure 29 Electron micrographs of purified RcGTA particles

WT-RcGTA (**A** and **C**) and ΔGhsB-RcGTA (**B** and **D**). Images show particles that are thought to have adsorbed to the carbon support sideways (**A** and **B**) and head down (**C** and **D).** Arrows indicate head spikes, and arrowheads indicate side tail fibers.

Furthermore, the micrographs clearly showed the presence of head spikes (Figure 29A, arrows). As the micrographs were of higher resolution than previously published RcGTA micrographs, the head spike dimension could be better measured as up to 12 nm long and estimated to be between 4 to 7 nm wide at the base. For the RcGTA particles attached head-down, the spikes are clearly shown to radiate out from the capsid structure (Figure 29C, arrows). Up to five spikes were observed per particle, and they appeared to be attached to the vertexes of the capsid. No head spikes were detected for the ΔGhsB-RcGTA particles in the side view (Figure 29B), nor for the particles attached head-down (Figure 29D). Therefore, we suggest that the *ghsB* gene is needed to obtain RcGTA head spikes.

These EMs also clearly reveal the presence of three to four fiber-like structures of about 20 nm length present at the tip of the tail (Figure 29A and B, arrowheads), which appear to be the side fiber previously suggested to exist by Yen *et al.* (1979). Newly visible in these images is an electron-dense structure approximately two to three times wider than the tail, present near the tip of the tail, above the side fiber, which could be a tail tip complex. Because of the size of this structure, I suggest that this is a baseplate structure, analogous to the baseplates formed by the *Myoviridae* T4 and many lactococcal *Siphoviridae* (Leiman *et al.*, 2010, Spinelli *et al.*, 2014). In contrast to the absence of head spikes on the *ΔghsB* mutant particles, the side fiber and baseplate-like structure were clearly present on ΔGhsB-RcGTA, indicating that GhsB is required for the formation of head spikes but not the side fiber, nor the baseplate-like structure.

3.5.2 CckA is required for correct tail assembly

ΔCckA-RcGTA migrated at a rate undistinguishable from the spike and tail-less DE442 *ΔghsBΔ1691* double mutant (Figure 27D). To investigate morphological differences in the

ΔCckA-RcGTA, French pressed, crude cell lysate from the RcGTA overproducer DE442 and a DE442*ΔcckA* mutant were analyzed by TEM. The DE442-derived lysate contained tailed as well as tail-less capsids (Figure 30A). In contrast, the majority of particles from DE442 *ΔcckA* lacked a recognizable tail structure, consisting of capsid only (Figure 30B). Furthermore, in the *ΔcckA* lysate sporadic particles were observed that contained tail-like structures which appeared to have aberrant lengths, and lacked a baseplate or tail-fiber like structure on the head-distal end (Figure 30C). These structures were similar to polytubes reported for certain tail mutants of phage lambda (Katsura, 1990, Mount *et al.*, 1968), and are therefore referred to as such.

To improve image quality, ΔCckA-RcGTA particles were purified from the crude lysate using the 6xHis-tagged capsid protein (pRhoG5CTH). Confirming the observations from cell lysate, the purified ΔCckA-RcGTA were composed mainly of isolated capsids (heads) (Figure 30D). Numerous polytubes were present (Figure 30D to F) and appeared in several instances to be attached to the capsid (Figure 30E). It appeared that the polytubes were sensitive to the purification or TEM procedure, as many appeared to have broken (Figure 30E and F). Furthermore, no spikes were observed on the capsids, consistent with the requirement of CckA for GhsB expression (Figure 26A). Therefore, the majority of particles produced by the *ΔcckA* mutant are tail- and spike-less DNA-filled capsids, consistent with the results from the gel migration assay. However, a minor fraction of the particles contains aberrant, long tail-like structures that appear to be rigid polytubes.

A

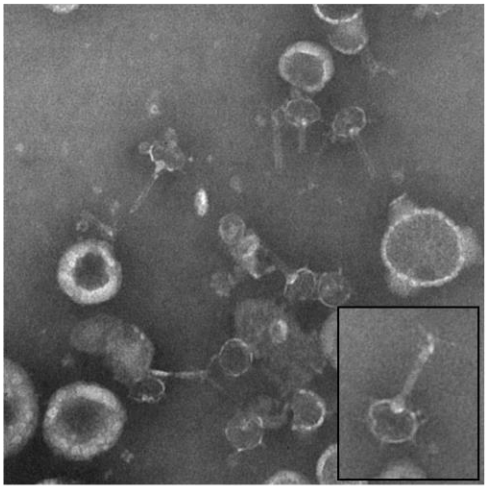

B

C

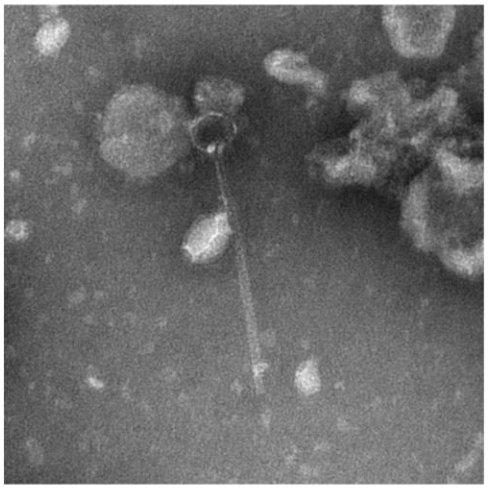

D

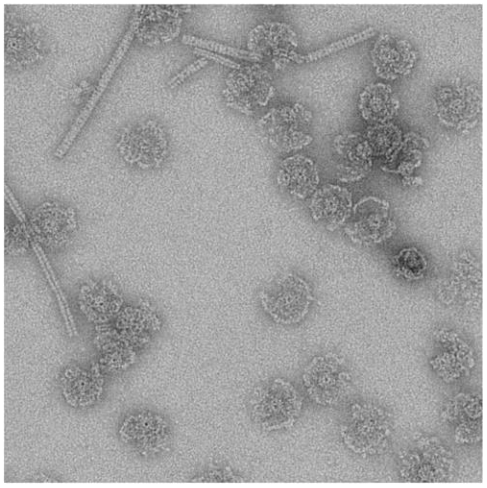

E

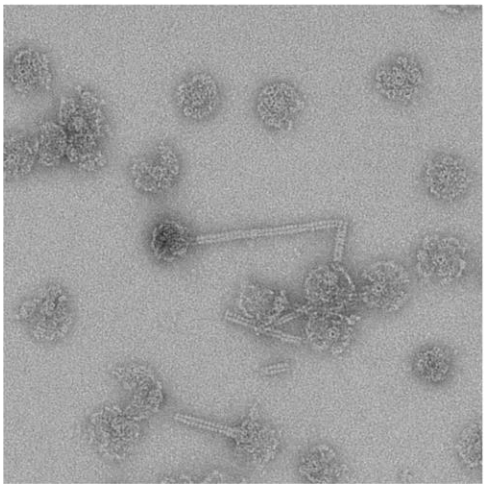

F

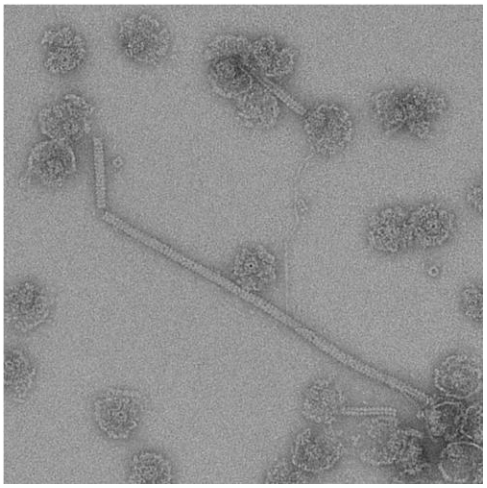

Figure 30 Polytube formation in the absence of CckA

TEM of crude lysate (**A** to **C**) or affinity purified (**D** to **F**) RcGTA particles produced by DE442 (**A**), or DE442 *ΔcckA* (**B** to **E**).

Inset shows an intact WT-RcGTA particle with head spikes, SFP and baseplate-like structure. The rounded vesicle-like structures observed in crude lysate are attributed to be membrane vesicles (chromatophores).

3.5.3 The *ΔclpX* mutant produces a spike-less prohead II-like structure

The capsid protein produced by the *ΔclpX* mutant had been proteolytically cleaved by the prohead protease (Figure 18A), indicating the assembly of a prohead II like structure or a later intermediate. To investigate the morphology of ΔClpX-RcGTA, particles were affinity purified using the 6xHis capsid tag from pRhoG5CTH and analyzed by TEM.

Electron micrographs of ΔClpX-RcGTA revealed numerous capsid-only structures Figure 31, with no sign of the tails or polytubes observed in WT-RcGTA or ΔCckA-RcGTA samples, respectively. Furthermore, very few of the structures contained spike-like structures.

It therefore appears that the *ΔclpX* mutant produces capsid-only particles, analogous to the HK97 Prohead II structures.

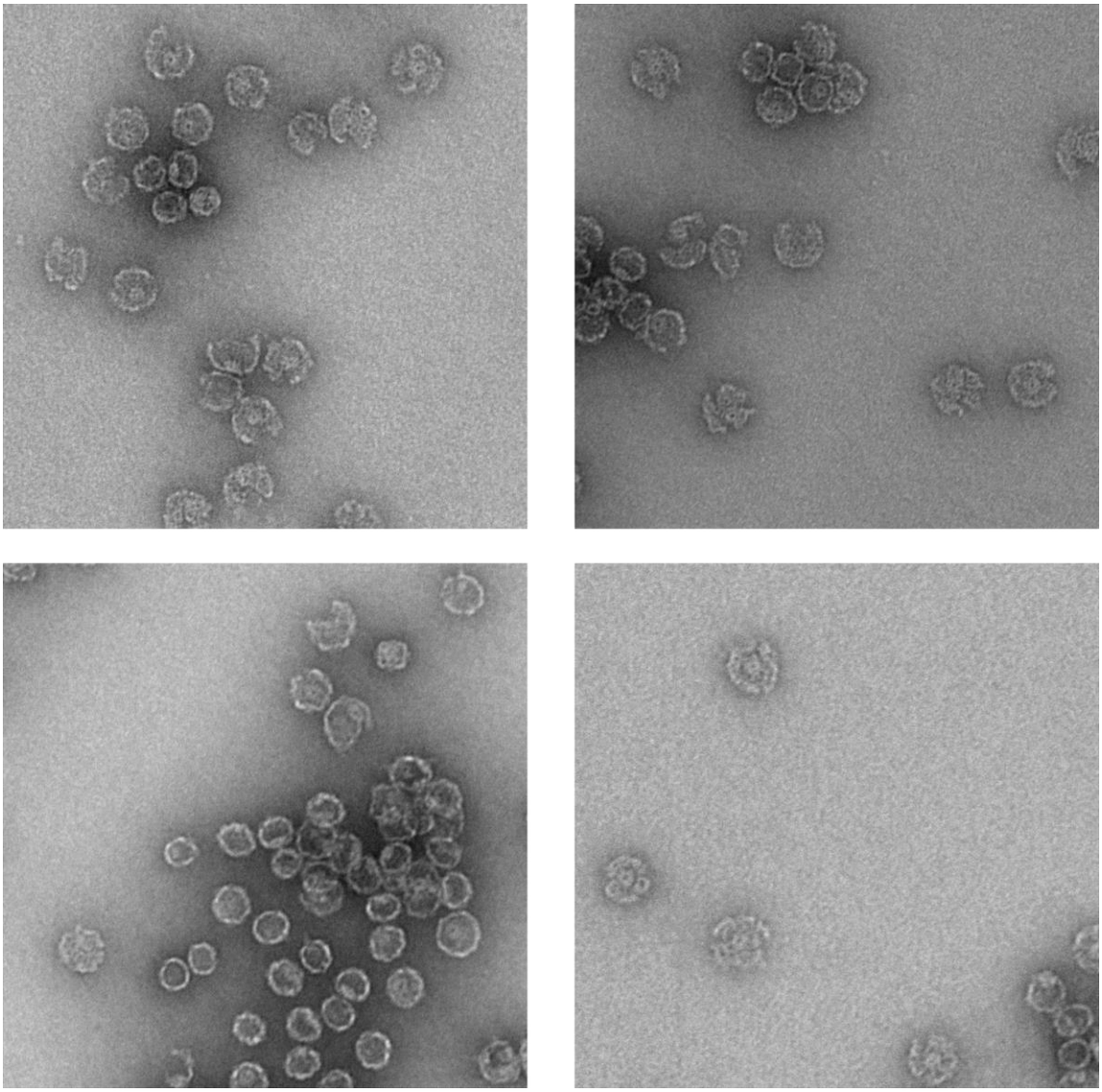

Figure 31 TEM of purified ΔClpX-RcGTA

Affinity purified ΔClpX-RcGTA produced by DE442 *ΔclpX* showing head-only structures.

3.6 RcGTA production is stimulated by amino acid depletion

3.6.1 Carbon depletion stimulates RcGTA transduction

RcGTA has been proposed to have an ancestor in common with a prophage, and shares several features with the temperate phages lambda and HK97 (Lang and Beatty, 2001, Lang and Beatty, 2007, Lang *et al.*, 2012). Induction of lambda from lysogenized cells is stimulated by DNA damage, but in contrast no stimulation of RcGTA production has been detected in response to DNA-damaging agents (Campbell, 2005, Marrs, 1974). Recently, mutation of the SOS response repressor LexA was found to inhibit RcGTA production (Kuchinski *et al.*, 2016). Production of RcGTA is increased when cultures enter the stationary phase (Florizone, 2006). This is at least partly explained by quorum sensing, because maximal RcGTA production requires homoserine lactone synthesis by GtaI (Leung *et al.*, 2012, Schaefer *et al.*, 2002). However, RcGTA is still produced in the absence of GtaI, indicating that RcGTA is likely induced by additional signals. Transition to stationary phase typically involves nutrient depletion, and previous work in the Beatty lab had shown RcGTA production to be influenced by the nutrient composition of the growth medium, with an increase in capsid production in media containing reduced carbon (Taylor, 2004). To learn more about the conditions that promote RcGTA-mediated transduction, I investigated the effects of specific nutrient depletions on RcGTA production.

R. capsulatus SB1003 was cultured photoheterotrophically in the minimal medium RCV, and temporarily depleted of the nutrients carbon, nitrogen or phosphate (malic acid, ammonium sulfate or potassium phosphate, respectively) for 2 h in the late exponential phase, and assayed for RcGTA production after 16 h of additional incubation in replete medium. Transient depletion of carbon greatly increased the amount of RcGTA capsid protein present in the culture medium

compared to a no-depletion control (Figure 32A). In contrast, small to no effects were observed for nitrogen and phosphate depletion, and so I focused on the effect of carbon. The role of phosphate concentration in the release of RcGTA has been described earlier, see Section 3.1.1. To confirm that the increased capsid protein represented functional RcGTA, I measured transduction frequencies of supernatant from carbon depleted cultures, and found that depletion increased the transduction frequency 21-fold compared to the no-depletion control (Figure 32B). Therefore, carbon depletion greatly stimulated RcGTA production.

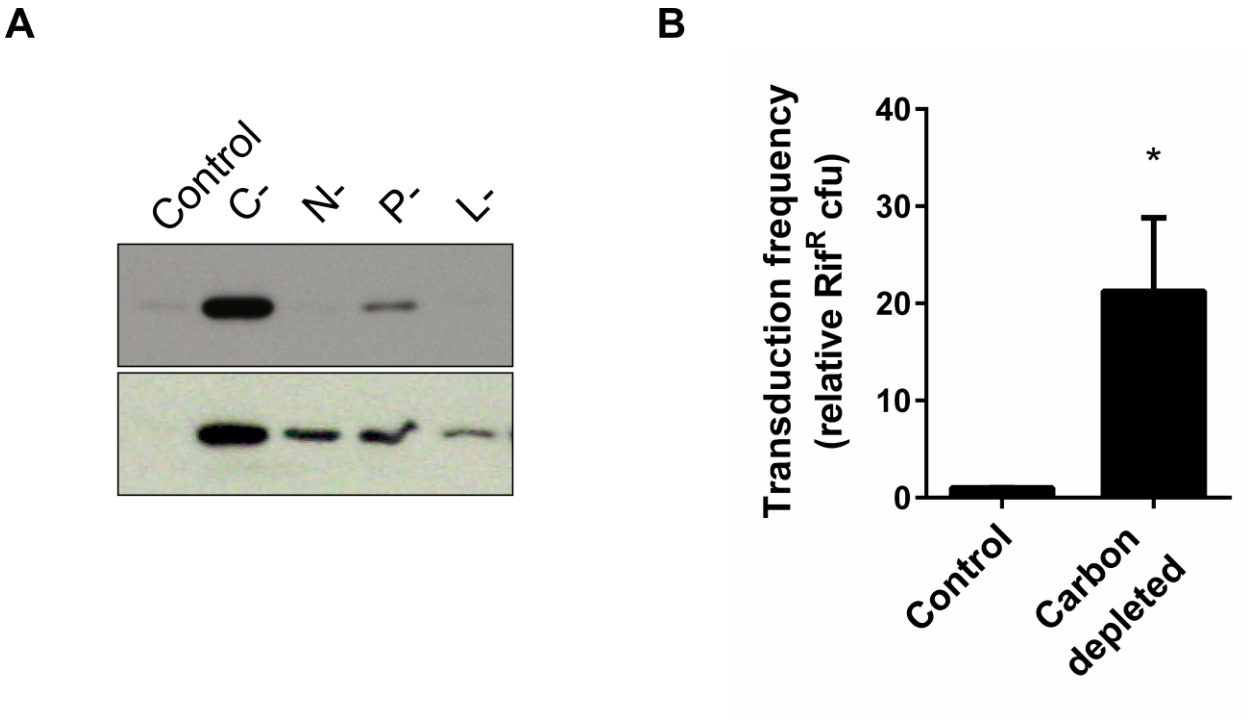

Figure 32 Temporary carbon depletion stimulates RcGTA production

A, Western blots of SB1003 culture supernatant after carbon (C-), nitrogen (N-), phosphate (P-) or light (L-) transient depletion, probed with RcGTA capsid antiserum. Blots from two independent experiments are shown. **B,** Transduction frequencies of carbon depleted cultures.

Because photoheterotrophic cultures of *R. capsulatus* utilize light, not carbon, as their energy source, it was unlikely that the effect of carbon depletion on RcGTA production was due to a lack of energy generation. To test this assumption, we similarly depleted cultures of light for 2 h. Cessation of growth was observed (not shown), however little to no increase in RcGTA capsid protein was detected (Figure 32A), indicating that depletion of an energy source does not stimulate RcGTA production.

3.6.2 Amino acid depletion induces RcGTA production

Carbon is a major nutrient and is involved in several metabolic pathways in the cell, including amino acid, nucleotide and fatty acid biosynthesis. To investigate the effects of amino acid depletion on RcGTA, I constructed a strain unable to synthesize the amino acid histidine by disrupting the orf *rcc01183*, predicted to encode a monofunctional HisB (imidazoleglycerol-phosphate dehydratase). The resultant SB1003 *ΔhisB* mutant was unable to grow on the minimal medium RCV unless supplemented with exogenous histidine, indicating that the strain was auxotrophic for histidine (not shown).

Temporary depletion of exogenous histidine increased transduction frequencies 8.2-fold for the *ΔhisB* mutant compared to replete control (Figure 33A). In contrast, no increase was observed for the prototrophic parental strain after depletion (0.76 of histidine-replete). Similarly, RcGTA capsid protein amounts were greatly increased in the culture supernatant and increased in the cell pellet fraction after histidine depletion of the *ΔhisB* mutant (Figure 33B). Similarly, addition of the histidine biosynthesis inhibitor 3-amino-1,2,4-triazole (3AT) to WT SB1003 cultures increased transduction levels 8.9-fold compared to the DMSO (solvent for 3AT) control (Figure 33C), and the effect of 3AT was offset by the addition of exogenous histidine (1.2-fold of DMSO control). 3AT-treated cultures also had increased levels of RcGTA capsid protein in

both cell pellet and supernatant fraction (Figure 33D). Therefore, RcGTA production is stimulated by histidine depletion.

The primary RcGTA cluster appears to be transcribed from a single promoter (Florizone, 2006). To investigate whether histidine depletion stimulated the activity of this promoter, cells containing the RcGTA promoter-*lacZ* reporter plasmid p601-g65 (Leung, 2010) were treated with 3AT. 4.7-fold greater β-galactosidase activity was observed in 3AT-treated cultures compared to a no-treatment control (Figure 33E), indicating that the stimulation of RcGTA production by histidine depletion is due to increased transcription of the RcGTA gene cluster.

To test whether stimulation of RcGTA production was specific to histidine or did also occur by depletion of other amino acids, I constructed a serine auxotroph by deleting *rcc03445,* the predicted *serB* homologue (phosphoserine phosphatase). Because phosphate concentrations modulate RcGTA release (Section 3.1.1), I also investigated the effect of amino acid depletion in growth medium containing reduced levels of KPO_4 (0.5 mM) to regular levels of phosphate (9.6 mM). Depleting the *ΔserB* mutant for exogenous serine increased transduction frequencies 9.2-fold and 5.9-fold for cells cultured in regular and reduced levels of phosphate (Figure 34A), respectively. Therefore, both serine and histidine depletion stimulated RcGTA production, indicating that this stimulation of RcGTA production is an effect due to the depletion of amino acids in general.

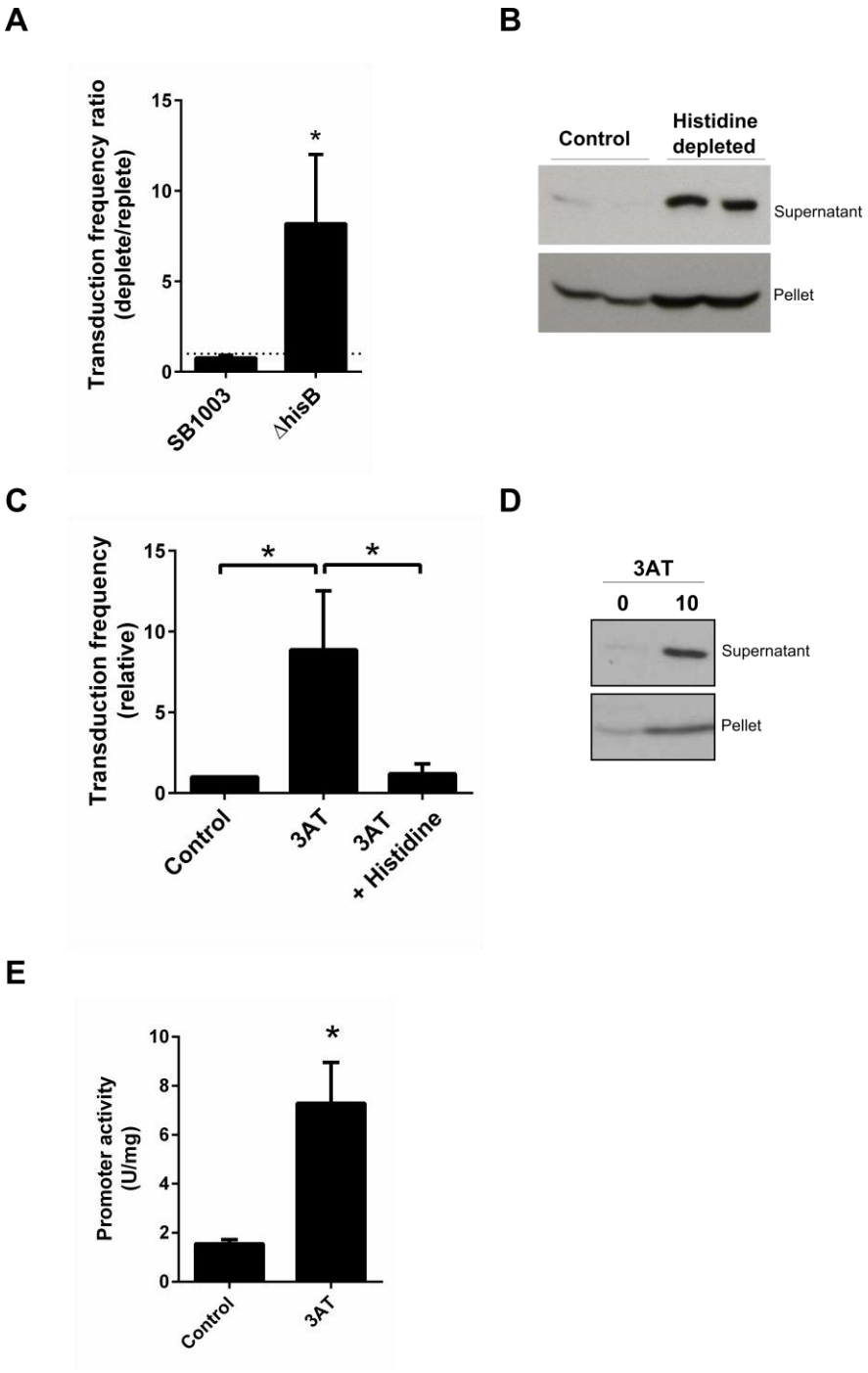

Figure 33 Histidine depletion stimulates RcGTA production

A, Ratio of transduction frequencies for samples temporary depleted of exogenous histidine to non-depleted samples for SB1003 and SB003 *ΔhisB*. **B,** Western blot of SB1003 *ΔhisB* culture supernatant and cell pellet fraction probed with RcGTA capsid antiserum. Duplicate cultures were temporary depleted of exogenous histidine as indicated

above blot. **C,** Transduction frequencies of SB1003 cultures treated with the histidine-biosynthesis inhibitor 3AT or 3AT and exogenous histidine. **D,** Western blot of SB1003 culture supernatant and cell pellet fraction after 3AT treatment (concentration in mM indicated) probed with RcGTA capsid antiserum. **E,** RcGTA promoter (β-galactosidase) activity for SB1003 containing the *lacZ* reporter plasmid p601-g65 after treatment with 3AT.

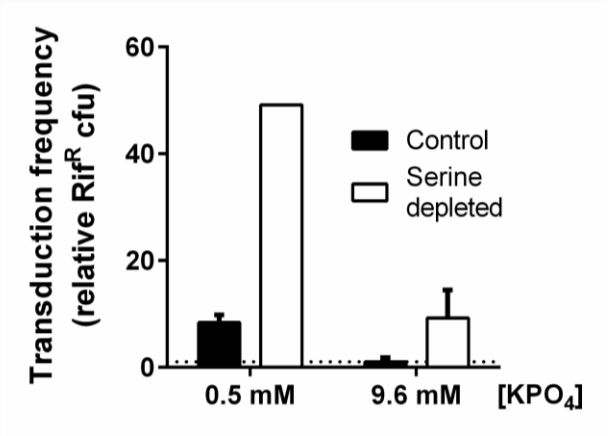

Figure 34 Serine depletion stimulates RcGTA production in media containing normal and reduced phosphate concentrations

Transduction frequencies of serine-depleted SB1003 *ΔserB* cultures. Transduction frequencies were normalized to serine-depleted cultures grown in 0.5 mM KPO_4 and expressed relative to non-depleted 9.6 mM culture for ease of comparison to previous data.

3.6.3 The stringent response is not required for RcGTA production but regulates biofilm formation

3.6.3.1 *spoT* can be disrupted in a WT background

The depletion of nutrients, particularly amino acids, results in the induction of the stringent response in many bacteria. This response is mediated by the "alarmones" ppGpp and pppGpp, which are global regulators of cell physiology (Hauryliuk *et al.*, 2015). *R. capsulatus*

encodes a single *spoT*/*relA* (*rcc03317*) homologue, which has been shown to be required for (p)ppGpp production after amino acid depletion (Masuda and Bauer, 2004). Masuda and Bauer (2004) attempted to disrupt this *spoT* homologue using a suicide plasmid approach, and concluded it was essential in a WT background, but could be deleted in a *hvrA* background. In contrast, *spoT* was reported to be non-essential in *C. crescentus* and the mutant exhibited normal doubling times when cultivated in a complex yeast-extract/peptone medium (Lesley and Shapiro, 2008). Because *R. capsulatus* produces (p)ppGpp in response to amino acid depletion and RcGTA production was stimulated by amino acid depletion, I hypothesized that induction of RcGTA production was mediated by (p)ppGpp.

Preliminary measurements indicated that the *ΔhvrA ΔspoT* mutant constructed by Masuda and Bauer (2004) produced RcGTA, and so I attempted to transduce the tetracycline resistance-marked *spoT* allele into the SB1003 WT strain. Tetracycline resistant colonies were obtained at a frequency typically observed for transduction (not shown), and a colony screened by PCR confirmed the absence of the WT-*spoT* allele and presence of WT-*hvrA* allele (Figure 35A). No major growth defect was observed for the *ΔspoT* mutant during photosynthetic growth in the complex medium YPS (Figure 35B). Plating of the mutant cultured in YPS onto RCV resulted in similar amounts of cfu as the parental strain, indicating that the mutant was not auxotrophic (not shown). The *R. capsulatus spoT* gene is therefore not essential for viability under laboratory conditions, in contrast to a previous report (Masuda and Bauer, 2004). Furthermore, the mutant is not auxotrophic, consistent with observations for a *C. crescentus ΔspoT* mutant (Lesley and Shapiro, 2008). However, inconsistent growth including long lag phases were observed when the mutant was cultured in minimal RCV medium, indicating a dysregulation of amino acid

biosynthesis operons as previously reported for ppGpp-deficient *E. coli* and *C. crescentus* (Lesley and Shapiro, 2008, Srivatsan and Wang, 2008).

In *E. coli*, *spoT* is expressed as a part of an operon together with the 5' *rpoZ* (Sarubbi *et al.*, 1989) and 3' genes *trmH* and *recG*. *R. capsulatus spoT* is similarly located 3' of *rpoZ* and possibly expressed in an operon with *rpoZ* and the gene downstream of *spoT* (not shown). To confirm that the *spoT* mutation is not polar, the *spoT* ORF was cloned under the control of a modified *lac* promoter and introduced in *trans* on the resultant plasmid *pIspoT*.

The *ΔspoT* mutant strain showed a reduced pigmentation (Figure 35C and D), and this was restored by addition of glucose to medium (Figure 35C), a phenotype previously associated with the *ΔspoT* mutation (Masuda and Bauer, 2004). The *spoT* provided in *trans* restored the *ΔspoT* pigmentation defect when cultured on plates (Figure 35D) and partially restored pigmentation for liquid culture, indicating that the *ΔspoT* mutation is not polar.

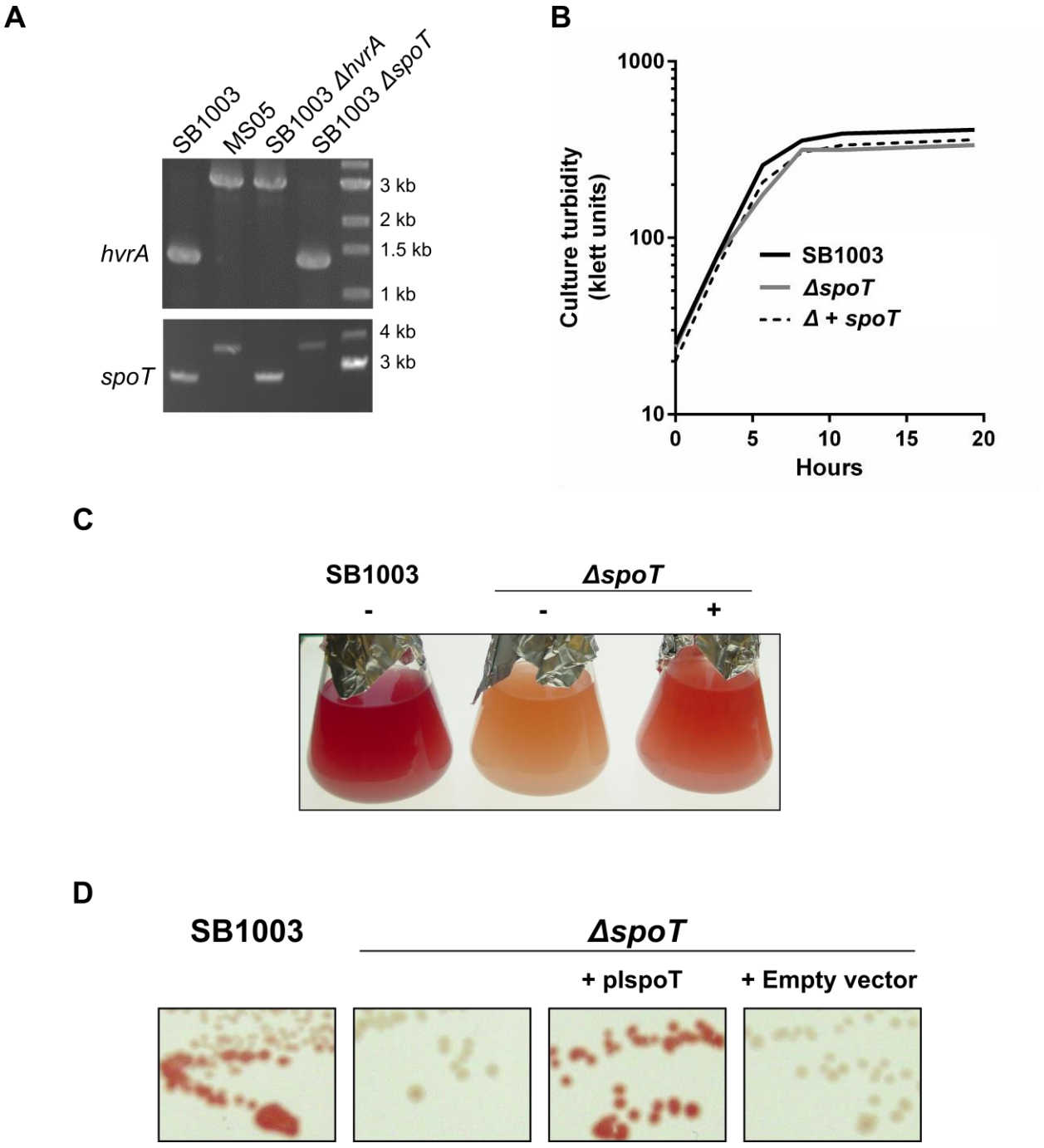

Figure 35 Pleiotropic phenotype of a *spoT* mutant

Genotypes (**A**) and phenotypes (**B** to **E**) of strains SB1003, SB1003 *ΔspoT* (single mutant) or SM05 (*ΔhvrAΔspoT* double mutant). **A,** Verification of allele replacement. PCR products were separated by agarose gel electrophoresis and visualized using ethidium bromide fluorescence. **B,** Turbidity of SB1003, SB1003 *ΔspoT* and *trans*-

complemented SB1003 *ΔspoT*(pIspoT) cultured photoheterotrophically in YPS medium. **C**, Culture pigmentation after 48 h of semi-aerobic growth in liquid YPS medium with no (-) or 0.5% wt/vol (+) glucose added. **D,** Colony pigmentation on solid YPS medium. Presence of complementation plasmid pIspoT or empty vector (pIND4) indicated.

Strain SM05 is a *ΔhvrAΔspoT* double mutant constructed by Masuda and Bauer (2004).

3.6.3.2 *A spoT* mutant has increased biofilm formation

After phototrophic growth of the *ΔspoT* mutant in YPS, an opaque layer on the walls of the culture tubes was observed and this layer was present, but greatly diminished, for the WT strain and by *trans*-complementation of *ΔspoT* with plasmid pIspoT. Inspection of the material by phase contrast microscopy revealed it to consist of cells (not shown), and the film stained blue with crystal violet (Figure 36A). Spectrophotometric quantification of eluted crystal violet indicated that the *ΔspoT* mutant produced 7.8-fold more of the film compared to WT strain SB1003 (Figure 36B). Based on these observations, I suggest that *R. capsulatus* forms a biofilm on glass during phototrophic growth and that biofilm formation is greatly increased for a *ΔspoT* mutant (lacking (p)ppGpp).

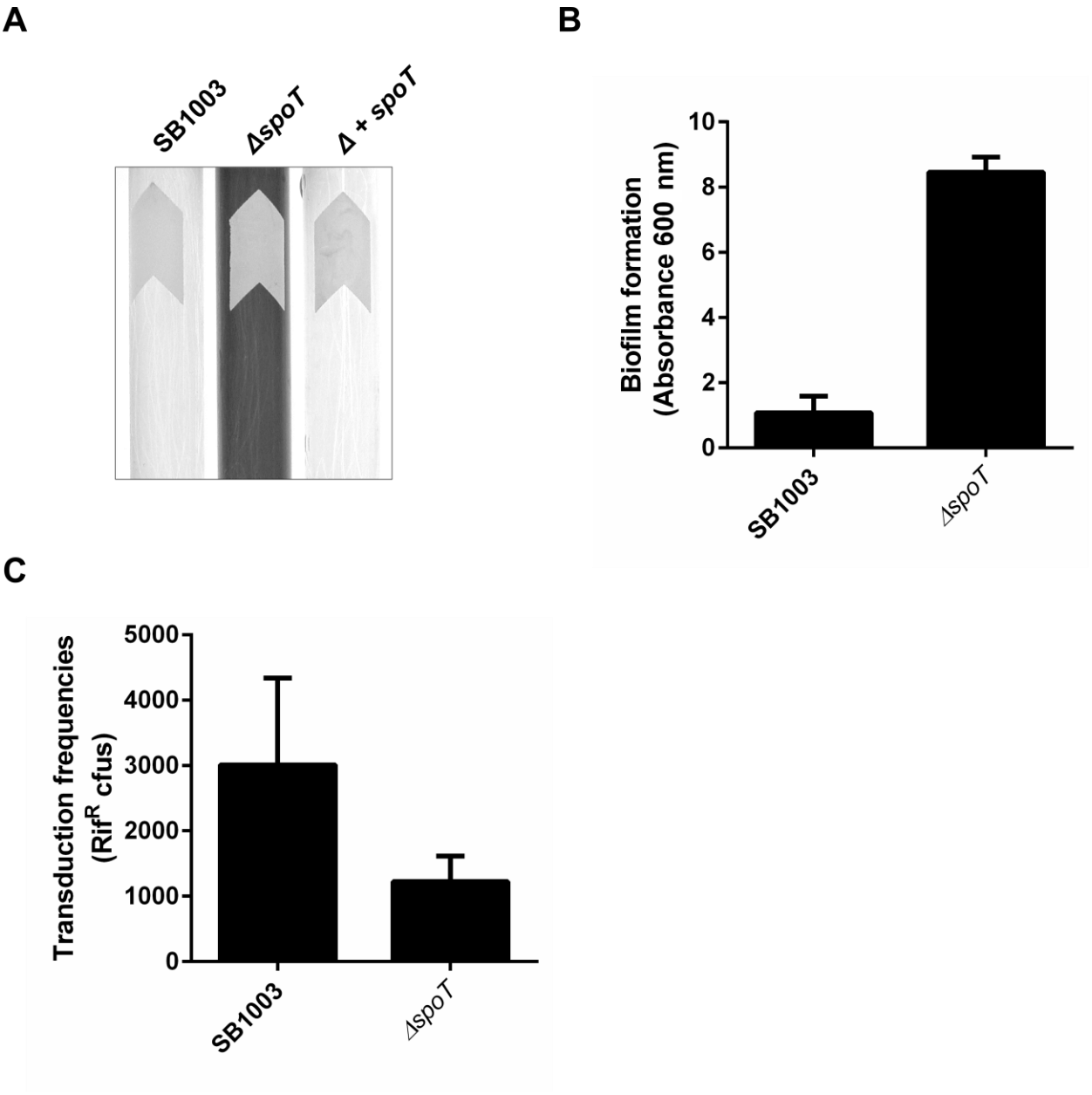

Figure 36 SpoT is required for biofilm formation, but not RcGTA production

Biofilm formation (**A** and **B**) and transduction (**C**) of SB1003, SB1003 *ΔspoT* and *trans*-complemented SB1003 *ΔspoT*(pIspoT) strains.

A, Crystal violet-stained culture tubes after photoheterotrophic growth. **B,** Quantification of crystal violet staining. **C,** Transduction frequency of culture supernatant.

Cells were cultured photoheterotrophically in YPS medium for all experiments. Error bars represent standard deviation of three biological replicates.

3.6.3.3 The (p)ppGpp-mediated stringent response is not required for RcGTA production

RcGTA production from the *ΔspoT* mutant was quantified using a transduction assay, and found to be reduced to 41% of the levels obtained for WT strain SB1003 (Figure 36C), consistent with the positive result obtained in transduction from SM05 (*ΔhvrAΔspoT*) to create the *ΔspoT* mutant in the SB1003 background. Therefore, *spoT* and its product (p)ppGpp are not required for RcGTA production.

3.6.4 The putative general stress sigma factor EcfG is not a regulator of RcGTA

Because RcGTA production is stimulated by carbon and amino acid depletion (Figure 32, Figure 33 and Figure 34), but does not require the stringent response (Figure 36C), I investigated alternative regulatory mechanisms.

The *R. capsulatus* homologues of EcfG, NepR and PhyR were identified using BLAST and found to be encoded by *rcc02291*, *rcc02290* and *rcc02289*, respectively. To investigate whether amino acid depletion stimulated RcGTA by this system, a *ΔecfG* (*Δrcc02291*) mutant was constructed and investigated for RcGTA production. No dramatic difference in transduction efficiency was observed compared to the WT strain SB1003 in the presence or absence of 3AT (Figure 37), indicating that the putative stress sigma factor EcfG is not involved in RcGTA production.

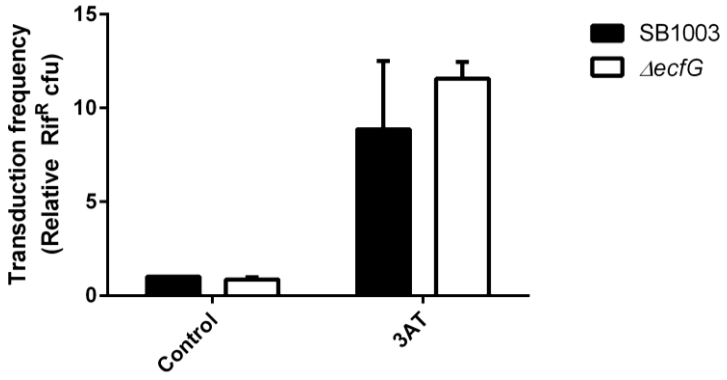

Figure 37 The putative general stress sigma factor EcfG is not required for stimulation of RcGTA production

Transduction frequencies of SB1003 and SB1003 *ΔecfG* treated in the presence or absence of 10 mM 3AT. Error bars represent standard deviation of the mean of at least two biological replicates.

Chapter 4: Discussion

4.1 Lytic release of RcGTA

In this thesis, I provide extensive evidence that RcGTA is released from cells through cell lysis, and that this is mediated by a canonical endolysin and holin system that is regulated by the phosphorylation state of CtrA (Section 3.1). The initial characterization of an RcGTA overproducer strain indicated that culture lysis was often observed, however no investigation into lysis or release was performed (Yen *et al.*, 1979). The RcGTA overproducer strain DE442, as well as an SB1003-derived overproducer strain SBpG*Δ280*, was found to undergo extensive cell lysis when cultured in media low in inorganic phosphate, with a marked decrease in culture turbidity at the entry to stationary phase. Furthermore, evidence for a low level of cell lysis was obtained from the WT strain SB1003 when cultured in media low in inorganic phosphate. This is similar to the release mechanism of many dsDNA tailed phages. Induction of lysogenized lambda results in a precisely timed cell lysis that can readily be monitored by turbidity (Garrett *et al.*, 1981). In contrast, the well-studied phage T4 does not exhibit a clear decrease in culture turbidity due to lysis inhibition by released virions (see below) (Young, 1992).

4.1.1 The endolysin 555

Hynes *et al.* reported that the open reading frame *rcc00555* encodes a putative endolysin that is required for release of RcGTA, and the downstream *rcc00556* a putative holin (Hynes *et al.*, 2012). 555 was found to be related to the endolysin gp61 from coliphage N4, a podovirus (see section 3.1.2.1). The gp61 murein hydrolase has been characterized in detail and found to cleave peptidoglycan in the same manner as the T4 lysozyme, an *N*-acetylmuramidase that cleaves the β1-4 glycosidic bond between *N*-acetylmuramic acid and *N*-acetyl-D-glucosamine in peptidoglycan (Stojkovic and Rothman-Denes, 2007, Young, 1992). Consistent with this,

recombinantly expressed 555 protein was capable of degrading purified peptidoglycan, as well as lysing *E. coli* cells, proving that 555 has muralytic activity. Combined with the requirement of 555 for release of RcGTA, it can be concluded that 555 is a genuine endolysin.

The 555 protein was predicted to contain two domains, an N-teminal catalytic domain involved in cleaving peptidoglycan and a C-terminal peptidoglycan binding domain. For the two endolysins Ply118 and Ply500, produced by phages infecting the Gram-positive *Listeria monocytogenes*, the cell wall (peptidoglycan) binding domain was required for lytic activity and sufficient for targeting the protein to the cell wall (Loessner *et al.*, 2002). It has therefore been suggested that the peptidoglycan binding domains of modular endolysins confer substrate recognition specificity and affinity to modular endolysins (Loessner, 2005). Although the role of the C-terminal domain of 555 was not investigated, it likely improves the lytic activity of the enzyme.

4.1.2 The holin 556

Like many endolysins, 555 was encoded next to the holin 556. 555 is the 5' gene in *R. capsulatus*, which is opposite to the arrangement of the lysis genes in phages lambda and P22, and the pinholin-encoding phage 21 (Young *et al.*, 2000).

Expression of 556 holin in *E. coli* halted growth and depolarized the cytoplasmic membrane (Figure 15), consistent with the predicted role as a holin. Furthermore, low level expression of this holin in *R. capsulatus* resulted in release of malate dehydrogenase to the culture supernatant, consistent with 556 encoding a canonical holin (Figure 14). Because hole formation would instantly kill the cell, the release of malate dehydrogenase from low level expression must be due to triggering of the holin in a small subset of the cells, rather than a small amount of leakage from the majority of cells. Related to this, the measured amount of pigment

release from the DE555 strain expressing both 555 and 556 was anecdotally observed to decrease with sub culturing (not shown), which I interpret to be a selection for mutants that no longer expressed the holin.

No antiholin was identified for the 556 holin. For many lambdoid phages, the antiholin is encoded by an alternate start codon of the holin gene, exemplified by lambda S105 and S107. The open reading frame of *rcc00556* does not contain the typical signature of such an antiholin, a positively charged amino acid sequestered between two alternate start codons such as for lambda S (Met-Lys-Met) and no likely alternate start codon is present nearby the annotated start codon of *rcc00556.* Furthermore, no likely antiholin candidate was located nearby *rcc00556*. However, this does not rule out the presence of an antiholin, as the phage T4 antiholin RI is encoded separately and distant from the holin T (Ramanculov and Young, 2001) and it appears that most endolysin-holin systems utilize an antiholin. However, precisely defined lysis is observed for phage lambda in the absence of the antiholin (Wang *et al.*, 2000), indicating that an antiholin is not absolutely required for a controlled lysis event.

Because homologues of 555 and 556 are present in several other Alphaproteobacteria, it is possible that most, if not all, RcGTA-related particles are released by this system.

4.1.3 The post-translational inhibition of cell lysis by inorganic phosphate

4.1.3.1 Inhibition of lysis is not a starvation response

In this thesis, I provide evidence that high concentrations of phosphate inhibit the lytic release of RcGTA from *R. capsulatus* cells, and that this inhibitory effect occurs in both a minimal medium (RCV) and a complex medium (YPS). This expands upon previous thesis results that initially reported a role of phosphate in release of RcGTA capsid from cells (Leung,

2010, Taylor, 2004). It had previously been hypothesized that the RR PhoB is involved in the phosphate-dependent effect on RcGTA release (Leung, 2010), because PhoB mediates a phosphate starvation response in several bacteria. Upon low (< 4 μM) levels of inorganic phosphate in the environment, PhoB becomes phosphorylated by the HK PhoR and activates expression of a large repertoire of genes, termed the Pho regulon, mainly involved in phosphate acquisition (Hsieh and Wanner, 2010, Lamarche *et al.*, 2008). Alkaline phosphatase is a member of the Pho regulon (Wanner, 1993), and alkaline phosphatase activity is considered an indicator of phosphate deprivation in many species.

R. capsulatus rcc03498 was found to encode a functional homologue of PhoB, as a strain lacking this gene had reduced growth in media containing trace amounts of phosphate and did not express alkaline phosphatase (Figure 10B and C). Because the mutant lacking PhoB produced and released RcGTA at levels similar to WT strain (Figure 10D and E), I conclude that RcGTA is not regulated by the PhoB-mediated phosphate starvation response. This conclusion is consistent with the release of RcGTA from cells cultivated in media containing 2 mM phosphate (initial concentration) (Figure 8C and E), that when harvested for RcGTA contained relatively high levels of residual inorganic phosphate (0.4 mM) compared to the < 4 μM concentrations needed to induce the Pho regulon, and very low alkaline phosphatase activity (Figure 10A and B).

Multiple results appear to indicate that the inhibitory effect of phosphate on RcGTA release is manifested at the level of protein activity, rather than a regulated genetic response to the concentration of phosphate. In addition to RcGTA release being independent of the Pho regulon (Figure 10), the expression of the endolysin/holin promoter was not decreased by high levels of phosphate (Figure S2). Furthermore, the inhibitory effect of addition of phosphate to a

culture undergoing lysis was rapid (Figure 11D), and lysis was not reduced by an inhibitor of protein synthesis (Figure 13B), and did not require cell growth (Figure 13A). Therefore, the effect of phosphate on lysis appears to be post-translational.

4.1.3.2 Inhibition requires phosphate in excess of typical concentrations in natural environments of *R. capsulatus*

The typical habitat for *Rhodobacter capsulatus* and other members of the *Rhodobacer* genus is eutrophic water with reduced oxygen and illumination, and several isolates have been obtained from sewage settling ponds (Pujalte *et al.*, 2014, Weaver *et al.*, 1975). Phosphate is typically a limiting nutrient for microbial growth in freshwater and marine environments (Schindler, 1977).

The phosphate concentration in a sewage settling pond was measured to be 95 uM (Olutiola *et al.*, 2010), however concentrations of phosphate have been measured as low as 27 pM in lakes (Hudson *et al.*, 2000). The maximal concentration of phosphate measured in the seasonally anoxic fjord Saanich Inlet was found to be 5.2 µM (Zaikova *et al.*, 2010). Therefore, the millimolar concentrations of phosphate required to inhibit release of RcGTA is higher than the concentration of phosphate found in most natural environments, except for highly eutrophic environments such as Lake Erie (Howell and Nakamoto, 2009). It therefore appears unlikely that the inhibition of RcGTA release by phosphate is an evolved regulatory mechanism, where the concentration of phosphate is sensed by *R. capsulatus* to be below a threshold that results in release of intracellularly-accumulated mature RcGTA particles.

However, optimization of the phosphate concentration in the growth medium used to cultivate strains for production of RcGTA-like particles has allowed for more controlled laboratory growth conditions to study RcGTA, compared to the previously used complex

medium YPS. Furthermore, consideration of the phosphate concentration in cultivation media may be essential for the discovery of additional RcGTA-like GTAs, and attention to the possible inhibition of GTA release by high concentrations of phosphate is essential when comparing levels of production of RcGTA-like particles from strains cultivated in various growth media (McDaniel *et al.*, 2012).

4.1.3.3 Post-translational modulation of lysis in phage systems

The mechanism by which phosphate inhibits lysis to release RcGTA is not clear and the results presented in this thesis do not differentiate between a post-translational regulation of lysis by a phosphate effect on activation of the endolysin or holin, or inhibition of an unknown antiholin resulting in triggering of the holin. However, with the exception of the complex myoviridae T4 and related phages, the timing of lysis is thought to not be regulated in real time but genetically encoded in the holin allele (Wang *et al.*, 2000, Young, 1992). T4 lysis inhibition requires an interaction between the soluble domains of T4 holin T and antiholin RI (Moussa *et al.*, 2012, Ramanculov and Young, 2001). No such soluble domain appears present in the holin Rcc00556 (WHAT 2.0 analysis, not shown).

No effect of phosphate concentration on the lytic activity of recombinantly expressed endolysin was detected (Figure 15A), indicating that phosphate does not inhibit the catalytic activity of the Rcc00555 endolysin. Because no signal anchor sequence for export through the *sec* pathway was detected for Rcc00555, and because Rcc00556 appears to encode a canonical holin (and not a pinholin, see section 4.1.2), the endolysin is most likely confined to the cytoplasm and only released to the periplasm by the activation of the holin. Phosphate could potentially inhibit the triggering of the Rcc00556 holin. However, DE555 expressing the holin constitutively in *trans* from pI556Gm was found to release increased levels of malate

dehydrogenase when cultured in 10 mM compared to 0.5 mM KPO_4 (Figure S6), apparently contradictory to an inhibition of Rcc00556 holin triggering by phosphate.

The spanin complex produced by phage lambda is required for lysis of *E. coli* in a medium containing millimolar but not low concentrations of divalent cations (Zhang and Young, 1999). No homologues of the lambda spanins Rz and Rz1 (Berry *et al.*, 2012) were identified in *R. capsulatus*, however an extensive systematic search was not attempted. There is a very large diversity of spanins encoded by phages that have an equivalent function to Rz/Rz1, yet little to no sequence similarity (Summer *et al.*, 2007). Spanins often require manual inspection of the genome to be located (Young, 2014), a daunting task considering the size of the 3.7 Mb chromosome of *R. capsulatus* (Strnad et al., 2010). Although it is possible that the effect of inorganic phosphate (an anion) on *R. capsulatus* cell lysis is due to stabilization of the cells, analogous to the effect of divalent cations in a spanin-deficient lambda infection, microscopic investigation indicate this to not be the case. In the absence of *Rz*/*Rz1* and high concentrations of divalent cations, *E. coli* cells round up (Berry *et al.*, 2012). In contrast, DE442 cells cultured in high levels of phosphate retain their rod-like shape, which appears to indicate an intact cell wall and that the effect of high concentrations of phosphate on lysis occurs prior to degradation of the peptidoglycan layer by the endolysin.

4.2 Regulation of RcGTA release by the phosphorelay CckA-ChpT-CtrA

The release of RcGTA from cells was reported to be influenced by the phosphorylation of CtrA (Mercer *et al.*, 2012).

I discovered that RcGTA is released from cells by lysis mediated by the endolysin 555 and holin 556 (see section 4.1). Expression of this lysis system was found to be regulated by

CckA, ChpT and CtrA, and the lysis-dependent release of LH2 pigments to the culture medium from RcGTA overproducers proved to be a good indicator of cell lysis.

4.2.1 Cell lysis requires phosphorylation of CtrA

The overproducer strain DE442 was used as a model for cell lysis, and *ctrA*, *chpT* and *cckA* were found to be required for lysis (Figure 16). Using a phosphomimetic CtrA mutant and a predicted kinase-deficient mutant of CckA, I have shown that the CckA-ChpT-CtrA phosphorelay is required for cell lysis, and that lysis appears to require phosphorylation of CtrA (Figure 16). The requirement for CtrA phosphorylation for lysis was confirmed by a *ΔcckA* mutation in the WT SB1003-derived SBpG*Δ280* mutant. This is consistent with a study on RcGTA capsid release by Mercer *et al* (2012) that found that phosphomimetic CtrA(D51E), but not non-phosphorylatable CtrA(D51A) resulted in release of capsid protein from a *ΔctrA* mutant.

4.3 Regulation of RcGTA maturation and lysis by the phosphorelay CckA-ChpT-CtrA

RcGTA was first visualized and described as a phage-like particle in in 1974 (Yen *et al.*, 1979). A subsequent TEM of affinity-purified RcGTA was later published (Chen *et al.*, 2009a), however the TEM provided were of inferior quality to the initial publication. In this thesis, I present TEM of affinity-purified RcGTA particles of a much higher resolution than the previously published ones. The TEM (Figure 29) clearly show that RcGTA has head spikes and side tail fibers, previously suggested to be present by Yen *et al.* (1979). Additionally, a baseplate-like structure was observed that had previously escaped notice.

Other Alphaproteobacteria that contain a gene cluster homologous to the RcGTA primary cluster have been reported to produce GTAs, and TEMs have been provided for GTAs from *R. pomeroyi* and *R. nubinhibens* (Biers *et al.*, 2008, McDaniel *et al.*, 2010, McDaniel *et al.*, 2012). However, caution should be taken in interpreting their TEM data, as the particles attributed to be

GTAs in these electron micrographs do not have tails, despite the presence of tail protein homologues in their RcGTA-like gene clusters. The requirement for the tail of RcGTA was confirmed by a *Δ1691* mutant, lacking the predicted tail tube protein-encoding gene, which was not capable of transduction (not shown).

4.3.1 RcGTA production and maturation is regulated by CtrA phosphorylation

The phosphorylation state of CtrA was previously reported to influence RcGTA production, with both phosphorylated and unphosphorylated forms reported to stimulate RcGTA production. Unphosphorylated CtrA strongly stimulated RcGTA capsid production, but not release, whereas CtrA~P was a weak stimulator of capsid production and allowed release (Mercer *et al.*, 2012). The lytic release of RcGTA was found to require CtrA~P (see section 3.1.3.2). The phosphorylation state of CtrA was also found to be important for the maturation of RcGTA. Both a *ΔcckA* mutant and *ΔctrA* strain expressing the unphosphorylated CtrA(D51A) produced the RcGTA-specific DNase I protected band indicative of capsid formation and DNA packaging. However, TEM analysis indicated that this particle differed from the WT-RcGTA particles by containing mostly heads lacking both spikes (see below) and tails. This is supported by gel electrophoresis migration of the particles: The migration rate of the DNase I-resistant band from a *ΔcckA* mutant was undistinguishable from that produced by a mutant lacking both the head spike protein GhsB and the predicted tail tube protein encoded by *rcc001691* (Figure 27D).

Tail and head assembly follow two separate pathways for long tailed dsDNA phages (*Myoviridae* and *Siphoviridae*), and these converge to form mature virions. Closer inspection of the particles produced by a *ΔcckA* mutant revealed what appear to be polytubes (or possibly

polytails). Similar structures have been reported for phage lambda and recently for phage TP901-1 (Katsura, 1990, Mount *et al.*, 1968, Stockdale *et al.*, 2015). The WT-RcGTA contained both a baseplate-like structure at the tip of the tail and side fibers, whereas none of the polymeric tail-like structures observed for the *ΔcckA* mutant contained these structures. Therefore, these RcGTA mutant structures appeared more similar to lambda polytubes than to polytails. Although it is possible that all the observed polytubes were broken polytails, and that the attributed ends were the middle of a polytail, this appears less likely than an explanation that the baseplate-like structure and fibers were never present. It therefore appears that in the absence of CtrA~P, polytubes are formed. Because the order of genes is conserved for many tailed phages, the homologues of lambda tail terminase gpU and the gpG/gpGT chaperones are likely the orfs *rcc01690* and *rcc01692/rcc01693*, respectively. RNA microarray expression data obtained in collaboration with A. Lang at Memorial University indicates that all orfs in the primary gene cluster, including the three above, are expressed in the *cckA* mutant. Furthermore, no dramatic changes in expression of any of the genes relative to the tail tube encoding *rcc01691* or capsid gene was observed for the *ΔcckA* mutant versus the WT strain SB1003 (not shown). Therefore, polytube formation appears not to be due to absence of mRNA for parts of the gene cluster in the *ΔcckA* mutant.

It is possible that CtrA~P is required for a post-transcriptional control of production or processing of a tail protein, however I have not performed experiments to investigate this in detail. The lambda TMP protein gpH is proteolytically cleaved during tail assembly after polymerization of the tail (Tsui and Hendrix, 1983). The central fiber proteins Tal_{2009} and ORF47 from the Gram-positive infecting phages Tuc2009 and TP901-1 are proteolytically processed with both fragments present in the tail of assembled particles, and for Tal_{2009} this cleavage was

shown to be self-mediated (Kenny *et al.*, 2004, Vegge *et al.*, 2005). Analogously, a small N-terminal peptide of RcGTA g15, the putative central fiber protein of RcGTA was present in purified RcGTA, indicating that g15 might similarly undergo proteolytic cleavage (Chen *et al.*, 2009a). Because the TMP and central fiber protein are required for tail assembly, a hypothetical absence of cleavage in the *ΔcckA* mutant could prevent RcGTA tail assembly.

The absence of a tail explains the extremely low transduction frequencies observed from the artificial French press lysate of the *ΔcckA* mutant (Figure 22). The tail of a tailed phage is required for infectivity and injection of DNA into the host (Davidson *et al.*, 2012), and so the tail-less ΔCckA-RcGTA would not be expected to transfer the DNA contained in the head to a recipient cell.

4.3.2 A bacterial protease or chaperone – possible roles for ClpX(P) in maturation

4.3.2.1 The RcGTA defects of a *ΔclpX* mutant

The ClpX protein, which is a subunit of the ClpXP protease in various bacteria, is required for RcGTA transduction and control of CtrA levels (Figure 18B and E). In the absence of ClpX, maturation of RcGTA appears to have stalled at a stage similar to Prohead II of HK97 (Figure 23D and Figure 31) (Hendrix and Johnson, 2012). It is possible that ClpX is required for full expansion of the RcGTA capsid, a step that is required for maturation of tailed phages and occurs alongside DNA packaging (Aksyuk and Rossmann, 2011). For lamba, expansion is thought to be triggered by DNA packaging whereas for T4 it can occur in the absence of DNA packaging (Fuller *et al.*, 2007, Rao and Black, 1985). Because no DNase I-protected DNA was observed for ΔClpX-RcGTA, such an absence of expansion could result from an absence of DNA packaging.

An absence of DNA from an immature capsid could also result from DNA-leakage after packaging, and so it is therefore also possible that ClpX is required for the retention of packaged DNA. For most phages, retention of DNA in the capsid after packaging requires two neck proteins, one which is a stopper protein that plugs the portal (Aksyuk and Rossmann, 2011, Tavares *et al.*, 2012). For phage lambda this stopper function is attributed to the protein gpW (Perucchetti *et al.*, 1988). The stopper function is provided by protein gp16 for phage SPP1. This protein forms a dodecameric ring that prevents DNA exit partly by formation of covalent disulfide bonds between the monomers (Lhuillier *et al.*, 2009). A mutant lacking the RcGTA orfs g6 to g15 was found to produce cleaved capsid protein, but no DNase I-resistant DNA was observed (not shown) indicating that DNA was likely not retained in the capsid, or less plausibly, not packaged. By comparison to phage SPP1 and HK97, this stopper is likely encoded by RcGTA g6 or g7 (not shown). Because spikes were not present in the ΔClpX-RcGTA, and such decorating proteins appear to typically be attached after DNA packaging (Aksyuk and Rossmann, 2011) it appear likely that the *ΔclpX* mutant never completes (or possibly, does not initiate) DNA packaging.

4.3.2.2 A protease component or standalone chaperone – two roles for ClpX

It is unclear how ClpX is required for proper maturation of RcGTA. ClpX is a component of the ClpXP protease in diverse species (where it acts as a chaperone, ClpP is the peptidase), and it is possible that in *R. capsulatus* ClpXP is required for complete or partial degradation of a protein (Baker and Sauer, 2012). However, ClpX also has chaperone activity independent of ClpP (see below).

Many phage (and viral) proteins, or proteins required for phage production, are proteolytically cleaved by host proteins (Gottesman, 2003, Hellen and Wimmer, 1992, Hershko

and Fry, 1975). ClpXP was shown to degrade the phage lambda DNA replication protein O by recognizing a C-terminal sequence (Gonciarz-Swiatek *et al.*, 1999). Lambda O is required for lambda DNA replication and binds to repeats in lambda *ori*, and together with lambda P and the *E. coli* helicase DnaB forms a preprimosomal complex to stimulate the initiation of DNA synthesis. Lambda O is considered extremely unstable with a half-life of 90 seconds *in vivo*, but formation of the preprimosomal complex stabilizes it against degradation by ClpXP (Zylicz *et al.*, 1998).

Lambda O is considered to have a similar role to the bacterial replication initiator factor DnaA (Mott and Berger, 2007). Although no role of DnaA has been reported for RcGTA production, it is noteworthy that the *Caulobacter crescentus* DnaA protein is degraded in the stationary phase by a ClpP-dependent protease, possibly ClpXP (Gorbatyuk and Marczynski, 2005). However, other researchers have reported DnaA to be degraded by the Lon protease (Leslie *et al.*, 2015).

The lambda cII protein, the master regulator of the lysis/lysogeny decision, is targeted by the membrane bound *E. coli* protease FtsH (also known as HflB) (Casjens and Hendrix, 2015). The C-terminal tail of cII is specifically recognized by FtsH, and the phage protein cIII acts as an inhibitor of proteolysis (Kobiler *et al.*, 2002).

In addition to control of protein turnover through complete degradation of targets, ClpXP has recently been found to partially degrade some proteins, such as the DNA clamp loader protein DnaX in *C. crescentus*. The processing generates a shorter γ isoform of DnaX that is required (together with the longer τ-form) for normal growth, and the ability to process the τ-form to the shorter γ was important for a DNA damage response (Vass and Chien, 2013). Therefore it is possible that ClpX is required for processing of an RcGTA protein.

Chaperones have been implicated in the assembly of several phages, and it is recognized that ClpX is active as a chaperone independent of ClpP. ClpX was found to promote binding of lambda O to DNA (Wawrzynow *et al.*, 1995). ClpX, but not ClpP, is essential for replication of *E. coli* phage Mu and is required to disassemble tetrameric complexes of the MuA transposase to allow for new rounds of transposition (Levchenko *et al.*, 1995). A role for ClpX independent of ClpP is also supported by the observation of Baker and Sauer (2012) that some organisms contain ClpX but lack ClpP.

The assembly of lambda and T4 heads, as well as T5 tails, requires the *E. coli* GroEL/GroES chaperonin. For lambda, the head deficiency was attributed to a requirement for GroEL/GroES in the assembly of the portal ((Ang *et al.*, 2000, Tilly *et al.*, 1981) and references therein).

ClpXP is known to degrade CtrA in *C. crescentus* (Jenal and Fuchs, 1998) and ClpXP appears to regulate the level of CtrA in *R. capsulatus* (Figure 18E). Both the presence of CtrA and the prosphorylation of CtrA are required for RcGTA production, maturation and release ((Mercer *et al.*, 2012), Figure 16 and Figure 23). It is possible that degradation of CtrA by ClpXP is required during the maturation process of RcGTA, although an absence of CtrA would have to be transient because phosphorylated CtrA is required for the release of mature particles (Figure 16). It could be speculated that ClpXP specifically degrades non-phosphorylated CtrA, however experiments on *C. crescentus* indicate that ClpXP degrades both phosphorylated and unphosphorylated CtrA (Domian *et al.*, 1997).

The experiments performed with *R. capsulatus* are unable to distinguish whether the requirement of ClpX for RcGTA maturation is due to a defect in ClpXP-dependent degradation of a protein, a ClpX-mediated chaperone activity or both. Furthermore, it is unclear whether the

defect is mediated by the absence of degradation/folding of a general regulatory protein (such as CtrA) or an RcGTA-specific protein.

4.3.3 RcGTA maturation requires the production of a CPS-binding head spike

In addition to regulating tail assembly, the CckA-ChpT-CtrA phosphorelay was found to be required for expression of *ghsA-ghsB* (formerly *rcc01079* and *rcc01080*). Head spike production required GhsB, an apparently carbohydrate-binding protein with a predicted Ig-like fold. In the absence of GhsB, RcGTA particles had reduced binding affinity to encapsulated cells, but not to non-encapsulated cells, indicating that the spikes are involved in binding to CPS (Figure 25). Because *ghsB* appears to be co-transcribed with the 5' *ghsA* and the gel migration of the *ΔghsA* mutant was the same as that of the *ΔghsB* mutant (Figure 27E), I propose that both are required for spike production.

In the absence of CckA, no spikes were visible on the RcGTA heads (Figure 30) consistent with the requirement for CckA for expression of GhsA and GhsB (Figure 26). This interpretation is supported by genome microarray data obtained from a *ΔctrA* mutant by Mercer *et al*. (2010; supplemental material), which indicated that *ghsA* and *ghsB* require CtrA for expression. In contrast, neither of the genes flanking *ghsA/ghsB* showed differential expression in the *ΔctrA* mutant, consistent with *ghsA/ghsB* being transcriptionally isolated and co-expressed. Additionally, expression of *ghsA/ghsB* was found to require GtaI, another regulator of RcGTA production and recipient capability. Because the *ghsA/ghsB* promoter was active in the *ΔclpX* mutant (Figure 18), but no spikes were present on the ΔClpX-RcGTA (Figure 31), it appears that formation of a procapsid and expression of *ghsA/ghsB* is not sufficient for the decoration of the procapsid with spikes.

4.3.4 Presence of exposed proteins involved in attachment to a cell on the capsids of tailed phage (and GTA) may be common

Because head spikes were not essential for transduction, but increased binding to cells, the spikes appear to be involved in the initial recognition and attachment to the cells. For tailed phages the initial binding to cells is often mediated by fibers located at the tail tip complex at the head-distal end of the tail (Fokine and Rossmann, 2014), and according to Casjens and Hendrix (2015): "In all [tailed] phages where it has been studied in detail, fibers or spikes at the distal tip of the tail make the first interaction with the host". In contrast, tail-less icosahedral phages have been reported to recognize and bind to their host using spike proteins present on the capsid. Phage phiX174 recognizes the lipopolysaccharide (LPS) of *E. coli* using spikes present on the capsid (Inagaki *et al.*, 2003). Similarly, the membrane-containing phage PRD1 has pentameric spikes, which were suggested to be involved in receptor-binding (Huiskonen *et al.*, 2004).

It has become clear that many phages display Ig-like domain proteins, and it was proposed that these Ig-like domains facilitate adsorption of phages to the carbohydrates present on the cell surface, or alternatively, to degrade polysaccharides to access the membrane (Fraser *et al.*, 2007, Fraser *et al.*, 2006). Although no Ig-like domains were detected by PFAM or SMART for GhsB, it appears that GhsB may be distantly related to carbohydrate-binding proteins that contain CBM folds or Ig-like domains based on my Phyre2 (Figure 24B and C, and Table S2) and Swissmodel analyses (not shown). The structure of the most common CBM folds and that of Ig-like domains are similar, as both contain a β-sandwich comprised of two sheets of antiparallel β-strands. Furthermore, some CBMs have a canonical Ig-like domain (Boraston *et al.*, 2004, Halaby and Mornon, 1998), and the majority of the CBMs (Table S2) are members of the Type B fold, which recognizes polymeric glycan chains (Boraston *et al.*, 2004).

Several tailed phages decorate their capsid scaffold with additional proteins, some of which contain Ig-like domains. The T4 highly immunogenic outer protein (Hoc) contains three Ig-like domains and binds to metazoan mucin, apparently increasing the concentration of phages in the intestinal tract (Barr *et al.*, 2013, Sathaliyawala *et al.*, 2010). The major capsid protein gp8 of phi29 contains an Ig-like domain and forms the attachment site for the head fiber protein gp8.5 (Xiang and Rossmann, 2011). Some decorating proteins may confer increased stability to the capsid structure, such as the T4 Soc protein (which lacks an Ig-domain) that acts as a clamp between neighbouring capsid hexamers (Qin *et al.*, 2010). However, most of such proteins have no known function. The *Bacillus subtilis* phage SPP1 has spikes made up from gp12, which contains a collagen-like fold, but the function is unknown (White *et al.*, 2012). The single horn per capsid produced by phage Syn5 has no recognized role (Pope *et al.*, 2007), although its triangular shape is morphologically similar to the spikes present on RcGTA, despite being larger (50 nm vs 12 nm long, respectively). Although the horn appears dispensable for infection of *Synechococcus* sp. WH8109, the laboratory host of Syn5, it is possible that the horn is involved in attachment to cells in the natural environment of Syn5. The flagellotropic phages CbK and Cb13 that infect *C. crescentus* have a hook-like structure on the head of phages that appears to aid in the attachment to the flagellum (Guerrero-Ferreira *et al.*, 2011). Because *C. crescentus*, *Synecococcus* and *R. capsulatus* are all aquatic bacteria, it is possible that these structures have evolved to aid in attachment to dispersed cells, and/or to prevent diffusion from local high concentrations of cells to the greater aquatic environment. Because RcGTA is produced by a small subset of the cells, and because both the production of and the ability to bind RcGTA particles are increased at high cell densities (Brimacombe *et al.*, 2013, Leung *et al.*, 2012), I speculate that one biological role of the head spikes is to prevent diffusion of RcGTA away from

a local community of related cells. Furthermore, it may be relatively common for tailed phages and phage-like particles to utilize proteins on the capsid for adhesion and attachment.

4.3.5 The GhsB protein may require another factor for capsule-binding activity

I attempted to biochemically characterise GhsB by expressing a C-terminally 6xHis tagged protein in *E. coli*. Although I was able to purify soluble protein (Figure 28A), I was not able to detect binding of the isolated protein to cells. This may indicate that despite appearing to be distantly related to carbohydrate-binding proteins and being required for efficient binding of RcGTA to CPS, GhsB may be a linker protein which itself does not bind CPS, but rather is required for a separate carbohydrate-binding protein to attach to RcGTA to form functional spikes. Alternatively, it is possible that the purified GhsB, despite being soluble in *E. coli*, requires an *R. capsulatus*-specific chaperone for proper folding, post-translational modification, or another component to yield a biologically active protein.

This possible accessory factor may be encoded by *ghsA*, which appears to be co-transcribed with *ghsB*. A *ΔghsA* mutant produced particles with a native gel migration indistinguishable from the *ΔghsB* mutant (Figure 27). It was reported that two proteins, gp53 and gp54, make up the horn of phage Syn5 (Raytcheva *et al.*, 2014). Analogously, several tail fibers require a chaperone for folding, including the lambda SFP and T4 gp37 proteins (Matsui *et al.*, 1997), and this chaperone gene is often located next to the fiber protein gene (Davidson *et al.*, 2012). I therefore speculate that GhsA interacts with GhsB, and may possibly be a chaperone required for proper GhsB folding, or associate with GhsB to form a polysaccharide-binding complex. Alternatively, GhsA may form a linker that anchors GhsB to the capsid, or (although unlikely) GhsB may be a linker that anchors a polysaccharide-binding GhsA to the capsid.

Fraser *et al.* (2007) suggested that many Ig-like domains encoded by phage genomes are attached to proteins by programmed translational frameshifts. Although the overlapping GhsA and GhsB appear *in silico* to have the potential for a frameshift, there is no indication that this occurs. GhsA and GhsB were detected to migrate in SDS-PAGE close to their predicted size of 10 kDa and 35 kDa, respectively, by Chen *et al.* (2009), and I similarly detected a 6xHis-tagged GhsB of ~35 kDa. Although it is conceivable that the two orfs are co-translated due to a frameshift and later proteolytically cleaved precisely at a residue close to the point of a frameshift, I consider this to be unlikely.

4.4 Possible roles of the enigmatic DivL

4.4.1 DivL regulates RcGTA apparently by modulating CckA kinase activity

A truncated homologue of the *C. crescentus* DivL was found to be involved in regulation of RcGTA (Figure 21A to C). Surprisingly, effect of a *ΔdivL* mutation on RcGTA production was opposite for the WT SB1003 and the RcGTA overproducer DE442 (Figure 21A and B).

In *C. crescentus*, DivL stimulates the kinase activity of CckA, presumably by a protein-protein interaction, and thereby promotes CtrA phosphorylation and stabilization against ClpXP-mediated degradation, and this activation of CckA by DivL is controlled by the RR DivK (Tsokos and Laub, 2012, Tsokos *et al.*, 2011). Phosphorylated DivK binds to the pseudo-DHp domain of DivL to inhibit CckA kinase activity (Childers *et al.*, 2014). The phosphorylation status of DivK is regulated by PleC and DivJ (Curtis and Brun, 2010). *R. sphaeroides* has been reported to lack the PleC-DivJ-DivK signaling system (Brilli *et al.*, 2010) and I did not detect homologues of this system in *R. capsulatus*. As with other Alphaproteobacteria that lack PleC-DivJ-DivK (Brilli *et al.*, 2010), *R. capsulatus* DivL lacks the DHp domain (Figure 20).

Experiments measuring CtrA~P-dependent lysis of DE442 indicated that DivL is required for CtrA phosphorylation, and involved in regulating CckA kinase activity (Figure 21D and E). Similarly, loss of DivL reduced, but did not abolish, cell lysis for a recent SB1003-derived *Δ280* overproducer strain, which indicate that DivL is not required for CckA kinase activity in SB1003*Δ280*.

No clear explanation for the opposite effects of a *ΔdivL* mutation on transduction in SB1003 and DE442 background presented itself. However, the opposite *ΔdivL* phenotype may indicate that there exist more factors in the regulation of CckA-ChpT-CtrA in *R. capsulatus* than currently appreciated. Strain DE442 contains multiple point mutations and lacks the 133 kb plasmid pRCB133 compared to SB1003 (Ding *et al.*, 2014, Hynes *et al.*, 2012). It is therefore possible that the difference between SB1003 and DE442 is due to absence of a CckA-stimulatory protein. A transposon screen was attempted to isolate such a mutant in a SBpG*Δ280ΔdivL* background using the *ghsA/ghsB* promoter-*lacZ* reporter (which produces β-galactosidase in SBpG*Δ280ΔdivL*, but not in DE442*ΔdivL*) however no putative candidates were identified.

Mutations that delay phage-mediated cell lysis have been shown to drastically increase the number of phages produced per cell (Josslin, 1970, Reader and Siminovitch, 1971). The *ΔdivL* mutation in the SBpG*Δ280* background decreased but did not abolish the number of cells that lysed, and because cell lysis requires CtrA~P, it is possible that an SB1003-derived *ΔdivL* mutant has decreased levels of CtrA~P or phosphorylates CtrA at a later stage during growth, resulting in a delayed lysis. This possibility could be tested by incubating cultures for longer periods of time, and monitoring the culture turbidity however this has not been investigated in detail.

Cells expressing the nonphosphorylatable CtrA(D51A) produce much more RcGTA capsid protein than cells expressing WT CtrA or the phosphomimetic CtrA(D51E) (Mercer *et al.*, 2012), although no explanation for this observation has been proposed.

The dramatic increase in RcGTA capsid production (and transduction) for SB1003 *ΔdivL* compared to SB1003 (Figure 21B and C) was not reflected at the transcriptional level. The beta-galactosidase activity of *ΔdivL* cells containing the RcGTA promoter-reporter plasmid p601-g65 was similar to that of the *ΔcckA* and *ΔchpT* mutants (Figure 21D), and no noticeable increase in the percentage of cells expressing the RcGTA promoter was observed using a fluorescent reporter (not shown, (Fogg *et al.*, 2012a)). Although a small increase in capsid production was observed from the *ΔcckA* mutant (Figure 22A), this increase appeared much smaller than the increase for the *ΔdivL* mutation. It is therefore possible that the effect of the absence of DivL occurs at the post-transcriptional level, by an unknown mechanism.

4.4.2 DivL likely regulates CckA through the PAS domains

Childers *et al.* (2014) reported that the DivL PAS domains were involved in modulating the specificity of DivL to DivK~P over DivK, and speculated that binding of DivK~P to DivL could alter the conformation of the PAS domain of DivL. This in turn could influence the structure and function of CckA, thereby regulating the CckA-ChpT-CtrA pathway (Childers *et al.*, 2014). The results obtained for *R. capsulatus* are consistent with DivL having a role in regulation of CckA activity, and since the *R. capsulatus* DivL protein lacks the DHp and CA domains, this supports the proposal by Childers *et al.* (2014) that it is the PAS domains of *C. crescentus* DivL modulates CckA.

4.5 Three separate clusters required for RcGTA production are regulated by the same regulatory systems

Despite RcGTA being encoded by (at least) three separate loci (the primary RcGTA cluster, the endolysin-holin genes, and the GhsA/GhsB head spike encoding genes), the promoters of all three clusters are regulated by the by the CckA-ChpT-CtrA phosphorelay. Expression of the primary gene cluster (Leung *et al.*, 2012) and the head spike genes (Figure 26C) are furthermore regulated by an acyl homoserine lactone synthesized by GtaI (regulation of the lysis genes by GtaI was not investigated). This phosphorelay also regulated maturation of RcGTA (see section 3.3 and 3.5.2), to my knowledge the first example of a HK and RR regulating assembly of a phage-like particle, or phage.

GtaI/GtaR and CckA-ChpT-CtrA are furthermore involved in regulating RcGTA recipient capability. GtaI is required for expression of the polysaccharide biosynthetic gene cluster located directly 3' of *ghsA/ghsB.* This biosynthesis cluster is required for the production of the CPS receptor for RcGTA (Brimacombe *et al.*, 2013). Recipient cells lacking CtrA are unable to receive alleles by RcGTA-mediated transduction (Brimacombe *et al.*, 2014), at least in part due to lack of expression in a *ΔctrA* mutant of a natural transformation-like system essential for RcGTA recipient capability (Brimacombe *et al.*, 2015).

4.6 Amino acid depletion and effects on RcGTA production

Bacteria monitor their physiological state and adjust their gene expression accordingly. Building on previous unpublished results from our lab, I've found that the stimulation of RcGTA production by carbon nutrient depletion is replicated by transient depletion of amino acids (Figure 32 and Figure 33). The depletion of nutrients, and particularly depletion of amino acids in several species initiates a global starvation response mediated by ppGpp. This stringent

response has been studied in several organisms including *E. coli* and *C. crescentus*. It appeared possible that a stringent response initiated at the entry to stationary phase induced RcGTA production. However, a mutant lacking SpoT, which is required for ppGpp production in *R. capsulatus* (Masuda and Bauer, 2004), still produces RcGTA indicating that the stringent response is not required for RcGTA production. It therefore appears likely that the increased production of RcGTA after carbon or amino acid depletion is not due to stimulation by the stringent response, although experiments depleting the *ΔspoT* mutant of of carbon or treatment with 3AT to test this directly did not yield consistent results (not shown).

CtrA is required for RcGTA production. In *C. crescentus*, the levels of CtrA fluctuate during the cell cycle, due in part to degradation by ClpXP (Curtis and Brun, 2010). Carbon depletion has been shown to influence levels of CtrA. Lesley *et al.* reported that carbon starvation of *C. crescentus* swarmer cells blocks the transition to stalked cells, and levels of CtrA are stabilized. However, levels of CtrA are restored in the non-starved samples as stalked cells initiate another round of replication and division, whereas it remains low in the swarmer cells (Lesley and Shapiro, 2008).

In contrast, nitrogen depletion does not appear to have a strong effect on CtrA levels (Gorbatyuk and Marczynski, 2005). Another study found that CtrA levels from a mixed population of *C. crescentus* cells were reduced to 50% after 30 min of carbon starvation, and reported that the re-accumulation of CtrA depended on the general stress response sigma factor SigT (EcfG) (Britos *et al.*, 2011). Combined nitrogen and carbon depletion has recently been shown to halt *Sinorhizobium meliloti* cells in the G1 phase, and allowed for cell synchronization. The growth arrest was assumed to be mediated by (p)ppGpp, however this assumption was not tested. (De Nisco *et al.*, 2014).

It is possible that altered levels of CtrA are responsible for the stimulation of RcGTA production (see below for one possible mechanism). If a fluctuation in the level of CtrA after carbon depletion is responsible for the observed effect on RcGTA, it would indicate that in contrast to *C. crescentus,* the levels of CtrA are not affected by EcfG in *R. capsulatus* (Figure 37).

Ribosomes that pause or stall during translation use the tmRNA system to modify and release the peptide, attaching a C-terminal ssrA tag (see section 1.7.5). In *E. coli*, this targets the peptide for degradation by cellular proteases, primarily ClpXP, but also ClpAP and FtsH (Barends *et al.*, 2011, Moore and Sauer, 2007). The tmRNA system has been implicated in the life cycle of several phages, including phage Mu, and is thought to allow the phage to monitor the fitness of the host (Moore and Sauer, 2007, Ranquet *et al.*, 2001). The ClpXP protease was reported to be present as a few copies in *E. coli* that could be saturated by overproducing proteins with artificial ssrA tags (Baker and Sauer, 2012). Interestingly, the *C. crescentus* ssrA RNA is cell-cycle regulated; strains lacking the tmRNA system have delayed replication initiation, and the timing of CtrA degradation relative to replication is dysregulated (Keiler and Shapiro, 2003b, Keiler and Shapiro, 2003a).

Amino acid depletion of *R. capsulatus* likely reduces the pool of aminoacylated tRNA, which could lead to a saturation of ClpXP by ssrA-tagged peptides and higher levels of CtrA. The CtrA levels in *R. capsulatus* after carbon or amino acid depletion was not investigated.

Because only temporary, but not continued, histidine depletion increased RcGTA production (Figure 33 and Figure S7) it appears possible that the effect on RcGTA production is a result of the sudden availability of nutrients rather than absence of nutrients. However, this is contradicted by previous unpublished experiments in which it was found that RcGTA production

was stimulated when cultures entered a premature stationary phase in a growth medium low in carbon, compared to a replete medium (Taylor, 2004).

4.7 Transduction assays can misrepresent GTA production

The classical method to determine the levels of GTA production is a transduction bioassay using a culture supernatant, filtered to remove cells. Such assays do not address whether different transduction levels are due to altered levels of GTA particles or an altered transduction-efficiency per GTA particle. As the transduction assay results for the production of RcGTA particles by mutant strain SB1003*ΔghsB* showed, a mutation that exhibited a decreased transduction efficiency per particle (Figure 25A) yielded an increased transduction frequency in the culture (Figure 25D), due to an increased amount of RcGTA present in the fraction (supernatant) used for the assay (Figure 25E). Therefore, the transduction efficiency measurments on cultures should be accompanied by western blots probed with antiserum raised against a GTA protein (such as a capsid protein) whenever possible.

4.8 Asymmetric growth in the Alphaproteobacteria and cell division control by CtrA

Asymmetric growth and/or division is found in several bacterial lineages but has been most intensively studied in *C. crescentus* (Kysela *et al.*, 2013). *C. crescentus* produces a sessile stalked and a motile swarmer cell after cell division, and this cell cycling is regulated by CtrA (Curtis and Brun, 2010, Quon *et al.*, 1996, Terrana and Newton, 1975). In addition to *C. crescentus*, there is ample evidence that certain other Alphaproteobacteria, such as *S. meliloti*, *Brucella abortus* and *Agrobacterium tumefaciens* and *Ochrobactrum anthropi* divide asymmetrically (Brown *et al.*, 2012, Hallez *et al.*, 2004, Lam *et al.*, 2003, Terrana and Newton, 1975). During symbiosis with plants, *S. meliloti* differentiates into non-replicative nitrogen-

fixing bacteroid cells. Although different than the dimorphic cell division of *C. crescentus*, this differentiation also appears to be controlled by CtrA (Pini *et al.*, 2015, Pini *et al.*, 2013).

The CtrA RR is well conserved in the Alphaproteobacteria, but not observed in bacteria from other classes (Brilli *et al.*, 2010). As in *C. crescentus*, perturbations of CtrA levels, or the control of CtrA phosphorylation, result in cell division defects for *A. tumefaciens, B. abortus* and *S. meliloti* (Bellefontaine et al., 2002, Kim et al., 2013, Pini et al., 2015, Willett et al., 2015). For *C. crescentus*, CtrA binds to DNA sequence motifs in the origin of replication to inhibit DNA replication in swarmer cells and control the cell cycle (Quon *et al.*, 1998). No binding of CtrA to the origin of replication was detected for *S. meliloti*, however depletion of CtrA resulted in a 20-fold increase in DNA content per cell, indicating that CtrA modulates DNA replication, and likely cell division, by an unknown mechanism (Pini *et al.*, 2015).

In contrast to *R. capsulatus*, CtrA is essential for *C. crescentus*, *S. meliloti, B. abortus*, and *A. tumefaciens* and all four organisms have the regulators DivJ, DivK and PleC that regulate CckA activity (Barnett *et al.*, 2001, Bellefontaine *et al.*, 2002, Brilli *et al.*, 2010, Kim *et al.*, 2013, Quon *et al.*, 1996, Willett *et al.*, 2015). Because in *R. capsulatus* CtrA, CckA and ChpT are not essential, and because mutants that lack these proteins have no gross growth or cell morphology defects, it has been suggested that these proteins are not involved in regulating *R. capsulatus* cell division (Hallez *et al.*, 2004, Mercer *et al.*, 2012).

Despite the fact that a loss of any of the above regulators does not result in an obvious change in phenotype, it appears that increased levels or over-phosphorylation of CtrA results in cell division defects of *R. capsulatus*, indicating that CtrA may regulate cell division or differentiation. A *ΔclpX* mutant was found to have increased levels of CtrA (Figure 18) which

indicates that CtrA is proteolytically degraded by ClpXP in *R. capsulatus* SB1003 as in *C. crescentus* (Jenal and Fuchs, 1998). The *ΔclpX* mutant was found to have a defect in cell division and formed long filamentous cells, and this defect was ameliorated by introducing a *ΔctrA* mutation (Figure 17). Furthermore, expression of the predicted constitutive kinase mutant CckA(Y589D) resulted in extensive CtrA-dependent cell filamentation (Figure 19). Because RcGTA production is confined to a small subset of the population of the WT SB1003 (Fogg *et al.*, 2012b, Hynes *et al.*, 2012), and the CckA(Y589D) allele did not result in detectable cell lysis typical of the strains that overexpress RcGTA, it appears that the cell division defects are independent of RcGTA production. It is uncertain how the increase in CtrA concentration elicits cell filamentation, however this effect on septation appears to be exerted only by the phosphorylated form of CtrA. This observation indicates that CtrA may also be involved in cell division for bacterial species where CtrA is not essential.

Chapter 5: Conclusion and Future Directions

The Alphaproteobacterium *R. capsulatus* produces a gene transfer agent called RcGTA. RcGTA shows similarities to the temperate phages lambda and HK97, and it has been proposed that RcGTA shares a common ancestor with a prophage (Lang and Beatty, 2001, Lang and Beatty, 2007, Lang *et al.*, 2012). This thesis presents several results which further strengthen the relationship between RcGTA and phages. Additionally, these results show that several levels of the production of RcGTA is regulated by bacterial regulatory systems, particularly the phosphorelay CckA-ChpT-CtrA.

Similar to most tailed ds DNA phages (Young, 2013), the RcGTA particle is released from cells by cell lysis, which requires an endolysin and holin system (Section 3.1). Release is inhibited by high (millimolar) concentrations of inorganic phosphate in the growth medium, by a mechanism that appears to be post-translational. Cell lysis is hard to detect for WT strains, consistent with the low percentage of cells producing RcGTA. In contrast, lysis is readily observable for RcGTA overproducer strains as a drop in culture turbidity, and the release from cells of membrane-bound pigments and the cytoplasmic enzyme malate dehydrogenase. Cell lysis is regulated by the CckA-ChpT-CtrA phosphorelay, and lysis requires phosphorylation of CtrA. This regulation is on the transcriptional level of the lysis system, as the promoter of the endolysin/holin requires CckA, ChpT and CtrA for activity.

Two new regulators of RcGTA were discovered: ClpX and DivL (Section 3.2). ClpX is predicted to be a component of the ClpXP protease, which in *C. crescentus* regulates CtrA levels by proteolytic degradation. Increased levels of CtrA were detected in a *ΔclpX* mutant, consistent with the degradation of CtrA by ClpXP in *R. capsulatus*. ClpX was required for RcGTA

transduction, but not for capsid production or cell lysis. Additionally, cells lacking ClpX had a cell division defect resulting in the formation of elongated, filamentous cells.

A loss of DivL produced opposite results for the WT strain SB1003 and the RcGTA overproducer DE442: DivL was required for maximal transduction frequency and cell lysis of DE442, similar to a *cckA* mutant. In contrast, a loss of DivL increased transduction for SB1003. Cell lysis could be restored for DE442 *ΔdivL* by introducing a putative constitutively kinase-active CckA allele, indicating that DivL modulates the kinase activity of CckA similar to the role of DivL in *C. crescentus* (Tsokos *et al.*, 2011). It is unclear what gives rise to the different phenotypes of the RcGTA overproducer and the WT *ΔdivL* mutants. It is possible that the overproducer strain lacks an additional regulator of CckA activity, and future studies could aim to elucidate the genetic background of this difference. Because the *ghsA/ghsB* promoter requires DivL for activity in DE442, but not SB1003, this promoter could be a useful reporter in such an investigation. A protein pulldown experiment using DivL and/or CckA, might allow for confirmation of the predicted interaction between CckA and DivL, and possibly allow identification of the hypothetical missing regulator of CckA in DE442. It is possible that phosphorylation of CtrA, and thereby cell lysis, is delayed in WT cells lacking DivL. This could be investigated by measuring particle release as a function of time. The phosphorylation level of CtrA could further be investigated using commercially available Phos-tag SDS-PAGE (Kinoshita *et al.*, 2006) to separate CtrA and CtrA~P followed by a western blot probed with CtrA antiserum.

Although the historical record is uncertain, it was thought that both SB1003 and DE442 were derived from B10 (see section 2.1), and the close relationship between SB1003 and DE442 was supported by comparison of genome sequences (Ding *et al.*, 2014). However, DE442 lacks

the 133 kb plasmid pRCB133 (Ding *et al.*, 2014, Hynes *et al.*, 2012) and has more than 700 single nucleotide polymorphisms compared to SB1003 (H. Ding, unpublished), and so it is likely that one or more of these differences causes the difference in the two *ΔdivL* phenotypes.

Similar to phages (Aksyuk and Rossmann, 2011), the RcGTA particle was found to undergo a maturation process to form transduction competent particles. This process was found to be regulated by a bacterial signaling system, the CckA-ChpT-CtrA phosphorelay (Section 3.3 and 3.5). In the absence of CckA, predominantly tail- and spike-less DNA-containing heads were produced. Additionally, the *ΔcckA* mutant produced tail-like polytube structures. The maturation defects of the *ΔcckA* mutant were partially overcome by introduction of phosphomimetic CtrA, indicating that phosphorylation of CtrA is required for successful particle assembly. A requirement for ClpX for particle maturation was also identified. The *ΔclpX* mutant produced tail-less heads that did not contain DNA, indicating that ClpX is required for the complete assembly of RcGTA heads.

RcGTA particles were found to contain head spikes and tail fibers, confirming initial observations of RcGTA (Yen *et al.*, 1979). Additionally, a baseplate-like structure was observed (Section 3.5). It would be interesting to do higher resolution structural studies of RcGTA and mutant derivatives, using electron cryo-tomography or X-ray crystallography to better understand assembly of RcGTA.

The production of head spikes required *ghsB*, which appears to be co-transcribed with *ghsA* (Section 3.4). Expression of *ghsA/ghsB* required the CckA-ChpT-CtrA phosphorelay and GtaI/GtaR quorum sensing systems. Homologues of GhsA and GhsB appear to be present in some phages that infect *R. capsulatus*. The RcGTA head spikes are required for binding to the polysaccharide capsule of *R. capsulatus* and needed for maximal frequencies of gene transfer per

particle, but are not essential for gene transduction. The *ghsA/ghsB* promoter was found to be active in a *ΔclpX* mutant; however the observed capsids from this mutant lacked spikes, indicating that the head spikes are attached to the capsid after DNA packaging.

The vast majority of phages have been reported to recognize their host using receptor-binding structures on the phage tail. However, many phages have additional proteins with no known function on their capsids. It is possible that several phages may also utilize such protein structures on the head to bind to cells. Although the GhsB protein was required for head spike production, no formal proof was obtained that the spike structure is made up of GhsB. Future studies could aim to confirm that this is the case by raising antibodies against GhsB, or by appending an epitope tag such as FLAG, and performing immunogold-TEM to identify the specific location of GhsB. Alternatively, fusing a protein such as maltose biding protein to GhsB to detect an increased size or altered shape of the spike structure by TEM could be performed. GhsB was predicted to be a carbohydrate-binding protein, but no binding of recombinantly produced protein to capsule coated cells was detected. Future studies could attempt to demonstrate that GhsB binds carbohydrate by co-expression of GhsA, which may be required for the formation of a biologically active protein complex.

Production of RcGTA is stimulated at high cell concentration in the stationary phase (Solioz *et al.*, 1975). It was found that temporary amino acid depletion stimulates RcGTA production, however *spoT*, required for the *R. capsulatus* stringent response (Masuda and Bauer, 2004), was not required for RcGTA production (Section 3.6). It therefore appears that the production of RcGTA is otherwise influenced by nutrient availabilities. The signaling mechanism responsible for this effect was not identified, and could be of interest for future studies. The analysis of gene expression profiles of amino acid depleted cells compared could be

a starting point for such an investigation. It would further be of interest to investigate the levels and phosphorylation state of CtrA after amino acid depletion, as this protein is a central regulator of RcGTA and its levels are altered by nutrient starvation in other organisms (see section 4.6).

To conclude, RcGTA has been shown to be a particle that undergoes maturation and release by mechanisms very similar to certain phages. However, the regulation of RcGTA production is more extensively intertwined with bacterial systems than are phages. Furthermore, unlike most prophages, the genes encoding RcGTA are found in at least three separate clusters in the bacterial genome.

References

Ackermann, H.W. (2003) Bacteriophage observations and evolution. *Res Microbiol* **154**: 245-251.

Adams, C.W., Forrest, M.E., Cohen, S.N. and Beatty, J.T. (1989) Structural and functional analysis of transcriptional control of the *Rhodobacter capsulatus puf* operon. *J Bacteriol* **171**: 473-482.

Aklujkar, M., Harmer, A.L., Prince, R.C. and Beatty, J.T. (2000) The *orf162b* sequence of *Rhodobacter capsulatus* encodes a protein required for optimal levels of photosynthetic pigment-protein complexes. *J Bacteriol* **182**: 5440-5447.

Aksyuk, A.A. and Rossmann, M.G. (2011) Bacteriophage assembly. *Viruses* **3**: 172-203.

Alahuhta, M., Luo, Y., Ding, S.Y., Himmel, M.E. and Lunin, V.V. (2011) Structure of CBM4 from Clostridium thermocellum cellulase K. *Acta Crystallogr Sect F Struct Biol Cryst Commun* **67**: 527-530.

Alahuhta, M., Xu, Q., Bomble, Y.J., Brunecky, R., Adney, W.S., Ding, S.Y. *et al.* (2010) The unique binding mode of cellulosomal CBM4 from Clostridium thermocellum cellobiohydrolase A. *J Mol Biol* **402**: 374-387.

Anderson, B., Goldsmith, C., Johnson, A., Padmalayam, I. and Baumstark, B. (1994) Bacteriophage-like particle of Rochalimaea henselae. *Mol Microbiol* **13**: 67-73.

Ang, D., Keppel, F., Klein, G., Richardson, A. and Georgopoulos, C. (2000) Genetic analysis of bacteriophage-encoded cochaperonins. *Annu Rev Genet* **34**: 439-456.

Bae, B., Ohene-Adjei, S., Kocherginskaya, S., Mackie, R.I., Spies, M.A., Cann, I.K. and Nair, S.K. (2008) Molecular basis for the selectivity and specificity of ligand recognition by the family 16 carbohydrate-binding modules from Thermoanaerobacterium polysaccharolyticum ManA. *J Biol Chem* **283**: 12415-12425.

Baker, T.A. and Sauer, R.T. (2012) ClpXP, an ATP-powered unfolding and protein-degradation machine. *Biochim Biophys Acta* **1823**: 15-28.

Barany, F. (1985) Single-stranded hexameric linkers: a system for in-phase insertion mutagenesis and protein engineering. *Gene* **37**: 111-123.

Barbian, K.D. and Minnick, M.F. (2000) A bacteriophage-like particle from Bartonella bacilliformis. *Microbiology* **146 (Pt 3)**: 599-609.

Barends, S., Kraal, B. and van Wezel, G.P. (2011) The tmRNA-tagging mechanism and the control of gene expression: a review. *Wiley Interdiscip Rev RNA* **2**: 233-246.

Barnett, M.J., Hung, D.Y., Reisenauer, A., Shapiro, L. and Long, S.R. (2001) A homolog of the CtrA cell cycle regulator is present and essential in Sinorhizobium meliloti. *J Bacteriol* **183**: 3204-3210.

Barr, J.J., Auro, R., Furlan, M., Whiteson, K.L., Erb, M.L., Pogliano, J. *et al.* (2013) Bacteriophage adhering to mucus provide a non-host-derived immunity. *Proc Natl Acad Sci U S A* **110**: 10771-10776.

Batchelor, J.D., Doucleff, M., Lee, C.J., Matsubara, K., De Carlo, S., Heideker, J. *et al.* (2008) Structure and regulatory mechanism of Aquifex aeolicus NtrC4: variability and evolution in bacterial transcriptional regulation. *J Mol Biol* **384**: 1058-1075.

Beatty, J.T. and Gest, H. (1981) Generation of Succinyl-Coenzyme-a in Photosynthetic Bacteria. *Archives of Microbiology* **129**: 335-340.

Bellefontaine, A.F., Pierreux, C.E., Mertens, P., Vandenhaute, J., Letesson, J.J. and De Bolle, X. (2002) Plasticity of a transcriptional regulation network among alpha-proteobacteria is supported by the identification of CtrA targets in Brucella abortus. *Mol Microbiol* **43**: 945-960.

Berry, J., Rajaure, M., Pang, T. and Young, R. (2012) The spanin complex is essential for lambda lysis. *J Bacteriol* **194**: 5667-5674.

Bertani, G. (1999) Transduction-like gene transfer in the methanogen Methanococcus voltae. *J Bacteriol* **181**: 2992-3002.

Bhate, M.P., Molnar, K.S., Goulian, M. and DeGrado, W.F. (2015) Signal transduction in histidine kinases: insights from new structures. *Structure* **23**: 981-994.

Biers, E.J., Wang, K., Pennington, C., Belas, R., Chen, F. and Moran, M.A. (2008) Occurrence and expression of gene transfer agent genes in marine bacterioplankton. *Appl Environ Microbiol* **74**: 2933-2939.

Bird, T.H. and MacKrell, A. (2011) A CtrA homolog affects swarming motility and encystment in Rhodospirillum centenum. *Arch Microbiol* **193**: 451-459.

Black, L.W. and Thomas, J.A. (2012) Condensed genome structure. *Adv Exp Med Biol* **726**: 469-487.

Bläsi, U. and Young, R. (1996) Two beginnings for a single purpose: the dual-start holins in the regulation of phage lysis. *Mol Microbiol* **21**: 675-682.

Boraston, A.B., Bolam, D.N., Gilbert, H.J. and Davies, G.J. (2004) Carbohydrate-binding modules: fine-tuning polysaccharide recognition. *Biochem J* **382**: 769-781.

Boraston, A.B., Nurizzo, D., Notenboom, V., Ducros, V., Rose, D.R., Kilburn, D.G. and Davies, G.J. (2002) Differential oligosaccharide recognition by evolutionarily-related beta-1,4 and beta-1,3 glucan-binding modules. *J Mol Biol* **319**: 1143-1156.

Boto, L. (2014) Horizontal gene transfer in the acquisition of novel traits by metazoans. *Proc Biol Sci* **281**: 20132450.

Bourret, R.B. (2010) Receiver domain structure and function in response regulator proteins. *Curr Opin Microbiol* **13**: 142-149.

Brilli, M., Fondi, M., Fani, R., Mengoni, A., Ferri, L., Bazzicalupo, M. and Biondi, E.G. (2010) The diversity and evolution of cell cycle regulation in alpha-proteobacteria: a comparative genomic analysis. *BMC Syst Biol* **4**: 52.

Brimacombe, C.A., Ding, H. and Beatty, J.T. (2014) Rhodobacter capsulatus DprA is essential for RecA-mediated gene transfer agent (RcGTA) recipient capability regulated by quorum-sensing and the CtrA response regulator. *Mol Microbiol* **92**: 1260-1278.

Brimacombe, C.A., Ding, H., Johnson, J.A. and Beatty, J.T. (2015) Homologues of Genetic Transformation DNA Import Genes Are Required for Rhodobacter capsulatus Gene Transfer Agent Recipient Capability Regulated by the Response Regulator CtrA. *J Bacteriol* **197**: 2653-2663.

Brimacombe, C.A., Stevens, A., Jun, D., Mercer, R., Lang, A.S. and Beatty, J.T. (2013) Quorum-sensing regulation of a capsular polysaccharide receptor for the Rhodobacter capsulatus gene transfer agent (RcGTA). *Mol Microbiol* **87**: 802-817.

Britos, L., Abeliuk, E., Taverner, T., Lipton, M., McAdams, H. and Shapiro, L. (2011) Regulatory response to carbon starvation in Caulobacter crescentus. *PLoS One* **6**: e18179.

Brown, P.J., de Pedro, M.A., Kysela, D.T., Van der Henst, C., Kim, J., De Bolle, X. *et al.* (2012) Polar growth in the Alphaproteobacterial order Rhizobiales. *Proc Natl Acad Sci U S A* **109**: 1697-1701.

Brun, E., Johnson, P.E., Creagh, A.L., Tomme, P., Webster, P., Haynes, C.A. and McIntosh, L.P. (2000) Structure and binding specificity of the second N-terminal cellulose-binding domain from Cellulomonas fimi endoglucanase C. *Biochemistry* **39**: 2445-2458.

Burrus, V., Pavlovic, G., Decaris, B. and Guedon, G. (2002) Conjugative transposons: the tip of the iceberg. *Mol Microbiol* **46**: 601-610.

Campbell, A. (1961) Sensitive mutants of bacteriophage lambda. *Virology* **14**: 22-32.

Campbell, A. (2005) General aspects of lysogeny. In: The Prophages. R.L. Calendar (ed). Oxford University Press, pp. 66-73.

Carattoli, A. (2013) Plasmids and the spread of resistance. *Int J Med Microbiol* **303**: 298-304.

Casino, P., Rubio, V. and Marina, A. (2010) The mechanism of signal transduction by two-component systems. *Curr Opin Struct Biol* **20**: 763-771.

Casjens, S.R. (2011) The DNA-packaging nanomotor of tailed bacteriophages. *Nat Rev Microbiol* **9**: 647-657.

Casjens, S.R. and Gilcrease, E.B. (2009) Determining DNA packaging strategy by analysis of the termini of the chromosomes in tailed-bacteriophage virions. *Methods Mol Biol* **502**: 91-111.

Casjens, S.R., Gilcrease, E.B., Winn-Stapley, D.A., Schicklmaier, P., Schmieger, H., Pedulla, M.L. *et al.* (2005) The generalized transducing Salmonella bacteriophage ES18: complete genome sequence and DNA packaging strategy. *J Bacteriol* **187**: 1091-1104.

Casjens, S.R. and Hendrix, R.W. (2015) Bacteriophage lambda: Early pioneer and still relevant. *Virology* **479-480**: 310-330.

Casjens, S.R. and Molineux, I.J. (2012) Short noncontractile tail machines: adsorption and DNA delivery by podoviruses. *Adv Exp Med Biol* **726**: 143-179.

Catalao, M.J., Gil, F., Moniz-Pereira, J., Sao-Jose, C. and Pimentel, M. (2013) Diversity in bacterial lysis systems: bacteriophages show the way. *FEMS Microbiol Rev* **37**: 554-571.

Chen, F., Spano, A., Goodman, B.E., Blasier, K.R., Sabat, A., Jeffery, E. *et al.* (2009a) Proteomic analysis and identification of the structural and regulatory proteins of the *Rhodobacter capsulatus* gene transfer agent. *J Proteome Res* **8**: 967-973.

Chen, Y.E., Tsokos, C.G., Biondi, E.G., Perchuk, B.S. and Laub, M.T. (2009b) Dynamics of two Phosphorelays controlling cell cycle progression in Caulobacter crescentus. *J Bacteriol* **191**: 7417-7429.

Cheung, J. and Hendrickson, W.A. (2010) Sensor domains of two-component regulatory systems. *Curr Opin Microbiol* **13**: 116-123.

Childers, W.S., Xu, Q., Mann, T.H., Mathews, II, Blair, J.A., Deacon, A.M. and Shapiro, L. (2014) Cell fate regulation governed by a repurposed bacterial histidine kinase. *PLoS Biol* **12**: e1001979.

Cid, M., Pedersen, H.L., Kaneko, S., Coutinho, P.M., Henrissat, B., Willats, W.G. and Boraston, A.B. (2010) Recognition of the helical structure of beta-1,4-galactan by a new family of carbohydrate-binding modules. *J Biol Chem* **285**: 35999-36009.

Claverys, J.P., Prudhomme, M. and Martin, B. (2006) Induction of competence regulons as a general response to stress in gram-positive bacteria. *Annu Rev Microbiol* **60**: 451-475.

Curtis, P.D. and Brun, Y.V. (2010) Getting in the loop: regulation of development in Caulobacter crescentus. *Microbiol Mol Biol Rev* **74**: 13-41.
Davidson, A.R., Cardarelli, L., Pell, L.G., Radford, D.R. and Maxwell, K.L. (2012) Long noncontractile tail machines of bacteriophages. *Adv Exp Med Biol* **726**: 115-142.
De Nisco, N.J., Abo, R.P., Wu, C.M., Penterman, J. and Walker, G.C. (2014) Global analysis of cell cycle gene expression of the legume symbiont Sinorhizobium meliloti. *Proc Natl Acad Sci U S A* **111**: 3217-3224.
Dewey, J.S., Savva, C.G., White, R.L., Vitha, S., Holzenburg, A. and Young, R. (2010) Micron-scale holes terminate the phage infection cycle. *Proc Natl Acad Sci U S A* **107**: 2219-2223.
Ding, H., Moksa, M.M., Hirst, M. and Beatty, J.T. (2014) Draft Genome Sequences of Six Rhodobacter capsulatus Strains, YW1, YW2, B6, Y262, R121, and DE442. *Genome Announc* **2**.
Domian, I.J., Quon, K.C. and Shapiro, L. (1997) Cell type-specific phosphorylation and proteolysis of a transcriptional regulator controls the G1-to-S transition in a bacterial cell cycle. *Cell* **90**: 415-424.
Dong, X., Xu, F., Gong, Y., Gao, J., Lin, P., Chen, T. *et al.* (2006) Crystal structure of the V domain of human Nectin-like molecule-1/Syncam3/Tsll1/Igsf4b, a neural tissue-specific immunoglobulin-like cell-cell adhesion molecule. *J Biol Chem* **281**: 10610-10617.
Duda, R.L., Hempel, J., Michel, H., Shabanowitz, J., Hunt, D. and Hendrix, R.W. (1995a) Structural transitions during bacteriophage HK97 head assembly. *J Mol Biol* **247**: 618-635.
Duda, R.L., Martincic, K. and Hendrix, R.W. (1995b) Genetic basis of bacteriophage HK97 prohead assembly. *J Mol Biol* **247**: 636-647.
Duda, R.L., Ross, P.D., Cheng, N., Firek, B.A., Hendrix, R.W., Conway, J.F. and Steven, A.C. (2009) Structure and energetics of encapsidated DNA in bacteriophage HK97 studied by scanning calorimetry and cryo-electron microscopy. *J Mol Biol* **391**: 471-483.
Eiserling, F., Pushkin, A., Gingery, M. and Bertani, G. (1999) Bacteriophage-like particles associated with the gene transfer agent of methanococcus voltae PS. *J Gen Virol* **80 (Pt 12)**: 3305-3308.
Feiss, M., Kobayashi, I. and Widner, W. (1983) Separate sites for binding and nicking of bacteriophage lambda DNA by terminase. *Proc Natl Acad Sci U S A* **80**: 955-959.
Feiss, M. and Rao, V.B. (2012) The bacteriophage DNA packaging machine. *Adv Exp Med Biol* **726**: 489-509.
Florizone, S.M. (2006) Studies on the Regulation of the Gene Transfer Agent (GTA) of *Rhodobacter capsulatus*. Vancouver, BC, Canada: Microbiology & Immunology, University of British Columbia.
Fogg, P.C., Hynes, A.P., Digby, E., Lang, A.S. and Beatty, J.T. (2011) Characterization of a newly discovered Mu-like bacteriophage, RcapMu, in Rhodobacter capsulatus strain SB1003. *Virology* **421**: 211-221.
Fogg, P.C., Westbye, A.B. and Beatty, J.T. (2012a) One for all or all for one: heterogeneous expression and host cell lysis are key to gene transfer agent activity in *Rhodobacter capsulatus*. *PLoS One* **7**: e43772.

Fogg, P.C.M., Westbye, A.B. and Beatty, J.T. (2012b) One for All or All for One: Heterogeneous Expression and Host Cell Lysis Are Key to Gene Transfer Agent Activity in Rhodobacter capsulatus. *Plos One* **7**.
Fokine, A. and Rossmann, M.G. (2014) Molecular architecture of tailed double-stranded DNA phages. *Bacteriophage* **4**: e28281.
Francez-Charlot, A., Kaczmarczyk, A., Fischer, H.M. and Vorholt, J.A. (2015a) The general stress response in Alphaproteobacteria. *Trends Microbiol* **23**: 164-171.
Francez-Charlot, A., Kaczmarczyk, A. and Vorholt, J.A. (2015b) The branched CcsA/CckA-ChpT-CtrA phosphorelay of Sphingomonas melonis controls motility and biofilm formation. *Mol Microbiol* **97**: 47-63.
Fraser, J.S., Maxwell, K.L. and Davidson, A.R. (2007) Immunoglobulin-like domains on bacteriophage: weapons of modest damage? *Curr Opin Microbiol* **10**: 382-387.
Fraser, J.S., Yu, Z., Maxwell, K.L. and Davidson, A.R. (2006) Ig-like domains on bacteriophages: a tale of promiscuity and deceit. *J Mol Biol* **359**: 496-507.
Friedman, D.I. and Court, D.L. (2005) Regulation of lambda gene expression by transcription termination and antitermination. In: The Bacteriophages. R.L. Calendar (ed). Oxford University Press, pp. 83-103.
Frost, L.S., Leplae, R., Summers, A.O. and Toussaint, A. (2005) Mobile genetic elements: the agents of open source evolution. *Nat Rev Microbiol* **3**: 722-732.
Fuller, D.N., Raymer, D.M., Rickgauer, J.P., Robertson, R.M., Catalano, C.E., Anderson, D.L. *et al.* (2007) Measurements of single DNA molecule packaging dynamics in bacteriophage lambda reveal high forces, high motor processivity, and capsid transformations. *J Mol Biol* **373**: 1113-1122.
Fulsundar, S., Harms, K., Flaten, G.E., Johnsen, P.J., Chopade, B.A. and Nielsen, K.M. (2014) Gene transfer potential of outer membrane vesicles of Acinetobacter baylyi and effects of stress on vesiculation. *Appl Environ Microbiol* **80**: 3469-3483.
Galperin, M.Y. (2010) Diversity of structure and function of response regulator output domains. *Curr Opin Microbiol* **13**: 150-159.
Gao, R. and Stock, A.M. (2010) Molecular strategies for phosphorylation-mediated regulation of response regulator activity. *Curr Opin Microbiol* **13**: 160-167.
Gardner, S.G., Johns, K.D., Tanner, R. and McCleary, W.R. (2014) The PhoU protein from Escherichia coli interacts with PhoR, PstB, and metals to form a phosphate-signaling complex at the membrane. *J Bacteriol* **196**: 1741-1752.
Garrett, J., Fusselman, R., Hise, J., Chiou, L., Smith-Grillo, D., Schulz, J. and Young, R. (1981) Cell lysis by induction of cloned lambda lysis genes. *Mol Gen Genet* **182**: 326-331.
Gelvin, S.B. (2003) Agrobacterium-mediated plant transformation: the biology behind the "gene-jockeying" tool. *Microbiol Mol Biol Rev* **67**: 16-37, table of contents.
Genthner, F.J. and Wall, J.D. (1984) Isolation of a recombination-deficient mutant of Rhodopseudomonas capsulata. *J Bacteriol* **160**: 971-975.
Gonciarz-Swiatek, M., Wawrzynow, A., Um, S.J., Learn, B.A., McMacken, R., Kelley, W.L. *et al.* (1999) Recognition, targeting, and hydrolysis of the lambda O replication protein by the ClpP/ClpX protease. *J Biol Chem* **274**: 13999-14005.
Gorbatyuk, B. and Marczynski, G.T. (2005) Regulated degradation of chromosome replication proteins DnaA and CtrA in Caulobacter crescentus. *Mol Microbiol* **55**: 1233-1245.

Gottesman, S. (2003) Proteolysis in bacterial regulatory circuits. *Annu Rev Cell Dev Biol* **19**: 565-587.
Gottesman, S., Clark, W.P., de Crecy-Lagard, V. and Maurizi, M.R. (1993) ClpX, an alternative subunit for the ATP-dependent Clp protease of Escherichia coli. Sequence and in vivo activities. *J Biol Chem* **268**: 22618-22626.
Greene, S.E., Brilli, M., Biondi, E.G. and Komeili, A. (2012) Analysis of the CtrA pathway in Magnetospirillum reveals an ancestral role in motility in alphaproteobacteria. *J Bacteriol* **194**: 2973-2986.
Guerrero-Ferreira, R.C., Viollier, P.H., Ely, B., Poindexter, J.S., Georgieva, M., Jensen, G.J. and Wright, E.R. (2011) Alternative mechanism for bacteriophage adsorption to the motile bacterium Caulobacter crescentus. *Proc Natl Acad Sci U S A* **108**: 9963-9968.
Haan, C. and Behrmann, I. (2007) A cost effective non-commercial ECL-solution for Western blot detections yielding strong signals and low background. *J Immunol Methods* **318**: 11-19.
Halaby, D.M. and Mornon, J.P. (1998) The immunoglobulin superfamily: an insight on its tissular, species, and functional diversity. *J Mol Evol* **46**: 389-400.
Hallez, R., Bellefontaine, A.F., Letesson, J.J. and De Bolle, X. (2004) Morphological and functional asymmetry in alpha-proteobacteria. *Trends Microbiol* **12**: 361-365.
Hauryliuk, V., Atkinson, G.C., Murakami, K.S., Tenson, T. and Gerdes, K. (2015) Recent functional insights into the role of (p)ppGpp in bacterial physiology. *Nat Rev Microbiol* **13**: 298-309.
Hellen, C.U. and Wimmer, E. (1992) The role of proteolytic processing in the morphogenesis of virus particles. *Experientia* **48**: 201-215.
Hendrix, R.W. and Johnson, J.E. (2012) Bacteriophage HK97 capsid assembly and maturation. *Adv Exp Med Biol* **726**: 351-363.
Hershko, A. and Fry, M. (1975) Post-translational cleavage of polypeptide chains: role in assembly. *Annu Rev Biochem* **44**: 775-797.
Hillmer, P. and Gest, H. (1977) H2 metabolism in the photosynthetic bacterium Rhodopseudomonas capsulata: H2 production by growing cultures. *J Bacteriol* **129**: 724-731.
Howell, T. and Nakamoto, L. (2009) Detroit River-Western Lake Erie Basin Indicator Project. In.: United States Environmental Protection Agency, pp.
Hsieh, Y.J. and Wanner, B.L. (2010) Global regulation by the seven-component Pi signaling system. *Curr Opin Microbiol* **13**: 198-203.
Hudson, J.J., Taylor, W.D. and Schindler, D.W. (2000) Phosphate concentrations in lakes. *Nature* **406**: 54-56.
Huiskonen, J.T., Kivela, H.M., Bamford, D.H. and Butcher, S.J. (2004) The PM2 virion has a novel organization with an internal membrane and pentameric receptor binding spikes. *Nat Struct Mol Biol* **11**: 850-856.
Hynes, A.P., Mercer, R.G., Watton, D.E., Buckley, C.B. and Lang, A.S. (2012) DNA packaging bias and differential expression of gene transfer agent genes within a population during production and release of the Rhodobacter capsulatus gene transfer agent, RcGTA. *Mol Microbiol* **85**: 314-325.
Inagaki, M., Kawaura, T., Wakashima, H., Kato, M., Nishikawa, S. and Kashimura, N. (2003) Different contributions of the outer and inner R-core residues of lipopolysaccharide to the

recognition by spike H and G proteins of bacteriophage phiX174. *FEMS Microbiol Lett* **226**: 221-227.
Ind, A.C., Porter, S.L., Brown, M.T., Byles, E.D., de Beyer, J.A., Godfrey, S.A. and Armitage, J.P. (2009) Inducible-expression plasmid for *Rhodobacter sphaeroides* and *Paracoccus denitrificans*. *Appl Environ Microbiol* **75**: 6613-6615.
Iniesta, A.A., McGrath, P.T., Reisenauer, A., McAdams, H.H. and Shapiro, L. (2006) A phospho-signaling pathway controls the localization and activity of a protease complex critical for bacterial cell cycle progression. *Proc Natl Acad Sci U S A* **103**: 10935-10940.
Jenal, U. and Fuchs, T. (1998) An essential protease involved in bacterial cell-cycle control. *EMBO J* **17**: 5658-5669.
Johnston, C., Martin, B., Fichant, G., Polard, P. and Claverys, J.P. (2014) Bacterial transformation: distribution, shared mechanisms and divergent control. *Nat Rev Microbiol* **12**: 181-196.
Josslin, R. (1970) The lysis mechanism of phage T4: mutants affecting lysis. *Virology* **40**: 719-726.
Jung, K., Fried, L., Behr, S. and Heermann, R. (2012) Histidine kinases and response regulators in networks. *Curr Opin Microbiol* **15**: 118-124.
Katsura, I. (1983) Tail Assembly and Injection. In: Lambda II. R.W. Hendrix, J.W. Roberts & F.W. Stahl (eds). Cold Spring Harbour: Cold Spring Harbour Laboratory Press, pp. 331-346.
Katsura, I. (1990) Mechanism of length determination in bacteriophage lambda tails. *Adv Biophys* **26**: 1-18.
Katsura, I. and Hendrix, R.W. (1984) Length determination in bacteriophage lambda tails. *Cell* **39**: 691-698.
Katzke, N., Arvani, S., Bergmann, R., Circolone, F., Markert, A., Svensson, V. *et al.* (2010) A novel T7 RNA polymerase dependent expression system for high-level protein production in the phototrophic bacterium Rhodobacter capsulatus. *Protein Expr Purif* **69**: 137-146.
Keen, N.T., Tamaki, S., Kobayashi, D. and Trollinger, D. (1988) Improved broad-host-range plasmids for DNA cloning in gram-negative bacteria. *Gene* **70**: 191-197.
Keiler, K.C. and Shapiro, L. (2003a) tmRNA in Caulobacter crescentus is cell cycle regulated by temporally controlled transcription and RNA degradation. *J Bacteriol* **185**: 1825-1830.
Keiler, K.C. and Shapiro, L. (2003b) TmRNA is required for correct timing of DNA replication in Caulobacter crescentus. *J Bacteriol* **185**: 573-580.
Kenny, J.G., McGrath, S., Fitzgerald, G.F. and van Sinderen, D. (2004) Bacteriophage Tuc2009 encodes a tail-associated cell wall-degrading activity. *J Bacteriol* **186**: 3480-3491.
Kim, J., Heindl, J.E. and Fuqua, C. (2013) Coordination of division and development influences complex multicellular behavior in Agrobacterium tumefaciens. *PLoS One* **8**: e56682.
Kinoshita, E., Kinoshita-Kikuta, E., Takiyama, K. and Koike, T. (2006) Phosphate-binding tag, a new tool to visualize phosphorylated proteins. *Mol Cell Proteomics* **5**: 749-757.
Kobayashi, H., De Nisco, N.J., Chien, P., Simmons, L.A. and Walker, G.C. (2009) Sinorhizobium meliloti CpdR1 is critical for co-ordinating cell cycle progression and the symbiotic chronic infection. *Mol Microbiol* **73**: 586-600.

Kobiler, O., Koby, S., Teff, D., Court, D. and Oppenheim, A.B. (2002) The phage lambda CII transcriptional activator carries a C-terminal domain signaling for rapid proteolysis. *Proc Natl Acad Sci U S A* **99**: 14964-14969.

Kuchinski, K., Brimacombe, C.A., Westbye, A.B., Ding, H. and Beatty, J.T. (2016) The SOS response master regulator LexA regulates the gene transfer agent of Rhodobacter capsulatus and represses transcription of the signal transduction protein CckA. *J Bacteriol*.

Kysela, D.T., Brown, P.J., Huang, K.C. and Brun, Y.V. (2013) Biological consequences and advantages of asymmetric bacterial growth. *Annu Rev Microbiol* **67**: 417-435.

Lam, H., Matroule, J.Y. and Jacobs-Wagner, C. (2003) The asymmetric spatial distribution of bacterial signal transduction proteins coordinates cell cycle events. *Dev Cell* **5**: 149-159.

Lamarche, M.G., Wanner, B.L., Crepin, S. and Harel, J. (2008) The phosphate regulon and bacterial virulence: a regulatory network connecting phosphate homeostasis and pathogenesis. *FEMS Microbiol Rev* **32**: 461-473.

Lang, A.S. and Beatty, J.T. (2000) Genetic analysis of a bacterial genetic exchange element: the gene transfer agent of *Rhodobacter capsulatus*. *Proc Natl Acad Sci U S A* **97**: 859-864.

Lang, A.S. and Beatty, J.T. (2001) The gene transfer agent of Rhodobacter capsulatus and "constitutive transduction" in prokaryotes. *Arch Microbiol* **175**: 241-249.

Lang, A.S. and Beatty, J.T. (2007) Importance of widespread gene transfer agent genes in alpha-proteobacteria. *Trends Microbiol* **15**: 54-62.

Lang, A.S., Taylor, T.A. and Beatty, J.T. (2002) Evolutionary implications of phylogenetic analyses of the gene transfer agent (GTA) of Rhodobacter capsulatus. *J Mol Evol* **55**: 534-543.

Lang, A.S., Zhaxybayeva, O. and Beatty, J.T. (2012) Gene transfer agents: phage-like elements of genetic exchange. *Nat Rev Microbiol* **10**: 472-482.

Langlois, C., Ramboarina, S., Cukkemane, A., Auzat, I., Chagot, B., Gilquin, B. *et al.* (2015) Bacteriophage SPP1 tail tube protein self-assembles into beta-structure-rich tubes. *J Biol Chem* **290**: 3836-3849.

Laub, M.T., Chen, S.L., Shapiro, L. and McAdams, H.H. (2002) Genes directly controlled by CtrA, a master regulator of the Caulobacter cell cycle. *Proc Natl Acad Sci U S A* **99**: 4632-4637.

Lazdunski, A.M., Ventre, I. and Sturgis, J.N. (2004) Regulatory circuits and communication in Gram-negative bacteria. *Nat Rev Microbiol* **2**: 581-592.

Leiman, P.G., Arisaka, F., van Raaij, M.J., Kostyuchenko, V.A., Aksyuk, A.A., Kanamaru, S. and Rossmann, M.G. (2010) Morphogenesis of the T4 tail and tail fibers. *Virol J* **7**: 355.

Leiman, P.G. and Shneider, M.M. (2012) Contractile tail machines of bacteriophages. *Adv Exp Med Biol* **726**: 93-114.

Lesley, J.A. and Shapiro, L. (2008) SpoT regulates DnaA stability and initiation of DNA replication in carbon-starved Caulobacter crescentus. *J Bacteriol* **190**: 6867-6880.

Leslie, D.J., Heinen, C., Schramm, F.D., Thuring, M., Aakre, C.D., Murray, S.M. *et al.* (2015) Nutritional Control of DNA Replication Initiation through the Proteolysis and Regulated Translation of DnaA. *PLoS Genet* **11**: e1005342.

Leung, M.M. (2010) CtrA and GtaR: Two systems that regulate the Gene Transfer Agent in *Rhodobacter capsulatus*. Vancouver, BC: Department of Microbiology & Immunology, University of British Columbia.

Leung, M.M., Brimacombe, C.A., Spiegelman, G.B. and Beatty, J.T. (2012) The GtaR protein negatively regulates transcription of the gtaRI operon and modulates gene transfer agent (RcGTA) expression in Rhodobacter capsulatus. *Mol Microbiol* **83**: 759-774.
Levchenko, I., Luo, L. and Baker, T.A. (1995) Disassembly of the Mu transposase tetramer by the ClpX chaperone. *Genes Dev* **9**: 2399-2408.
Lhuillier, S., Gallopin, M., Gilquin, B., Brasiles, S., Lancelot, N., Letellier, G. *et al.* (2009) Structure of bacteriophage SPP1 head-to-tail connection reveals mechanism for viral DNA gating. *Proc Natl Acad Sci U S A* **106**: 8507-8512.
Li, C., Wen, A., Shen, B., Lu, J., Huang, Y. and Chang, Y. (2011) FastCloning: a highly simplified, purification-free, sequence- and ligation-independent PCR cloning method. *BMC Biotechnol* **11**: 92.
Little, J.W. (2005) Gene regulatory circuitry of phage lambda. In: The Bacteriophages. R.L. Calendar (ed). Oxford University Press, pp. 74-82.
Loessner, M.J. (2005) Bacteriophage endolysins--current state of research and applications. *Curr Opin Microbiol* **8**: 480-487.
Loessner, M.J., Kramer, K., Ebel, F. and Scherer, S. (2002) C-terminal domains of Listeria monocytogenes bacteriophage murein hydrolases determine specific recognition and high-affinity binding to bacterial cell wall carbohydrates. *Mol Microbiol* **44**: 335-349.
Lori, C., Ozaki, S., Steiner, S., Bohm, R., Abel, S., Dubey, B.N. *et al.* (2015) Cyclic di-GMP acts as a cell cycle oscillator to drive chromosome replication. *Nature* **523**: 236-239.
Madigan, M.T. and Jung, D.O. (2009) An overview of purple bacteria: Systematics, Physiology, and habitats. In: The purple phototrophic bacteria. C.N. Hunter, F. Daldal, M.C. Thurnauer & J.T. Beatty (eds). pp. 1-15.
Marrs, B. (1974) Genetic recombination in Rhodopseudomonas capsulata. *Proc Natl Acad Sci U S A* **71**: 971-973.
Marx, C.J. and Lidstrom, M.E. (2001) Development of improved versatile broad-host-range vectors for use in methylotrophs and other Gram-negative bacteria. *Microbiology* **147**: 2065-2075.
Masuda, S. and Bauer, C.E. (2004) Null mutation of HvrA compensates for loss of an essential relA/spoT-like gene in Rhodobacter capsulatus. *J Bacteriol* **186**: 235-239.
Matson, E.G., Thompson, M.G., Humphrey, S.B., Zuerner, R.L. and Stanton, T.B. (2005) Identification of genes of VSH-1, a prophage-like gene transfer agent of Brachyspira hyodysenteriae. *J Bacteriol* **187**: 5885-5892.
Matsui, T., Griniuviene, B., Goldberg, E., Tsugita, A., Tanaka, N. and Arisaka, F. (1997) Isolation and characterization of a molecular chaperone, gp57A, of bacteriophage T4. *Journal of Bacteriology* **179**: 1846-1851.
McDaniel, L.D., Young, E., Delaney, J., Ruhnau, F., Ritchie, K.B. and Paul, J.H. (2010) High frequency of horizontal gene transfer in the oceans. *Science* **330**: 50.
McDaniel, L.D., Young, E.C., Ritchie, K.B. and Paul, J.H. (2012) Environmental factors influencing gene transfer agent (GTA) mediated transduction in the subtropical ocean. *PLoS One* **7**: e43506.
Mercer, R.G., Callister, S.J., Lipton, M.S., Pasa-Tolic, L., Strnad, H., Paces, V. *et al.* (2010) Loss of the response regulator CtrA causes pleiotropic effects on gene expression but does not affect growth phase regulation in Rhodobacter capsulatus. *J Bacteriol* **192**: 2701-2710.

Mercer, R.G., Quinlan, M., Rose, A.R., Noll, S., Beatty, J.T. and Lang, A.S. (2012) Regulatory systems controlling motility and gene transfer agent production and release in Rhodobacter capsulatus. *FEMS Microbiol Lett* **331**: 53-62.
Moglich, A., Ayers, R.A. and Moffat, K. (2009) Structure and signaling mechanism of Per-ARNT-Sim domains. *Structure* **17**: 1282-1294.
Moore, S.D. and Sauer, R.T. (2007) The tmRNA system for translational surveillance and ribosome rescue. *Annu Rev Biochem* **76**: 101-124.
Mott, M.L. and Berger, J.M. (2007) DNA replication initiation: mechanisms and regulation in bacteria. *Nat Rev Microbiol* **5**: 343-354.
Mount, D.W., Harris, A.W., Fuerst, C.R. and Siminovitch, L. (1968) Mutations in bacteriophage lambda affecting particle morphogenesis. *Virology* **35**: 134-149.
Moussa, S.H., Kuznetsov, V., Tran, T.A., Sacchettini, J.C. and Young, R. (2012) Protein determinants of phage T4 lysis inhibition. *Protein Sci* **21**: 571-582.
Musovic, S., Oregaard, G., Kroer, N. and Sorensen, S.J. (2006) Cultivation-independent examination of horizontal transfer and host range of an IncP-1 plasmid among gram-positive and gram-negative bacteria indigenous to the barley rhizosphere. *Appl Environ Microbiol* **72**: 6687-6692.
Nagao, N., Yamamoto, J., Komatsu, H., Suzuki, H., Hirose, Y., Umekage, S. *et al.* (2015) The gene transfer agent-like particle of the marine phototrophic bacterium *Rhodovulum sulfidophilum*. *Biochemistry and Biophysics Reports* **4**: 369-374.
Neher, S.B., Villen, J., Oakes, E.C., Bakalarski, C.E., Sauer, R.T., Gygi, S.P. and Baker, T.A. (2006) Proteomic profiling of ClpXP substrates after DNA damage reveals extensive instability within SOS regulon. *Mol Cell* **22**: 193-204.
Neiditch, M.B., Federle, M.J., Pompeani, A.J., Kelly, R.C., Swem, D.L., Jeffrey, P.D. *et al.* (2006) Ligand-induced asymmetry in histidine sensor kinase complex regulates quorum sensing. *Cell* **126**: 1095-1108.
Norman, A., Hansen, L.H. and Sorensen, S.J. (2009) Conjugative plasmids: vessels of the communal gene pool. *Philos Trans R Soc Lond B Biol Sci* **364**: 2275-2289.
Olutiola, P.O., Awojobi, K.O., Oyedeji, O., Ayansina, A.D.V. and Cole, O.o. (2010) Relationship between bacterial density and chemical composition of a tropical sewage oxidation pond. *African Journal of Environmental Science and Technology* **4**: 595-602.
Omar, A.S., Flammann, H.T., Golecki, J.R. and Weckesser, J. (1983) Detection of Capsule and Slime Polysaccharide Layers in 2 Strains of Rhodopseudomonas-Capsulata. *Archives of Microbiology* **134**: 114-117.
Pang, T., Savva, C.G., Fleming, K.G., Struck, D.K. and Young, R. (2009) Structure of the lethal phage pinhole. *Proc Natl Acad Sci U S A* **106**: 18966-18971.
Pappas, K.M., Weingart, C.L. and Winans, S.C. (2004) Chemical communication in proteobacteria: biochemical and structural studies of signal synthases and receptors required for intercellular signalling. *Mol Microbiol* **53**: 755-769.
Pell, L.G., Liu, A., Edmonds, L., Donaldson, L.W., Howell, P.L. and Davidson, A.R. (2009) The X-ray crystal structure of the phage lambda tail terminator protein reveals the biologically relevant hexameric ring structure and demonstrates a conserved mechanism of tail termination among diverse long-tailed phages. *J Mol Biol* **389**: 938-951.

Perucchetti, R., Parris, W., Becker, A. and Gold, M. (1988) Late stages in bacteriophage lambda head morphogenesis: in vitro studies on the action of the bacteriophage lambda D-gene and W-gene products. *Virology* **165**: 103-114.

Peterson, G.L. (1983) Determination of total protein. *Methods Enzymol* **91**: 95-119.

Pini, F., De Nisco, N.J., Ferri, L., Penterman, J., Fioravanti, A., Brilli, M. *et al.* (2015) Cell Cycle Control by the Master Regulator CtrA in Sinorhizobium meliloti. *PLoS Genet* **11**: e1005232.

Pini, F., Frage, B., Ferri, L., De Nisco, N.J., Mohapatra, S.S., Taddei, L. *et al.* (2013) The DivJ, CbrA and PleC system controls DivK phosphorylation and symbiosis in Sinorhizobium meliloti. *Mol Microbiol* **90**: 54-71.

Pope, W.H., Weigele, P.R., Chang, J., Pedulla, M.L., Ford, M.E., Houtz, J.M. *et al.* (2007) Genome sequence, structural proteins, and capsid organization of the cyanophage Syn5: a "horned" bacteriophage of marine synechococcus. *J Mol Biol* **368**: 966-981.

Pujalte, M.J., Lucena, T., Ruvira, M.A., Arahal, D.R. and Macián, M.C. (2014) The Family Rhodobacteraceae. In: The Prokaryotes - Alphaproteobacteria and Betaproteobacteria. E. Rosenberg, E. DeLong, S. Lory, E. Stackebrandt & F. Thompson (eds). Springer Berlin Heidelberg, pp. 439-512.

Qin, L., Fokine, A., O'Donnell, E., Rao, V.B. and Rossmann, M.G. (2010) Structure of the small outer capsid protein, Soc: a clamp for stabilizing capsids of T4-like phages. *J Mol Biol* **395**: 728-741.

Quon, K.C., Marczynski, G.T. and Shapiro, L. (1996) Cell cycle control by an essential bacterial two-component signal transduction protein. *Cell* **84**: 83-93.

Quon, K.C., Yang, B., Domian, I.J., Shapiro, L. and Marczynski, G.T. (1998) Negative control of bacterial DNA replication by a cell cycle regulatory protein that binds at the chromosome origin. *Proc Natl Acad Sci U S A* **95**: 120-125.

Ramanculov, E. and Young, R. (2001) An ancient player unmasked: T4 rI encodes a t-specific antiholin. *Mol Microbiol* **41**: 575-583.

Ranquet, C., Geiselmann, J. and Toussaint, A. (2001) The tRNA function of SsrA contributes to controlling repression of bacteriophage Mu prophage. *Proc Natl Acad Sci U S A* **98**: 10220-10225.

Rao, V.B. and Black, L.W. (1985) DNA packaging of bacteriophage T4 proheads in vitro. Evidence that prohead expansion is not coupled to DNA packaging. *J Mol Biol* **185**: 565-578.

Rapp, B.J., Landrum, D.C. and Wall, J.D. (1986) Mehylammonium uptake by Rhodobacter capsulatus. *Arch Microbiol* **146**: 134-141.

Raytcheva, D.A., Haase-Pettingell, C., Piret, J. and King, J.A. (2014) Two novel proteins of cyanophage Syn5 compose its unusual horn structure. *J Virol* **88**: 2047-2055.

Reader, R.W. and Siminovitch, L. (1971) Lysis defective mutants of bacteriophage lambda: genetics and physiology of S cistron mutants. *Virology* **43**: 607-622.

Rubinstein, R., Ramagopal, U.A., Nathenson, S.G., Almo, S.C. and Fiser, A. (2013) Functional classification of immune regulatory proteins. *Structure* **21**: 766-776.

Sambrook, J., Fritsch, E.F. and Maniatis, T. (1989) *Molecular cloning: a laboratory manual*. Cold Spring Harbor, NY: Cold Spring Harbor Laboratory Press.

Sarre, S.G. and Hahn, F.E. (1967) Mode of action of gentamicin. *Trans N Y Acad Sci* **29**: 575-578.

Sarubbi, E., Rudd, K.E., Xiao, H., Ikehara, K., Kalman, M. and Cashel, M. (1989) Characterization of the spoT gene of Escherichia coli. *J Biol Chem* **264**: 15074-15082.
Sathaliyawala, T., Islam, M.Z., Li, Q., Fokine, A., Rossmann, M.G. and Rao, V.B. (2010) Functional analysis of the highly antigenic outer capsid protein, Hoc, a virus decoration protein from T4-like bacteriophages. *Mol Microbiol* **77**: 444-455.
Schaefer, A.L., Taylor, T.A., Beatty, J.T. and Greenberg, E.P. (2002) Long-chain acyl-homoserine lactone quorum-sensing regulation of Rhodobacter capsulatus gene transfer agent production. *J Bacteriol* **184**: 6515-6521.
Schindler, D.W. (1977) Evolution of phosphorus limitation in lakes. *Science* **195**: 260-262.
Schwechheimer, C. and Kuehn, M.J. (2015) Outer-membrane vesicles from Gram-negative bacteria: biogenesis and functions. *Nat Rev Microbiol* **13**: 605-619.
Serwer, P. and Griess, G.A. (1999) Advances in the separation of bacteriophages and related particles. *J Chromatogr B Biomed Sci Appl* **722**: 179-190.
Simon, R., Priefer, U. and Puhler, A. (1983) A broad host range mobilization system for in vivo genetic-engineering—transposon mutagenesis in gram-negative bacteria. *Biotechnology* **1**: 784-791.
Simpson, P.J., Jamieson, S.J., Abou-Hachem, M., Karlsson, E.N., Gilbert, H.J., Holst, O. and Williamson, M.P. (2002) The solution structure of the CBM4-2 carbohydrate binding module from a thermostable Rhodothermus marinus xylanase. *Biochemistry* **41**: 5712-5719.
Solioz, M. (1975) The gene transfer agent of *Rhodopseudomonas capsulata*. Ph.D. thesis. St. Louis: Saint Louis University.
Solioz, M. and Marrs, B. (1977) The gene transfer agent of Rhodopseudomonas capsulata. Purification and characterization of its nucleic acid. *Arch Biochem Biophys* **181**: 300-307.
Solioz, M., Yen, H.C. and Marris, B. (1975) Release and uptake of gene transfer agent by *Rhodopseudomonas capsulata*. *J Bacteriol* **123**: 651-657.
Solovyev, V. and Salamov, A. (2011) Automatic Annotation of Microbial Genomes and Metagenomic Sequences. In: Metagenomics and its Applications in Agriculture, Biomedicine and Environmental Studies. R.W. Li (ed). Nova Science Publishers, pp. 61-78.
Soucy, S.M., Huang, J. and Gogarten, J.P. (2015) Horizontal gene transfer: building the web of life. *Nat Rev Genet* **16**: 472-482.
Spano, A.J., Chen, F.S., Goodman, B.E., Sabat, A.E., Simon, M.N., Wall, J.S. *et al.* (2007) In vitro assembly of a prohead-like structure of the Rhodobacter capsulatus gene transfer agent. *Virology* **364**: 95-102.
Spinelli, S., Veesler, D., Bebeacua, C. and Cambillau, C. (2014) Structures and host-adhesion mechanisms of lactococcal siphophages. *Front Microbiol* **5**: 3.
Srivatsan, A. and Wang, J.D. (2008) Control of bacterial transcription, translation and replication by (p)ppGpp. *Curr Opin Microbiol* **11**: 100-105.
Stanton, T.B. (2007) Prophage-like gene transfer agents-novel mechanisms of gene exchange for Methanococcus, Desulfovibrio, Brachyspira, and Rhodobacter species. *Anaerobe* **13**: 43-49.
Sternberg, N. and Weisberg, R. (1977) Packaging of coliphage lambda DNA. II. The role of the gene D protein. *J Mol Biol* **117**: 733-759.

Stewart, R.C. (2010) Protein histidine kinases: assembly of active sites and their regulation in signaling pathways. *Curr Opin Microbiol* **13**: 133-141.
Stockdale, S.R., Collins, B., Spinelli, S., Douillard, F.P., Mahony, J., Cambillau, C. and van Sinderen, D. (2015) Structure and Assembly of TP901-1 Virion Unveiled by Mutagenesis. *PLoS One* **10**: e0131676.
Stojkovic, E.A. and Rothman-Denes, L.B. (2007) Coliphage N4 N-acetylmuramidase defines a new family of murein hydrolases. *J Mol Biol* **366**: 406-419.
Strnad, H., Lapidus, A., Paces, J., Ulbrich, P., Vlcek, C., Paces, V. and Haselkorn, R. (2010) Complete genome sequence of the photosynthetic purple nonsulfur bacterium *Rhodobacter capsulatus* SB 1003. *J Bacteriol* **192**: 3545-3546.
Summer, E.J., Berry, J., Tran, T.A., Niu, L., Struck, D.K. and Young, R. (2007) Rz/Rz1 lysis gene equivalents in phages of Gram-negative hosts. *J Mol Biol* **373**: 1098-1112.
Sun, S., Kondabagil, K., Draper, B., Alam, T.I., Bowman, V.D., Zhang, Z. *et al.* (2008) The structure of the phage T4 DNA packaging motor suggests a mechanism dependent on electrostatic forces. *Cell* **135**: 1251-1262.
Szurmant, H., White, R.A. and Hoch, J.A. (2007) Sensor complexes regulating two-component signal transduction. *Curr Opin Struct Biol* **17**: 706-715.
Tavares, P., Zinn-Justin, S. and Orlova, E.V. (2012) Genome gating in tailed bacteriophage capsids. *Adv Exp Med Biol* **726**: 585-600.
Taylor, D.P., Cohen, S.N., Clark, W.G. and Marrs, B.L. (1983) Alignment of genetic and restriction maps of the photosynthesis region of the Rhodopseudomonas capsulata chromosome by a conjugation-mediated marker rescue technique. *J Bacteriol* **154**: 580-590.
Taylor, T.A. (2004) Evolution and Regulation of the Gene Transfer Agent (GTA) of *Rhodobacter capsulatus*. Vancouver, BC: Department of Microbiology & Immunology, University of British Columbia.
Terrana, B. and Newton, A. (1975) Pattern of unequal cell division and development in Caulobacter crescentus. *Dev Biol* **44**: 380-385.
Tews, I., Perrakis, A., Oppenheim, A., Dauter, Z., Wilson, K.S. and Vorgias, C.E. (1996) Bacterial chitobiase structure provides insight into catalytic mechanism and the basis of Tay-Sachs disease. *Nat Struct Biol* **3**: 638-648.
Thomas, C.M. and Nielsen, K.M. (2005) Mechanisms of, and barriers to, horizontal gene transfer between bacteria. *Nat Rev Microbiol* **3**: 711-721.
Tilly, K., Murialdo, H. and Georgopoulos, C. (1981) Identification of a second Escherichia coli groE gene whose product is necessary for bacteriophage morphogenesis. *Proc Natl Acad Sci U S A* **78**: 1629-1633.
Tsokos, C.G. and Laub, M.T. (2012) Polarity and cell fate asymmetry in Caulobacter crescentus. *Curr Opin Microbiol* **15**: 744-750.
Tsokos, C.G., Perchuk, B.S. and Laub, M.T. (2011) A dynamic complex of signaling proteins uses polar localization to regulate cell-fate asymmetry in Caulobacter crescentus. *Dev Cell* **20**: 329-341.
Tsui, L.C. and Hendrix, R.W. (1983) Proteolytic processing of phage lambda tail protein gpH: timing of the cleavage. *Virology* **125**: 257-264.
Vass, R.H. and Chien, P. (2013) Critical clamp loader processing by an essential AAA+ protease in Caulobacter crescentus. *Proc Natl Acad Sci U S A* **110**: 18138-18143.

Vega-Baray, B., Domenzain, C., Rivera, A., Alfaro-Lopez, R., Gomez-Cesar, E., Poggio, S. *et al.* (2015) The flagellar set Fla2 in Rhodobacter sphaeroides is controlled by the CckA pathway and is repressed by organic acids and the expression of Fla1. *J Bacteriol* **197**: 833-847.

Vegge, C.S., Brondsted, L., Neve, H., Mc Grath, S., van Sinderen, D. and Vogensen, F.K. (2005) Structural characterization and assembly of the distal tail structure of the temperate lactococcal bacteriophage TP901-1. *J Bacteriol* **187**: 4187-4197.

Wall, J.D., Weaver, P.F. and Gest, H. (1975) Gene transfer agents, bacteriophages, and bacteriocins of *Rhodopseudomonas capsulata*. *Arch Microbiol* **105**: 217-224.

Wang, H., Ziesche, L., Frank, O., Michael, V., Martin, M., Petersen, J. *et al.* (2014) The CtrA phosphorelay integrates differentiation and communication in the marine alphaproteobacterium Dinoroseobacter shibae. *BMC Genomics* **15**: 130.

Wang, I.N., Deaton, J. and Young, R. (2003) Sizing the holin lesion with an endolysin-beta-galactosidase fusion. *J Bacteriol* **185**: 779-787.

Wang, I.N., Smith, D.L. and Young, R. (2000) Holins: the protein clocks of bacteriophage infections. *Annu Rev Microbiol* **54**: 799-825.

Wanner, B.L. (1993) Gene regulation by phosphate in enteric bacteria. *J Cell Biochem* **51**: 47-54.

Wawrzynow, A., Wojtkowiak, D., Marszalek, J., Banecki, B., Jonsen, M., Graves, B. *et al.* (1995) The ClpX heat-shock protein of Escherichia coli, the ATP-dependent substrate specificity component of the ClpP-ClpX protease, is a novel molecular chaperone. *EMBO J* **14**: 1867-1877.

Weaver, P.F., Wall, J.D. and Gest, H. (1975) Characterization of Rhodopseudomonas capsulata. *Arch Microbiol* **105**: 207-216.

West, A.H. and Stock, A.M. (2001) Histidine kinases and response regulator proteins in two-component signaling systems. *Trends Biochem Sci* **26**: 369-376.

Westbye, A.B., Leung, M.M., Florizone, S.M., Taylor, T.A., Johnson, J.A., Fogg, P.C. and Beatty, J.T. (2013) Phosphate concentration and the putative sensor kinase protein CckA modulate cell lysis and release of the Rhodobacter capsulatus gene transfer agent. *J Bacteriol* **195**: 5025-5040.

White, H.E., Sherman, M.B., Brasiles, S., Jacquet, E., Seavers, P., Tavares, P. and Orlova, E.V. (2012) Capsid structure and its stability at the late stages of bacteriophage SPP1 assembly. *J Virol* **86**: 6768-6777.

White, R., Tran, T.A., Dankenbring, C.A., Deaton, J. and Young, R. (2010) The N-terminal transmembrane domain of lambda S is required for holin but not antiholin function. *J Bacteriol* **192**: 725-733.

Willett, J.W., Herrou, J., Briegel, A., Rotskoff, G. and Crosson, S. (2015) Structural asymmetry in a conserved signaling system that regulates division, replication, and virulence of an intracellular pathogen. *Proc Natl Acad Sci U S A* **112**: E3709-3718.

Wu, H., Sampson, L., Parr, R. and Casjens, S. (2002) The DNA site utilized by bacteriophage P22 for initiation of DNA packaging. *Mol Microbiol* **45**: 1631-1646.

Xiang, Y. and Rossmann, M.G. (2011) Structure of bacteriophage phi29 head fibers has a supercoiled triple repeating helix-turn-helix motif. *Proc Natl Acad Sci U S A* **108**: 4806-4810.

Xie, H., Gilbert, H.J., Charnock, S.J., Davies, G.J., Williamson, M.P., Simpson, P.J. *et al.* (2001) Clostridium thermocellum Xyn10B carbohydrate-binding module 22-2: the role of conserved amino acids in ligand binding. *Biochemistry* **40**: 9167-9176.
Xu, J., Hendrix, R.W. and Duda, R.L. (2014) Chaperone-protein interactions that mediate assembly of the bacteriophage lambda tail to the correct length. *J Mol Biol* **426**: 1004-1018.
Xu, M., Struck, D.K., Deaton, J., Wang, I.N. and Young, R. (2004) A signal-arrest-release sequence mediates export and control of the phage P1 endolysin. *Proc Natl Acad Sci U S A* **101**: 6415-6420.
Yen, H.C., Hu, N.T. and Marrs, B.L. (1979) Characterization of the gene transfer agent made by an overproducer mutant of Rhodopseudomonas capsulata. *J Mol Biol* **131**: 157-168.
Yoo, S.J., Seol, J.H., Kang, M.S., Ha, D.B. and Chung, C.H. (1994) clpX encoding an alternative ATP-binding subunit of protease Ti (Clp) can be expressed independently from clpP in Escherichia coli. *Biochem Biophys Res Commun* **203**: 798-804.
Young, I., Wang, I. and Roof, W.D. (2000) Phages will out: strategies of host cell lysis. *Trends Microbiol* **8**: 120-128.
Young, R. (1992) Bacteriophage lysis: mechanism and regulation. *Microbiol Rev* **56**: 430-481.
Young, R. (2013) Phage lysis: do we have the hole story yet? *Curr Opin Microbiol* **16**: 790-797.
Young, R. (2014) Phage lysis: three steps, three choices, one outcome. *J Microbiol* **52**: 243-258.
Zaikova, E., Walsh, D.A., Stilwell, C.P., Mohn, W.W., Tortell, P.D. and Hallam, S.J. (2010) Microbial community dynamics in a seasonally anoxic fjord: Saanich Inlet, British Columbia. *Environ Microbiol* **12**: 172-191.
Zan, J., Heindl, J.E., Liu, Y., Fuqua, C. and Hill, R.T. (2013) The CckA-ChpT-CtrA phosphorelay system is regulated by quorum sensing and controls flagellar motility in the marine sponge symbiont Ruegeria sp. KLH11. *PLoS One* **8**: e66346.
Zhang, N. and Young, R. (1999) Complementation and characterization of the nested *Rz* and *Rz1* reading frames in the genome of bacteriophage lambda. *Mol Gen Genet* **262**: 659-667.
Zhang, S., Lu, G., Qi, J., Li, Y., Zhang, Z., Zhang, B. *et al.* (2013) Competition of cell adhesion and immune recognition: insights into the interaction between CRTAM and nectin-like 2. *Structure* **21**: 1430-1439.
Zylicz, M., Liberek, K., Wawrzynow, A. and Georgopoulos, C. (1998) Formation of the preprimosome protects lambda O from RNA transcription-dependent proteolysis by ClpP/ClpX. *Proc Natl Acad Sci U S A* **95**: 15259-15263.

Appendix

Appendix A : supplementory figures and tables

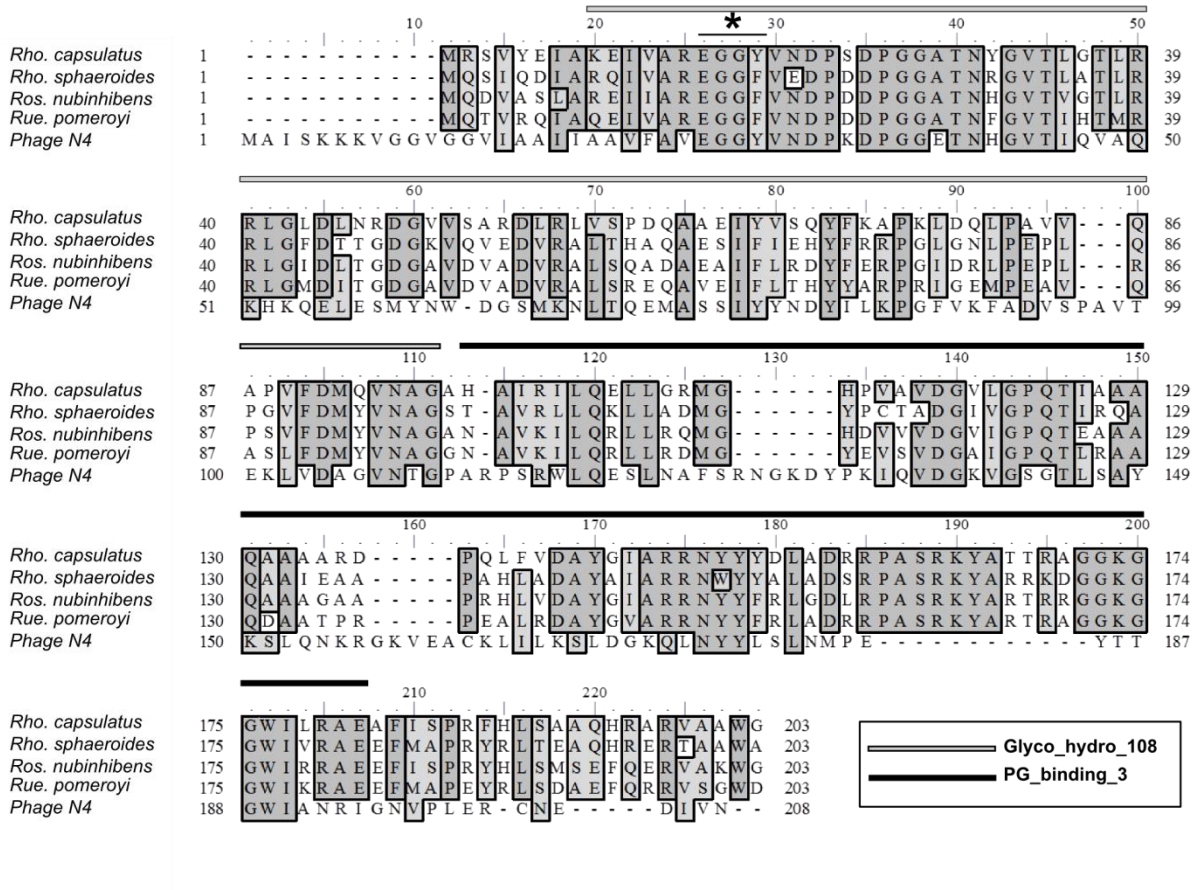

Figure S1 Conserved sequence of endolysins

ClustalO alignment of best BlastP hits of *Rhodobacter capsulatus* endolysin Rcc00555 in selected organisms. *Rhodobacter sphaeroides* 2.4.1 (WP_011337867.1), *Roseovarius nubinhibens* (WP_009814954.1), *Ruegeria pomeroyi* (WP_011047611.1), *Escherichia* phage N4 (YP_950539.1). PFAM domains in Rcc00555 indicated by bars above sequence. Star (*) indicates the conserved catalytic site characterized for the N-acetylmuramidase from phage N4. Shading threshold 80%.

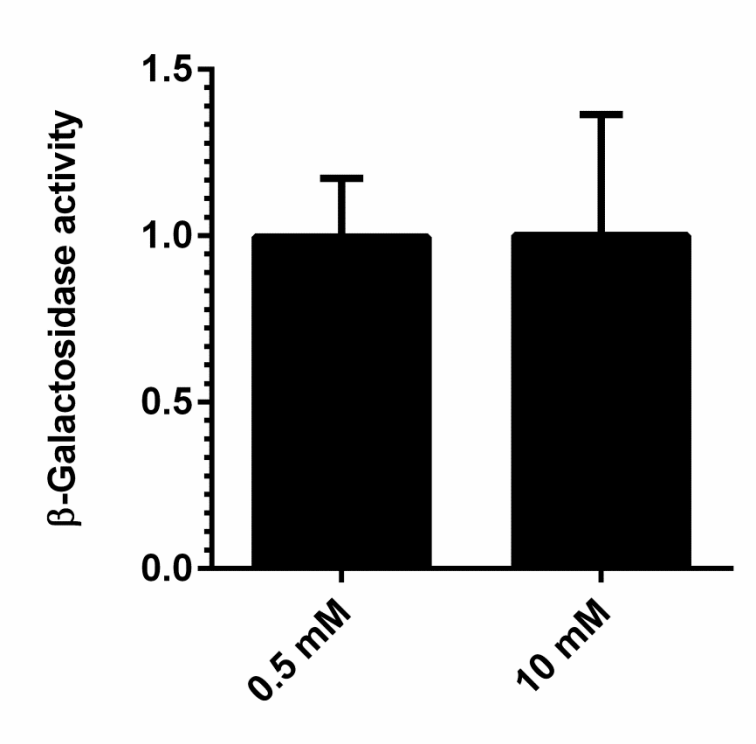

Figure S2 *rcc00555* promoter activity is not influenced by phosphate concentration

Promoter (β-galactosidase) activity of DE555(pXCA-555) cells cultured in RCVm containing 0.5 or 10 mM KPO_4 for 24h.

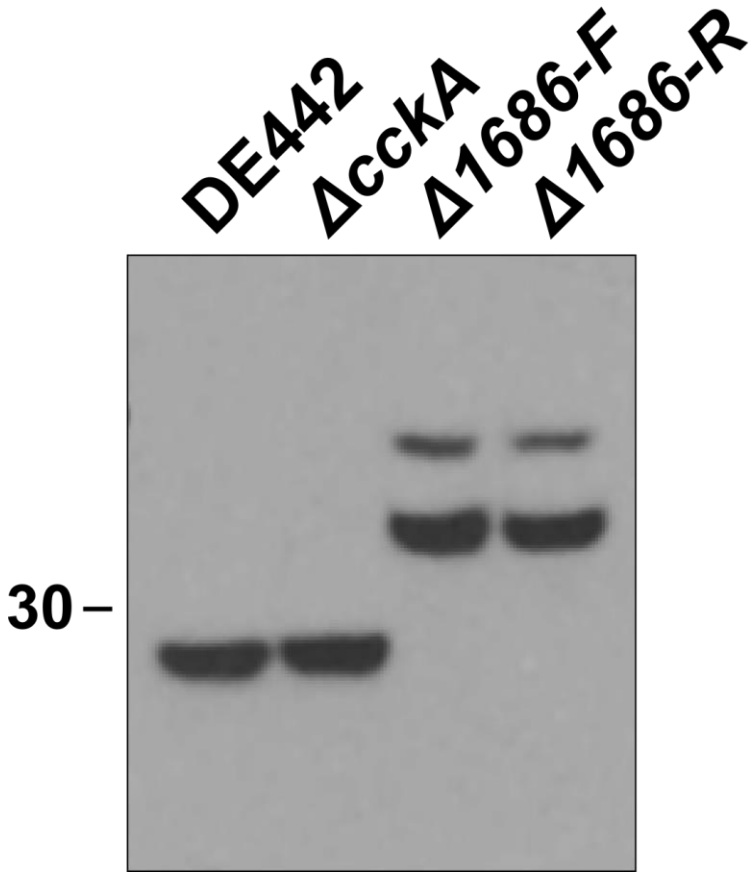

Figure S3 The g4 capsid prohead protease mutant *Δ1686*

Migration of the capsid protein for mutants lacking the capsid prohead protease. Western blot of culture supernatant probed with RcGTA capsid anti-serum. F and R indicate orientation of KIXX relative to reading frame of Rcc01686.

A

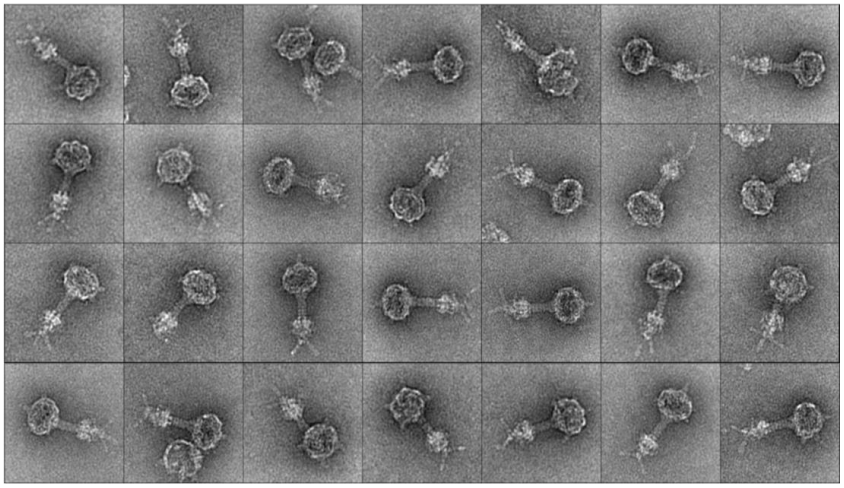

B

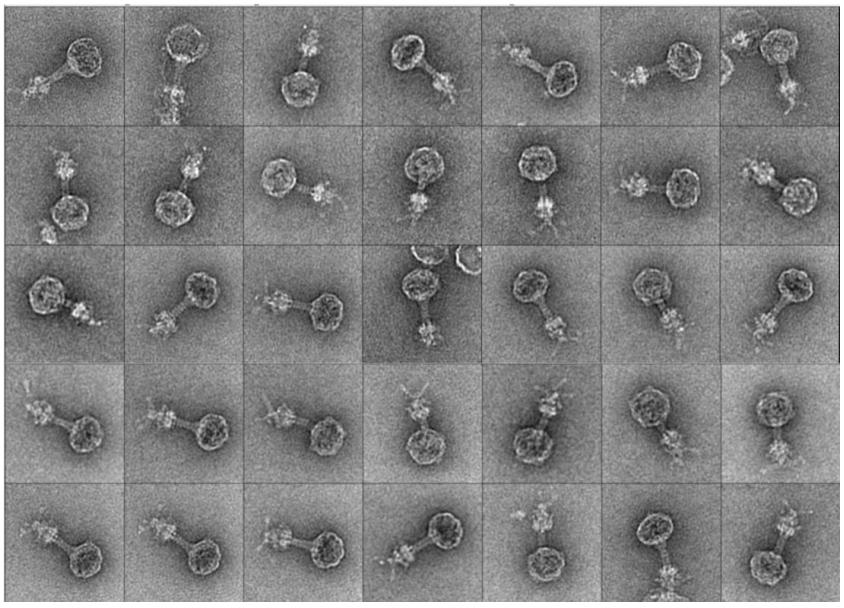

Figure S4. TEMs of RcGTA particles, side view

Negatively stained TEM of 6xHis purified RcGTA particles. **A.** DE442. **B.** DE442*ΔghsB*

A

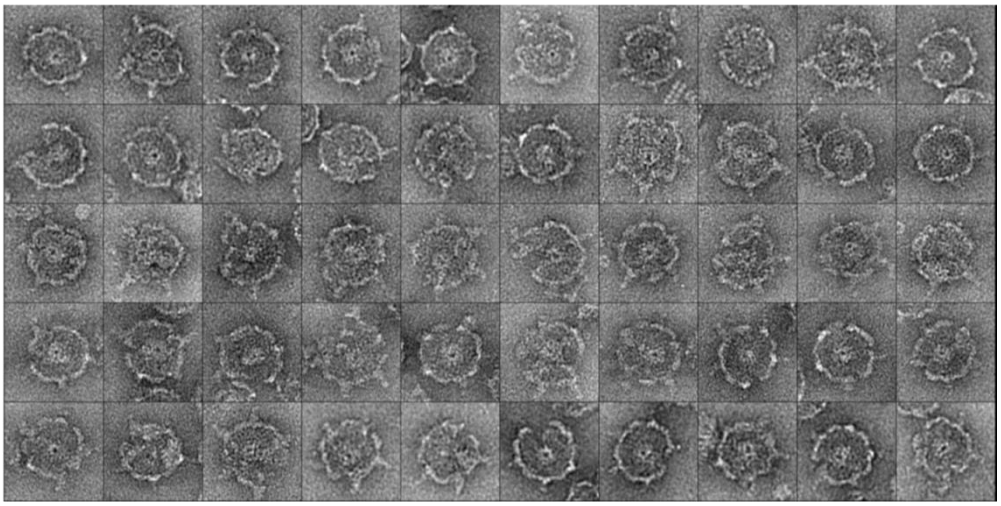

B

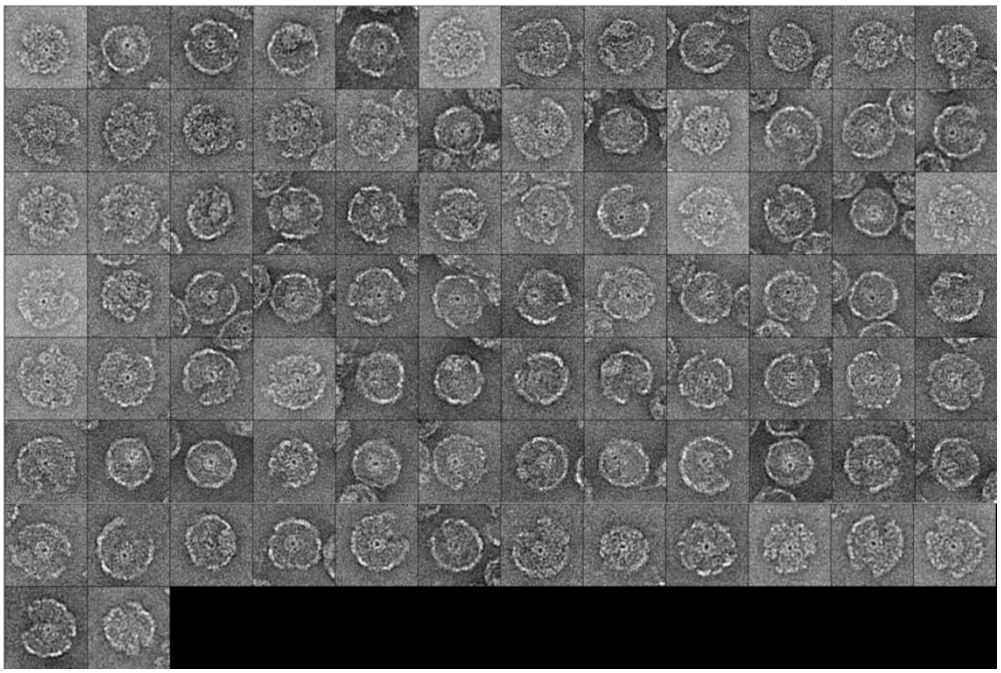

Figure S5. TEMs of RcGTA particles, top view

Negatively stained TEM of 6xHis purified RcGTA particles. **A.** DE442. **B.** DE442*ΔghsB*

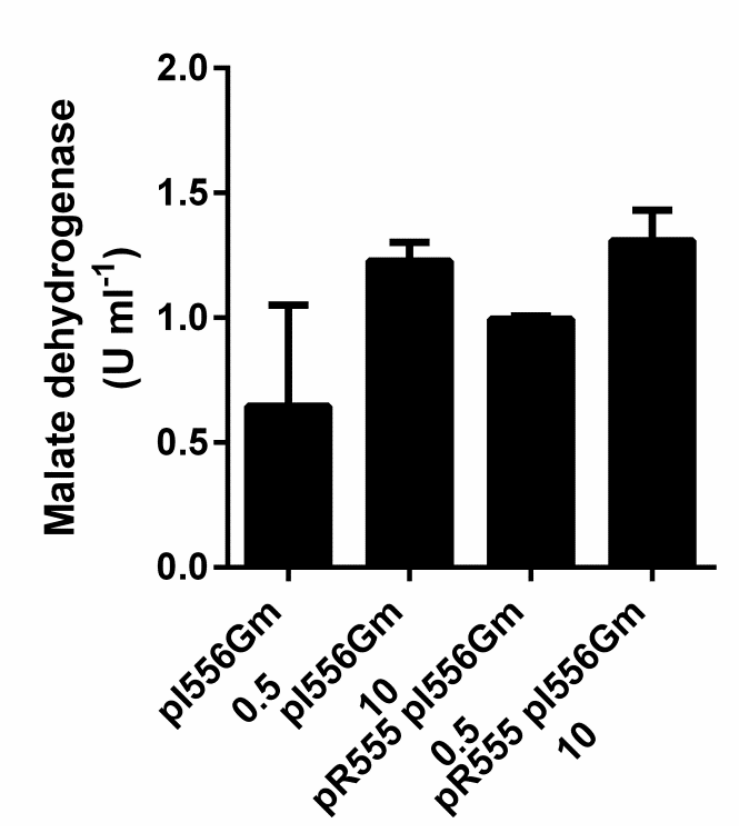

Figure S6 High phosphate concentration does not inhibit malate dehydrogenase release from cells constitutively expressing *rcc00556*

DE555 containing plasmids pI556 and pR555 cultivated in RCVm containing 0.5 mM or 10 mM KPO_4 as indicated.

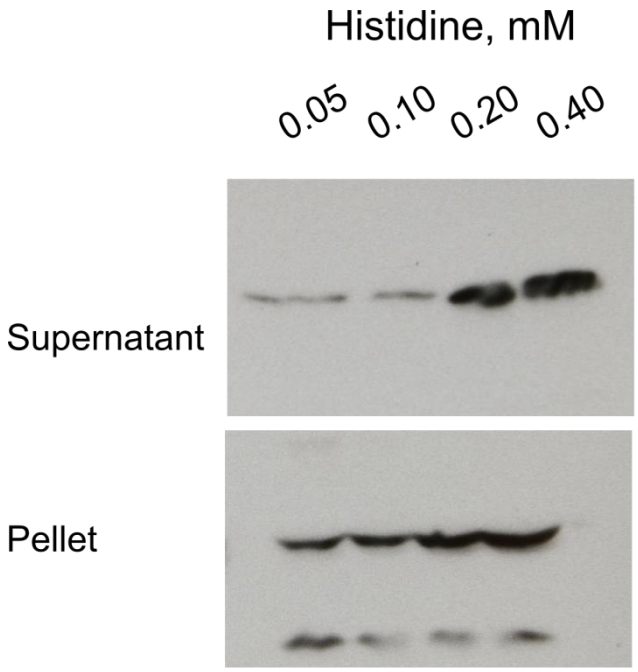

Figure S7 Continued depletion of histidine does not stimulate RcGTA

Depletion of histidine by cultivation in media containing growth limiting concentrations of histidine does not increase RcGTA production and release for the histidine auxotroph SB1003*ΔhisB.* Media containing 0.05 and 0.10 mM were considered growth limiting based on growth curve (not shown) and final OD_{660} measurements. Western blot of OD_{660} normalized supernatant or cell fraction probed with anti-RcGTA capsid serum.

Table S1 Bacterial strains

Strain	Reference	Description[1]
Rhodobacter capsulatus		
SB1003	(Solioz and Marrs, 1977)	RcGTA-WT producer, Rif^r
B10	(Marrs, 1974)	WT-isolate
DE442	?[2]	RcGTA-overproducer, Rif^r
B10 *Δ1081*	(Brimacombe *et al.*, 2013)	Capsular polysaccharide-negative mutant, Rif^s
B10 *Δ1032*	(Brimacombe *et al.*, 2013)	Capsular polysaccharide-negative mutant, Rif^s
B10 *ΔgtaI*	(Leung *et al.*, 2012)	Acyl-homoserine lactone synthase mutant, Rif^s
SB1003 *ΔphoB*	This work	Response regulator mutant *ΔphoB* (*Δrcc03498*), markerless, alkaline phosphatase-negative, Rif^r
SB1003 *ΔcckA*	(Mercer *et al.*, 2012)	Hybrid histidine kinase mutant *ΔcckA*, Kan^r Rif^r
DE442 *ΔcckA*	This work	Hybrid histidine kinase mutant *ΔcckA*, Kan^r Rif^r
SB1003 *ΔchpT*	(Mercer *et al.*, 2012)	Phosphotransferase mutant *ΔchpT*, Kan^r Rif^r
DE442 *ΔchpT*	This work	Phosphotransferase mutant *ΔchpT*, Kan^r Rif^r
SBRM1	(Mercer *et al.*, 2010)	Response regulator mutant *ΔctrA*, SB1003-derived, Kan^r Rif^r
DE442 *ΔctrA*	This work	Response regulator mutant *ΔctrA*, Kan^r Rif^r

Strain	Reference	Description[1]
SB555	(Hynes *et al.*, 2012)	Endolysin mutant *Δrcc00555::KIXX*, lysis-negative, SB1003-derived, Kan^r Rif^r
DE555	This work	Lysis-negative *Δrcc00555::KIXX*, lysis negative, DE442-derived, Kan^r Rif^r
SB1003 *ΔghsB*	This work	Head spike mutant *ΔghsB* (*Δrcc01080::aacC1*, Gm^r Rif^r
DE442 *ΔghsB*	This work	Head spike mutant *ΔghsB::aacC1*, Gm^r Rif^r
DE442 *ΔghsA*	This work	Head spike mutant *ΔghsA* (*Δrcc01079*), markerless, Rif^r
DE442 *Δ1691*	This work	Tail tube mutant *Δrcc01691::KIXX*, Kan^r Rif^r
DE442 *ΔghsB Δ1691*	This work	Head spike *ghsB* and tail tube *1691* double mutant, Gm^r Kan^r Rif^r
DE442 *ΔghsB ΔcckA*	This work	Head spike *ghsB* and hybrid histidine kinase *cckA* double mutant, Gm^r Kan^r Rif^r
SB1003 *ΔclpX*	This work	Chaperone *clpX* mutant *Δrcc02608::aacC1*, Gm^r Kan^r
DE442 *ΔclpX*	This work	Chaperone mutant *ΔclpX* (*Δrcc02608::aacC1*), Gm^r Kan^r
SB1003 *ΔclpX ΔctrA*	This work	Chaperone *clpX* and response regulator *ctrA* double mutant, Gm^r Kan^r Rif^r

Strain	Reference	Description[1]
SB1003 *ΔhisB*	This work	Histidine auxotroph *ΔhisB* (*Δrcc01183::KIXX*), Kan^r Rif^r
SB1003 *ΔserB*	This work	Serine auxotroph *ΔserB* (*Δrcc03445*), markerless, Rif^r
SM05	(Masuda and Bauer, 2004)	*Δhvra* and *ΔspoT* double mutant, $ppGpp^0$, SB1003-derived. Kan^r Tet^r Rif^r
SB1003 *ΔspoT*	This work	*ΔspoT* mutant, $ppGpp^0$, Tet^r Rif^r
SB1003 *ΔhvrA*	This work	*ΔhvrA* mutant, Kan^r Rif^r
SB1003 *ΔecfG*	This work	General stress response sigma-factor mutant *ΔecfG* (*Δrcc02291*), markerless, Rif^r
SB1003 *ΔdivL*	This work	PAS domain protein mutant *ΔdivL* (*Δrcc00042::aacC1*), Gm^r Rif^r
DE442 *ΔdivL*	This work	PAS domain protein mutant *ΔdivL* (*Δrcc00042::aacC1*), Gm^r Rif^r
SBpG	H. Ding unpublished	Chromosomal RcGTA promoter-mCherry reporter, SB1003 derived, Rif^r
SBpG*Δ280*	H. Ding unpublished	RcGTA-overproducer, SBpG-derived, Rif^r
SBpG*Δ280 ΔdivL*	This work	*ΔdivL* in an *Δ280* RcGTA-overproducer background, Gm^r Rif^r
SBpG*Δ280 ΔcckA*	This work	*ΔcckA* in an *Δ280* RcGTA-overproducer background, Kan^r Rif^r

Strain	Reference	Description[1]
Escherichia coli		
DH5α	(Sambrook *et al.*, 1989)	General cloning strain
S17-1 λ pir	(Simon *et al.*, 1983)	Plasmid conjugation, *pir*
TEC5	(Taylor *et al.*, 1983)	Plasmid conjugation
BL21(DE3)	Invitrogen	Protein overexpression

[1] Gene locus are referred to using the *rccXXXXX* of *R. capsulatus* SB1003 for all *R. capsulatus* strains.

[2] The strain is of uncertain provenance but is a *crtD* mutant probably derived from Y262 (Yen *et al.* 1079; B. Marrs, personal communication).

Table S2 Genetic constructs

Name	Reference	Description
pUC19	Invitrogen	General cloning plasmid, Amp^r
pZJD29A	J. Jiang and C. E. Bauer, unpublished data	Broad host range suicide plasmid, *sacB* Gm^r
pRK415	(Keen *et al.*, 1988)	Broad host range plasmid, Tet^r
pCM62	(Marx and Lidstrom, 2001)	Broad host range plasmid, Tet^r
pXCA601	(Adams *et al.*, 1989)	Reporter plasmid, *lacZ* Tet^r
pZKOphoB	This work	*ΔphoB* marker-less mutation, *sacB* Gm^r
pUCckAKO	This work	*cckA*::Kan^r fragment for transduction. Amp^r Kan^r
pRCckA	This work	*cckA* complementation plasmid, Tet^r
pD51A	(Mercer *et al.*, 2012)	CtrA(D51A), non-phosphorylatable. Tet^r
pD51E	(Mercer *et al.*, 2012)	CtrA(D51E), phosphomimetic. Tet^r
pR555	(Hynes *et al.*, 2012)	*rcc00555* complementation plasmid, Tet^r
pIND4	(Ind *et al.*, 2009)	IPTG-inducible expression plasmid, Kan^r
pIND4Gm	This work	*aacC1* containing variant of pIND4, Gm^r
pI556	This work	*rcc00556* expression plasmid, Kan^r
pI556Gm	This work	*rcc00556* complementation plasmid, Gm^r
pU1080Gm	This work	*ΔghsB*::*aacC1* mutation, Amp^r Gm^r
pUC4KIXX	(Barany, 1985)	Plasmid containing KIXX cassette, Kan^r Amp^r

Name	Reference	Description
pC1691KIXX	This work	*Δ1691* tail tube mutation, Tet^r Kan^r
pZKOghsA	This work	*ΔghsA* marker-less mutation, Gm^r
pCghsA	This work	*ghsA* complementation plasmid, Tet^r
pCghsA-ghsB	This work	*ghsA-ghsB* complementation plasmid, Tet^r
pCghsA-ghsB_His	This work	GhsB C-terminal 6 His tag, complementation plasmid, Tet^r
pCdivL	This work	*divL* complementation plasmid, Tet^r
pCclpX	This work	*clpX* complementation plasmid, Tet^r
pCclpXGm	This work	*ΔclpX::aacC1* mutation, Tet^r Gm^r
pCclpXP	This work	*clpP-clpX* complementation plasmid, Tet^r
pUhisBKIXX	This work	*ΔhisB::KIXX* mutant, Amp^r Kan^r
pZKOserB	This work	*ΔserB* markerless mutant, Gm^r
pIspoT	This work	*spoT* complementation plasmid, Kan^r
pZKOecfG	This work	*ΔecfG* marker-less mutant, Gm^r
p601-g65	(Leung *et al.*, 2012)	RcGTA promoter-lacZ reporter plasmid, Tet^r
pXCA-555	This work	555 promoter-lacZ reporter, Tet^r
pXCA-ghsA	This work	*ghsA* promoter-lacZ reporter, Tet^r
pET28a(+)	Novagen	*E. coli* T7 expression plasmid, inducible, Kan^r
pET-555C	This work	555 C-terminal 6 His tag *E. coli* expression plasmid, inducible, Kan^r

Name	Reference	Description
pETghsB_C	This work	GhsB C-terminal 6 His tag *E. coli* expression plasmid, inducible, Kan^r
pRhokHi-6	(Katzke *et al.*, 2010)	Kan^r $Spec^r$
pOrf5CTH	(Chen *et al.*, 2009a)	6 His tagged RcGTA major capsid expressed from RcGTA cluster promoter, Tet^r
pRhoG5CTH	This work	6 His tagged RcGTA major capsid expressed by constitutive read-through from *aphII*. Kan^r $Spec^r$

Table S3 Phyre2 templates for GhsB modelling

Phyre2 rank[1]	**Type**	**Enzyme/Protein**	**Organism**	**PDB code and chain**	**Reference**
1	CBM4	Cellulase K (CelK)	*Clostridium thermocellum*	3P6B-A	(Alahuhta *et al.*, 2011)
2	CBM16	Mannanase (ManA, module 1)	*Thermoanaerobacterium polysaccharolyticum*	2ZEW-B	(Bae *et al.*, 2008)
3	CBM61	Endo-β-1,4-galactanase (TM1201)	*Thermotoga maritima*	2XON-A	(Cid *et al.*, 2010)
4	CBM16	Mannanase (ManA, module 2)	*Thermoanaerobacterium polysaccharolyticum*	2ZEZ-C	(Bae *et al.*, 2008)
5	CBM22	Xylanase (Xyn10B)	*Clostridium thermocellum*	1H6Y-A	(Xie *et al.*, 2001)
6	CBM4	Xylanase (Xyn10A)	*Rhodothermus marinus*	1K42-A	(Simpson *et al.*, 2002)
7	CBM4	1,4-beta-glucanase (CenC)	*Cellulomonas fimi*	1CX1-A	(Brun *et al.*, 2000)

Phyre2 rank[1]	**Type**	**Enzyme/Protein**	**Organism**	**PDB code and chain**	**Reference**
8	CBM4	Cellobiohydrolase (CbhA)	*Clostridium thermocellum*	3K4Z-A	(Alahuhta *et al.*, 2010)
9	CBM4	Laminarinase (Lam16A)	*Thermotoga maritima*	1GUI-A	(Boraston *et al.*, 2002)
10	CBM4	endo-β-1,4-glucanase (Cel9B)	*Cellulomonas fimi*	1GU3-A	(Boraston *et al.*, 2002)
11	Ig superfamily/ Nectin	Cell adhesion molecule 1 (Cadm1/NecI-2/Tslc1)	*Homo sapiens*	4H5S-B	(Zhang *et al.*, 2013)
12	Ig superfamily	Programmed cell death protein 1 (PD-1)	*Homo sapiens*	3RRQ-A	Lazar-Molnar, Unpublished
13	Ig superfamily/ Nectin-like	Class-I MHC restricted T cell associated molecule (CRTAM)	*Homo sapiens*	3RBG-B	(Rubinstein *et al.*, 2013)

Phyre2 rank[1]	**Type**	**Enzyme/Protein**	**Organism**	**PDB code and chain**	**Reference**
14	Ig superfamily/ Nectin-like	Nectin-like molecule 1 (NecI-1)	*Homo sapiens*	1Z9M-A	(Dong *et al.*, 2006)
15	Glycoside Hydrolase Family 20	Chitobiase (ChB)	*Serratia marcescens*	1QBA-A	(Tews *et al.*, 1996)

CBM: Carbohydrate-binding module

[1] Rank adjusted after excluding identical proteins/modules. Excluded protein PDB code: 2W5F-B